Université catholique de Louvain
Institute of Condensed Matter and Nanosciences (IMCN)
Molecules, Solids and Reactivity (MOST)
Laboratoire de chimie organique et médicinale

Bâtiment Lavoisier
Place Louis Pasteur 1, bte L4.01.02, 1348 Louvain-la-Neuve, Belgique
Tél. : + 32 (0) 10 47 87 73 – fax : +32 (0) 10 47 27 88
Email : steve.dierick@gmail.com
URL : http://www.uclouvain.be/groupe-marko.html

A new generation of *N*-heterocyclic carbene platinum catalysts has been developed for the hydrosilylation of alkenes, alkynes and allenes. These complexes possess high activities and display exquisite stereoselectivities whilst being efficient at low catalyst loadings. They tolerate a wide range of functional groups and the precatalyst precursor is readily available, insensitive towards air and moisture, bench-stable for extended periods of time and easy to handle. These qualities make them the ideal user-friendly catalysts for hydrosilylation. In general, all the reagents are mixed directly from their bottles and stirred in air without any precaution. Furthermore, the use of solventless conditions, coupled with a fully atom-economical transformation, leads to a true green process, attractive for industry.
Additionally, an exceptionally bulky *N*-heterocyclic carbene has been designed, fully characterized and engaged in the formation of several organometallic complexes. IPr*$^{(2\text{-Np})}$ appears to be the most sterically demanding NHC reported to date. It is noteworthy that its ability to modify its overall shape enables IPr*$^{(2\text{-Np})}$ to accommodate various coordination environments whilst still remaining one of the most σ-donating NHCs.

Steve Dierick studied at the Université catholique de Louvain, where he received a M.Sc. degree in chemistry in 2009. During his undergraduate studies, he went to the Université de Montréal as a Mercator's Fellow and worked on the asymmetric aziridination reaction under the supervision of Prof. Hélène Lebel. Afterward, he joined the group of Prof. István E. Markó and conducted his master thesis on the total synthesis of teuvincentins. Between 2009 and 2013, he prepared his Ph.D. thesis, supported by a FRIA scholarship. In November 2013, he will move to the University of Texas Southwestern Medical Center, for post-doctoral research with Prof. Jef K. De Brabander, as an Honorary B.A.E.F. Fellow.

Steve Dierick 329 | 2013
New NHC Complexes for Catalytic Hydrosilylation and Organometallic Chemistry

UCL

New *N*-Heterocyclic Carbene Complexes for Catalytic Hydrosilylation and Organometallic Chemistry

Steve Dierick

Août 2013

Thèse présentée en vue de l'obtention
du grade de docteur en sciences

Faculté des sciences

Université catholique de Louvain

Université catholique de Louvain

Institute of Condensed Matter and Nanosciences
Molecules, Solids and Reactivity
Laboratoire de chimie organique et médicinale

New *N*-Heterocyclic Carbene Complexes for Catalytic Hydrosilylation and Organometallic Chemistry

A Thesis Presented for the
Degree of Doctor of Sciences by

Steve Dierick

Louvain-la-Neuve
August 2013

"My mama always said life was like a box of chocolates, you never know what you're gonna get"

Tom Hanks playing Forrest Gump
Forrest Gump (1994)
Screenplay by Eric Roth
Directed by Robert Zemeckis

Members of the Jury

Prof. Edward Anderson (University of Oxford)
Prof. Benjamin Elias (UCL, Secretary)
Prof. Jean-François Gohy (UCL, Chairperson)
Prof. István Markó (UCL, Supervisor)
Prof. Olivier Riant (UCL)
Prof. Christian Stevens (Ghent University)

Financial support of this work by the Fond pour la formation à la Recherche dans l'Industrie et l'Agriculture (Ph.D. fellowship to the Author) and the Université catholique de Louvain is gratefully acknowledged.

Acknowledgements — Remerciements

Now comes the time to put in lines what will be the most read part of this manuscript. It is also the opportunity for me to acknowledge all of you, who helped me throughout the years.

"Boss", depuis mon entrée à l'université, vous m'impressionnez par votre charisme, votre savoir, votre créativité et votre entièreté. J'ai beaucoup apprécié vos enseignements, vos conseils, vos encouragements et votre confiance. Merci de m'avoir laissé gérer mes projets, sans pression, et surtout de me laisser partir après quatre ans seulement ! [1]

Fabio, l'homme sans qui la boutique ne tournerait pas. Je voudrais te remercier, avec Gullu, de m'avoir tendu la main quand j'étais au plus bas et de m'avoir embrigadé dans votre labo. Merci pour tes nombreux conseils, ton franc-parler, les cafés du matin bien salutaires et les parties endiablées de kicker.
Go Redskins !

Le travail administratif qui accompagne une thèse est parfois lourd et déroutant. Heureusement, Chantal et Juliette étaient là pour veiller au grain. Merci pour votre patience et votre dévouement à vos « chers chercheurs », toujours avec le sourire et dans la bonne humeur.

Une thèse, ce n'est pas seulement un apprentissage, c'est aussi une aventure humaine. J'ai rencontré quatre amis formidables pendant mon séjour au labo Markó. Gullu, grâce à toi, et Fabio, j'ai remonté la pente et je vous en suis reconnaissant. Nos discussions sur la science,

[1] Copyright Gullu

la religion, la vie et le reste me manquent… y compris les soirées resto double-entrée, double-dessert pour Gullu ! Quand est-ce qu'on lance notre projet secret d'entreprise ? Simon, ou Simon-Smith, aka le MacGyver du rota, enfin quelqu'un d'aussi maniaque que moi au labo ! Merci pour tous tes trucs et astuces, tes déguisements et ton humour trop swaggy. Coryse, chère Coryse, quel bonheur de passer ses journées en compagnie d'une personne aussi gentille et souriante que toi. Promis, si je deviens auteur de parodie musicale, tu seras ma manager ! Alex, le caribou, déjà si longtemps que tu es parti avec femme et enfants. Merci pour les jurons québécois, le néerlandais déformé… et d'avoir ravivé mon manque de St-Hubert.

Je dois absolument remercier mon armée de correcteurs. Boss, Coryse, François, Lio, Pol, Thomas et Simon, merci pour les heures passées à relire, annoter, corriger et critiquer ce manuscrit dans des délais aussi brefs.

J'ai eu la chance de travailler avec des « jeunes » remplis de promesses. Emilie, pas facile pour toi de travailler sur l'hydrosilylation… alors que tu t'intéressais aux légumes ! Merci pour ta détermination et ton dynamisme. Damien, enthousiaste et bosseur, merci pour ta bonne humeur, je te souhaite le meilleur. Thibaut, ton travail n'a pas été facile, mais tu n'as jamais abandonné. Merci pour ton acharnement à vouloir tout comprendre, c'était un plaisir de chercher les réponses avec toi. J'espère que vous aurez appris autant de moi, que moi avec vous.

Coupe du monde de kicker, congrès, projections de matchs de foot, soupers et jeux de noël, cafés améliorés, tournois de mini-foot, séminaires interminables, engueulades et autres fous rires, voilà ce qui a rythmé mon quotidien au labo. Tout ça grâce à la complicité des nombreux membres du groupe et du Lavoisier. Merci à/Many thanks

to Akina, Alécia, Ben (la blonde), Alice, Brigitte, Cécile, Charlotte, Christophe (Chris), Cristian (Marcel), Eleonora, Florian (Flo), François (Mister Bee), Freddi, Fred, Emilie (VDB), Géraldine (Gégé), Grégory (Greg), Hodney (Hodneynouney), Goody, Guiz, Huoming (Mister Li), Jean-François (Justiiin !!), Jack-Philippe, Jemina, Jiri (George), Joséphine, Kevin (Kev-l'ancien), Kevin (Kev-le-nouveau), Koen, Laeti, Lio, Loïc, Marion, Mélanie, Pilou, Pipoune, Pol (le polyol), Quentin L. (Qwan-tine), Quentin D., Seb, Sophie, Thierry, Thomas X. (Mister Ur-de-bise), Thomas V., Tomas, Virginie, Winai, Xiaofeng (Chinese boy), Xiya, Yile et tous ceux qui se reconnaîtront, d'avoir égayé mes journées.

Mon cher MacBook. Fidèle au poste tous les jours, tu as supporté mon tapotage incessant sans te venger par un bug dévastateur pour mes documents. Merci pour ta machine à remonter le temps, ta réactivité au quart de tour et ton traitement de texte qui n'a jamais « rencontré un problème et doit fermer » !

Je remercie mes parents, Yolande et Claude, et ma grande sœur, Stéphanie. Vous m'avez enseigné le goût du travail bien fait mais aussi l'envie d'apprendre et d'aider les autres. Merci de m'avoir appris à ne pas craindre les difficultés, à toujours repousser les limites et à me dépasser. J'espère que vous serez fiers de moi.

Toutes ces années, une femme extraordinaire m'a fait le privilège de sa présence quotidienne à mes côtés. Ma fabuleuse amie/compagne/fiancée/cohabitante/future épouse, Jesla. Sans ton soutien, en particulier cette dernière année et encore plus ces dernières semaines, je n'y serais pas arrivé. Merci pour ta complicité, tes rires, tes réprimandes, ta patience et ton amour. Tu rends ma vie plus douce et notre avenir ne m'a jamais paru aussi radieux.

Publications

1. "Highly chemoselective reduction of carbonyl groups in the presence of aldehydes"
   Gulluzar Bastug, Steve Dierick, Frédéric Lebreux and István E. Markó
   Organic Letters **2012**, *14*, 1306–1309
2. "Platinum [1,3-bis[2,6-bis(1-methylethyl)-phenyl]-1,3-dihydro-2*H*-imidazol-2-ylidene][1,3-bis(η^2-ethenyl)-1,1,3,3-tetramethyldisiloxane]"
   Steve Dierick and István E. Markó
   Encyclopedia of Reagents for Organic Synthesis **2013**, John Wiley & Sons, DOI: 10.1002/047084289X.rn01545
3. "NHC platinum(0) complexes: unique catalysts for the hydrosilylation of alkenes and alkynes"
   Steve Dierick and István E. Markó
   In *N-Heterocyclic Carbenes. Effective Tools for Organometallic Synthesis*, Steven P. Nolan, ed.; Wiley, In press
4. "IPr*$^{(2\text{-Np})}$ — An exceedingly bulky *N*-heterocyclic carbene"
   Steve Dierick, Damien F. Dewez and István E. Markó
   Submitted
5. "Stereoselective hydrosilylation of alkynes and alkenes catalyzed by NHC platinum(0) complexes"
   Steve Dierick, Gulluzar Bastug and István E. Markó
   Organic Syntheses, Accepted for checking
6. "Bis-silyl platinum NHC catalysts for the hydrosilylation of alkynes and alkenes"
   Steve Dierick, Emilie Vercruysse and István E. Markó
   Manuscript in preparation
7. "Base-catalysed hydroamination of vinylsilanes"
   Alexandre Drouin, Marie-Claude Tremblay, Fabio Lucaccioni, Steve Dierick and István E. Markó
   Manuscript in preparation

Abbreviations

A	Pre-exponential factor in the Arrhenius' law
$A^{1,2}$	1,2-Allylic
$A^{1,3}$	1,3-Allylic
AIBN	Azobisisobutyronitrile
AE	Diallyl ether
Alk	Alkyl
APCI	Atmospheric-pressure chemical ionization
aq.	Aqueous
ax	Axial
Ar	Aryl
ATR	Attenuated total reflectance
BArF	Tetrakis(3,5-bis(trifluoromethyl)phenyl)borate
BHT	2,6-di-*tert*-Butyl-4-methylphenol
BINAP	Bis(diphenylphosphino)-1,1′-binaphthalene
bp	Boiling point
CI	Chemical ionization
cod	1,5-Cyclooctadiene
Cp*	Pentamethylcyclopentadienyl
D	Bond-dissociation energy
dba	Dibenzylideneacetone
dct	Dibenzo[*a*,*e*]cyclooctatetraene
dec	Decomposition
DFT	Density functional theory
DIBALH	Diisobutylaluminum hydride
DIOP	2,3-*O*-Isopropylidene-2,3-dihydroxy-1,4-bis(diphenylphosphino)butane
Dipp	2,6-Diisopropylphenyl
DMB	2,4-Dimethoxybenzyl
DMDO	Dimethyldioxirane
DMF	*N*,*N*-Dimethylformamide
dvtms	Divinyltetramethyldisiloxane
E_a	Activation Energy

EDG	Electron-donating group
EI	Electron ionization
eq	Equatorial
equiv	Equivalent
ESI	Electrospray ionization
EWG	Electron-withdrawing group
FGI	Functional group interconversion
FID	Flame ionization detector
FTIR	Fourier transform infrared spectroscopy
GC	Gas–liquid chromatography
ΔH^0	Standard enthalpy of reaction
HMPA	Hexamethylphosphoramide
HRMS	High-resolution mass spectrometry
IR	Infrared spectroscopy
KHMDS	Potassium hexamethyldisilazide
L.A.	Lewis acid
LUMO	Lowest-energy unoccupied molecular orbital
temp.	Temperature
M	Metal *or* mol L^{-1}
m-CPBA	*meta*-Chloroperoxybenzoic acid
MD'M	Bis(trimethylsilyloxy)methyl silane
mp	Melting point
MS	Mass spectrometry
n.c.	No conversion
n.d.	Not determined
NHC	*N*-heterocyclic carbene
NMR	Nuclear magnetic resonance
2-Np	2-Naphthyl
Nu	Nucleophile
Ox	Oxidizing agent
PDI	Polydispersity index
PE	Petroleum ether
phen	1,10-Phenanthroline
ppm	Parts per million

rt	Room temperature
TBAF	Tetra-butylammonium fluoride
TBS	*tert*-Butyldimethylsilyl
TBDPS	*tert*-Butyldiphenylsilyl
temp	Temperature
TES	Triethylsilyl
TFAA	Trifluoroacetic anhydride
TfO	Triflate
THF	Tetrahydrofuran
THP	Tetrahydropyran
TLC	Thin layer chromatography
TMS	Trimethylsilyl
TMEDA	Tetramethylethylenediamine
Tol	Toluene
Ts	*para*-Toluenesulfonyl
UHP	Urea hydrogen peroxide
UV	Ultraviolet
$\%V_{\mathrm{Bur}}$	Percent buried volume
Vi	Vinyl
X-MOP	2-(Diphenylphosphino)-2′-X-1,1′-binaphthyl
XPhos	2-Dicyclohexylphosphino-2',4',6'-triisopropylbiphenyl
Xyl	Xylene

Standard Ligands

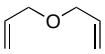

AE

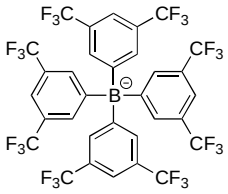

BArF

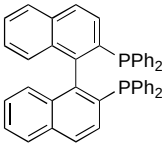

BINAP

cod

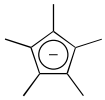

Cp*

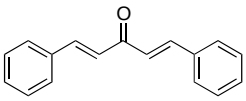

dba

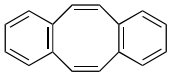

dct

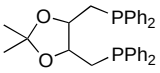

diop

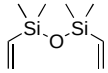

dvtms

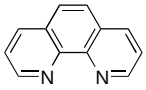

phen

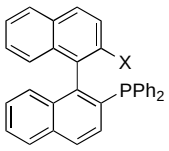

X-MOP

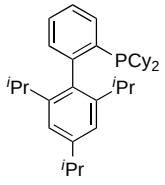

XPhos

N-Heterocyclic Carbenes

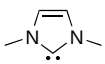

IMe

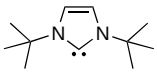

I*t*Bu

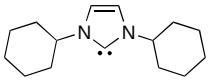

ICy

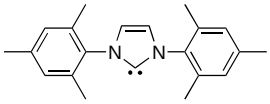

IMes

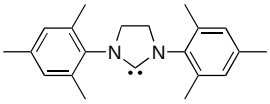

SIMes

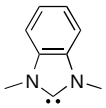

BIMe

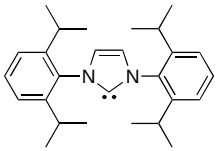

IPr

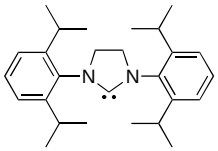

SIPr

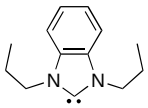

BI*n*Pr

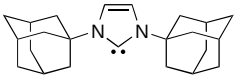

IAd

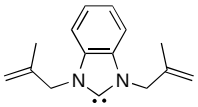

BI*m*Allyl

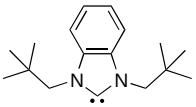

BI*neo*Pent

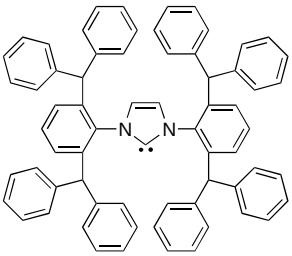

IPr*

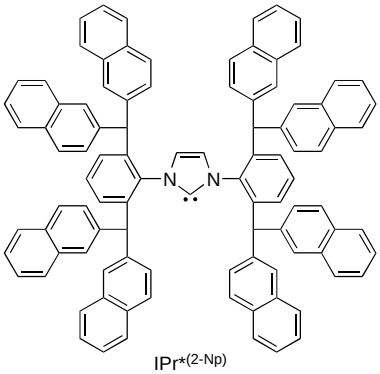

IPr*$^{(2\text{-Np})}$

Summary

The initial aim of this Ph.D. thesis was to study in detail the hydrosilylation of silylated alkynes **1**, catalyzed by the *N*-heterocyclic carbene platinum catalyst **3** (Figure 1) (see Chapter 2). We rapidly confirmed that the origin of the regioselectivity observed in this reaction was governed by steric differentiation between the R' and R_3Si substituents rather than by electronic factors. Moreover, it appeared that silylated alkynes bind strongly to platinum(0) species, promoting deactivation pathways and leading to the desired adducts in modest yields and with low selectivities.

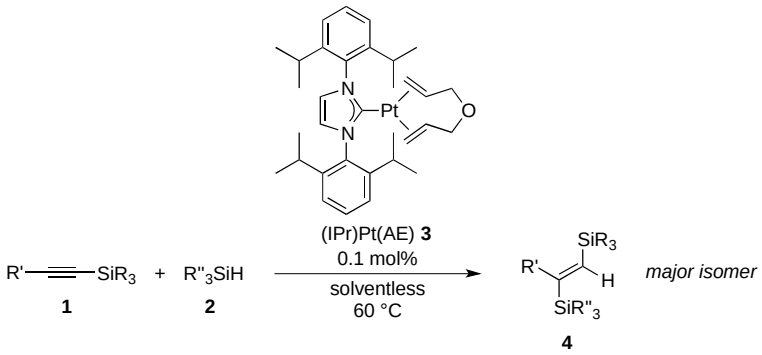

Figure 1. Hydrosilylation of silylated alkynes.

Subsequent optimization of this transformation led to the discovery of a 3rd generation of NHC platinum(0) precatalysts **6** (Figure 2) (see Chapter 2). The advantages of these bis-silyl complexes over the previous families of precatalysts are (i) their faster initiation rate and (ii) their reduced sensitivity to deactivation by substrate binding. These features enable them to afford higher levels of selectivity, whilst reacting faster than the initial precatalysts. Therefore, recognizing complexes $(IPr)Pt(SiR_3)_2$ as exceptional hydrosilylation precatalysts, we established their scope and limitation in the transformation of silylated alkynes and terminal alkynes and olefins, using various silanes.

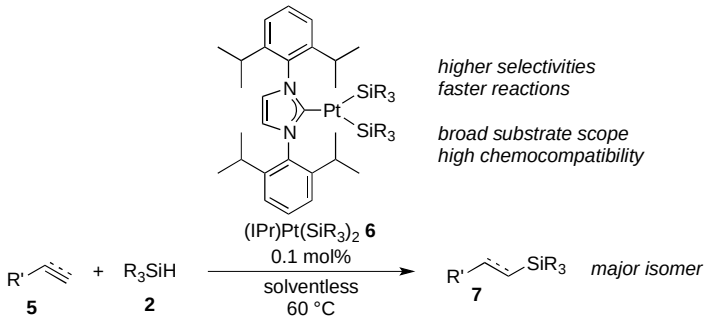

Figure 2. Third generation of hydrosilylation precatalysts.

During the course of these studies, we became interested in the development of highly sterically demanding, yet flexible, *N*-heterocyclic carbenes (see Chapter 4). Using a rational approach, we designed a new NHC. The desired imidazolium salt proved to be easily synthesized, in only four steps and on a large-scale (Figure 3). This new ligand, IPr*$^{(2\text{-Np})}$ (**8**), was fully characterized and was engaged in the formation of complexes with silver(I), copper(I), rhodium(I) and palladium(II). It appears to be the bulkiest NHC reported to date, while still being flexible and highly σ-donating.

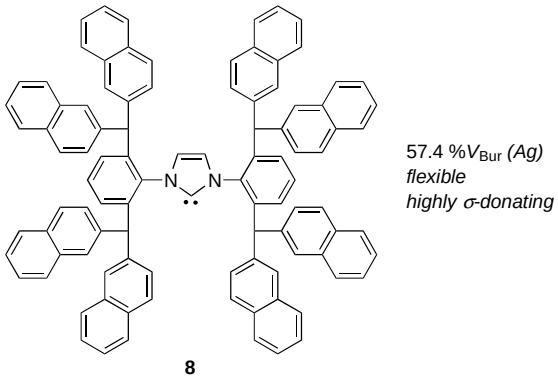

Figure 3. Structure of IPr*$^{(2\text{-Np})}$.

Finally, we collaborated to the study on the exquisite ability of diethylaluminum benzenethiolate to selectively react with aldehydes over other carbonyl functions, enabling the chemoselective in situ reduction of ketones and methyl esters in the presence of aldehydes (Figure 4) (see Annex Chapter). This potent strategy avoids the usual drawbacks of traditional protecting group methodologies and could be extended to various other transformations.

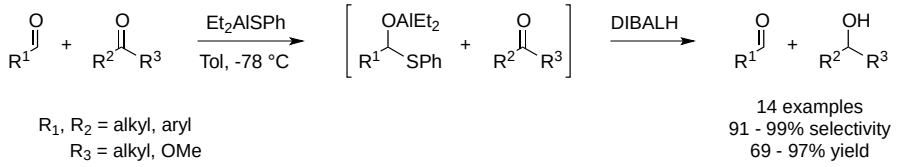

Figure 4. Highly chemoselective reduction of carbonyl groups in the presence of aldehydes.

Table of Contents

Chapter 1: Hydrosilylation of Alkenes and Alkynes **1**

1. Introduction 1
2. Hydrosilylation of Alkenes 2
   - 2.1 Radical Mediated Hydrosilylation 2
   - 2.2 Ionic Hydrosilylation 3
   - 2.3 Transition Metal Catalyzed Hydrosilylation 5
     - 2.3.1 Chalk–Harrod Mechanism 6
     - 2.3.2 Mononuclear Platinum Species or Colloids? 7
     - 2.3.3 Modified Chalk–Harrod Mechanisms 9
   - 2.4 Applications 11
     - 2.4.1 Functional Group Tolerance 12
     - 2.4.2 Internal Double Bonds 13
     - 2.4.3 Allylic Substrates 13
     - 2.4.4 Asymmetric Hydrosilylation 15
   - 2.5 Remaining Challenges in Alkenes Hydrosilylation 19
3. Hydrosilylation of Alkynes 20
   - 3.1 Radical Mediated Hydrosilylation 21
   - 3.2 Ionic Hydrosilylation 23
   - 3.3 Transition Metal Catalyzed Hydrosilylation 23
     - 3.3.1 Chalk–Harrod Mechanism 23
     - 3.3.2 Ojima–Crabtree Mechanism 24
     - 3.3.3 Trost–Ball Mechanism 26
   - 3.4 Applications 30
     - 3.4.1 Preparation of β-(*E*) Vinylsilanes 30
     - 3.4.2 Preparation of β-(*Z*) Vinylsilanes 34
     - 3.4.3 Preparation of α Vinylsilanes 38
     - 3.4.4 Hydrosilylation of Internal Alkynes 41
   - 3.5 Remaining Challenges in Alkynes Hydrosilylation 52
4. Conclusions 53

Chapter 2: Hydrosilylation and Platinum *N*-Heterocyclic Carbene Complexes **55**

1. Introduction 56
2. Hydrosilylation of Alkenes, the Beginning 57
3. Initial Results with Phosphine Ligands 59
4. NHC Platinum(0) Complexes, the Breakthrough 61
   - 4.1 Synthesis of NHC Platinum(0) Complexes and Kinetic Assays 61
   - 4.2 Functional Group Tolerance and Substrate Scope 67
   - 4.3 Mechanistic Studies 69
     - 4.3.1 Activation Period 70
     - 4.3.2 Catalyst Deactivation Pathways 74
     - 4.3.3 Semi-Quantitative Kinetic Studies 76
     - 4.3.4 Quantitative Kinetic Modeling 79
     - 4.3.5 Conclusions 84
5. Hydrosilylation of Alkynes 85
   - 5.1 Catalyst Screening and the Impact of NHCs on Regioselectivity 85
   - 5.2 Influence of the Silane on the Regioselectivity 89
   - 5.3 A Second Generation Catalyst for the Hydrosilylation of Alkynes 90
   - 5.4 Functional Group Tolerance and Substrate Scope 92
   - 5.5 Mechanistic Studies 96
     - 5.5.1 Qualitative Kinetic Studies 96
     - 5.5.2 Catalyst Activation and Deactivation Pathways 99
     - 5.5.3 Proposed Mechanism 100
6. Conclusions 102

Chapter 3: New Platinum *N*-Heterocyclic Carbene Complexes for Catalytic Hydrosilylation **103**

1. Origin and Objectives of this Research Project 103
2. Preparation of the Starting Materials 104
   2.1 Synthesis of (IPr)Pt(dvtms) and (IPr)Pt(AE) 104
   2.2 Synthesis of Silylated Alkynes 107
3. An Unexpectedly Challenging Class of Substrates 110
   3.1 Unpromising first results 110
   3.2 Optimization of the Reaction Conditions 113
   3.3 A 3rd Generation of Precatalysts 116
   3.4 Exploring the Potential of the 3rd Generation of Precatalysts 121
      3.4.1 Silylated Alkynes 121
      3.4.2 Terminal Alkynes 122
      3.4.3 Alkenes 125
      3.4.4 Allenes 128
   3.5 Combining Hydrosilylation and Peterson Elimination 133
   3.6 Combining Hydrosilylation and Hydroamination 136
   3.7 Combining Hydrosilylation, Cyclopropanation and Hiyama Cross-Coupling 140
4. Conclusions and Perspectives 142
   4.1 Conclusions 142
   4.2 Perspectives 143

Chapter 4: IPr*(2-Np) — An Exceedingly Bulky *N*-Heterocyclic Carbene **145**

1. Introduction 145
2. A New Generation of Sterically Demanding NHC 148
   2.1 Synthesis of the Imidazolium Salt IPr*(2-Np)•HCl 148
   2.2 Coordination Chemistry of IPr*(2-Np) 151
3. Conclusions and perspectives 156

Chapter 5: Conclusions **159**

Chapter 6: Experimental Section **163**

1. Instrumentation 163
2. Procedures 165
3. Compounds Synthesized in Chapter 3 166
   - 3.1 Preparation of the Precatalysts 166
   - 3.2 Preparation of the Substrates. 171
   - 3.3 Hydrosilylation 172
     - 3.3.1 Hydrosilylation of Silylated Alkynes 173
     - 3.3.2 Hydrosilylation of Terminal Alkynes 176
     - 3.3.3 Hydrosilylation of Alkenes 183
   - 3.4 Transformations of the Vinylsilanes 187
4. Compounds Synthesized in Chapter 4 189
   - 4.1 Synthesis of the Imidazolium Salt IPr*$^{(2\text{-Np})}$•HCl 189
   - 4.2 Synthesis of the organometallic complexes 193
   - 4.3 X-Ray Structures Determination 199
5. Compounds Synthesized in the Annex Chapter 201

Annex Chapter: Chemoselective Reduction of Carbonyl Groups in the Presence of Aldehydes **207**

1. State of the Art 207
2. When Serendipity Comes into Play 210
3. Chemoselective Reduction of Carbonyl Groups in the Presence of Aldehydes 212
   - 3.1 Optimization Study 212
   - 3.2 Chemoselective Reduction of Ketones 214
   - 3.3 Chemoselective Reduction of Methyl Esters 216
4. Conclusions and Perspectives 217

Chapter 1

Hydrosilylation of Alkenes and Alkynes

This chapter does not intend to be an exhaustive review on the hydrosilylation reaction but a concise, comprehensive and meaningful overview of the state of the art. It is the Author's wish to guide the Reader to the most appropriate methodology for the synthesis of his desired organosilane. The contributions of *N*-heterocyclic carbene platinum(0) complexes from the Markó research group to this synthetic endeavor will be described in the Chapter 2 and 3.

1. Introduction

The hydrosilylation of alkenes and alkynes, i.e., the addition of silanes across carbon–carbon double or triple bonds, represents the ideal pathway to produce organosilicon compounds (Figure 1). Indeed, this reaction is usually straightforward to perform and fully atom-economical. Moreover, the starting reagents are stable, cheap and readily available. Therefore, it is hardly surprising that this transformation constitutes the core of the organosilicon industry together with the Rochow–Müller process.[1] Accordingly, it is used to produce various silicon compounds ranging from bulk commodities to fine chemicals and specialty products, e.g., lubricating oils, paper release

[1] (a) E. G. Rochow, *J. Am. Chem. Soc.* **1945**, *67*, 963. (b) R. Müller, *Chem. Tech.* **1950**, 41. (c) D. Seyferth, *Organometallics* **2001**, *20*, 4978.

coatings, or grafting agents. In addition, the organosilane products are valuable building blocks for organic synthesis by taking advantage of the richness and versatility of organosilicon chemistry. Furthermore, they can be carried out through long synthetic sequences without decomposition.

Figure 1. General scheme for alkenes and alkynes hydrosilylation.

2. Hydrosilylation of Alkenes

2.1 Radical Mediated Hydrosilylation

In 1947, Whitmore described the thermal reaction of 1-octene (**1.4**) with trichlorosilane (**1.5**) in the presence of a catalytic amount of diacetyl peroxide, affording the corresponding organosilane **1.6** (Figure 2).[2] This report, which constitutes the first example in history of multiple carbon–carbon bond hydrosilylation, relies on a radical process.[3]

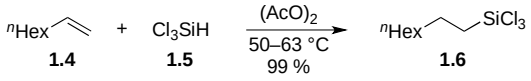

Figure 2. Hydrosilylation of 1-octene with trichlorosilane.

The general mechanism of free radical mediated hydrosilylation, similar to that of the Kharasch addition,[4] is depicted in Figure 3.[5] Hydrogen

[2] L. H. Sommer, E. W. Pietrusza, F. C. Whitmore, *J. Am. Chem. Soc.* **1947**, *69*, 188.
[3] For a review, see: C. Chatgilialoglu, *Organosilanes in Radical Chemistry*; John Wiley & Sons: Chichester, 2004.
[4] M. S. Kharasch, E. V. Jensen, W. H. Urry, *Science* **1945**, *102*, 128.
[5] K. Y. Choo, P. P. Gaspar, *J. Am. Chem. Soc.* **1974**, *96*, 1284.

abstraction from the silane **1.2** produces a silicon-centered radical **1.7**. Subsequent addition to olefin **1.8** engenders adduct **1.9**, which finally abstracts a hydrogen atom from another silane **1.2** affording product **1.10** and regenerating the silyl radical **1.7**.

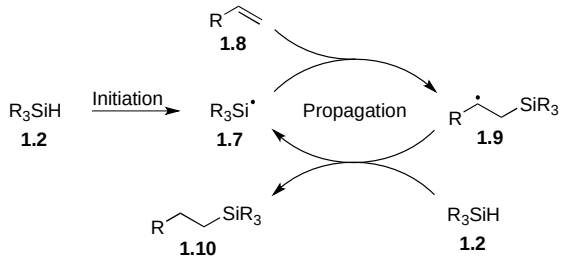

Figure 3. Mechanism of radical-mediated hydrosilylation.

The initiation step can be triggered in various ways. If the silyl radical **1.7** is relatively stable – as for trichlorosilane – heating the reaction mixture above 160 °C might induce hydrosilylation.[6] Obviously, the use of chemical initiators, like peroxides or AIBN, requires much milder conditions. One can also employ UV-radiation, although it usually results in significantly lower yields.[2] It is noteworthy that radical hydrosilylation is not widely used with trialkylsilanes, due to the very slow abstraction of the hydrogen atom from these reagents, even in the presence of thiols as hydrogen transfer catalysts.[7]

2.2 Ionic Hydrosilylation

In 1962, Pike demonstrated that tertiary amines are good catalysts for the addition of chlorosilanes, especially trichlorosilane, to alkenes at high temperature (Figure 4).[8] This methodology is particularly efficient for electrophilic olefins.

---

6 A. J. Barry, L. DePree, J. W. Gilkey, D. E. Hook, *J. Am. Chem. Soc.* **1947**, *69*, 2916.

7 For a review, see: B. P. Roberts, *Chem. Soc. Rev.* **1999**, *28*, 25.

8 R. A. Pike, *J. Org. Chem.* **1962**, *27*, 2186.

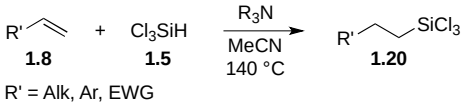

Figure 4. Tertiary amine catalyzed hydrosilylation.

Whilst the mechanism of this reaction has not been thoroughly investigated, Benkeser[9] and Bernstein[10] independently established that (i) tertiary amines **1.21** are sufficiently basic to deprotonate trichlorosilane (**1.5**) in acetonitrile at room temperature and (ii) this equilibrium is considerably shifted toward the conjugate base **1.22** and acids **1.23** (Figure 5). The polarization of the Si–H bond in chlorosilanes – opposite to that of alkylsilanes – explains this phenomenon.

It is worth noting that Fleming[11] and Pulido[12] developed the addition of silylcuprates to Michael acceptors and allenes.

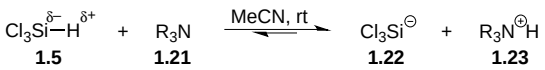

Figure 5. Deprotonation of trichlorosilane with tertiary amines.

Lewis acid catalysis enables the use of alkylsilanes in the ionic *anti* hydrosilylation of alkenes. Among them, aluminum chloride appeared to be the best choice (Figure 6).[13] In this approach, the more electron-donating the substituents on silicon, the higher the yields. It

[9] R. A. Benkeser, K. M. Voley, J. B. Grutzner, W. E. Smith, *J. Am. Chem. Soc.* **1970**, *92*, 697.

[10] S. C. Bernstein, *J. Am. Chem. Soc.* **1970**, *92*, 699.

[11] For a review, see: I. Fleming, *Lithium Bis[dimethyl(phenyl)silyl]-cuprate* in Encyclopedia of Reagents for Organic Synthesis**, 2001**, John Wiley & Sons.

[12] For a review, see: A. Barbero, F. J. Pulido, *Acc. Chem. Res.* **2004**, *37*, 817.

[13] a) K. Oertle, H. Wetter, *Tetrahedron Lett.* **1985**, *26*, 5511. b) K. Yamamoto, M. Takemae, *Synlett* **1990**, 259. c) T. Kubota, M. Endo, T. Hirahara, Jpn. Pat. 09316087, **1997**. d) N. Asao, T. Sudo, Y. Yamamoto, *J. Org. Chem*. **1996**, *61*, 7654. e) T. Sudo, N. Asao, V. Gevorgyan, Y. Yamamoto, *J. Org. Chem*. **1999**, *64*, 2494. f) Y.-S. Song, B. R. Yoo, G.-H. Lee, I. N. Jung, *Organometallics* **1999**, *18*, 3109.

has been proposed that the role of the Lewis acid could either be (i) to form a π-complex with the olefin, prior to hydride addition and transmetallation[13e] or (ii) to generate a silylium cation which adds to the olefin, affording a stable carbocation that is trapped by an hydride.[13f]

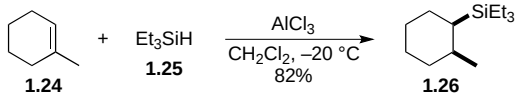

Figure 6. Aluminum chloride catalyzed hydrosilylation.

For a long time, this approach suffered from the low functional group compatibility associated with aluminum chloride. Gevorgyan addressed this issue by employing $B(C_6F_5)_3$ as a mild Lewis acid and extended the scope of this transformation.[14]

2.3 Transition Metal Catalyzed Hydrosilylation

Transition metal catalysis is the method of choice to carry out the hydrosilylation of C–C multiple bonds. Numerous metals (e.g. Pd, Ni, Co, Rh, Ru, Fe, Ir,…) have been studied for this purpose. However, since the breakthrough of Speier in 1957,[15] platinum(0) has become the work-horse of alkene hydrosilylation. The most popular complexes are the Speier catalyst, i.e., hexachloroplatinic acid in isopropanol, and the Karstedt catalyst: $Pt_2(dvtms)_3$.[16] This is due to its exquisite ability to insert into the rather strong silicon–hydrogen bond (D = 75–100 kcal mol^{-1}) and produce relatively stable platinum silicon hydride complexes.[17] Nevertheless, concerning their mode of action, most of the metal catalysts follow either (i) the Chalk–Harrod mechanism

14 M. Rubin, T. Schwier, V. Gevorgyan, *J. Org. Chem.* **2002**, *67*, 1936.

15 a) J. L. Speier, J. A. Webster, G. H. Barnes, *J. Am. Chem. Soc.* **1957**, *79*, 974. b) J. L. Speier, *Adv. Organomet. Chem.* **1979**, *17*, 407.

16 a) B. D. Karstedt, (1973) US Patent 3,775,452. For a review about the elucidation of the Karstedt's catalyst structure, see: L. N. Lewis, J. Stein, Y. Gao, R. E. Colborn, G. Hutchins, *Platinum Metals Rev.* **1997**, *41*, 66.

17 J. Y. Corey, *Chem. Rev.* **2011**, *111*, 863.

(hydrometallation) or (ii) the modified Chalk–Harrod mechanism (silylmetallation).[18] These catalytic cycles, along with some discussion on platinum nuclearity, are the objects of the two following sections.

2.3.1 Chalk–Harrod Mechanism

Group 10 metals ($Ni^{(0)}$, $Pd^{(0)}$, $Pt^{(0)}$) are known to react according to the general mechanism described by Chalk and Harrod in 1965 (Figure 7).[19] Hence, the oxidative addition of the metal catalyst **1.27** into the silicon–hydrogen bond, followed by coordination of the alkene **1.8** affords the key intermediate **1.29**. The consecutive 1,2-migratory insertion of the terminal double bond can then lead to two regioisomers, i.e. **1.30** and **1.31**. The major regioisomer **1.30** undergoes an irreversible reductive elimination yielding the desired organosilane **1.10** and regenerating the catalytic species **1.27**. On the other hand, the minor regioisomer **1.31** either goes through (i) a rapid β-hydride elimination affording the isomerized olefin **1.33** or (ii) a reductive elimination producing the internal adduct **1.34**. This catalytic cycle is based upon both kinetic studies and product distribution.

[18] Two minor mechanisms have also been proposed. For early transition metals, see: a) T. D. Tilley, *Acc. Chem. Res.* **1993**, *26*, 22. b) N. S. Radu, T. D. Tilley, *J. Am. Chem. Soc.* **1995**, *117*, 5863. c) T. I. Gountchev, T. D. Tilley, *Organometallics* **1999**, *18*, 5661. d) S. Sakaki, T. Takayama, M. Sumimoto, M. Sugimoto, *J. Am. Chem. Soc.* **2004**, *126*, 3332. For cationic ruthenium(II) and primary silanes, see: e) P. B. Glaser, T. D. Tilley, *J. Am. Chem. Soc.* **2003**, *125*, 13640.

[19] A. J. Chalk, J. F. Harrod, *J. Am. Chem. Soc.* **1965**, *87*, 16.

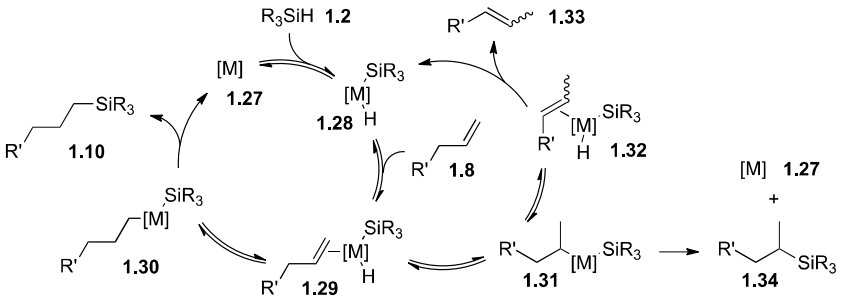

Figure 7. Chalk–Harrod mechanism.

When platinum is used, silanes bearing a chiral silicon center have been shown to react with complete retention of configuration.[20] These experiments rule out an S_N2-type oxidative addition and support a concerted 3-centers mechanism, in agreement with the literature on Si–H oxidative additions.[17]

Moreover, the hydrometallation step for platinum is further substantiated by DFT based calculations.[21] All the catalytic cycle is thought to be reversible, except for the reductive elimination step. According to two different investigations, the rate limiting step could either be (i) the 1,2-migratory insertion (E_a = 23 kcal mol^{-1})[21a] or (ii) the reductive elimination (E_a = 16 kcal mol^{-1}).[21b]

2.3.2 Mononuclear Platinum Species or Colloids?

The reaction mixtures obtained when the hydrosilylation reaction is performed with platinum catalysts are often dark colored, and precipitated platinum black is regularly observed at the end of the process. Therefore, the implication of platinum colloids as actual

[20] a) L. H. Sommer, J. E. Lyons, H. Fujimoto, *J. Am. Chem. Soc.* **1969**, *91*, 7051. b) F. Carre, E. Colomer, R. J. P. Corriu, A. Vioux, *Organometallics* **1984**, *3*, 1272. c) C. Eaborn, D. J. Tune, D. R. M. Walton, *J. Chem. Soc., Dalton Trans.* **1973**, 2255.

[21] a) S. Sakaki, N. Mizoe, M. Sugimoto, *Organometallics* **1998**, *17*, 2510. b) C. A. Tsipis, C. E. Kefalidis, *J. Organomet. Chem.* **2007**, *692*, 5245.

catalysts for this transformation has been placed under debate by Lewis.[22,23]

In response, independent studies by Osborn and Lewis himself have concluded that the real catalytically active species are mononuclear platinum complexes.[24] This conclusion is based upon the following experimental observations:

- During the most active phase of hydrosilylation, no species containing a Pt–Pt bond has ever been detected, regardless of the nature or amount of the reagents employed.
- The stoichiometry of the reagents and the coordination ability of the alkene are of paramount importance for the characteristics of the platinum species obtained at the end of the reaction. Indeed, either (i) the olefin is strongly coordinating and the final compounds contain Pt–C bonds only or (ii) the alkene is weakly coordinating and/or the silane is present in excess and the ending molecules contain Pt–Si and Pt–Pt bonds.
- There is an oxygen effect for several hydrosilylation systems. Explicitly, in its absence, hydrosilylation of certain olefins does not occur. This is attributed to the fact that oxygen breaks multinuclear platinum species that are formed when poorly coordinating alkenes are used.
- Finally, the addition of elemental mercury, a selective poison for heterogeneous catalysts, [25] has no deleterious effects on

[22] For a review about resolving between homogeneous and heterogeneous catalysis, see: R. H. Crabtree, *Chem. Rev.* **2012**, *112*, 1536.
[23] L. N. Lewis, N. Lewis, *J. Am. Chem. Soc.* **1986**, *108*, 7228.
[24] a) P. Steffanut, J. A. Osborn, A. DeCian, J. Fisher, *Chem. Eur. J.* **1998**, *4*, 2008. b) J. Stein, L. N. Lewis, Y. Gao, R. A. Scott, *J. Am. Chem. Soc.* **1999**, *121*, 3693.
[25] G. M. Whitesides, M. Hackett, R. L. Brainard, J.-P. P. M. Lavalleye, A. F. Sowinski, A. N. Izumi, S. S. Moore, D. W. Brown, E. M. Staudt, *Organometallics* **1985**, *4*, 1819.

hydrosilylation. However, the introduction of dct, an inhibitor of homogeneous catalysts,[26] suppresses all reactivity.

Additionally, the Author would like to stress that homogeneous platinum-based hydrosilylation catalysts have regularly been passing the Collman's test for more than 50 years (see Section 2.4). This test is based upon the catalytic ability of a substance to transform polymer-based substrates.[27] In this procedure, homogeneous catalysts have higher mobility in the polymer matrix and are thus active, whilst heterogeneous ones are, in general, inactive.

Interestingly, the studies of Osborn and Lewis have also revealed two fundamental findings:

- The induction periods observed with the Karstedt and the Speier catalysts (from 5 min to 1 h), respectively correspond to the time required for the hydrosilylation of the divinylsiloxane ligands (see Chapter 2) and the reduction of platinum(IV) to platinum(0).
- The colloidal platinum species are probably responsible for the hydrogenation of the olefins (see Chapter 2).

To conclude, the exact nature of the homogeneous platinum complex **1.27** (Figure 7) is still questioned. However, it is generally accepted that this compound contains either an alkene or an ancillary ligand (see Chapter 2).

2.3.3 Modified Chalk–Harrod Mechanisms

Hydrosilylation of alkenes, mediated by metals other than the platinum triad, is accompanied by an increased amount of hydrogenated olefins

[26] D. R. Anton, R. H. Crabtree, *Organometallics* **1983**, *2*, 855.
[27] J. P. Collman, K. M. Kosydar, M. Bressan, W. Lamanna, T. Garrett, *J. Am. Chem. Soc.* **1984**, *106*, 2569.

and the appearance of vinylsilanes as side products. With the classical Chalk–Harrod mechanism failing to take this phenomenon into account, another pathway has been proposed for $Rh^{(I)}$, $Ir^{(I)}$ and $Ru^{(0)}$ catalyzed processes: the modified Chalk–Harrod mechanism.[28] While it shares the same first two steps as its parent catalytic cycle (Figure 8), the common intermediate **1.29**, undergoes a 1,2-migratory insertion of the alkene into the metal–silicon bond (silylmetallation) instead of the metal–hydrogen bond (hydrometallation). Then, the subsequent metal hydride species **1.35** can follow two distinct pathways: (i) a reductive elimination to produce the desired alkylsilane **1.10** and complete the catalytic cycle or (ii) a β-hydride elimination leading to the observed vinylsilane **1.37**, concomitant with the hydrogenation of a double bond to regenerate the catalyst **1.27**.

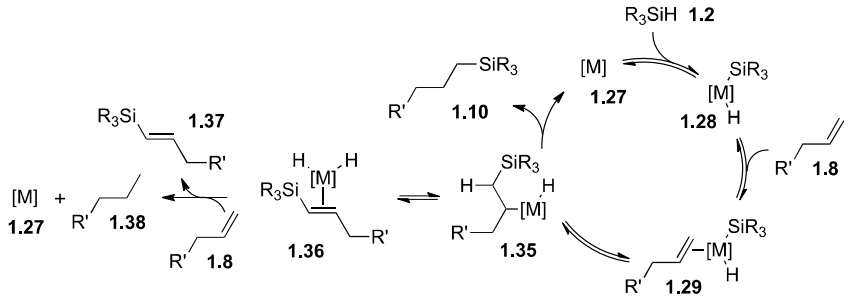

Figure 8. Modified Chalk–Harrod mechanism.

Additionally to the isolation of side products, this mechanism is further supported by a DFT study realized for the $RhCl(PH_3)_3$ mediated hydrosilylation of ethylene.[29] In this report, the oxidative addition was found to be the rate limiting step (E_a = 16 kcal mol^{-1}).

[28] a) A. Onopchenko, E. T. Sabourin, D. L. Beach, *J. Org. Chem.* **1983**, *48*, 5101. b) A. Onopchenko, E. T. Sabourin, D. L. Beach, *J. Org. Chem.* **1984**, *49*, 3389. c) R. S. Tanke, R. H. Crabtree, *Organometallics* **1991**, *10*, 415. d). Y. Seki, K. Takeshita, K. Kawamoto, S. Murai, N. Sonoda, *J. Org. Chem.* **1986**, *51*, 3890.

[29] S. Sakaki, M. Sumimoto, M. Fukuhara, M. Sugimoto, H. Fujimoto, S. Matsuzaki, *Organometallics*, **2002**, *21*, 3788.

An alternative version of the modified Chalk–Harrod mechanism has been proposed for $Co^{(I)}$, $Rh^{(I)}$ and $Pd^{(II)}$ catalysts.[30] While the key step of this variant remains a silylmetallation, the active metal species **1.39** bears only a silyl ligand (Figure 9), and no hydrogen atom is present as in complex **1.28** (see Figure 7 and Figure 8). This mechanistic proposal is based upon the isolation of intermediates.

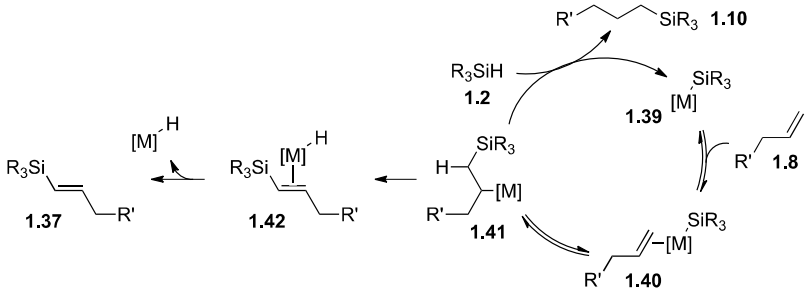

Figure 9. Variant of the modified Chalk-Harrod mechanism.

2.4 Applications

The main applications of alkene hydrosilylation are found in industry and the vast majority of the manufacturing hydrosilylation processes is based upon transition metal catalysis.[31] It is used to produce functional organosilanes (particularly γ-substituted propylsilanes), silicone polymers (silicone oils, functional siloxanes, silicone resins…), silicone elastomers, silicone-based release coatings, polysiloxane-grafted, silane-modified polymers (as adhesive and sealing materials), and so on…

[30] a) F. Seitz, M. S. Wrighton, *Angew. Chem. Int. Ed.* **1988**, *27*, 289. b) S. B. Duckett, R. N. Perutz, *Organometallics*, **1992**, *11*, 90. c) A. M. LaPointe, F. C. Rix, M. Brookhart, *J. Am. Chem. Soc.* **1997**, *119*, 906.

[31] For a review about the recent advances and the actual challenges in this area, see: D. Troegel, J. Stohrer, *Coord. Chem. Rev.* **2011**, *255*, 1440.

In this context, most of the examples are collected in the patent literature and, since these studies use non-uniform reaction conditions, the comparison of several catalytic systems is particularly difficult.[31] Nevertheless, it is undeniable that the Karstedt's catalyst and, to a lesser extent, the Speier's catalyst are at the heart of industrial processes in reason of their excellent catalytic behaviors, ease of access, and very low catalytic loadings, which counterbalances the high cost of platinum (33,276 €/kg on July 5, 2013).[31]

2.4.1 Functional Group Tolerance

Examples of functionalized alkene hydrosilylation are scarce in the literature, due to the low functional group compatibility of traditional catalysts (including the Speier and Karstedt catalysts). However, in addition to the *N*-heterocyclic carbene platinum(0) complexes studied by Markó (see Chapter 2 and 3), platinum oxide was found to be excellent catalyst for this purpose by Wagner and Mioskowski (Figure 10).[32]

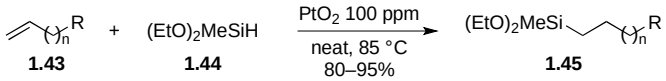

1.43 **1.44** **1.45**

R = NH_2, $N(Alk)_2$, CO_2H, COMe, OAc, CN, OAlk

Figure 10. Platinum oxide catalyzed hydrosilylation.

It is also worth mentioning that transition metals have their favored silanes for hydrosilylation. Indeed, while platinum catalysts tolerate any silane (alkyl-, alkoxy-, chloro-…), rhodium ones prefer alkyl- or arylsilanes and palladium complexes are mostly restricted to $Cl_nR_{3-n}SiH$ (n = 2, 3).[33]

[32] N. Sabourault, G. Mignani, A. Wagner, C. Mioskowski, *Org. Lett.* **2002**, *4*, 2117.

[33] T. Hayashi, in *Comprehensive Asymmetric Catalysis I-III*; E. N. Jacobsen, A. Pfaltz, H. Yamamoto, eds; Springer-Verlag: Berlin, 1999, vol. 1, p 319.

2.4.2 Internal Double Bonds

The hydrosilylation of internal olefins is particularly troublesome. Generally, these substrates are either unreactive or the catalysts afford very low levels of regioselectivity. The rare successful methodologies display a very narrow scope, being efficient for a selection of activated substrates and/or requiring particular catalysts.[34] In this context, an interesting tandem migration–hydrosilylation sequence, triggered by the Speier's catalyst, was reported (Figure 11).[15a,35] Unfortunately, the harsh conditions necessary to achieve this transformation preclude its use on functionalized molecules. As an alternative, a tether tactic can be used to perform the reaction intramolecularly (see Sections 2.4.4.2 and 2.4.4.3).

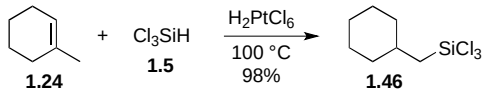

Figure 11. Tandem migration–hydrosilylation.

2.4.3 Allylic Substrates

The hydrosilylation of alkenes **1.47**, bearing allylic functional groups, furnishes γ-functionalized propylsilanes **1.52**, highly desired for industrial applications.[31] Unfortunately, allylic compounds constitute one of the most difficult classes of substrates for hydrosilylation catalysts since they are easily prone to reduction. This reactivity is depicted in Figure 12. As shown, besides following a classical hydrosilylation pathway, the catalyst can insert into the allyl–X bond of **1.47** to generate the π-allyl complex **1.48**. Then, the silane transfers its

[34] B. Marciniec, H. Maciejewski, C. Pietraszuk, P. Pawluć, in *Hydrosilylation: A Comprehensive Review on Recent Advances*; B. Marciniec, ed; Springer: New York, 2009, p 3.

[35] J. W. Ryan, J. L. Speier, *J. Am. Chem. Soc.* **1964**, *86*, 895.

hydride to the metal and a reductive elimination follows to produce propene (**1.50**) and close the catalytic cycle.

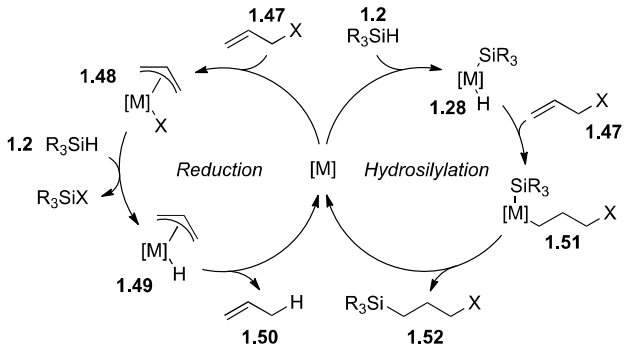

Figure 12. Reduction and hydrosilylation of allylic substrates.

In complete agreement with this mechanism, it has been observed that the lower the hydride character of the silane and the stronger the allyl–X bond, the lower the amount of reduced allyl compounds.

So far, no catalytic system proved to be universal. Nevertheless, the Shin-Etsu Corporation has optimized a beautiful process for the hydrosilylation of allyl chloride with chlorodimethylsilane (Figure 13).

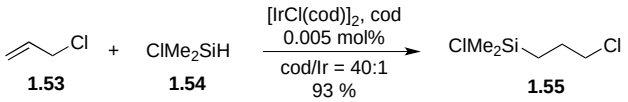

Figure 13. Shin-Etsu process for the hydrosilylation of allyl chloride.

During this thesis, the Author and Ms. Emilie Vercruysse have tackled this research theme, with some success, using *N*-heterocyclic carbene platinum(0) complexes (see Chapter 3).

2.4.4 Asymmetric Hydrosilylation

In opposition to the usual topic of alkene hydrosilylation, the development of asymmetric versions of this reaction is mainly of academic interest and not industrial.[36] This transformation is appealing because a consecutive Tamao–Kumada–Fleming oxidation would deliver optically enriched alcohols. It is worth noting that this sequence is equivalent to an asymmetric hydration of a double bond. However, two difficulties rapidly arise: (i) the non-symmetrical nature of the R_3Si–H bond (contrarily to the H–H bond in asymmetric hydrogenation) and (ii) the limited number of olefin types amenable to hydrosilylation (see Section 2.4.2).

2.4.4.1 Enantioselective Intermolecular Hydrosilylation

The first example of an asymmetric hydrosilylation was accomplished by Kumada and Hayashi in 1971.[37] It was based upon a platinum complex bearing a *P*-stereogenic monodentate ligand and afforded modest levels of enantioselectivity (Figure 14, Equation 1). Since platinum introduces the silicon group onto the terminal carbon, the olefins have to be 1,1-disubstituted to produce a chiral center β to silicon. Therefore, in order to extend the scope of the methodology, Kumada and Tamao replaced platinum by palladium. Combined with trichlorosilane, this system favors the placement of silicon onto the internal carbon, thus enabling the use of terminal alkenes (Equation 2).[38] Interestingly, this combination of palladium and trichlorosilane is the only one able to deliver selectively branched hydrosilylation products.

---

[36] For reviews, see: a) ref 33. b) B. Marciniec, H. Maciejewski, C. Pietraszuk, P. Pawluć, in *Hydrosilylation: A Comprehensive Review on Recent Advances*; B. Marciniec, ed; Springer: New York, 2009, p 125.

[37] K. Yamamoto, T. Hayashi, M. Kumada, *J. Am. Chem. Soc.* **1971**, *93*, 5301.

[38] Y. Kiso, K. Yamamoto, K. Tamao, M. Kumada, *J. Am. Chem. Soc.* **1972**, *94*, 4373.

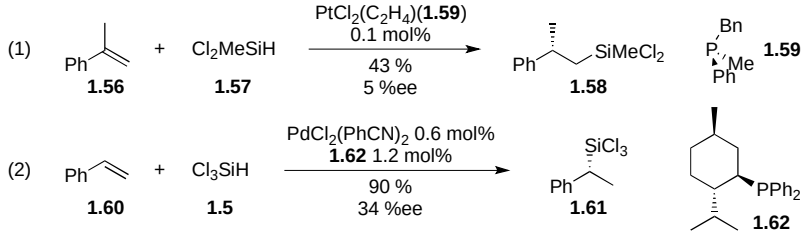

Figure 14. Kumada, Hayashi and Tamao asymmetric hydrosilylations.

After 20 years of ligand screening, Hayashi discovered that the X-MOP family of ligands was impressive for the enantioselective intermolecular hydrosilylation of terminal alkenes, styrene derivatives and norbornene type structures (Figure 15).[39] He also demonstrated that this catalytic system follows a Chalk–Harrod mechanism (hydropalladation) through the isolation of side products and deuterium labeling studies.[39d,40]

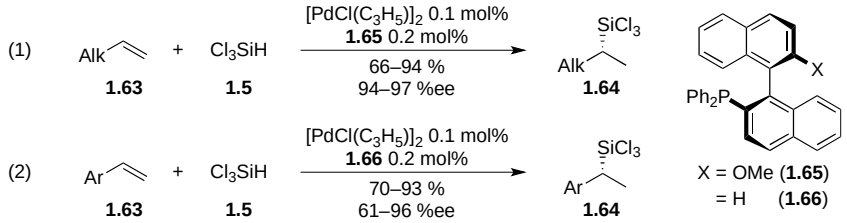

Figure 15. Hayashi asymmetric hydrosilylation with X-MOP ligands.

A few years later, Johannsen revealed that readily accessible chiral phosphoramidites are also efficient ligands for the application of this methodology to styrene derivatives.[41]

---

[39] a) Y. Uozumi, T. Hayashi, *J. Am. Chem. Soc.* **1991**, *113*, 9887. b) Y. Uozumi, K. Kitayama, T. Hayashi, K. Yanagi, E. Fukuyo, *Bull. Chem. Soc. Jpn.* **1995**, *68*, 713. c) K. Kitayama, Y. Uozumi, T. Hayashi, *J. Chem. Soc., Chem. Commun.* **1995**, 1533. d) T. Hayashi, S. Hirate, K. Kitayama, H. Tsuji, A. Torii, Y. Uozumi, *J. Org. Chem.* **2001**, *66*, 1441.

[40] Y. Uozumi, H. Tsuji, T. Hayashi, *J. Org. Chem.* **1998**, *63*, 6137.

[41] a) J. F. Jensen, B. Y. Svendsen, T. V. la Cour, H. L. Pedersen, M. Johannsen, *J. Am. Chem. Soc.* **2002**, *124*, 4558. b) X.-X. Guo, J.-H. Xie, G.-H. Hou, W.-J. Shi, L.-X. Wang, Q.-L. Zhou, *Tetrahedron: Asymm.* **2004**, *15*, 2231.

2.4.4.2 Enantioselective Intramolecular Hydrosilylation

To circumvent the limitation to terminal double bonds, the use of tethered silane groups in order to control the regioselectivity of the hydrosilylation of internal olefins has been introduced. This brilliant tactic enables the stereoselective synthesis of 1,3-diols,[42] important subunits found in numerous natural products, starting from allylic or homoallylic alcohols. It is particularly effective for rhodium(I) coordinated by bidentate phosphines and enables the preparation of two chiral centers in a single operation (Figure 16).[43] Interestingly, a deuterium labeling study has confirmed a silylrhodation pathway, in agreement with the expected modified Chalk–Harrod mechanism.[44]

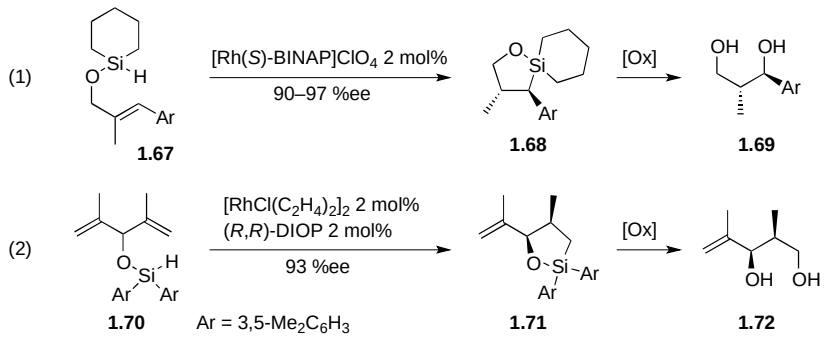

Figure 16. Representative enantioselective intramolecular hydrosilylations.

2.4.4.3 Diastereoselective Intramolecular Hydrosilylation

Generally, if an olefin tethered with a silane is already chiral, its hydrosilylation proceeds with high diastereoselectivity. For instance,

---

[42] For a review on the stereoselective synthesis of 1,3-diols, see: S. E. Bode, M. Wolberg, M. Müller, *Synthesis* **2006**, 557.

[43] a) K. Tamao, T. Tohma, N. Inui, O. Nakayama, Y. Ito, *Tetrahedron Lett.* **1990**, *31*, 7333. b) S. H. Bergens, P. Noheda, J. Whelan, B. Bosnich, *J. Am. Chem. Soc.* **1992**, *114*, 2121. c) R. W. Barnhart, X. Wang, P. Noheda, S. H. Bergens, J. Whelan, B. Bosnich, *Tetrahedron* **1994**, *50*, 4335.

[44] S. H. Bergens, P. Noheda, J. Whelan, B. Bosnich, *J. Am. Chem. Soc.* **1992**, *114*, 2128.

this method has successfully been used for the construction of *syn*-1,3-diols.[45] Recently, Roush has achieved the stereoselective synthesis of *syn*,*syn*- and *syn*,*anti*-1,3,5-triols through this powerful tactic (Figure 17).[46]

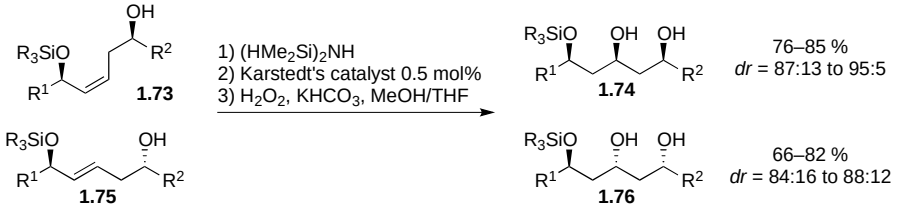

Figure 17. Roush synthesis of *syn*,*syn*- and *syn*,*anti*-1,3,5-triols.

Assuming that a Chalk–Harrod mechanism is at work, the diastereoselectivity is derived from intermediate **1.77** adopting a chairlike conformation, with the double bond in a pseudoequatorial position, for the hydroplatination step.

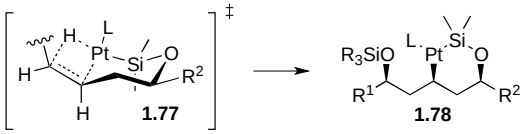

Figure 18. Model for the diastereoselective intramolecular hydrosilylation.

2.4.4.4 Diastereoselective Intermolecular Hydrosilylation

In 2005, Oestreich reported that the chiral information embedded in an optically enriched *Si*-stereogenic silane could be transferred to carbon through the hydrosilylation of an olefin catalyzed by Brookhart's

[45] For a review, see: a) S. Bracegirdle, E. A. Anderson, *Chem. Soc. Rev.* **2010**, *39*, 4114. b) B. Marciniec, H. Maciejewski, C. Pietraszuk, P. Pawluć, in *Hydrosilylation: A Comprehensive Review on Recent Advances*; B. Marciniec, ed; Springer: New York, 2009, p 87.

[46] F. Li, W. R. Roush, *Org. Lett.* **2009**, *11*, 2932.

complex (Figure 19).[47] However, this type of silane is difficult to prepare,[48] making this approach less attractive for organic synthesis.

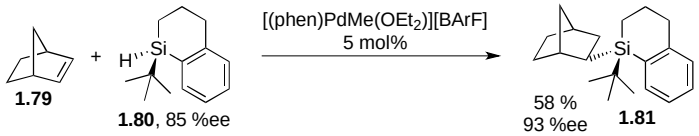

Figure 19. Chirality transfer from silicon to carbon through hydrosilylation.

Interestingly, a positive non-linear effect has been measured for this transformation. This is in support of a modified Chalk–Harrod mechanism for palladium(II) catalysts, in agreement with Brookhart studies.[30c]

2.5 Remaining Challenges in Alkenes Hydrosilylation

Although being a mature field, the hydrosilylation of alkenes still faces some challenges. Mostly required for industrial applications, new generations of catalysts are necessary in order to address the following issues:[31]

- Improving processes hampered by the formation of significant amount of side products, particularly during the production of γ-functionalized propylsilanes.
- Increasing resistance to sulfur and nitrogen contamination.
- Achieving the synthesis of switchable catalysis with perfectly clear-cut activation.[31,49]
- Replacing precious metal-based catalysts by low-cost ones.

---

[47] a) M. Oestreich, S. Rendler, *Angew. Chem. Int. Ed.* **2005**, *44*, 1661. b) M. Oestreich, *Chem. Eur. J.* **2005**, *12*, 30.

[48] For a review, see: L.-W. Xu, G.-Q. Lai, J.-X. Jiang, *Chem. Soc. Rev.* **2011**, *40*, 1777.

[49] R. Karch, V. Raab, A. Rivas Nass, Umicore AG, personal communication 2013.

This last statement is particularly important due the very high and volatile price of platinum. New catalysts based upon ruthenium and iron have demonstrated promising results, but are still far from achieving the activities and selectivities of well-established complexes.[31,50]

From an academic point of view, it is the Author's opinion that the development of new catalysts for the regio- and stereoselective intermolecular hydrosilylation of internal alkenes is a valuable research theme. Likewise, extending the Hayashi enantioselective hydrosilylation scope beyond trichlorosilane and terminal olefins would be of benefit to organic synthesis.

3. Hydrosilylation of Alkynes

The hydrosilylation of terminal and internal alkynes can afford theoretically three or four different stereoisomers (Figure 20).[51] Considering the synthetic potential of each of these vinylsilanes, efficient methodologies, enabling their selective formations, are highly desirable.[52,53]

[50] For a promising iron(0) catalyst, although extremely air and moisture sensitive, see: A. M. Tondreau, C. C. H. Atienza, K. J. Weller, S. A. Nye, K. M. Lewis, J. G. P. Delis, P. J. Chirik, *Science* **2012**, *335*, 567.

[51] For reviews on the hydrosilylation of alkynes, see: a) T. Hiyama, T. Kusumoto, in *Comprehensive Organic Synthesis*; B. M. Trost, I. Fleming, eds; Pergamon Press: Oxford, 1991, vol. 8, p 763. b) J. A. Reichl, D. H. Berry, *Adv. Organomet. Chem.* **1998**, *43*, 197. c) I. Ojima, Z. Li, J. Zhu, in *The Chemistry of Organosilicon Compounds*; Z. Rappoport, Y. Apeloig, eds; Wiley: Chichester, 1998, vol. 2, p 1687. d) B. M. Trost, Z. T. Ball, *Synthesis*, **2005**, 853. e) B. Marciniec, H. Maciejewski, C. Pietraszuk, P. Pawluć, in *Hydrosilylation: A Comprehensive Review on Recent Advances*; B. Marciniec, ed; Springer: New York, 2009, p 53.

[52] For reviews on the synthetic utility of vinylsilanes, see: a) W. P. Weber, *Silicon Reagents for Organic Synthesis*; Springer-Verlag: Berlin, 1983, p 79. b) T. A. Blumenkopf, L. E. Overman, *Chem. Rev.* **1986**, *86*, 857. c) E. W. Colvin, in *Comprehensive Organometallic Chemistry II*; E. W. Abel, F. G. A. Stone, G. Wilkinson, eds; Pergamon: Oxford, 1995, vol. 11, p 313. d) E. Langkopf, D.

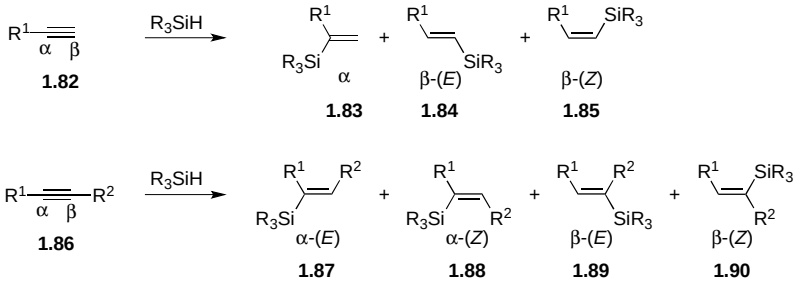

Figure 20. Stereochemical outcome of alkynes hydrosilylation.

3.1 Radical Mediated Hydrosilylation

Under radical free conditions, hydrosilylation of terminal alkynes affords a mixture of β-(*Z*) and β-(*E*) vinylsilanes.[3] The mechanism associated with this transformation is similar to the one reported for alkenes and depicted in Figure 3. However, in this case, the initial (*Z*) vinyl radical adduct **1.91** is in equilibrium with its (*E*) isomer **1.92** (Figure 21). Therefore, the stereoselectivity of the reaction strongly depends upon whether it is performed under kinetic or thermodynamic control.

Schinzer, *Chem. Rev.* **1995**, *95*, 1375. e) I. Fleming, A. Barbero, D. Walter, *Chem. Rev.* **1997**, *97*, 2063. f) T.-Y. Luh, S.-T. Liu, in *The Chemistry of Organosilicon Compounds*; Z. Rappoport, Y. Apeloig, eds; Wiley: Chichester, 1998, vol. 2, p 1793. g) A. Hosomi, K. Miura, in *Comprehensive Organometallic Chemistry III: From Fundamentals to Applications*; R. H. Crabtree, D. M. P. Mingos, eds; Elsevier: Oxford, 2007, vol. 9, p 297. h) M. J. Curtis-Long, Y. Aye, *Chem. Eur. J.* **2009**, *15*, 5402. i) S. E. Denmark, J. H.-C. Liu, *Angew. Chem. Int. Ed.* **2010**, *49*, 2978.

[53] For reviews on the synthesis of vinylsilanes, see: a) L. Birkofer, O. Sthul, in *The Chemistry of Organic Silicon Compounds*; Z. Rappoport, S. Patai, eds; Wiley: Chichester, 1989, vol. 1, p 655. b) B. Marciniec, C. Pietraszuk, I. Kownacki, M. Zaidlewicz, in *Comprehensive Organic Functional Group Transformations II*; A. R. Katritzky, R. J. K. Taylor, eds; Elsevier: Amsterdam, 2004, vol. 2, p 941. c) D. S. W. Lim, E. A. Anderson, *Synthesis* **2012**, 983.

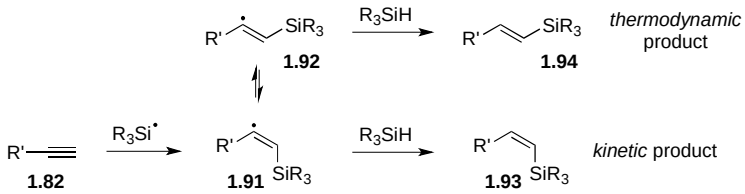

Figure 21. Radical hydrosilylation of alkynes.

Chlorosilanes, which are particularly efficient in the case of radical hydrosilylation of olefins (see Section 2.1), are notably unselective for alkynes.[54] As for alkenes, trialkylsilanes are not efficient due to their slow hydrogen abstraction. In stark contrast, tris(trimethylsilyl)silane, initiated by Et_3B/O_2 at room temperature, adds to terminal triple bonds to afford the β-(*Z*) vinylsilanes **1.96** with exquisite selectivities (Figure 22).[55] However, 2,2-dimethyl-3-butyne is a notable exception as it gives cleanly the β-(*E*) vinylsilane. This has been putatively attributed to the higher $A^{1,3}$ strain caused by the *tert*-butyl substituent in the (*Z*) radical adduct **1.91**.

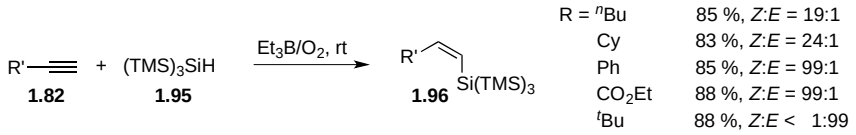

Figure 22. Hydrosilylation of terminal alkynes using tris(trimethylsilyl)silane.

It is noteworthy that, till this day, no reaction conditions or reagents have been developed that allows the systematic production of the β-(*E*) isomer **1.94**.

[54] a) R. A. Benkeser, R. A. Hickner, *J. Am. Chem. Soc.* **1958**, *80*, 5298. b) R. A. Benkeser, M. L. Burrous, L. E. Nelson, J. V. Swisher, *J. Am. Chem. Soc.* **1961**, *83*, 4385.

[55] a) B. Kopping, C. Chatgilialoglu, M. Zehnder, B. Giese, *J. Org. Chem.* **1992**, *57*, 3994. b) K. Miura, K. Oshima, K. Utimoto, *Bull. Chem. Soc. Jpn.* **1993**, *66*, 2356.

3.2 Ionic Hydrosilylation

β-(*Z*) vinylsilanes **1.93** can be easily formed, with excellent regioselectivities, through the aluminum chloride mediated *anti* hydrosilylation of terminal alkynes **1.82** (Figure 23).[13d,e] However, these conditions are limited to alkylsilanes and suffer from low functional group tolerance. Nonetheless, they have found applications in an intramolecular version to prepare silacycles.[56]

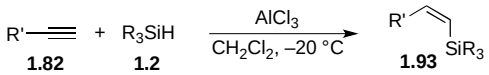

Figure 23. Hydrosilylation of alkynes catalyzed by aluminum chloride.

3.3 Transition Metal Catalyzed Hydrosilylation

The metal catalyzed hydrosilylation of carbon–carbon triple bonds constitutes the most efficient access to the highly valuable vinylsilanes. Unfortunately – or fortunately? – the stereochemical outcome of this transformation strongly depends upon the metal employed, its ligands, the catalytic loading, the substituents on both the alkyne and the silane, the temperature, the solvent and even the order of addition of the reagents. Frequently, the modification of one of these parameters leads to impressive effects on the reaction's result.

3.3.1 Chalk–Harrod Mechanism

Although mechanistic studies are scarce,[57] the hydrosilylation of carbon–carbon triple bonds catalyzed by platinum(0) and palladium(0)

[56] T. Sudo, N. Asao, Y. Yamamoto, *J. Org. Chem.* **2000**, *65*, 8919.

[57] a) C. A. Tsipis, *J. Organomet. Chem.* **1980**, *188*, 53. b) A. K. Roy, R. B. Taylor, *J. Am. Chem. Soc.* **2002**, *124*, 9510. c) C. A. Tsipis, C. E. Kefalidis, *Organometallics* **2006**, *25*, 1696.

complexes are thought to follow a mechanism similar to the one proposed by Chalk and Harrod for alkenes (see Section 2.3.1).[19] Accordingly, oxidative addition of the metal catalyst **1.27** into the silicon–hydrogen bond, followed by coordination of the alkyne **1.82** affords the key intermediate **1.97** (Figure 24). The consecutive 1,2-migratory insertion of the terminal triple bond can then produce two regioisomers, i.e. **1.98** and **1.99**. The major regioisomer **1.98**, undergoes an irreversible reductive elimination yielding the desired β-(*E*) vinylsilane **1.94** and releasing the catalytic species **1.27**. On the other hand, the minor regioisomer **1.99**, destabilized by the $A^{1,2}$ strain between the alkyne substituent and the metal ligands, can either afford the α vinylsilane or regenerate the metal hydride **1.97**. Interestingly, both regioisomers result from a *syn* addition of the silane across the triple bond.

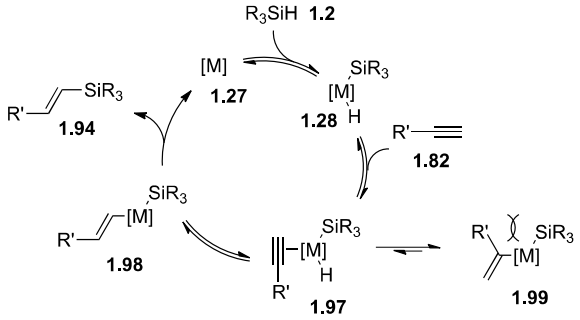

Figure 24. Chalk–Harrod mechanism.

3.3.2 Ojima–Crabtree Mechanism

When catalyzed by metals other than platinum(0) and palladium(0), the hydrosilylation of alkynes results in increased amounts of β-(*Z*) vinylsilanes, which are often predominant. Occasionally, the formation of olefins and silylated alkynes can also be detected. Regarding these observations, Ojima, for rhodium(I),[58] and Crabtree, for iridium(I),[59]

[58] I. Ojima, N. Clos, R. J. Donovan, P. Ingallina, *Organometallics* **1990**, *9*, 3127.

introduced a working mechanism based upon a silylmetallation reminiscent of the modified Chalk–Harrod mechanism for alkenes (see Section 2.3.3). This mechanism begins with the same first two steps described by Chalk and Harrod (Figure 25). However, the common intermediate **1.97** undergoes a 1,2-migratory insertion of the alkyne into the metal–silicon bond (silylmetallation) instead of the metal–hydride bond (hydrometallation). Then, the subsequent (*Z*) metal hydride species **1.100** can follow two distinct pathways: (i) a reductive elimination affording the β-(*E*) vinylsilane **1.94** and closing the catalytic cycle or (ii) an *E*/*Z* isomerization process favoring its (*E*) isomer **1.103**. The isomerization driving force is assumed to be the release of steric strain between the metal and the silicon group in **1.100**. It is suggested to involve the zwitterionic carbene **1.101** or the metallacyclopropene **1.102**. Afterward, the metal species **1.103** can either (i) reductively eliminate to produce the β-(*Z*) vinylsilane **1.93** or (ii) undergo a β-hydride elimination delivering the silylated alkyne **1.104**. The metal hydride species **1.105** resulting from this latter possibility is putatively responsible for the formation of hydrogenated products.

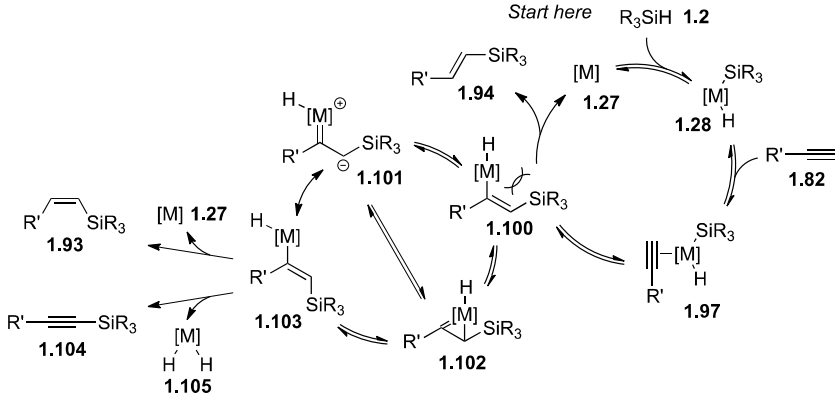

Figure 25. Ojima–Crabtree mechanism.

[59] a) R. S. Tanke, R. H. Crabtree, *J. Am. Chem. Soc.* **1990**, *112*, 7984. b) C.-H. Jun, R. H. Crabtree, *J. Organomet. Chem.* **1993**, *447*, 177.

Due to the lack of in-depth mechanistic studies, it is particularly difficult to rationalize the influence of the reaction parameters and hence to anticipate the selectivity outcome of hydrosilylation governed by the Ojima–Crabtree mechanism. Nevertheless, a few reliable experimental observations can be summarized:

- Increasing the temperature favors the β-(*E*) vinylsilane **1.94**.
- Electron-withdrawing groups on silicon favor the β-(*E*) vinylsilane **1.94**, whilst electron-donating groups afford preferentially the β-(*Z*) vinylsilane **1.93**.
- Electron-poor metal centers preferentially produce the β-(*E*) vinylsilane **1.94**.
- Bulky substituents on both the carbon–carbon triple bond and the silane favor the silylated alkyne **1.104** and the β-(*E*) vinylsilane **1.94**.

3.3.3 Trost–Ball Mechanism

In 2001, Trost and Ball discovered that a cationic ruthenium(II) complex, $[Cp^*Ru(MeCN)_3]PF_6$, catalyzes the hydrosilylation of alkynes with various silanes to afford the corresponding α vinylsilanes as the major products.[60] In a subsequent work, they carried out the intramolecular hydrosilylation of homo- and bis-homopropargylic alcohols **1.106** leading to the formation of the *anti* endo-dig cyclized products **1.107**.[61] This result stands in stark contrast to the one obtained using platinum(0) catalysts that produce the *syn* exo-dig products **1.108** (Figure 26).[62] It is critical to point out that compounds

[60] B. M. Trost, Z. T. Ball, *J. Am. Chem. Soc.* **2001**, *123*, 12726.
[61] B. M. Trost, Z. T. Ball, *J. Am. Chem. Soc.* **2003**, *125*, 30.
[62] a) K. Tamao, K. Maeda, T. Tanaka, M. Kumada, *Tetrahedron Lett.* **1988**, *29*, 6955. b) J. A. Marshall, M. M. Yanik, *Org. Lett.* **2000**, *2*, 2173. c) S. E. Denmark, W. T. Pan, *Org. Lett.* **2001**, *3*, 61.

1.107 are incompatible with a *syn* hydro- or silylmetallation, which would respectively result in the formation of cyclic species **1.109** or **1.110** with internal *trans* double bonds.[63]

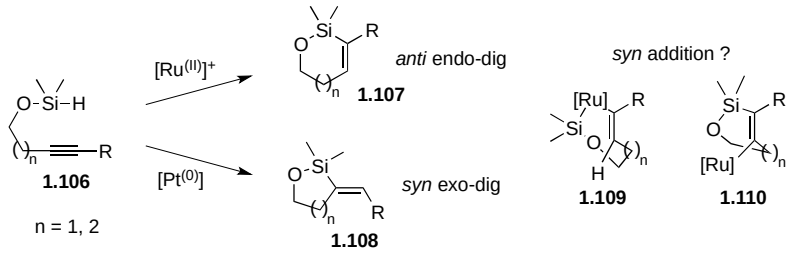

Figure 26. Cyclization products of transition metal catalyzed hydrosilylation.

Intrigued by this unexpected behavior, they reexamined the hydrosilylation of a terminal alkyne in a labeling experiment (Figure 27).[61] Remarkably, the same apparent *anti* addition of the silane was observed, with complete deuterium incorporation in a single isomer. Moreover, since no crossover or doubly deuterated compounds were produced, this study rules out a pathway involving the external delivery of a hydride to a π-coordinated triple bond (see Sections 2.2 and 3.2), or a process involving two discrete ruthenium complexes.

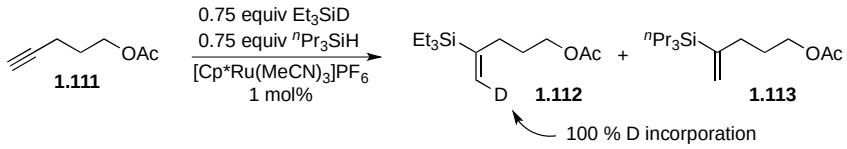

Figure 27. Labeling experiment for [Cp*Ru(MeCN)$_3$]PF$_6$.

In order to discriminate between a stereospecific *anti* addition and a stereoselective *E*/*Z* isomerization process (see Section 3.3.2), they performed the hydrosilylation of the hindered alkyne **1.114** with

[63] For a meaningful discussion, see: R. H. Crabtree, *New. J. Chem.* **2003**, *27*, 771.

deuterated triethylsilane (Figure 28).[64] Again, the hydrosilylation product **1.115** was obtained with complete deuterium incorporation in a single isomer. Therefore, an isomerization route between a hypothetical initial *syn* adduct **1.116** and intermediate **1.117** is unlikely.

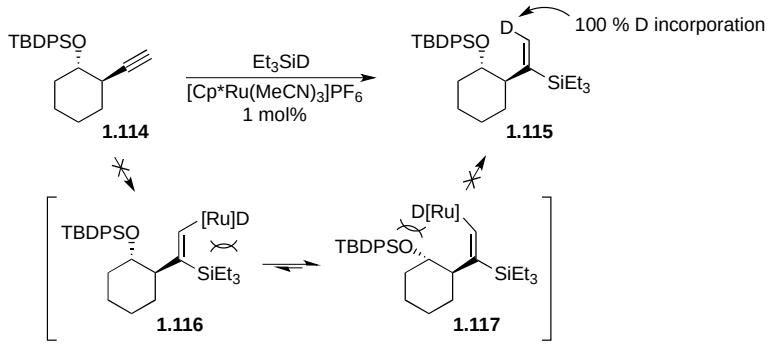

Figure 28. Deuterium labeling experiment for [Cp*Ru(MeCN)$_3$]PF$_6$.

Concerning the reactivity of the ruthenium complex with the silane, Trost and Ball noticed that no ruthenium hydride formation is observed by ^{1}H NMR spectroscopy when an equimolar amount of silane is mixed with [Cp*Ru(MeCN)$_3$]PF$_6$.[65] Thus, a pathway involving a direct oxidative addition step is uncertain.

With all these experimental results in hand, a theoretical study of the reaction was realized using DFT calculations.[65] The resulting mechanistic pathway is depicted in Figure 29. Accordingly, the cationic ruthenium(II) catalyst **1.118** coordinates both the unsaturated compound **1.82** and the silane **1.2**. The resulting complex **1.119** then undergoes a concerted oxidative addition–1,2-migratory insertion,[66] immediately followed by a stereospecific counterclockwise C–C bond rotation (indicated by a curved arrow in **1.120**); leading directly to the

[64] B. M. Trost, Z. T. Ball, *J. Am. Chem. Soc.* **2005**, *127*, 17644.

[65] L. W. Chung, Y.-D. Wu, B. M. Trost, Z. T. Ball, *J. Am. Chem. Soc.* **2003**, *125*, 11578.

[66] A similar concerted mechanism is operating in the hydrosilylation of alkenes catalyzed by (NHC)Pt(dvtms) complexes (see Chapter 2).

ruthenacyclopropene **1.121**. Afterward, a α-migration of the silyl group results in the net *anti* addition adduct **1.122**, which releases the α vinylsilane **1.83** and regenerates the catalytic species **1.118**.

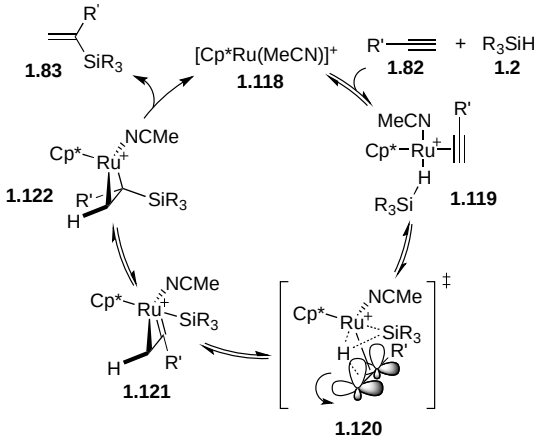

Figure 29. Trost–Ball mechanism.

Interestingly, this mechanism does not only account for the stereospecific *anti* addition but it also explains the origin of the unusual regioselectivity. Indeed, the hypervalency of the hydrogen atom in the transition state **1.120** favors its delivery to the more sterically accessible carbon of the triple bond. Importantly, in the case of internal alkynes, electronic factors must be taken into account in order to rationalize the selectivity (see Section 3.4.4.2). For example, propargylic alcohols and α,β-alkynyl carbonyl compounds direct the addition of the silicon group onto the most electron-rich carbon of the unsaturation, notwithstanding the steric hindrance in its environment. This directing effect is attributed to the disfavored formation of a carbenoid center adjacent to an electronegative substituent.

3.4 Applications

In stark contrast to olefin hydrosilylation, the hydrosilylation of alkynes is mostly an academic research topic. The resulting vinylsilanes, although absent in natural products, have proved to be remarkably valuable in various synthetic methodologies. For example, they serve as partners for the Hiyama–Denmark cross-coupling, as Michael acceptors, masked ketones, terminators for cationic cyclization, stereodivergent vinyl-halogen precursors, nucleophiles for aldehydes or activated Michael acceptors…[52] Moreover, they are particularly appreciated in reason of their low-cost, low-toxicity, ease of handling, simplicity of by-products removal and high stability throughout several synthetic steps, making them attractive surrogates to their tin and boron counterparts.

3.4.1 Preparation of β-(E) Vinylsilanes

Since platinum(0) complexes are essentially selective for the formation of β-(*E*) vinylsilanes (see Section 3.3.1), the overwhelming majority of catalytic hydrosilylations targeting this particular isomer are centered upon this metal. The principal outcomes are summarized in Table 1 (p 32). Benkeser and Lewis studied the use of Speier and Karstedt catalysts with various alkynes and silanes (entries 1–7).[67] Sadly, these complexes exhibit a moderate tolerance to functional groups (see Section 2.4.1) and a highly substrate dependent selectivity. To overcome these shortcomings, Stone and Tsipis introduced phosphine ligands to improve the selectivity of the Karstedt catalyst and focused

[67] a) R. A. Benkeser, M. L. Burrous, L. E. Nelson, J. V. Swisher, *J. Am. Chem. Soc.* **1961**, *83*, 4385. b) L. N. Lewis, K. G. Sy, G. L. Bryant, P. E. Donahue, *Organometallics* **1991**, *10*, 3750.

their effort on tricyclohexylphosphine (entries 8–11).[57a, 68] This approach led to higher selectivities with lower platinum loadings. Undoubtedly, due to the lowered Lewis acidity of these new complexes, the functional group compatibility was also increased. In a very similar way, Procter used the bulkier tri-*tert*-butylphosphine to further improve the selectivities (entries 12–17), particularly for propargylic alcohols.[69,70] However, alkoxysilanes are not well tolerated by platinum catalysts and these complexes are air and moisture sensitive (tri-*tert*-butylphosphine is pyrophoric), which hampered their use on large scale.

By harnessing the tri-*tert*-butylphosphine/Karstedt's complex couple, Denmark was able to achieve an elegant one-pot hydrosilylation–Hiyama cross-coupling with siloxanes (Figure 30).[71,72] The same sequence has subsequently been applied to internal alkynes (see Section 3.4.4.4).

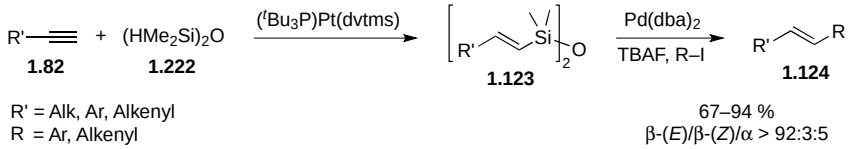

Figure 30. Denmark one-pot hydrosilylation–Hiyama cross-coupling.

[68] a) M. Green, J. L. Spencer, G. A. F. Stone, C. A. Tsipis, *J. Chem. Soc., Dalton Trans.* **1977**, 1519. b) M. Green, J. L. Spencer, G. A. F. Stone, C. A. Tsipis, *J. Chem. Soc., Dalton Trans.* **1977**, 1525.

[69] P. J. Murphy, J. L. Spencer, G. Procter, *Tetrahedron Lett.* **1990**, *31*, 1051.

[70] It has been reported that a catalytic amount of $Na^{(0)}$ might be necessary to achieve high levels of regioselectivity, see: R. T. Beresis, J. S. Solomon, M. G. Yang, N. F. Jain, J. S. Panek, *Org. Synth.* **2004**, *75*, 78.

[71] a) S. E. Denmark, Z. Wang, *Org. Lett.* **2001**, *3*, 1073. b) S. E. Denmark, Z. Wang, *Org. Synth.* **2005**, *81*, 54. c) S. E. Denmark, L. Neuville, M. E. L. Christy, S. A. Tymonko, *J. Org. Chem.* **2006**, *71*, 8500. d) S. E. Denmark, Z. Wang, *Org. Synth.* **2011**, *88*, 102.

[72] For earlier approach, see: a) K. Tamao, K. Kobayashi, Y. Ito, *Tetrahedron Lett.* **1989**, *30*, 6051. b) K. Takahashi, T. Minami, Y. Ohara, T. Hiyama, *Tetrahedron Lett.* **1993**, *34*, 8263. c) K. Takahashi, T. Minami, Y. Ohara, T. Hiyama, *Bull. Chem. Soc. Jpn.* **1995**, *68*, 2649. d) A. Mori, E. Takahisa, H. Kajiro, K. Hirabayashi, Y. Nishihara, T. Hiyama, *Chem. Lett.* **1998**, 443.

Table 1. Platinum-catalyzed hydrosilylation of 1-heptyne.

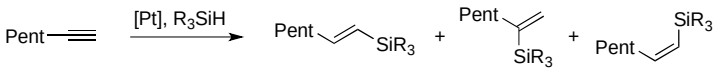

entry	catalyst	silane	yield	$E/\alpha/Z$
1	Speier	Cl(^{i}Pr)$_2$SiH	80 %	100:0:0
2	(0.1 mol%)	(HMe$_2$Si)$_2$O	100 %	84:16:0
3		(EtO)Et$_2$SiH	58 %	66:34:0
4[(a)]	Karstedt	Et$_3$SiH	—	89:0:11
5	(0.2–0.4 mol%)	Cl(^{i}Pr)$_2$SiH	—	dec
6		(HMe$_2$Si)$_2$O	100 %	85:15:0
7		(EtO)Et$_2$SiH	54 %	72:28:0
8	[Cy$_3$P(R$_3$Si)(μ-H)Pt]$_2$	Et$_3$SiH	97 %	95:5:0
9	(0.01 mol%)	Cl$_2$MeSiH	95 %	96:4:0
10		Cl$_3$SiH	93 %	96:4:0
11[(b)]		(EtO)$_3$SiH	83 %	82:18:0
12	(^{t}Bu$_3$P)Pt(dvtms)	Et$_3$SiH	95 %	98:0:2
13	(0.1 mol%)	(HMe$_2$Si)$_2$O	100 %	98:2:0
14		(EtO)$_3$SiH	52 %	—
15		(EtO)$_2$MeSiH	49 %	—
17		(EtO)Me$_2$SiH	55 %	92:8:0
18		Cl(^{i}Pr)$_2$SiH	—	dec

[a] 1-Pentyne was used. [b] 1-Butyne was used. This table is adapted from reference 53c, courtesy of Prof. Edward Anderson.

With the desire to address the shortcomings of the phosphine-based methodologies, Markó developed, since 1998, a whole family of platinum(0) carbene catalysts (see Chapter 2 and 3). These complexes are able to hydrosilylate terminal triple bonds with high activities, exquisite stereoselectivities and low catalyst loading, while tolerating a wide range of functional and protecting groups.

Regarding the hydrosilylation of phenylacetylene derivatives **1.125**, Alami reported an efficient protocol based upon a combination of platinum(II) chloride and the Buchwald ligand XPhos (Figure 31).[73] Despite high catalytic loadings, this system affords nearly perfect selectivities for a broad substrate scope (electron-rich and electron-poor aromatics) with various silanes, including alkoxysilanes. It is putatively admitted that platinum(II) is reduced in situ to the catalytically active platinum(0).

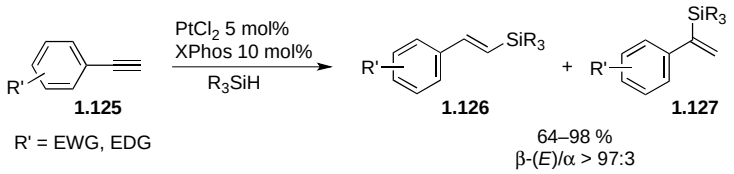

Figure 31. Hydrosilylation of phenylacetylenes with $PtCl_2$/XPhos.

Recently, Cook adapted the methodology of Alami to the hydrosilylation of propargylic alcohols **1.128** (Figure 32).[74] Strikingly, the catalytic loading was dramatically lowered and secondary as well as tertiary alcohols, possessing various substitution patterns, deliver one single isomer **1.129** when reacted with various silanes. Disappointingly, internal triple bonds could not be efficiently hydrosilylated using this protocol.

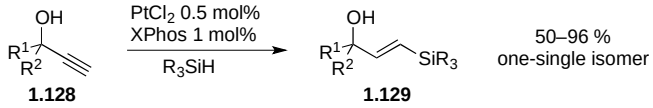

Figure 32. Hydrosilylation of propargylic alcohols with $PtCl_2$/XPhos.

[73] a) A. Hamze, O. Provot, J.-D. Brion, M. Alami, *Tetrahedron Lett.* **2008**, *49*, 2429. b) A. Hamze, O. Provot, J.-D. Brion, M. Alami, *J. Organomet. Chem.* **2008**, *693*, 2789.

[74] a) M. G. McLaughlin, M. J. Cook, *Chem. Comm.* **2011**, *47*, 11104. b) C. A. McAdam, M. G. McLaughlin, A. J. S. Johnston, J. Chen, M. W. Walter, M. J. Cook, *Org. Biomol. Chem.* **2013**, *11*, 4488.

The β-(*E*) vinylsilanes are not only accessible by platinum catalysis. For instance, Oshima[75] and Takeuchi[76] revealed that $Pd_2(dba)_3/Cy_3P$ and $[Rh(cod)_2]BF_4/2\ PPh_3$ complexes afford excellent results as well. Unfortunately, these catalysts are limited to the use of arylsilanes and trialkylsilanes, respectively. Nevertheless, the cationic rhodium catalyst has been used in the multi-gram scale hydrosilylation of propargyl alcohol for total synthesis purposes.[77]

Addressing the lower selectivities associated with alkoxysilanes, Mori and Hiyama established a brilliant catalytic system which affords both the β-(*E*) and the β-(*Z*) adducts, at will, simply by changing the order of addition of the reagents (Figure 33).[78]

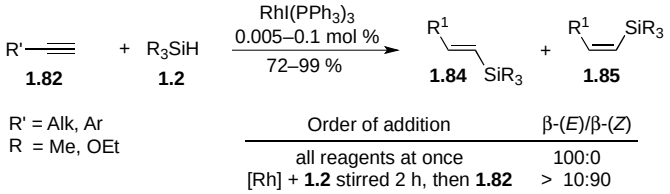

Figure 33. Mori–Hiyama stereodivergent hydrosilylation.

3.4.2 Preparation of β-(Z) Vinylsilanes

The metals of choice to reach β-(*Z*) vinylsilanes are rhodium, ruthenium and, to a lesser extent, iridium. The major achievements are reviewed in Table 2 (p 37).[79] Ojima discovered that the Wilkinson's catalyst

[75] D. Motoda, H. Shinokubo, K. Oshima, *Synlett* **2002**, 1529.
[76] R. Takeuchi, S. Nitta, D. Watanabe, *J. Org. Chem.* **1995**, *60*, 3045.
[77] a) J. Robichaud, F. Tremblay, *Org. Lett.* **2006**, *8*, 597. b) J. Hayashida, V. H. Rawal, *Angew. Chem. Int. Ed.* **2008**, *47*, 4373.
[78] a) A. Mori, E. Takahisa, H. Kajiro, Y. Nishihara, T. Hiyama, *Polyhedron* **2000**, *19*, 567. b) A. Mori, E. Takahisa, Y. Yamamura, T. Kato, A. P. Mudalige, H. Kajiro, K. Hirabayashi, Y. Nishihara, T. Hiyama, *Organometallics* **2004**, *23*, 1755.
[79] For other highlights of rhodium and ruthenium-based catalytic systems, see references 51c and 52d

produces the desired isomer (entry 1).[80] Unfortunately, this method is limited to the addition of triethylsilane to unhindered alkynes. Moreover, the reaction is capricious and isomerization between the β-(*Z*) and β-(*E*) isomers has been observed.[81] Twenty years later, Takeuchi described that the dimer $[Rh(cod)Cl]_2$ in ethanol or dimethylformamide is able to catalyze the apparent *anti* addition of triethylsilane to alkyl-substituted alkynes (entry 2).[82] However, Mori and Hiyama indicated that the arylacetylenes polymerize under these conditions.[78] Therefore, they used $RhI(PPh_3)_3$, activated with alkoxysilanes, to prepare β-(*Z*) vinylsilanes with excellent selectivities. This catalytic system displays a relatively broad substrate scope (entries 3,4; see also Figure 33).

As mentioned, ruthenium-based systems are also able to catalyze the hydrosilylation of alkynes, even if they require significantly higher catalytic loadings. Oro[83] and Ozawa[84] inaugurated this topic with encouraging results using arylsilanes. However five equivalents of the acetylenes were used and the substrate scope remains to be explored (entry 5). The best selectivities were obtained by Chang with the use of the dimer $[RuCl_2(p\text{-cymene})]_2$ (entries 6,7).[85] Although limited to the addition of triphenylsilane or triethylsilane, this catalytic system tolerates benzyl ethers, esters, chlorides and alcohols. Aryl- and alkyl-acetylenes could be hydrosilylated under these mild conditions in high yields. Notable exceptions are propargylic and homopropargylic –

[80] a) I. Ojima, M. Kumagai, Y. Nagai, *J. Organomet. Chem.* **1974**, *66,* C14. b) I. Ojima, N. Clos, R. J. Donovan, P. Ingallina, *Organometallics* **1990**, *9*, 3127.

[81] a) H. Watanabe, T. Kitahara, T. Motegi, Y. Nagai, *J. Organomet. Chem.* **1977**, *139*, 215. b) H. M. Dickers, R. N. Haszeldine, A. P. Mather, R. V. Parish, *J. Organomet. Chem.* **1978**, *161*, 91.

[82] R. Takeuchi, N. Tanouchi, *J. Chem. Soc. Perkin Trans. 1* **1994**, 2909.

[83] a) M. A. Esteruelas, J. Herrero, L. A. Oro, *Organometallics* **1993**, *12*, 2377. b) M. Martín, E. Sola, F. J. Lahoz, L. A. Oro, *Organometallics* **2002**, *21*, 4027.

[84] a) Y. Maruyama, K. Yamamura, I. Nakayama, K. Yoshiuchi, F. Ozawa, *J. Am. Chem. Soc.* **1998**, *120*, 1421. b) H. Katayama, K. Taniguchi, M. Kobayashi, T. Sagawa, T. Minami, F. Ozawa, *J. Organomet. Chem.* **2002**, *645*, 192.

[85] Y. Na, S. Chang, *Org. Lett.* **2000**, *2*, 1887.

but not bis-homopropargylic – alcohols, which afford the corresponding α vinylsilanes with high selectivities (see Section 3.4.3). Interestingly, these results are complementary to those obtained by Cook and his platinum catalyst (see Figure 32). It is worth mentioning that the simple protection of these alcohol functions as benzyl ethers reinstated the β-(*Z*) selectivity. Recently, some reports have indicated that 1st generation Grubbs metathesis catalyst triggers the hydrosilylation of alkynes, providing that there is no oxygen atom to direct the silicon group at the α position (entries 8,9).[86] Hence, organosilanes under solventless conditions afford interesting selectivities. However, shifting to triethoxysilane and/or using dichloromethane as the solvent unexpectedly lead to a complete reversal of regioselectivity in favor of the α vinylsilanes (see Section 3.4.3).

Recently, Oro has shown recently that a bis-NHC iridium(III) complex **1.130** was also a selective catalyst for the transformation of aryl- and alkylacetylenes into β-(*Z*) vinylsilanes (entries 10–12).[87] Although the catalyst loadings are high, especially considering the price of iridium, electron-rich and electron-poor phenylacetylene derivatives give the adducts with uniformly high selectivity levels (> 90:10:0) and with either alkyl- or arylsilanes.

It is worth noting that Faller has demonstrated that phenylacetylene could also be selectively hydrosilylated with triphenyl- and triethoxysilane with exquisite selectivities using $[Cp^*RhCl_2]_2$, though high catalytic loadings are required.[88] Unfortunately, this system has never been exemplified furthermore.

[86] a) C. S. Aricó, L. R. Cox, *Org. Biomol. Chem.* **2004**, *2*, 2558. b) S. V. Maifeld, M. N. Tran, D. Lee, *Tetrahedron Lett.* **2005**, *46*, 105.

[87] M. Iglesias, M. Pérez-Nicolás, P. J. S. Miguel, V. Polo, F. J. Fernández-Alvarez, J. J. Pérez-Torrente, L. A. Oro, *Chem. Commun.* **2012**, *48*, 9480.

[88] J. W. Faller, D. G. D'Alliessi, *Organometallics* **2002**, *21*, 1743.

Table 2. Rhodium- and ruthenium-catalyzed hydrosilylation of 1-hexyne.

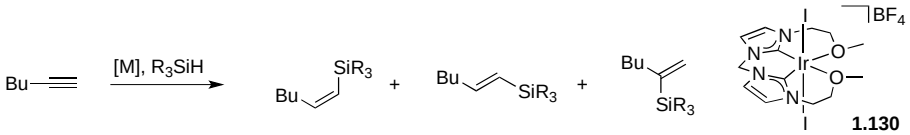

entry	catalyst	silane	yield	$Z/E/\alpha$
1	$RhCl(PPh_3)_3$ (0.01 mol%)	Et_3SiH	95 %	96:2:2
2	$[Rh(cod)Cl]_2$ (0.05 mol%)	Et_3SiH	85 %	94:4:2
3[a]	$RhI(PPh_3)_3$	$(Me_3SiO)Me_2SiH$	95 %	87:13:0
4[a]	(0.05–0.1 mol%)	$(EtO)_2MeSiH$	99 %	97:3:0
5[a],[b]	$Ru(SiMe_2Ph)Cl(CO)(P^iPr_3)_2$ (5 mol%)	$PhMe_2SiH$	98 %	91:9:0
6	$[RuCl_2(p\text{-cymene})]_2$	Et_3SiH	88 %	96:4:0
7	(5 mol%)	Ph_3SiH	98 %	98:2:0
8[c]	$Cl_2(PCy_3)_2Ru{=}CHPh$	Et_3SiH	86 %	90:0:10
9[c]	(1 mol%)	Ph_2MeSiH	75 %	74:5:21
10	**1.130**	Et_3SiH	86 %	85:15:0
11	(5 mol%)	$PhMe_2SiH$	82 %	73:27:0
12		Ph_2MeSiH	86 %	87:13:0

[a] 1-Octyne was used. [b] Five equivalents of alkyne were used. [c] Solventless.

3.4.3 Preparation of α Vinylsilanes

The hydrosilylation of alkynes to afford selectively the corresponding α vinylsilanes is a recent area of research dominated exclusively by ruthenium complexes. The leading results are presented in Table 3. In 2001, Trost and Ball paved the way using the cationic compound $[Cp^*Ru(MeCN)_3]^+$, which provides excellent yields and selectivities (entries 1–6).[58,62,89] It tolerates numerous functionalities, including: alcohols, silyl and benzyl ethers, ketones, enones, acetals, carboxylic acids, esters, halides and tertiary tosylamines. In addition to the silanes already included in Table 3 (p 40), this catalyst has been used successfully with allyl-, phenyl-, ethoxy- and (2-furanylmethyl)-dimethylsilane. Triisopropylsilane, though, is not accepted and α quaternary centers as well as 1,6-diynes – in contrast to 1,5- and 1,6-enynes – are unreactive under the reaction conditions. In 2002, Yamamoto reported that another pentamethylcyclopentadienyl ruthenium complex, $Cp^*RuH_3(PPh_3)$, produces α vinylsilanes starting from alkylacetylenes and chlorosilanes (entries 7–9).[90] The best results were obtained when dichloromethylsilane was employed; ester and ether functions were compatible. However, hydrosilylation with trialkylsilanes, or using arylacetylenes or alkynes bearing α quaternary centers as substrates, were sluggish and gave mixtures of stereoisomers.

While the Grubbs 1st generation metathesis catalyst usually affords the β-(*Z*) vinylsilanes selectively (see Section 3.4.2), Cox described that using triethoxysilane and alkylacetylenes switched the selectivity outcome in favor of the α isomers (entries 10–12).[86a] This combination appeared to be particularly effective if an oxygenated function, available for coordination, was present in the vicinity of the triple bond. Independently, Cossy and Dalko revealed that, by employing

[89] B. M. Trost, M. R. Machacek, Z. T. Ball, *Org. Lett.* **2003**, *5*, 1895.
[90] Y. Kawanami, Y. Sonoda, T. Mori, K. Yamamoto, *Org. Lett.* **2002**, *4*, 2825.

triphenylsilane in dichloromethane, nearly perfect yields and selectivities, also in favor of the α isomers, could be obtained using the Grubbs I catalyst.[91] Under these conditions, silyl ethers, esters, vinylogous esters and ynoates are well tolerated.

Finally, it is noteworthy that propargylic and, to a greater extend, homopropargylic alcohols **1.131** – but not bis-homopropargylic alcohols – are good stereo-directing groups. Indeed, they allow the smooth formation of α vinylsilanes **1.132** using a combination of $[RuCl_2(p\text{-cymene})]_2$ and triphenylsilane, albeit in relatively low yields (Figure 34). In the absence of these stereo-directing groups, this ruthenium catalyst affords the β-(*Z*) isomers in high yields and selectivities (see Section 3.4.2).

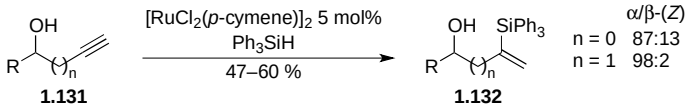

1.131 **1.132**

Figure 34. Propargylic and homopropargylic alcohols as stereo-directing groups.

[91] C. Menozzi, P. I. Dalko, J. Cossy, *J. Org. Chem.* **2005**, *70*, 10717.

Table 3. Ruthenium-catalyzed hydrosilylation of 1-alkynes.

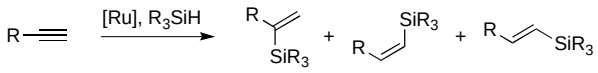

entry	catalyst	silane	yield	α/(*Z*/*E*)
1[a]	$[Cp^*Ru(MeCN)_3]PF_6$	Et_3SiH	86 %	>95:(5)
2[b]	(1 mol%)	$BnMe_2SiH$	100 %	>95:(5)
3[a]		$(EtO)_2MeSiH$	88 %	93:(7)
4[a]		$(EtO)_3SiH$	86 %	90:(10)
5[a]		$ClMe_2SiH$	67 %	n.d.[c]
6[a]		Et_2SiH_2	<10 %	—
7[d]	$Cp^*RuH_3(PPh_3)$	Cl_2MeSiH	89 %	89:10:1
8[d]	(3 mol%)	$ClMe_2SiH$	65 %	85:13:2
9[d]		Cl_3SiH	79 %	69:16:15
10[e]	$Cl_2(PCy_3)_2Ru=CHPh$	$(EtO)_3SiH$	>90 %	73:17:10
11[e]	(2.5 mol%)	Et_3SiH	86 %	9:91:0
12[e]		$PhMe_2SiH$	87 %	24:69:7
13[f]	(5 mol%)	Ph_3SiH	98 %	97:3:0
14[f]		$(EtO)_3SiH$	76 %	86:7:7
15[f]		Et_3SiH	86 %	77:20:3
16[f]		(2-thiophenyl)Me_2SiH	80 %	58:21:21
17[f]		$EtMe_2SiH$	70 %	56:26:18
18[f]		$^tBuMe_2SiH$	75 %	30:70:0
19[f]		$^iPr_3SiH$	0 %	—

[a] 5-Acetoxypentyne was used. [b] Methyl 10-undecynoate was used. [c] Not determined but subsequent reactions afforded one single stereoisomer originating from the α vinylsilane. [d] 1-Heptyne was used. [e] 1-Decyne was used in toluene. [f] 4-(*tert*-Butyldimethylsilyloxy)butyne was used in dichloromethane.

3.4.4 Hydrosilylation of Internal Alkynes

The selective hydrosilylation of internal C–C triple bonds is an important endeavor which attracted major interests in the recent years. Undeniably, achieving the stereocontroled synthesis of trisubstituted vinylsilanes opens the door to a myriad of useful synthetic building blocks, including geometrically defined trisubstituted olefins. This section will only consider unsymmetrical alkynes, due to the lack of difficulty and the limited utility of symmetrical ones.[92]

It is interesting to mention that Trost and Ball implemented a useful strategy for the reduction of alkynes **1.86** to (*E*) alkenes **1.134** based upon an *anti* hydrosilylation–protodesilylation sequence (Figure 35).[93] This approach is notably milder and more chemoselective than a Birch-type reduction. Obviously, this methodology does not require the control of the regioselectivity of the silane addition and could be extended to the synthesis of (*Z*) olefins using *syn* selective catalysts. Recently, Plietker accomplished a similar transformation affording either (*E*) or (*Z*) styrene derivatives.[94]

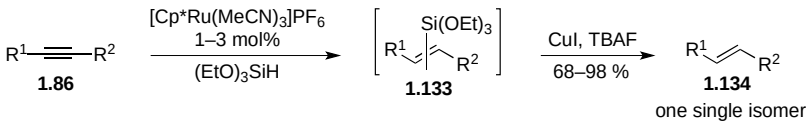

Figure 35. Synthesis of (*E*)-alkenes by *anti* hydrosilylation–protodesilylation.

3.4.4.1 Steric Differentiation

Due to the inherent cylindrical shape of carbon–carbon triple bonds, it is particularly challenging for an organometallic complex to differentiate between each end of these unsaturations, in the absence of electronic

[92] For more information about this topic, see reference 51.
[93] B. M. Trost, Z. T. Ball, T. Jöge, *J. Am. Chem. Soc.* **2002**, *124*, 7922.
[94] C. Belger, B. Plietker, *Chem. Commun.* **2012**, *48*, 5419.

bias, stereo-directing groups or steric effects. Nevertheless, in 1995, Molander showed that an yttrium compound was able to discriminate between the two sp-hybridized carbons of an alkyne substituted on one end by a linear alkyl group and on the other by a branched alkyl chain. The hydrosilylation afforded a single isomer **1.136** via a stereospecific *syn* addition (Figure 36).[95] Even if this approach is limited to the addition of phenylsilane, it tolerates silyl, tetrahydropyranyl and trityl protected alcohols, as well as tertiary amines. The presence of a tertiary propargylic carbon also leads to one isomer, albeit in low yield (23 %).

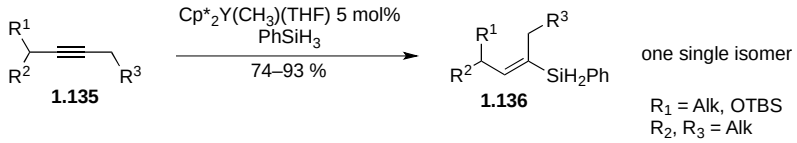

Figure 36. Molander hydrosilylation of internal alkynes.

Remarkably, this catalytic system also distinguishes between a methyl and an *n*-hexyl or a 2-methylbutyl group (Table 4, entries 1–3). Loss of selectivity only arises when a linear alkyl chain faces another one substituent branched at the position 3 (alkyne numbering) (entries 4,5).

Since Molander's tour de force, no other studies have competed with these superb results. Nowadays, Markó's platinum(0) complexes are also able to catalyze the selective hydrosilylation of internal alkynes based upon steric discrimination (see Chapter 2 and 3). Interestingly, various silanes can be successfully engaged as reaction partners and a *tert*-butyl substituent on the alkyne is perfectly tolerated, making both methodologies highly complementary.

[95] G. A. Molander, W. H. Retsch, *Organometallics* **1995**, *14*, 4570.

Table 4. Molander hydrosilylation of internal alkynes with $Cp^*_2Y(CH_3)(THF)$.

entry	substrate	major product	yield	β/α
1	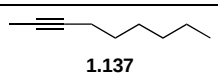 **1.137**	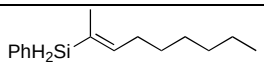 **1.138**	81 %	4.1:1
2[a]			n.d.	7.2:1
3	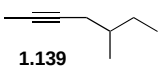 **1.139**	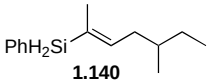 **1.140**	40 %	7.3:1
4	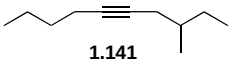 **1.141**	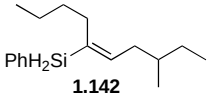 **1.142**	73 %	1:1
5	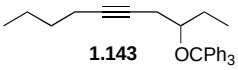 **1.143**	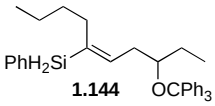 **1.144**	64 %	2.5:1

[a] $Cp^*_2YbCH(TMS)_2$ was used as catalyst.

It is interesting to point out that Montgomery carried out preliminary experiments using *N*-heterocyclic nickel(0) catalysts.[96] Despite the encouraging results obtained, this system deserves further work to delineate its possibilities and compare it properly to the existing methods.

3.4.4.2 Electronic Differentiation

In 2003, Trost and Ball discovered that $[Cp^*Ru(MeCN)_3]PF_6$ promotes the *anti* addition of silanes to internal propargylic alcohols **1.145**, positioning selectively the silicon group onto the β carbon of the triple bond (see Section 3.3.3) (Figure 37).[64,97] A stereo-directing effect of the proximal hydroxyl group by coordination was ruled out because terminal propargylic alcohols afford the opposite regioisomer.[60] Unfortunately, triethoxysilane leads to unstable vinylsilanes, therefore

[96] M. R. Chaulagain, G. M. Mahandru, J. Montgomery, *Tetrahedron* **2006**, *62*, 7560.

[97] B. M. Trost, Z. T. Ball, T. Jöge, *Angew. Chem. Int. Ed.* **2003**, *42*, 3415.

benzyldimethylsilane, triethylsilane and ethoxydimethylsilane were used: the latter being employed in only one example. This catalytic system tolerates numerous functional groups (see Section 3.4.3) and proved to accept substantial steric bulk, even for α-branched R^2 groups. Regarding homo- and bis-homopropargylic alcohols, lower selectivities were achieved, the remote inductive effect being too weak. The use of silicon tethers was very successful to solve this problem (see Section 3.4.4.4).

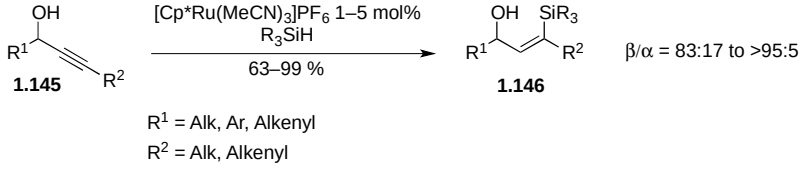

Figure 37. Trost–Ball hydrosilylation of propargylic alcohols.

Remarkably, starting from optically enriched propargylic alcohols **1.147**, Ru-catalyzed hydrosilylation reaction, followed by a Tamao–Kumada oxidation, furnishes stereocontrolled aldol adducts **1.149**. This synthetic pathway, which could be performed as a one-pot process, corresponds to the addition of methyl ketone enolates to aldehydes, a challenge in asymmetric synthesis (Figure 38).[97] This oxidation strategy has been extended to the synthesis of *syn* α,β-dihydroxy ketones **1.151**, through the introduction of an epoxidation step consecutive to the hydrosilylation reaction.[98]

[98] B. M. Trost, Z. T. Ball, K. M. Laemmerhold, *J. Am. Chem. Soc.* **2005**, *127*, 10028.

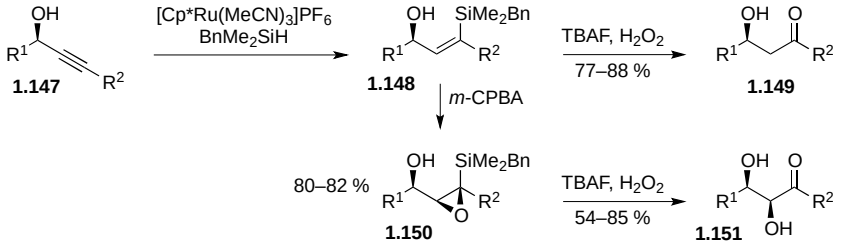

Figure 38. Formal stereocontrolled synthesis of aldol products.

Recently, Ferreira used the same electronic differentiation in propargylic alcohols **1.152**, to accomplish their *syn* hydrosilylation under platinum(0) catalysis, with a regioselectivity opposite to the method of Trost and Ball (Figure 39).[99] This complementary selectivity is attributed to a Chalk–Harrod mechanism, in which the hydride is introduced onto the most electron-poor position. Accordingly, as he was extending this strategy to various substrates, Ferreira was able to correlate the levels of selectivity to the ^{13}C chemical shifts of the sp-hybridized carbon atoms of the substrates, though steric effects also have a substantial influence. Furthermore, this approach is not limited to the addition of triethylsilane and bis(trimethylsilyloxy)methylsilane could also be employed. The hydroxyl group can be replaced by an acetoxy or a trifluoroacetoxy substituent. Finally, homopropargylic derivatives have been evaluated with some success.

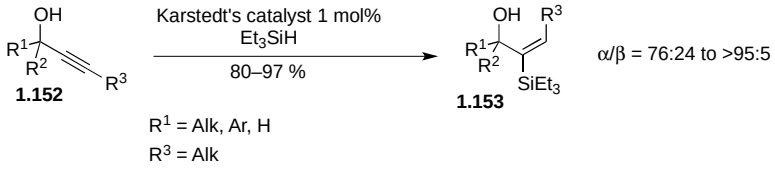

Figure 39. Platinum catalyzed hydrosilylation of propargylic alcohols.

Expectedly, in this strategy, increasing the electronegativity of the directing group increases the regioselectivity. Indeed, after the propargylic alcohols, Trost and Ball rapidly realized that α,β-alkynyl

[99] D. A. Rooke, E. M. Ferreira, *Angew. Chem. Int. Ed.* **2012**, *51*, 3225.

carbonyl compounds **1.154** are excellent substrates for their ruthenium catalyst. Usually, the β-silyl adducts **1.155** are obtained with selectivities above 95:5 (Figure 40).[100] It should be noted that these molecules are also accessible via the addition of stoichiometric silylcuprate reagents.[11] However, this approach is less functional group tolerant, little atom-economical and usually limited to the introduction of a $SiMe_2Ph$ group.

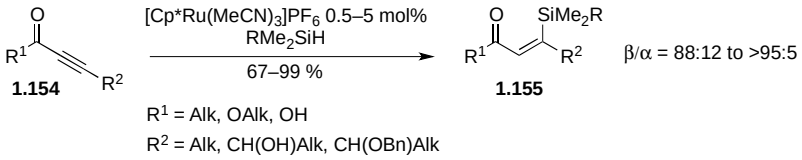

Figure 40. Trost–Ball hydrosilylation of α,β-alkynyl carbonyl compounds.

Subsequently, a protocol for the intramolecular delivery of the R substituent of the silyl group in **1.156**, followed by an oxidation, has been implemented (Figure 41). This process, leading to aldol compounds **1.157** containing tertiary alcohol groups, proved to be diastereoselective when R^2 was chiral.[100]

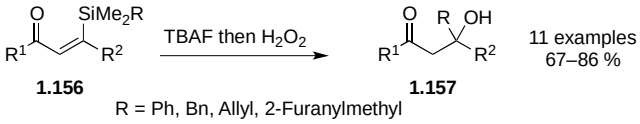

Figure 41. Geminal alkylation–oxidation of 1.156.

Ferreira also explored the use of carbonyl functions as directing groups for platinum-catalyzed hydrosilylation of α,β-alkynyl carbonyl compounds **1.158** (Figure 42).[99,101] While nearly perfect selectivities could occasionally be obtained, the results were particularly dependent upon the electronic effect of the other substituent.

[100] B. M. Trost, Z. T. Ball, *J. Am. Chem. Soc.* **2004**, *126*, 13942.
[101] D. A. Rooke, E. M. Ferreira, *J. Am. Chem. Soc.* **2010**, *132*, 11926.

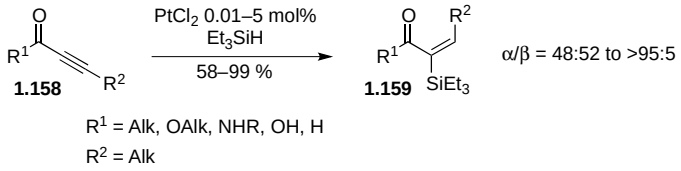

Figure 42. Platinum-catalyzed hydrosilylation of α,β-alkynyl carbonyl compounds.

Shortly after Ferreira, Sumida and Hosoya undertook a catalyst screening, which revealed that a combination of $Pd_2(dba)_3$ and tricyclohexylphosphine promotes the *syn* addition of various silanes to alkynes **1.160** bearing diverse electron-withdrawing groups.[102] This catalytic cocktail, previously proposed by Oshima (see Section 3.4.1),[75] affords the corresponding α vinylsilanes **1.161** as the sole products in outstanding yields. Interestingly, a large number of silanes, including alkoxysilanes, performed well under these conditions. However, to ensure reproducible results, it was crucial to use only 1 equivalent or less of the silane in order to avoid E/Z isomerization.

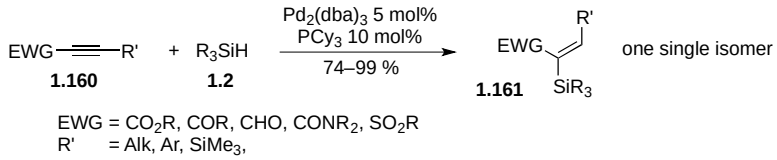

Figure 43. Palladium-catalyzed hydrosilylation of internal alkynes.

In 2009, Konno demonstrated that the dinuclear complex $Co_2(CO)_8$ catalyzes the *syn* addition of triethylsilane across the triple bond of **1.162**, substituted by fluoroalkyl chains, with good to excellent yields and stereoselectivities (Figure 44).[103] Phenyldimethylsilane and triethoxysilane also react smoothly but give very poor selectivities. Finally, triisopropylsilane and triphenylsilane are unreactive.

[102] Y. Sumida, T. Kato, S. Yoshida, T. Hosoya, *Org. Lett.* **2012**, *14*, 1552.
[103] T. Konno, K.-i. Taku, S. Yamada, K. Moriyasu, T. Ishihara, *Org. Biomol. Chem.* **2009**, *7*, 1167.

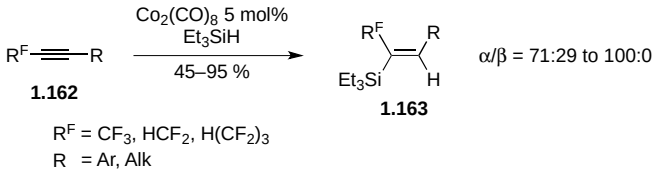

Figure 44. Hydrosilylation of internal fluoroalkyl-acetylenes.

When secondary propargylic alcohol substituents were present in the substrates, the yields and selectivities of the reaction were dramatically improved (Figure 45). However, tertiary propargylic alcohols were not tolerated. Interestingly, phenyldimethylsilane was also a good substrate (93 %, α/β = 92:8), though in only one reported example.

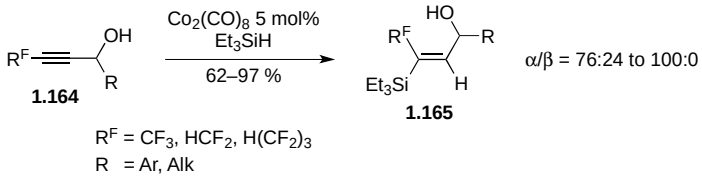

Figure 45. Hydrosilylation of fluoroalkyl propargylic alcohols.

Finally, Alami applied the same electronic discrimination principle to the platinum oxide catalyzed transformation of arylacetylenes **1.166** (Figure 46).[104] Useful selectivities were obtained while numerous functional groups were tolerated on the aromatic ring as well as various organo- and alkoxysilanes. Intriguingly, *ortho* substitution leads systematically to higher levels of regioselectivity than *para* substitution, for the same electron-withdrawing or electron-donating substituent. This "ortho effect" has not been rationalized.

[104] a) A. Hamze, O. Provot, M. Alami, J.-D. Brion, *Org. Lett.* **2005**, *7*, 5625. b) A. Hamze, O. Provot, J.-D. Brion, M. Alami, *Synlett* **2007**, 2025.

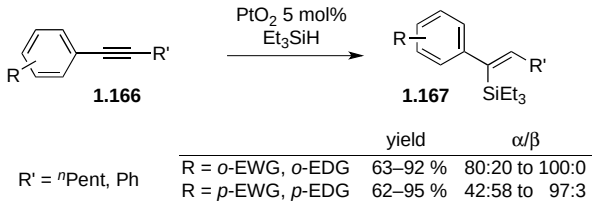

Figure 46. Hydrosilylation of arylacetylenes.

3.4.4.3 Dimethylvinylsilyl Ethers as Stereo-Directing Groups

In 2011, Tomooka studied an elegant strategy to achieve the stereoselective hydrosilylation of propargylic, homopropargylic and bishomopropargylic alcohols.[105] This approach is based upon two properties of the Karstedt's catalyst: (i) alkynes, even internal, are hydrosilylated faster then alkenes, because of their higher π-acidity and (ii) platinum(0) binds strongly to vinylsilanes (see Chapter 2). Therefore, Tomooka selected dimethylvinylsilyl ethers as temporary stereo-directing groups (Figure 47). Rewardingly, the silyl portions of the silanes were directed onto the proximal carbon atoms to afford the corresponding vinylsilanes **1.169** as the sole products in the case of propargylic and homopropargylic alcohols. An electronic effect was ruled out since replacement of the silyl ether group by other electronically similar functions leads to severe erosion of the selectivity. Various silanes were tolerated, including the bulky triisopropylsilane, halogeno- and alkoxysilanes.

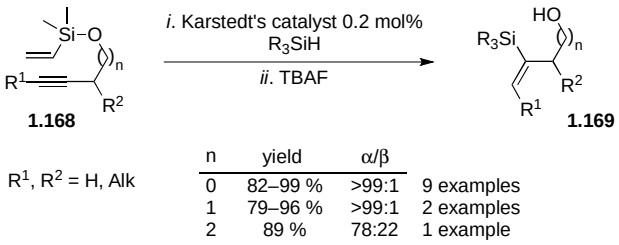

Figure 47. Dimethylvinylsilyl ethers as stereo-directing groups.

[105] Y. Kawasaki, Y. Ishikawa, K. Igawa, K. Tomooka, *J. Am. Chem. Soc.* **2011**, *133*, 20712.

3.4.4.4 Silicon Tethers for Intramolecular Hydrosilylation

Initiated by Tamao in 1988,[62a] the use of silicon tethers for the intramolecular hydrosilylation of internal alkynes has mainly been developed by Marshall and Denmark. Initially, they both reported that platinum (Speier or Karstedt catalysts) could efficiently trigger the intramolecular *syn* exo-dig hydrosilylation of homopropargylic hydridosilyl ethers **1.170** (Figure 48).[62b,c] Single stereoisomers **1.171** were obtained in good yields and submitted to Tamao–Kumada oxidation to afford stereodefined aldol products. Hiyama cross-coupling afforded tri-substituted olefins.

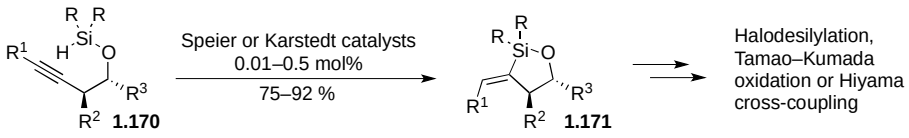

Figure 48. *Syn* exo-dig hydrosilylation of homopropargylic hydridosilyl ethers.

Rapidly afterward, Denmark completed this approach with the achievement of an *anti* exo-dig hydrosilylation, using a ruthenium dimer catalyst (Figure 49).[106] Unfortunately, only two examples were reported.

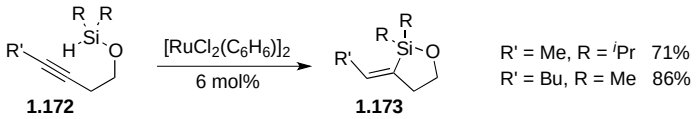

Figure 49. *Anti* exo-dig hydrosilylation of homopropargylic hydridosilyl ethers.

The application of this strategy to propargylic alcohols was plagued by the instability of the resulting oxasilacyclobutane ring. Nevertheless, Denmark rapidly overcame this limitation through the introduction of a longer tether group, a disiloxane chain (Figure 50).[107] Whilst again limited to only two examples, a *syn* and an *anti* exo-dig addition, the

[106] S. E. Denmark, W. Pan, *Org. Lett.* **2002**, *4*, 4163.
[107] S. E. Denmark, W. Pan, *Org. Lett.* **2003**, *5*, 1119.

resulting polymeric vinylsilanes **1.175** and **1.176** were successfully submitted to a consecutive Hiyama cross-coupling with various aryl iodide partners.

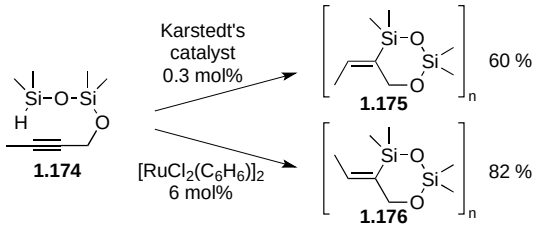

Figure 50. ***Syn*** **and** ***anti*** **exo-dig hydrosilylation of propargylic hydridosilyl ethers.**

Finally, Trost and Ball found the missing piece of the puzzle: the *anti* endo-dig hydrosilylation of homopropargylic and bis-homopropargylic alcohol hydridosilyl ethers **1.177** using $[Cp^*Ru(MeCN)_3]PF_6$ (Figure 51).[61,98] This approach is perfectly complementary to the *syn* and *anti* exo-dig additions of Tamao, Marshall and Denmark (vide supra). Together, these silicon-tethered tactics are completing the electronically directed intermolecular hydrosilylation of propargylic alcohols (see Section 3.4.4.2). Furthermore, as for β-silyl allylic alcohols, Trost and Ball established an oxidative methodology leading to either homo- or bis-homo aldol products **1.179** and **1.181**, with or without an α-hydroxy group. Gratifyingly, depending upon the substitution patterns of the starting hydridosilyl ethers **1.177**, the resulting products were prepared with good to perfect diastereoselectivities.

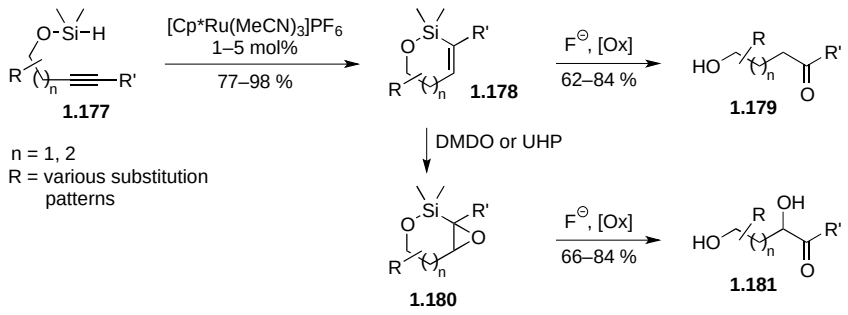

Figure 51. ***Anti*** **endo-dig hydrosilylation of dimethylsilyl ethers.**

3.5 Remaining Challenges in Alkynes Hydrosilylation

Prodigious progress has been made in the hydrosilylation of carbon–carbon triple bonds in the last decade, particularly for internal substrates. Nevertheless, there is still room for improvement:

- As for olefin hydrosilylation, the hydrosilylation of alkynes is mostly based upon noble metals and would benefit from the development of low-cost catalysts for economic reasons.
- Catalytic loadings of ruthenium-based hydrosilylation should be diminished to the range of their platinum and rhodium counterparts, by improving their turnover numbers.
- In general, the substrate scopes of catalysts selective for β-(*Z*) vinylsilanes are not thoroughly delineated. Furthermore, the range of compatible silanes should be extended, notably toward heteroatom-substituted silanes. Nevertheless, the advent of masked silanols offers an alternative.[108]
- No catalyst has been reported to promote the *anti* regioselective hydrosilylation of internal alkynes, using a steric discrimination approach. Moreover, the very selective system reported by Molander for the *syn* addition is limited to the sole condensation of phenylsilane.
- The electronic discrimination strategy for the hydrosilylation of internal alkynes should be pursued and the development of catalysts more sensitive to these inductive effects is a valuable research theme.

[108] For more information, see reference 89a and: a) J. C. Anderson, R. H. Munday, *J. Org. Chem.* **2004**, *69*, 8971. b) K. Itami, T. Nakami, J. Yoshida, *J. Am. Chem. Soc.* **2001**, *123*, 5600. c) K. Hosoi, K. Nozaki, T. Hiyama, *Chem. Lett.* **2002**, 138.

In order to face these challenges, it is particularly important to undertake in-depth mechanistic studies. Indeed, most of the proposed pathways described in the literature are merely speculative and based upon alkene hydrosilylation catalytic cycles. Therefore, thorough mechanistic studies, including deactivation pathways, are needed to guide the development of new catalytic systems.

4. Conclusions

Since 1947, the hydrosilylation of carbon–carbon multiple bonds has grown from a laboratory curiosity to the heart of the silicone industry, together with the Rochow–Müller process. Among all the methods available to promote this reaction, transition metal catalysis is the most used and studied. Numerous metals (e.g. Rh, Ru, Ir, Co, Ni, Pd,…) have been introduced for this purpose.

Concerning alkenes hydrosilylation, platinum is particularly effective for the synthesis of linear or tethered alkylsilanes with excellent selectivities, low catalyst loadings and high functional group compatibility (see Sections 2.4.1 and 2.4.4.3, Chapters 2 and 3). On the other hand, palladium and rhodium enable the enantioselective synthesis of branched alkyl silanes (see Sections 2.4.4.1 and 2.4.4.2).

Regarding alkynes hydrosilylation, platinum is ideal for the preparation of β-(*E*) vinylsilanes (see Section 3.4.1, Chapters 2 and 3), while rhodium and ruthenium share the first place to access the β-(*Z*) isomer (see Section 3.4.2). However, the α vinylsilanes are best produced under ruthenium catalysis (see Section 3.4.3). The challenging hydrosilylation of internal alkynes is dominated by yttrium and platinum, for steric differentiation (see Section 3.4.4.1); and by platinum and ruthenium, for electronic discrimination as well as silicon-tethered tactics (see Sections 3.4.4.2 and 3.4.4.4). The importance of the complementarity of each pair of metal for these applications cannot be understated.

Nowadays, hydrosilylation is considered as a powerful and atom-economical tool. Hence, it is more and more implemented as a platform for the development of synthetic methodologies and strategies, taking advantage of the richness and versatility of organosilicon chemistry. Accordingly, in the very recent years, there has been an explosion in the number of natural product total syntheses in which hydrosilylation plays a pivotal role.[109]

[109] For selected examples, see reference 95 and: a) S. Diethelm, E. M. Carreira, *J. Am. Chem. Soc.* **2013**, *135*, 8500. b) Y. Sridhar, P. Srihari, *Eur. J. Org. Chem.* **2013**, 578. c) B. M. Trost, M. J. Bartlett, *Org. Lett.* **2012**, *14*, 1322. d) A. ElMarrouni, R. Lebeuf, J. Gebauer, M. Heras, S. Arseniyadis, J. Cossy, *Org. Lett.* **2012**, *14*, 314. e) D. J. Clausen, S. Wan, P. E. Floreancig, *Angew. Chem. Int. Ed.* **2011**, *50*, 5178. f) K. Lehr, R. Mariz, L. Leseurre, B. Gabor, A. Fürstner, *Angew. Chem. Int. Ed.* **2011**, *50*, 11373. g) D. Gallenkamp, A. Fürstner, *J. Am. Chem. Soc.* **2011**, *133*, 9232. h) Y. Cui, W. Tu, P. E. Floreancig, *Tetrahedron* **2010**, *66*, 4867. i) B. M. Trost, J. D. Sieber, W. Qian, R. Dhawan, Z. T. Ball, *Angew. Chem. Int. Ed.* **2009**, *48*, 5478. j) C. Bressy, J.-P. Vors, S. Hillebrand, S. Arseniyadis, J. Cossy, *Angew. Chem. Int. Ed.* **2008**, *47*, 10137. k) C. Rodriguez-Escrich, F. Urpí, J. Vilarrasa, *Org. Lett.* **2008**, *10*, 5191. l) S. Y. F. Mak, N. R. Curtis, A. N. Payne, M. S. Congreve, A. J. Wildsmith, C. L. Francis, J. E. Davies, S. I. Pascu, J. W. Burton, A. B. Holmes, *Chem. Eur. J.* **2008**, *14*, 2867. m) A. Fürstner, M. Bonnekessel, J. T. Blank, K. Radkowski, G. Seidel, F. Lacombe, B. Gabor, R. Mynott, *Chem. Eur. J.* **2007**, *13*, 8762. n) E. O. Onyango, J. Tsurumoto, N. Imai, K. Takahashi, J. Ishihara, S. Hatakeyama, *Angew. Chem. Int. Ed.* **2007**, *46*, 6703. o) S. A. Burova, F. E. McDonald, *J. Am. Chem. Soc.* **2004**, *126*, 2495. p) J. A. Marshall, K. C. Ellis, *Org. Lett.* **2003**, *5*, 1729. q) S. A. Kozmin, *Org. Lett.* **2001**, *3*, 755. r) J. A. Marshall, M. M. Yanik, *J. Org. Chem.* **2001**, *66,* 1373. s) R. A. Robinson, J. S. Clark, A. B. Holmes, *J. Am. Chem. Soc.* **1993**, *115*, 10400. t) G. D. Annis, L. A. Paquette, *J. Am. Chem. Soc.* **1982**, *104*, 4504.

Chapter 2

Hydrosilylation and Platinum *N*-Heterocyclic Carbene Complexes

This chapter describes how the use of *N*-heterocyclic carbenes has enabled the research group of the Author to discover unique platinum(0) catalysts for the hydrosilylation of unsaturated carbon–carbon bonds.[1] It will provide the Reader with (i) the background knowledge required for the proper understanding of the Chapter 3 and (ii) the state of the art prior to the beginning of this Ph.D. thesis.

Independently, a similar strategy has been explored by Elsevier.[2] NHC platinum(0) complexes have also been used as hydroboration and diboration catalysts as well as precursors of platinum(II) carbene complex.[3] Supported platinum carbene complexes on meso-porous

[1] Part of this chapter has been accepted for publication in: Dierick, S.; Markó, I. E. In *N-Heterocyclic Carbenes. Effective Tools for Organometallic Synthesis*; Nolan, S. P. Ed.; Wiley, *In press*.

[2] (a) J. W. Sprengers, M. J. Mars, M. A. Duin, K. J. Cavell, C. J. Elsevier, *J. Organomet. Chem.* **2003**, *679*, 149. (b) J. W. Sprengers, M. de Greef, M. A. Duin, C. J. Elsevier, *Eur. J. Inorg. Chem.* **2003**, 3811. (c) J. W. Sprengers, M. J. Agerbeek, C. J., Elsevier, H. Kooijman, A. L. Spek, *Organometallics* **2004**, *23*, 3117.

[3] For a review, see: a) S. Dierick, I. E. Markó, Platinum [1,3-bis[2,6-bis(1-methylethyl)-phenyl]-1,3-dihydro-2*H*-imidazol-2-ylidene][1,3-bis(η²-ethenyl)-1,1,3,3-tetramethyldisiloxane], in *e-EROS Encyclopedia of Reagents for Organic Synthesis*, Wiley-VCH. 2013. For the original contributions, see: b) V. Lillo, J. Mata, J. Ramírez, E. Peris, E., Fernandez, *Organometallics* **2006**,

cross-linked polystyrene particles, precipitated silica and porous glass beads have been reported as well as their application in hydrosilylation.[4] Hydrosoluble analogs have also been prepared.[5] They will not be discussed here.

1. Introduction

Though thermodynamically favored, hydrosilylation must be catalyzed in order to be operative (see Chapter 1). Various methods have been explored to this end but the most effective processes use transition metal-based homogeneous catalysis. For decades, the Speier catalyst, i.e., hexachloroplatinic acid in isopropanol, has been widely used for hydrosilylation. In 1973, Karstedt described a platinum catalyst obtained from the reaction of hexachloroplatinic acid with 1,3-divinyltetramethyldisiloxane.[6] Whilst the structure of this catalyst remained unclear for several years,[7] its popularity grew for a number of reasons, two of which are its shorter induction period and its higher activity. Gradually, it replaced Speier's catalyst in industrial and academic applications. Nowadays, the Karstedt complex (**2.1**) is an indispensable tool for hydrosilylation and the standard against which every new catalyst is compared (Figure 1). Despite this success, several drawbacks still persist. Most noteworthy amongst them are that this promoter is not completely selective and affords, in the case of olefins, undesired side products, such as isomerized and reduced starting

25, 5829. c) V. Lillo, J. A. Mata, A. M. Segarra, E. Peris, E., Fernandez, *Chem. Commun.* **2007**, 2184. d) D. Brissy, M. Skander, P. Retailleau, A. Marinetti, *Organometallics* **2007**, *26*, 5782.

4 a) Y. Zhang, L. Zhao, P. K. Patra, J. Y. Ying, *Adv. Synth. Catal.* **2008**, *350*, 662. b) G. L. Larson, B. C. Arkles, R. A. Cameron, (2010) US Patent 2010/0280266.

5 G. F. Silbestri, J. C. Flores, E. de Jesús, *Organometallics* **2012**, *31*, 3355.

6 B. D. Karstedt, (1973) US Patent 3,775,452.

7 For a review about the elucidation of the Karstedt's catalyst structure, see: L. N. Lewis, J. Stein, Y. Gao, R. E. Colborn, G. Hutchins, *Platinum Metals Rev.* **1997**, *41*, 66.

materials (see Section 2). The hydrosilylation of alkynes catalyzed by Karstedt complex (**2.1**), usually affords mixtures of regioisomeric vinyl silanes (see Chapter 1). Furthermore, Karstedt catalyst is not stable under the reaction conditions and produces platinum colloids that can taint the final product.

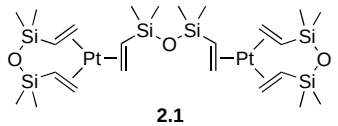

2.1

Figure 1. Structure of the Karstedt's complex.

2. Hydrosilylation of Alkenes, the Beginning

Our interest in the hydrosilylation reaction began with a partnership with Rhodia Silicones in the late nineties.[8] Their benchmark reaction for testing new catalysts was the hydrosilylation of 1-octene (**2.2**) with bis(trimethylsilyloxy)methylsilane (MD'M) (**2.3**) in hot xylene (Figure 2). While 1-octene is a representative olefin, MD'M is a cheap silane mimicking the linkage of siloxane polymers (Si–O–Si). Under these conditions, the Karstedt catalyst produces various side products, among which the isomerized olefin **2.5** and *n*-octane (**2.6**) are preponderant. Moreover, the reaction medium usually turns yellow due to the presence of colloidal platinum species.[9]

[8] In 2007, Rhodia Silicones was acquired by the China National Bluestar Corporation and renamed Bluestar Silicones.

[9] Platinum colloids can be detected by dynamic light scattering or by UV-visible spectroscopy.

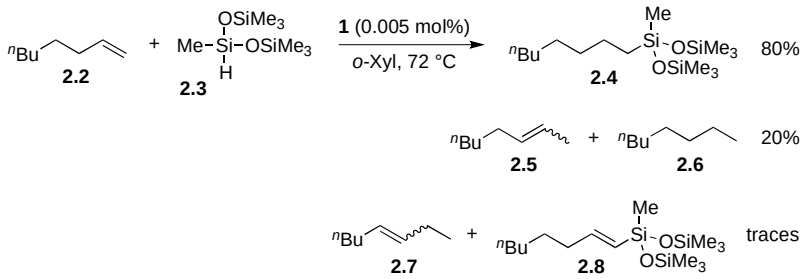

Figure 2. Benchmark reaction for new hydrosilylation catalysts.

Karstedt catalyst is known to follow the general mechanism described by Chalk and Harrod (Figure 3).[10] According to this mechanism, oxidative addition of the platinum(0) species **A** into the silicon–hydrogen bond of **2.9** followed by coordination of the alkene **2.10**, affords the key intermediate **C**. 1,2-Migratory insertion of the terminal double bond can produce two regio-isomers, i.e., **D** and **D'**. The major regioisomer, **D**, undergoes an irreversible reductive elimination to produce the desired silane **2.11** and regenerates the catalytic active platinum species **A**. On the other hand, the minor regioisomer **D'** suffers a rapid β-hydride elimination and, after dissociation, produces the isomerized olefin **2.12** and the platinum(II) intermediate **B**. In addition, colloidal Pt species, generated in situ from ligandless platinum, appear to be responsible for the hydrogenation of the olefins present in the reaction mixture.

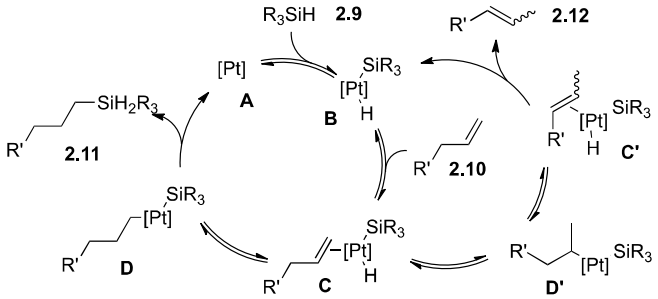

Figure 3. Chalk and Harrod mechanism.

[10] A. J. Chalk, J. F. Harrod, *J. Am. Chem. Soc.* **1965**, *87*, 16.

With these mechanistic insights in mind, we recognized that the introduction of a sterically demanding and strongly binding ancillary ligand onto the Karstedt complex (**2.1**) could give rise to a new generation of platinum catalysts with improved properties. Indeed, increasing the steric hindrance around the metal should enhance the propensity of platinum to add on the less hindered side of the olefin, resulting in a decrease in the amount of isomerized alkenes. Furthermore, a strong metal–ligand bond with high dissociation energy should prevent the formation of platinum colloids and thus suppress the reduction of the alkenes.

3. Initial Results with Phosphine Ligands

At the onset of our investigations, phosphines were selected as the ancillary ligand because of their long and successful history in this field. Therefore, addition of different phosphines to Karstedt complex (**2.1**) afforded the corresponding monophosphine platinum(0) complexes **2.13** bearing one dvtms ligand (Table 1, p 60).[11]

The reactivity of these new compounds **2.13** was compared to that of the Karstedt catalyst (**2.1**) using the benchmark hydrosilylation (see Figure 2). In all cases, they proved to be slightly less active than their parent complex, the least reactive being the tri(2-furyl)phosphine derivative **2.13c** (Figure 4a, p 60). Interestingly, it transpired from these experiments that the less active the catalyst, the better the selectivity. As can be seen from Figure 4b, the amount of isomerized material increases initially before decreasing gradually. One notable exception entails the use of complex **2.13c**. The lowering of isomerized products is concomitant with the appearance of *n*-octane and Pt-colloids in the reaction medium and supports the proposal that colloidal platinum

[11] I. E. Markó, S. Stérin, O. Buisine, G. Mignani, P. Branlard, B. Tinant, J.-P. Declercq, *Science* **2002**, *298*, 204.

species are responsible, at least in part, for the hydrogenation phenomenon.

Table 1. Synthesis of (phosphine)Pt(dvtms) complexes.

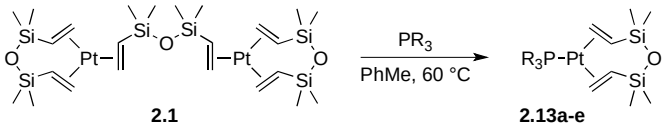

2.1 **2.13a-e**

product	R	yield (%)
13a	Phenyl	54
13b	Cyclohexyl	49
13c	2-Furyl	90
13d	*t*-Butyl	60
13e	*o*-Tolyl	55

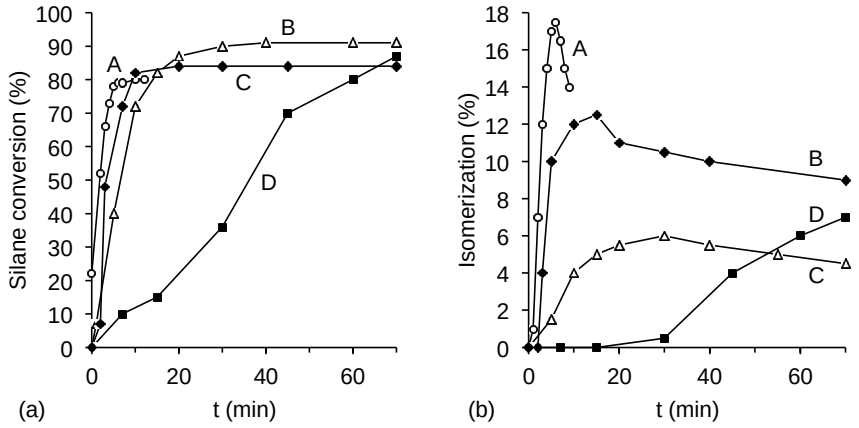

Figure 4. (a) Silane conversion curves for the hydrosilylation of 1-octene (**2.2**) by MD'M (**2.3**) catalyzed by platinum complexes. (b) Isomerization curves. Reaction conditions: MD'M (0.5 mol L^{-1}), 1-octene (0.5 mol L^{-1}), [Pt] (0.005 mol%), *o*-xylene, 72 °C. Karstedt's catalyst **2.1** (A), (Ph_3P)Pt(dvtms) **2.13a** (B), ($^tBu_3P$)Pt(dvtms) **2.13d** (C) and **2.13c** (D).

These results indicate that the phosphine ligands are still too labile for our purpose.

4. NHC Platinum(0) Complexes, the Breakthrough

4.1 Synthesis of NHC Platinum(0) Complexes and Kinetic Assays

In order to increase the binding between the ancillary ligand and platinum(0), we turned our attention to an emerging class of more robust σ-donor ligands: the *N*-heterocyclic carbenes. In analogy to the preparation of the phosphine derivatives **2.13**, the addition of various NHC carbenes (generated *in situ* by deprotonation of the corresponding imidazolium salts) to the Karstedt's catalyst (**2.1**) enabled the preparation of a new family of platinum(0) complexes **2.15** (Table 2).[11,12] Unlike the Karstedt catalyst (**2.1**) or the phosphine complexes **2.13**, these readily available crystalline compounds are insensitive to air and moisture, are bench-stable for extended periods of time and are easy to handle.

[12] a) I. E. Markó, S. Stérin, O. Buisine, G. Berthon, G. Michaud, B. Tinant, J.-P. Declercq, *Adv. Synth. Catal.* **2004**, *346*, 1429. b) O. Buisine, G. Berthon-Gelloz, J.-F. Brière, S. Stérin, G. Mignani, P. Branlard, B. Tinant, J.-P. Declercq, I. E. Markó, *Chem. Commun.* **2005**, 3856. c) G. Berthon-Gelloz, O. Buisine, J.-F. Brière, G. Michaud, S. Stérin, G. Mignani, B. Tinant, J.-P. Declercq, D. Chapon, I. E. Markó, *J. Organomet. Chem.* **2005**, *690*, 6156. d) S. Dierick, G. Bastug, I. E. Markó, *Org. Synth.*, *Accepted for checking*.

Table 2. Selected syntheses of (NHC)Pt(dvtms) complexes.

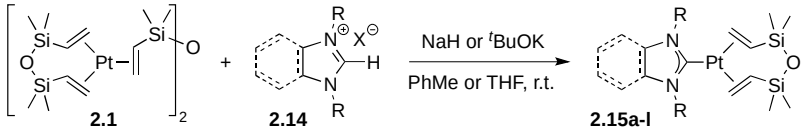

2.1 + **2.14** → **2.15a-l**

complex	yield (%)	complex	yield (%)
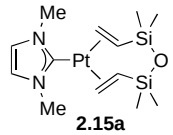 **2.15a**	77	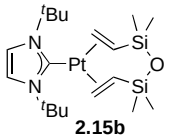 **2.15b**	65
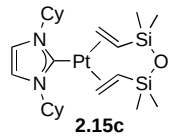 **2.15c**	90	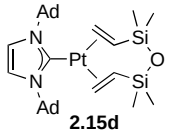 **2.15d**	66
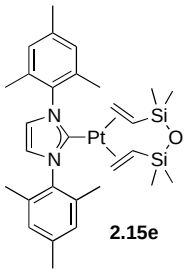 **2.15e**	85	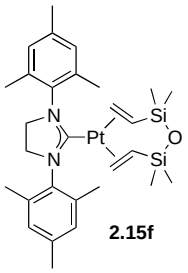 **2.15f**	50
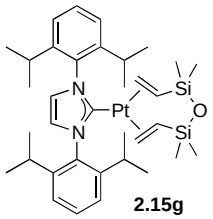 **2.15g**	70	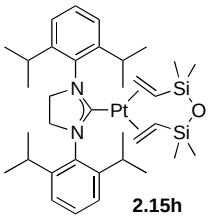 **2.15h**	50
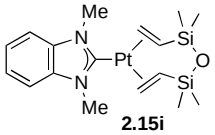 **2.15i**	80	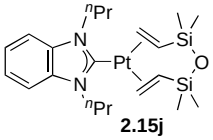 **2.15j**	60
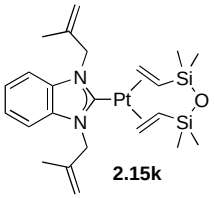 **2.15k**	78	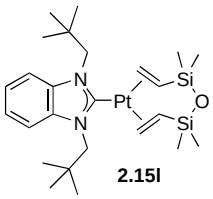 **2.15l**	50[(a)]

[a] Benzimidazoylidene obtained by reduction of the corresponding thiourea.

The intimate structure of theses complexes, revealed by single-crystal X-ray diffraction analyses, presents a trigonal planar arrangement around the platinum center (Figure 5).[13] This disposition is characteristic of $(L)Pt^0(alkene)_2$ compounds and optimizes the back-bonding phenomenon by enhancing the overlap between the metal d-orbitals and the alkene π^* systems.[14] The diene ligand (dvtms) adapts itself to this arrangement by adopting a chair-like chelating conformation, minimizing the steric interactions. The carbene ring is usually orthogonal to the coordination-plane for *N*-alkyl substituted NHCs (θ = 82.4–88.9°) but tilted for *N*-aryl substituted NHCs (θ = 52.1–63.8°). This torsion away from orthogonality appears to avoid destabilizing steric repulsions. As will be seen later on, this property will have a significant influence in the hydrosilylation of alkynes (see Section 5.1) and on the initiation period of the catalytic process (vide infra).

[13] For a detailed discussion about the structural features of (NHC)Pt(dvtms) complexes, see: References 12 and 19.

[14] F. R. Hartley, in *Comprehensive Organometallic Chemistry*; E. W. Abel, F. G. A. Stone, G. Wilkinson, eds.; Pergamon: Oxford, 1982, vol. 6., p 471.

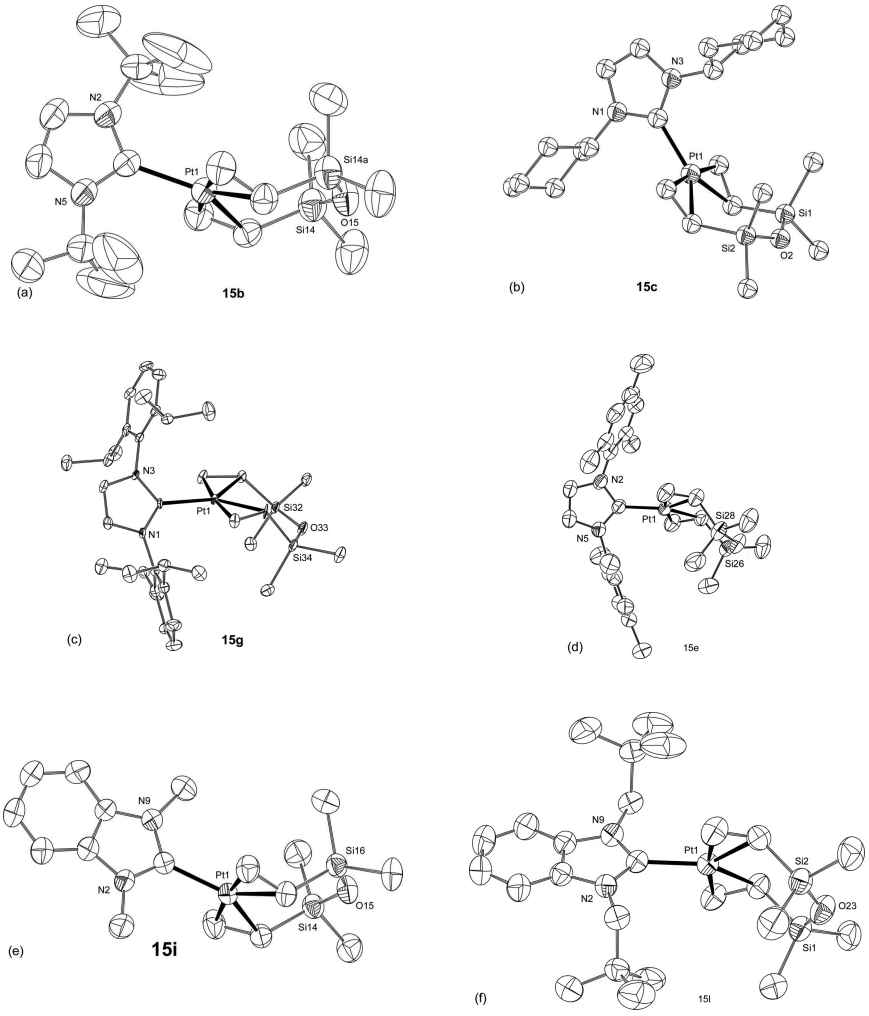

Figure 5. Selected X-ray structures of various (NHC)Pt(dvtms) complexes.
Ellipsoids at the 50% probability level.

When tested in the benchmark hydrosilylation (see Section 2), the platinum NHC complexes **2.15** proved to be less active but far more selective than the Karstedt catalyst (**2.1**) and the phosphine analogs **2.13**.[11,12] Remarkably, none of these compounds produce platinum colloids during the reaction and only the anti-Markovnikov adduct is

detected. These NHC-Pt complexes can be divided in two families, according to their slightly different catalytic behaviors. Thus, the *N*-alkyl substituted NHC class, **2.15a-d** and **2.15i-k**, is characterized by fast initiation rates and low amounts of isomerized octene (<4.5%) (Figure 6 and Figure 7). On the other hand, the *N*-aryl substituted NHC class, **2.15e-h**, has significantly longer initiation periods and more isomerization is observed (>4.5%) (Figure 8). Interestingly, after an initial latency time, the reactions proceed with remarkably high rates, almost comparable to that of the Karstedt catalyst (**2.1**). Additionally, both classes display sigmoidal conversion curves but these are more marked for the *N*-aryl substituted complexes. It is worth mentioning that the BIneoPent compound **2.15l** has a distinctive behavior in somewhere between the two classes (Figure 7, curve E). Indeed though belonging to the *N*-alkyl substituted family, its carbene ring system is tilted away from its coordination plane (θ = 70.3°) much like the *N*-aryl substituted NHC derivatives. Hence, this complex is less active than the *N*-alkyl type catalysts but more active than its *N*-aryl counterparts. It presents also a noticeable sigmoidal conversion curve.

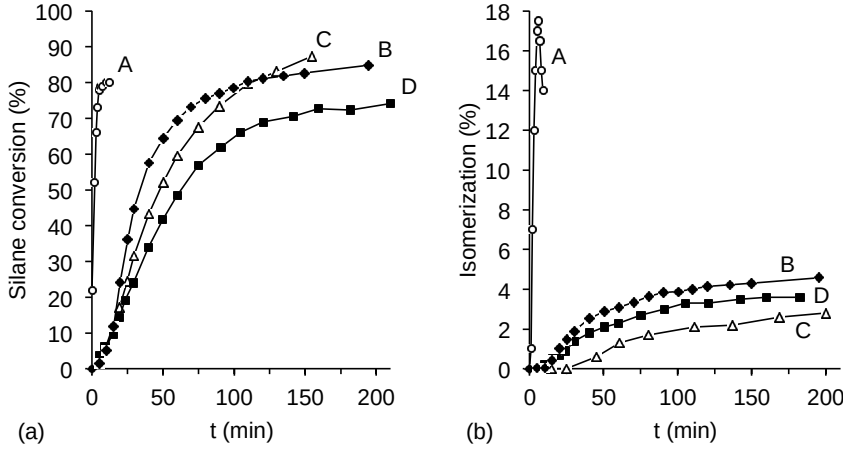

Figure 6. (a) Silane conversion curves for the hydrosilylation of 1-octene (**2.2**) by MD'M (**2.3**) catalyzed by platinum complexes. (b) Isomerization curves. Reaction conditions: MD'M (0.5 mol L^{-1}), 1-octene (0.5 mol L^{-1}), [Pt] (0.005 mol%), *o*-xylene, 72 °C. Karstedt's catalyst **2.1** (A), (I^{t}Bu)Pt(dvtms) **2.15b** (B), (ICy)Pt(dvtms) **2.15c** (C) and (IMe)Pt(dvtms) **2.15a** (D).

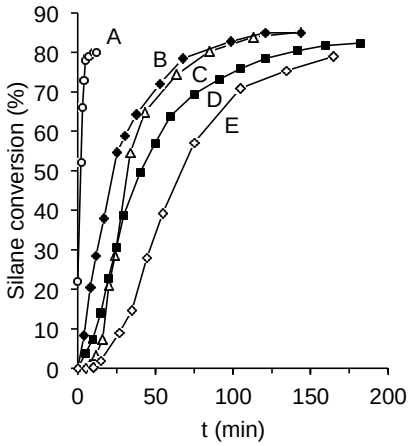

Figure 7. Silane conversion curves for the hydrosilylation of 1-octene (**2.2**) by MD'M (**2.3**) catalyzed by platinum complexes. Reaction conditions: MD'M (0.5 mol L^{-1}), 1-octene (0.5 mol L^{-1}), [Pt] (0.005 mol%), *o*-xylene, 72 °C. Karstedt's catalyst **2.1** (A), (BI*n*Pr)Pt(dvtms) **2.15j** (B), (BI*m*Allyl)Pt(dvtms) **2.15k** (C), (BIMe)Pt(dvtms) **2.15i** (D) and (BI*neo*Pent)Pt(dvtms) **2.15l** (E).

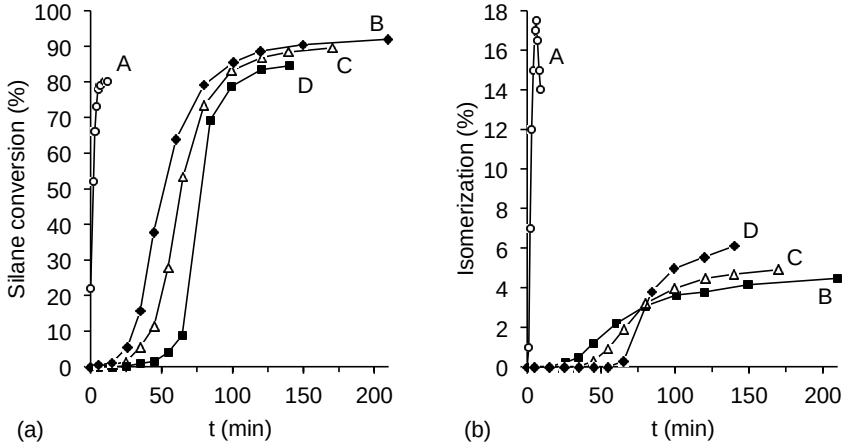

Figure 8. (a) Silane conversion curves for the hydrosilylation of 1-octene (**2.2**) by MD'M (**2.3**) catalyzed by platinum complexes. (b) Isomerization curves. Reaction conditions: MD'M (0.5 mol L^{-1}), 1-octene (0.5 mol L^{-1}), [Pt] (0.005 mol%), *o*-xylene, 72 °C. Karstedt's catalyst **2.1** (A), (IMes)Pt(dvtms) **2.15e** (B), (IPr)Pt(dvtms) **2.15g** (C) and (SIPr)Pt(dvtms) **2.15h** (D).

4.2 Functional Group Tolerance and Substrate Scope

Among all these new NHC platinum(0) catalysts, (ICy)Pt(dvtms) **2.15c** displays a fast reaction rate whilst still retaining a high selectivity (see Figure 6, curve C). Accordingly, it was elected for further optimization. Whereas modifications of several reaction conditions proved fruitless, a simple inverse addition protocol, i.e., a slow addition of the silane to the reaction mixture, led to the desired alkylsilane **2.4** in an outstanding 96% isolated yield. Less than 1% of the isomerized alkenes were contaminating the crude reaction product (Figure 9).[11]

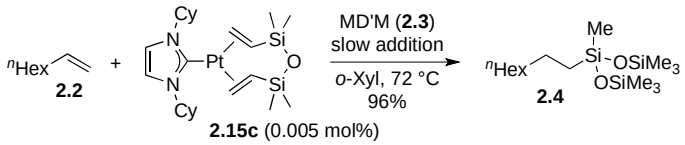

Figure 9. Inverse addition protocol.

The Karstedt complex (**2.1**) is known to be particularly intolerant towards functional groups that are sensitive towards Lewis acids. Pleasingly, **2.15c** demonstrates high chemocompatibility with a wide range of functions and protecting groups (Table 3).[12a] In all cases, excellent yields and purities are obtained. It is noteworthy that tetrahydropyranyl ethers and epoxides survive under the reaction conditions (entries 1–3). Scrambling in the silyl ether protecting groups, silylation of free alcohols and hydrosilylation of ketones are not detected (entries 4–6). Esters could equally be smoothly hydrosilylated (entry 7). It is worth mentioning that internal alkenes are inert under these reaction conditions (entry 8).

Table 3. Hydrosilylation of functionalized alkenes catalyzed by 2.15c.

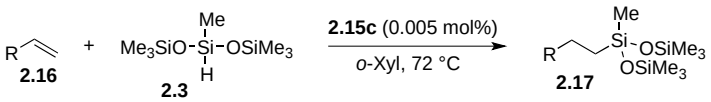

entry	alkene	product	yield (%)[a,b]
1	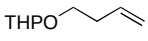	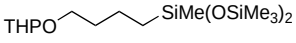	92
2	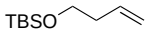	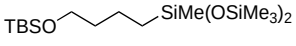	90
3	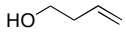	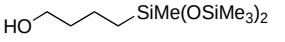	92
4	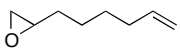	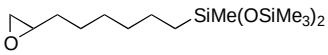	81
5	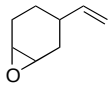	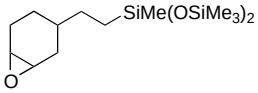	96
6	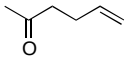	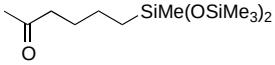	78[c]
7	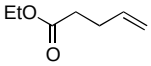	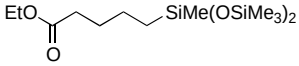	80
8	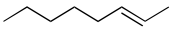	—	n.c.

[a] All yields are for isolated, pure compounds. Unless otherwise mentioned, the conversions are all quantitative. [b] In all cases, the use of Karstedt catalyst (**2.1**) leads to a mixture of products and to the formation of colloidal platinum species. [c] The reaction was stopped after 80% conversion.

Applying our platinum(0) NHC complexes, Rieger has demonstrated that linear and hyperbranched polycarbosilanes can be obtained by hydrosilylation polymerization of AB and AB_2 monomers, respectively (Figure 10).[15] The use of the Karstedt or the Speier catalyst resulted in significant isomerization into unreactive internal double bonds (ca. 6–29%). In sharp contrast, no isomerized olefin was detected when (IMes)Pt(dvtms) **2.15e** was employed. As the isomerization constitutes a termination reaction, its suppression leads to polymers of significantly

[15] U. Will, D. Veljanovski, P. Härter, B. Rieger, *Macromolecules* **2010**, *43*, 934.

higher molecular weight. Furthermore, Pt–NHC complexes being less active than catalyst **2.1** and H_2PtCl_6/*i*-PrOH, the polymer growth is slower but more uniform, resulting in highly homogeneous polymers with smaller polydispersity indices.

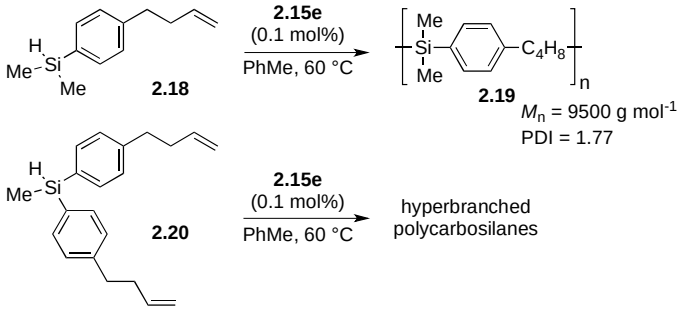

Figure 10. Polymerizations by hydrosilylation induced by (IMes)Pt(dvtms) 2.15e.

Although platinum(0) complexes are able to mediate hydrosilylation with various silanes, bis(trimethylsilyloxy)methylsilane (**2.3**) constitutes our favorite reagent. Indeed, it is cheap, stable and mimics the linkage of siloxane polymers (Si–O–Si). On the other hand, it is small and displays a low reactivity akin to that of dialkoxysilanes, which makes it a challenging substrate for highly selective hydrosilylations. Gratifyingly, the Tamao–Kumada oxidation of alkyl bis(trimethylsilyloxy)methyl silanes can be successfully performed under mild and neutral conditions.[12a,16–17]

4.3 Mechanistic Studies

Delighted by the unique features of (NHC)platinum(dvtms) complexes **2.15**, it was decided to investigate in detail the mechanism of the

[16] a) For the seminal publication by Tamao and Kumada, see: K. Tamao, N. Ishida, T. Tanaka, M. Kumada, *Organometallics* **1983**, *2*, 1694. b) For a review about the Tamao–Kumada–Fleming oxidation, see: G. R. Jones, Y. Landais, *Tetrahedron* **1996**, *52*, 7599.

[17] D. A. Rooke, E. M. Ferreira, *Angew. Chem., Int. Ed.* **2012**, *51*, 3225.

hydrosilylation triggered by these catalysts. Prior to these studies, several research groups had already demonstrated the homogeneous nature of the active platinum species in hydrosilylation (see Chapter 1).[18] This remains true even if colloidal platinum is detected during the reaction. Moreover, such colloids have never been observed in hydrosilylation using platinum carbene complexes. Thus, it was assumed that for such compounds the active species are also homogeneous.

4.3.1 Activation Period

A distinctive characteristic of the NHC platinum complexes **2.15** is their long activation period as compared to other platinum(0) sources (see Figure 4, 4–6). Moreover, all these catalysts present a sigmoidal shape for their conversion and isomerization curves, particularly at moderate temperatures. Both features, especially pronounced for the *N*-aryl substituted derivatives **2.15e-h**, are typical for catalytic systems in which formation of the catalytically active species is a slow process occurring throughout the whole course of the reaction. Additionally, closer examination of the graphs presented in Section 4.1 reveals that, as a general rule, the more active the catalyst, the higher the amount of isomerized olefins. Hence, hydrosilylation and isomerization appear to be linked by a common intermediate, as in the Chalk and Harrod mechanism (see Figure 3).[10]

In order to confirm that the precatalyst initiation rate is slower than the catalytic cycle, we devised a simple experiment in which the kinetic profile of the reaction is monitored upon addition of fresh reactants at the end of the reaction (Figure 11).[19] Usually, this protocol is used to

[18] a) P. Steffanut, J. A. Osborn, A. DeCian, J. Fisher, *Chem. Eur. J.* **1998**, *4*, 2008. b) J. Stein, L. N. Lewis, Y. Gao, R. A. Scott, *J. Am. Chem. Soc.* **1999**, *121*, 3693.

[19] G. Berthon-Gelloz, I. E. Markó, Efficient and selective hydrosilylation of alkenes and alkynes catalyzed by novel N-heterocyclic carbene Pt^0

probe catalyst longevity and gives rise to slower reaction upon successive additions. In stark contrast, an 8-fold increase in rate, relative to the initial reaction rate (curve A), was observed upon the second addition of fresh reactants (curve B). Even more impressive was the 16-fold increase in the reaction rate when a third batch of reactants was added (curve C). This meaningful experiment demonstrates that the generation of the active catalytic species is significantly slower than the hydrosilylation itself. Furthermore, it emphasizes the importance of precatalyst activation in the overall transformation.

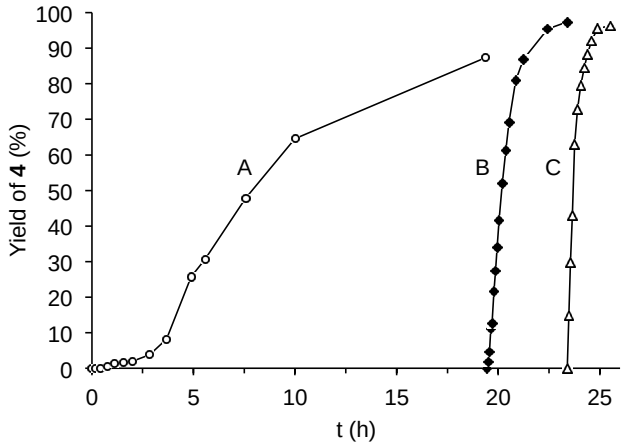

Figure 11. Effect of the addition of fresh reactants on the kinetic profile of the reaction for the hydrosilylation of 1-octene (**2.2**) by MD'M (**2.3**) catalyzed by (ICy)Pt(dvtms) **2.15c**. Reaction conditions: MD'M (0.05 mol L^{-1}), 1-octene (0.05 mol L^{-1}), [Pt] (0.05 mol%), *o*-xylene, 72 °C. On the 2nd and 3rd addition, MD'M (0.05 mol L^{-1}) and 1-octene (0.05 mol L^{-1}) were added to the reaction mixture. For clarity, the reaction profile for the formation of **2.4** is corrected by subtraction of the previously formed product. First addition (A), second addition (B) and third addition (C).

A reasonable mechanism for the initiation of compounds **2.15** requires an unfavorable decoordination of one double bond of the chelating ligand dvtms to afford intermediate **2.21** (Figure 12). The opening of a coordination site enables the oxidative addition of the silane necessary

complexes, in *N-heterocyclic carbenes in synthesis*; S. P. Nolan, ed., Wiley-VCH, Weinheim, 2006, p 119.

to achieve the hydrosilylation of the diene, driving the equilibrium towards the real catalyst **2.22**.

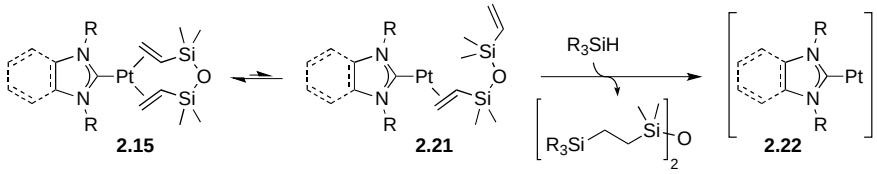

Figure 12. Proposed mechanism for the activation of (NHC)Pt(dvtms) 2.15.

If such a pathway is operating and since hydrosilylation itself is fast, the initiation process must be slow because of the low concentration of intermediate **2.21** in the reaction mixture. Indeed, in addition to the chelate effect, dvtms is a vinylsilane known to possess strong affinities for late, low-valent transition metals. This enhanced coordination ability of vinylsiloxanes is due to a strong interaction between the $\sigma^*_{(Si-O)}$ orbital and the double bond π^* orbital. This effect lowers the energy level of the vinylsiloxane LUMO, increasing its π-acidity and thus strengthening the backbonding from the electron rich metal center.[20] According to this analysis, replacing the dvtms ligand by less coordinating dienes should increase the initiation rate. In order to confirm this hypothesis, two new (ICy)Pt(η^2-diene) complexes **2.23** and **2.24** were prepared (Figure 13).[21]

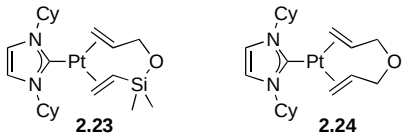

Figure 13. Modification of the chelating moiety of (ICy)Pt(η^2-diene) complexes.

[20] a) H. Bock, H. Seidl, H. *J. Am. Chem. Soc.* **1968**, *90*, 5694. b) J. W. Fitch, D. P. Flores, J. E. George, *J. Organomet. Chem.* **1971**, *29*, 263. c) J. W. Fitch, K. C. Chan, J. A. Froelich, J. A. *J. Organomet. Chem.* **1978**, *160*, 477.

[21] a) G. Berthon-Gelloz, I. E. Markó, *Unpublished results*. b) G. Berthon-Gelloz, J.-M. Schumers, F. Lucaccioni, B. Tinant, J. Wouters, I. E. Markó, I. E. *Organometallics* **2007**, *26*, 5731.

The catalytic behavior of the (ICy)Pt(η^2-diene) derivatives **2.15c**, **2.23** and **2.24** in the benchmark hydrosilylation is perfectly explicit (Figure 14).[21b] Indeed, replacing one vinylsilane moiety of the dvtms ligand by its allyl analog results in a 4.5-fold increase in the reaction rate (Figure 14a, curve B vs C). Moreover, a second substitution leads to an 8-fold increase (Figure 14a, curve A vs C). These results fully agree with that the first dissociative step determining the overall rate of the initiation process. Unfortunately, the amounts of isomerized olefins also appear to increase with the enhanced activity of the catalyst (Figure 14b). Besides, the stability of the precatalysts diminishes as the coordinating ability of the chelating dienes decreases. Osborn and Elsevier have also demonstrated that the nature of the alkene fragment is a key parameter determining the stability and the activity of (L)Pt(η^2-alkene)$_2$ and (L)$_2$Pt(η^2-alkene) complexes. The same dissociative mechanism, being the rate determining step, has also been invoked.[18a]

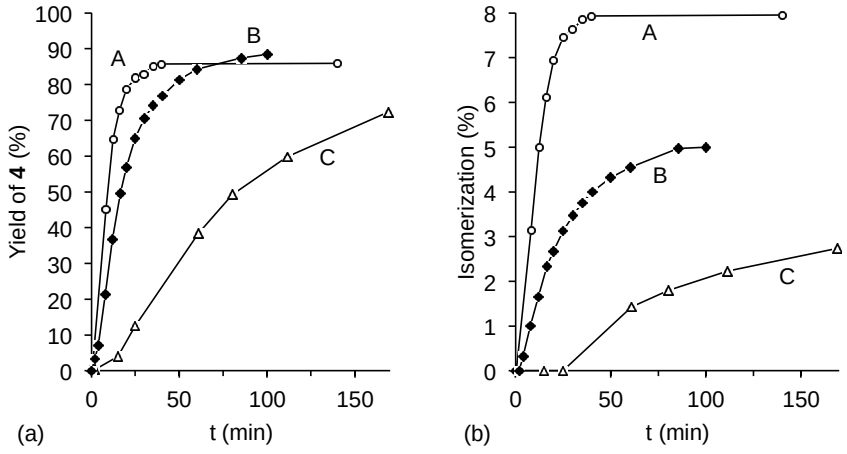

Figure 14. (a) Kinetic reaction profile for the hydrosilylation of 1-octene (**2.2**) by MD'M (**2.3**) catalyzed by (ICy)Pt(η^2-diene) complexes. (b) Isomerization curves. Reaction conditions: MD'M (0.5 mol L^{-1}), 1-octene (0.5 mol L^{-1}), [Pt] (0.005 mol%), *o*-xylene, 70 °C. (ICy)Pt(AE) **2.24** (A), **2.23** (B) and (ICy)Pt(dvtms) **2.15c** (C).

4.3.2 Catalyst Deactivation Pathways

Precious insights into a reaction mechanism can be collected through the isolation of reactive intermediates. While no reaction occurs between 1-octene (**2.2**) and bis(trimethylsilyloxy)methylsilane (**2.3**) in the absence of a suitable catalyst, mixtures of (NHC)Pt(dvtms) **2.15** and 1-octene (**2.2**) are unreactive even under harsh conditions.[22] However, treatment of (ICy)Pt(dvtms) **2.15c** with five equivalents of MD'M (**2.3**), in hot and degassed toluene, yields the dimeric complex **2.25** and the hydrosilylated diene **2.26** (Figure 15).[19] The intimate structure of **2.25** was unambiguously revealed by a single crystal X-ray diffraction analysis.[23]

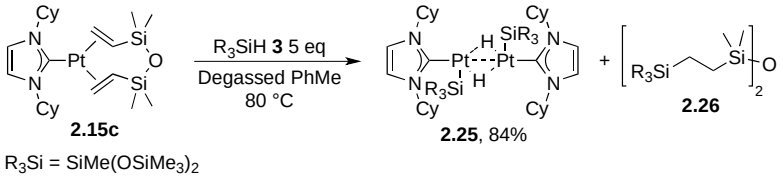

Figure 15. Synthesis of platinum dimer 2.25.

Interestingly, phosphine analogs of dimer **2.25** have already been reported by Stone and Tsipis. They proved to be efficient hydrosilylation mediators at room temperature.[24] Surprisingly, when submitted to our model reaction, **2.25** turned out to be less active than its precursor **2.15c** (Figure 16).[19] Additionally, compound **2.25** presents a significantly prolonged activation period resulting from a particularly slow generation of the active species.

[22] G. Berthon-Gelloz, S. Dierick, I. E. Markó, *Unpublished results*.

[23] G. Berthon-Gelloz, N. Scott, S. P. Nolan, I. E. Markó, *Unpublished results*.

[24] a) M. Green, J. L. Spencer, G. A. F. Stone, C. A. Tsipis, *J. Chem. Soc., Dalton Trans.* **1977**, 1519. b) M. Green, J. L. Spencer, G. A. F. Stone, C. A. Tsipis, *J. Chem. Soc., Dalton Trans.* **1979**, 1525. c) M. Ciriano, M. Green, J. A. K. Howard, J. Proud, J. L. Spencer, G. A. F. Stone, C. A. Tsipis, *J. Chem. Soc., Dalton Trans.* **1978**, 801.

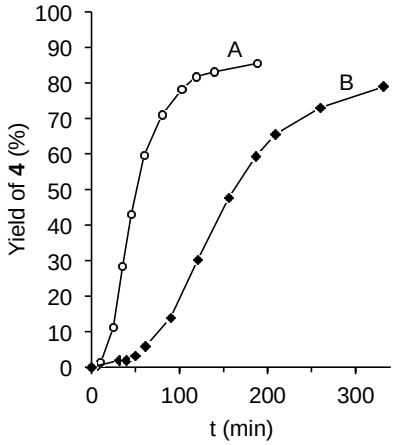

Figure 16. Kinetic reaction profile for the hydrosilylation of 1-octene (**2.2**) by MD'M (**2.3**) catalyzed by (ICy)Pt(dvtms) **2.15c** and complex **2.25**. Reaction conditions: MD'M (0.5 mol L^{-1}), 1-octene (0.5 mol L^{-1}), [Pt] (0.005 mol%), *o*-xylene, 70 °C. (ICy)Pt(dvtms) **2.15c** (A) and complex **2.25** (B).

This marked difference between phosphine and carbene platinum dimers might be due to the stronger σ-donating ability of NHCs. Indeed, this effect strengthens the Pt–H–Pt bond hence disfavoring the release of the monomeric species **2.27** required to initiate the hydrosilylation catalytic cycle (Figure 17).

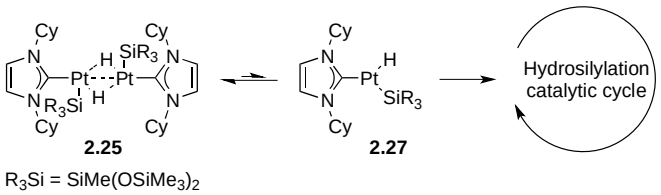

R_3Si = $SiMe(OSiMe_3)_2$

Figure 17. Proposed equilibrium for the initiation of dimer 2.25.

To further probe the reactivity of complex **2.25**, its reaction with 10 equivalents of 1-octene (**2.2**) in hot [d_8]-toluene was monitored by ^{1}H NMR spectroscopy (Figure 18).[19] After 4 h, complete conversion of **2.25** into (ICy)Pt(1-octene)$_2$ **2.28** was observed, along with the hydrosilylated product **2.29**. Unfortunately, compound **2.28** is too unstable to be isolated from the reaction mixture. Nevertheless, this experiment demonstrates that there is an equilibrium operating

between **2.25** and its monomer **2.27**, which can complete the hydrosilylation reaction without any added silane.

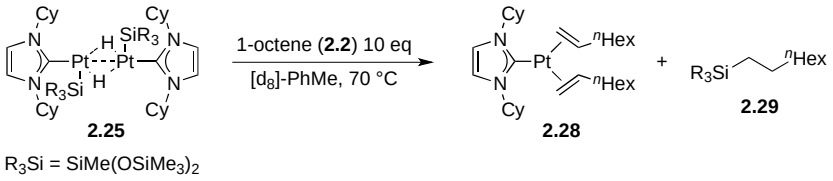

$R_3Si = SiMe(OSiMe_3)_2$

Figure 18. Reaction of dimer 2.25 with excess 1-octene.

To summarize our findings, the platinum dimer **2.25** appears to act as a dormant species. Indeed, while affording a competent monomeric hydrosilylation precatalyst, its dissociation rate is rather low and the overall hydrosilylation proceeds more slowly than with the precatalyst (ICy)Pt(dvtms) **2.15c**. Therefore, its formation has to be considered as a deactivation pathway on the hydrosilylation timescale.

4.3.3 Semi-Quantitative Kinetic Studies

In mechanistic investigation, kinetic studies occupy a fundamental position inherent to in-depth understanding of the chemical reaction. However, in catalysis, unless activation of the precatalyst can be made so fast as to become negligible as compared to the rate of the catalytic cycle, the initial rate measurement under conventional kinetic conditions is impossible. Concerning (ICy)Pt(dvtms) complex **2.15c**, preactivation of the catalyst cannot be accomplished without forming the less active dimer **2.25** (see Section 4.3.2). Moreover, the conditions for the measurement of the kinetic data are usually far from the real catalytic system, e.g., different catalyst loadings or pseudo-first order conditions, and might produce some artifacts. Consequently, we decided to conduct basic semi-quantitative analysis of the hydrosilylation rate, under the usual reaction conditions, by measuring the tangent of the most active phase of the kinetic curve: "V_{max}". This value represents the maximum rate attainable by the entire catalytic system and it enables

the quantitative comparison between the different kinetic curves. Eventually, the information gained through this rudimentary investigation has facilitated the development of a numerical kinetic modeling of the overall process, which enabled the accurate determination of its elementary rate constants (see Section 4.3.4).

Through this first approach, a first order in silane (**2.3**) was observed (Figure 19), in agreement with the Chalk and Harrod mechanism (see Figure 3).[10,18b]

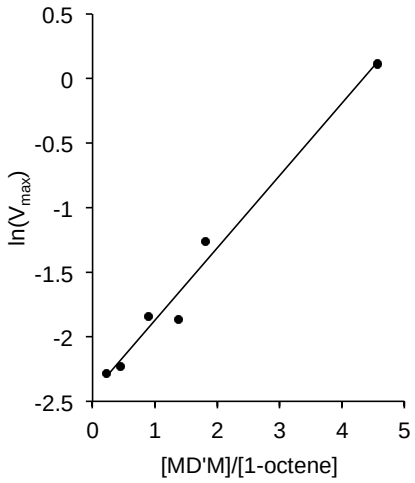

Figure 19. Relationship between the [MD'M]/[1-octene] ratio and the logarithm of V_{max} (s^{-1}). Reaction conditions: 1-octene (0.5 mol L^{-1}), (ICy)Pt(dvtms) **2.15c** (0.005 mol%), *o*-xylene, 72 °C. R^2 = 0.980.

Unexpectedly, the reaction is also first order in 1-octene (**2.2**), for alkene to silane ratio below 3 (Figure 20). Increasing further the amount of olefin decreases the reaction rate. Generally, this behavior is only encountered with strongly binding alkenes.[25] This inhibition by the substrate is attributed to a reversible deactivation pathway leading to the formation of (ICy)Pt(1-octene)$_2$ **2.28**.

[25] a) L. N. Lewis, R. E. Colborn, H. Grade, R. A. Garold, *Organometallics* **1995**, *14*, 2202. b) L. N. Lewis, J. Stein, R. E. Colborn, Y. Gao, J. Dong, *J. Organomet. Chem.* **1996**, *521*, 221.

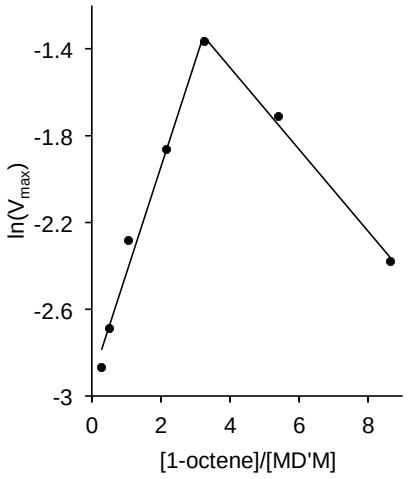

Figure 20. Relationship between the [1-octene]/[MD'M] ratio and the logarithm of V_{max} (s^{-1}). Reaction conditions: MD'M (0.5 mol L^{-1}), (ICy)Pt(dvtms) **2.15c** (0.005 mol%), *o*-xylene, 70 °C. R^2 = 0.986 for the linearized segment up to [1-octene]/[MD'M] = 4. R^2 = 0.996 for the linearized segment down to [1-octene]/[MD'M] = 4.

Surprisingly, the effect of precatalyst **2.15c** loading on the hydrosilylation rate displays a plateau above 0.005 mol% (Figure 21). This trend suggests that the solution becomes "saturated" in catalyst. Indeed, increasing the catalyst concentration favors its transformation into its dimer **2.25**, while the unimolecular rate determining step, that is, the dissociative process in the precatalyst initiation (see Figure 12), remains unaffected. Thus, raising the amount of precatalyst is not necessarily directly correlated to an increase in catalyst concentration. Besides, the linear correlation between V_{max} and precatalyst loading below 0.005 mol% would suggest a zero order in platinum. Obviously, this indicates the limits of our rudimentary analysis. Indeed, this method does not take into account the variation of catalyst concentration throughout the measures of V_{max}. Additionally, platinum is not only involved in the hydrosilylation catalytic cycle, but also in the activation process and the deactivation pathways, definitely affecting its observed reaction order. Consequently, this approach is unable to determine kinetic order in platinum.

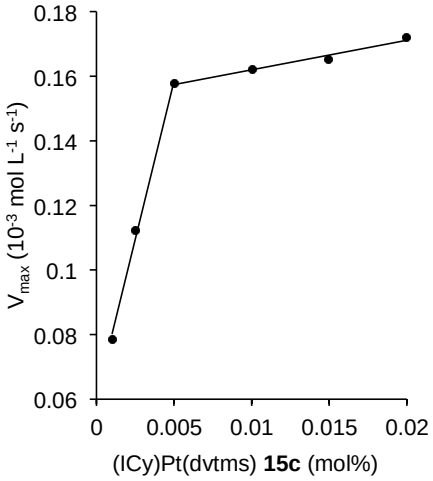

Figure 21. Relationship between the catalyst loading and V_{max} (10^{-3} mol L^{-1} s^{-1}). Reaction conditions: MD'M (0.5 mol L^{-1}), 1-octene (0.5 mol L^{-1}), *o*-xylene, 70 °C. R^2 = 0.996 for the linearized segment up to catalyst loading = 0.005 mol%. R^2 = 0.979 for the linearized segment down to catalyst loading = 0.005 mol%.

In conclusion, though being unelaborated, this semi-quantitative analysis allows us to define a first order in silane and alkene in the reaction rate law, while the kinetic order in platinum remains inaccessible. Rewardingly, these insights have been determined under reaction conditions nearly identical to those used to conduct the actual hydrosilylation.

4.3.4 Quantitative Kinetic Modeling

In order to circumvent the limitations of our semi-quantitative analysis and to acquire significant and precise kinetic information from our catalytic system, we considered using numerical kinetic modeling. The underlying principle of this approach is that numerical integration of the system of differential equations corresponding to the elementary transformations can be used to determine the elementary rate constants

by least-squares fitting.[26] In practice, a software is used to solve a set of differential equations, representing a mechanistic model proposed by its user, to fit for the given experimental kinetic data.[27] The software used in this study, ReactOp®, associates two variables to each step within the kinetic model: the activation energy (E_a) and the pre-exponential factor (A) derived from the Arrhenius' law (Equation 1). Therefore, the software varies their values in order to fit the experimental data.

$$k = A\, e^{\frac{-E_a}{RT}}$$

Equation 1. Arrhenius' law.

To establish an effective kinetic model, every reasonable mechanism based upon previous experimental studies is analyzed. Discrimination between each of them is then performed by comparison of their fit with the experimental kinetic data. Importantly, this mathematical treatment can be used to deconvolute the initiation rate constant of the active catalyst from the actual rate constant of the catalytic cycle, thereby alleviating the need for parameters outside the actual regime of the catalytic reaction.

Through the use of this procedure, 15 different mechanistic models were confronted with 16 independent experimental kinetic records. Finally, we identified a proposed mechanism in excellent agreement with the kinetic data.[19,21a] Representative examples of the fits obtained with this model for different temperatures are presented in Figure 22.

[26] For leading references, see: a) R. Hartmann, P. Chen, *Adv. Synth. Catal.* **2003**, *345*, 1353. b) G. Rothenberg, S. C. Cruz, G. P. F. van Strijdonck, H. C. J. Hoefsloot *Adv. Synth. Catal.* **2004**, *346*, 467.

[27] Any software able to solve a set of differential equations can be used, e.g., ReactOp® or MATLAB®.

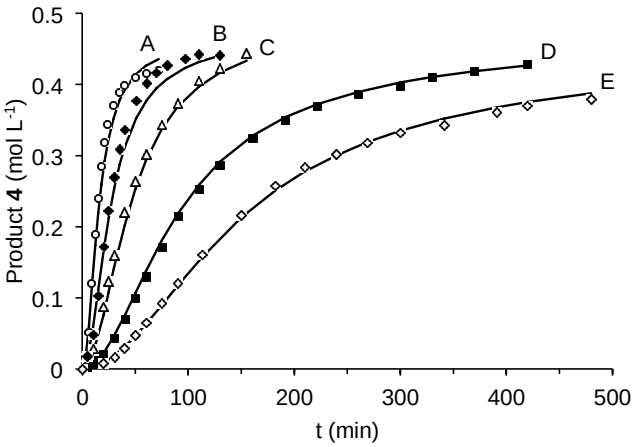

Figure 22. Representative fit of the kinetic model with experimental curves for the formation of product **2.4** at different reaction temperatures. Reaction conditions: MD'M (0.5 mol L^{-1}), 1-octene (0.5 mol L^{-1}), (ICy)Pt(dvtms) **2.15c** (0.005 mol%), *o*-xylene. Kinetic model (solid lines), experimental data (dots); *T* (°C) = 90 (A), 80 (B), 70 (C), 59 (D), 51 (E).

In this kinetic model, depicted in Figure 23 (p 83), the activation process (k_{ini}) appears to be first order in precatalyst **2.15c** and is independent of both 1-octene (**2.2**) and the silane **2.3** (incorporating a silane and/or an alkene in the activation step resulted in poorer fit). This result is in full agreement with an activation pathway governed by the initial decoordination of one double bond of the chelating ligand dvtms (see Figure 12). The resulting active catalyst **E** subsequently coordinates reversibly both substrates **2.2** and **2.3** and proceeds to a concerted oxidative addition – 1,2 migratory insertion, leading directly to the (ICy)Pt(alkyl)(silyl) intermediate **G**. Finally, reductive elimination yields the hydrosilylated product **2.4**, closing the catalytic cycle and regenerating the active species **E**. It is worth noting that all these elementary steps are kinetically indistinguishable and are collected together in the rate constant k_{hydro}. Though the formation of intermediate **F** and **G** are thought to be reversible, the final reductive elimination is associated with a significant driving force, that is, the formation of the strong silicon–carbon bond. Hence, the best kinetic model depicts the catalytic cycle as an overall irreversible reaction. Importantly, this mechanism, involving a concerted oxidative addition –

1,2 migratory insertion, fits significantly better with the experiments than its equivalents based upon two distinct steps, as in the Chalk and Harrod mechanism (see Figure 3).[10] It is further supported by the first order on both silane and alkene determined by our semi-quantitative analysis (see Section 4.3.3). Inhibition of the catalyst **E** at high alkene concentration is modeled by an equilibrium (K_{eq}) between complex **E** and (ICy)Pt(1-octene)$_2$ (**2.30**). Additionally, the formation of dimer **2.25** is modeled as an irreversible deactivation pathway (k_{dimer}), as estimated in Section 4.3.2. Finally, the isomerization process (k_{iso}) is definitely linked to the hydrosilylation process, presumably through the formation of the other regioisomer of **G** derived from **F**. Again, the intimate steps of this transformation are kinetically indistinguishable. However, since no regio-isomer of **2.4** could be detected in the reaction mixture, the rate of β-hydride elimination towards 2-octene (**2.5**) must be higher than the concurrent reductive elimination. Furthermore, the isomerization process is irreversible, as expected, since internal alkenes cannot be hydrosilylated under the reaction conditions (see Table 3, entry 8).

The rate constants obtained through the Arrhenius' law via this numerical kinetic modeling are collected in Table 4 (p 83). These calculated values reveal that the rate constant for the activation step is 900,000 times smaller than the rate constant for the catalytic cycle and support the fact that (ICy)Pt(dvtms) **2.15c** releases slowly the catalytically active species. The equilibrium constant between (ICy)Pt **E** and (ICy)Pt(1-octene)$_2$ **2.30** slightly favors the former. This is coherent with alkene inhibition occurring for alkene to silane ratios above 3 (see Figure 20). Unfortunately, the high errors associated with k_{iso} and k_{dimer} preclude any discussion on their intrinsic values.[28] Nonetheless, the rate of dimer formation is five orders of magnitude higher than the initiation

[28] Although the activation energy (E_a) and the pre-exponential factor (A) are calculated with excellent precision, the propagation of uncertainty is dramatic upon calculation of the rate constants (k) with these terms because two exponential functions are involved.

rate indicating that, as soon as a high concentration of the active species is achieved, dimerization will occur readily.

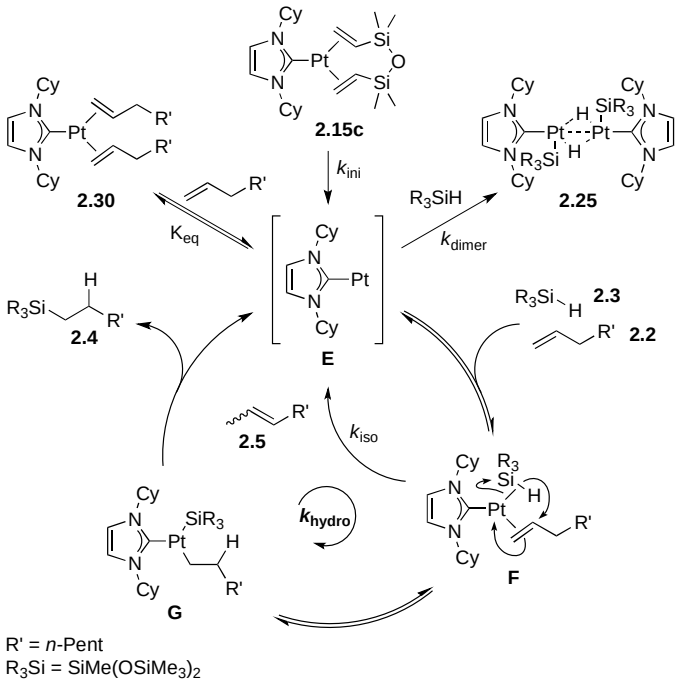

Figure 23. Proposed mechanism for the hydrosilylation of alkenes catalyzed by (ICy)Pt(dvtms) 2.15c.

Table 4. Rate constants calculated by fitting the kinetic model to the experimental data at 70 °C.

constant	fitting	error
k_{ini}	1.40×10^{-4} s^{-1}	0.01×10^{-4} s^{-1}
k_{hydro}	127 L^2 mol^{-2} s^{-1}	1 L^2 mol^{-2} s^{-1}
k_{iso}	8 L^2 mol^{-2} s^{-1}	98 L^2 mol^{-2} s^{-1}
k_{dimer}	16 L^1 mol^{-1} s^{-1}	20 L^1 mol^{-1} s^{-1}
K_{eq}	0.32 L^2 mol^{-2}	0.02 L^2 mol^{-2}

Pleasantly, this kinetic modeling enables us to extract interesting features of this catalytic system, e.g., platinum species distribution over time, catalyst loading or temperature effects on products distribution and reaction rates, etc…, thereby demonstrating its practical usefulness.[19,21a]

Further supported by extensive *ab initio* calculations,[29] the concerted oxidative addition – 1,2 migratory insertion mechanism might be substantiated by the observation of a large primary kinetic isotope effect. Accordingly, we performed the hydrosilylation or 1-octene (**2.2**) in the standard conditions but using the deuterated derivative of silane **2.3**.[19] Unfortunately, the error related to the extracted hydrosilylation rate constant is too high to allow any quantitative conclusions ($k_{\text{D-hydro}}$ = 7 ± 159 L^2 mol^{-2} s^{-1}). However, this experiment disclosed a significant increase of the activation energy for the hydrosilylation catalytic cycle ($E_{a(\text{D-hydro})}$ = 176 ± 5 kJ mol^{-1} vs $E_{a(\text{H-hydro})}$ = 80.58 ± 0.05 kJ mol^{-1}), thus supporting the concerted pathway.

4.3.5 Conclusions

This in-depth mechanistic study of alkenes hydrosilylation mediated by (NHC)Pt(dvtms) complexes afforded a better understanding of this catalytic process. Its two main lessons are:

- Hydrosilylation and isomerization cycles are intimately coupled and increasing the hydrosilylation rate will predictably raise the isomerization extent.
- The precatalyst acts as a reservoir for the catalytically active species and its slow release is the key for minimizing the isomerization process.

[29] G. Mignani, Rhodia Silicones, personal communication, 2002.

5. Hydrosilylation of Alkynes

5.1 Catalyst Screening and the Impact of NHCs on Regioselectivity

Encouraged by the exciting results obtained with the *N*-heterocyclic carbene platinum(0) complexes in alkene hydrosilylation, we focused our efforts on the more challenging hydrosilylation of alkynes. At the onset of this study, we chose to employ the previous benchmark conditions, at a slightly higher temperature, using 1-octyne (**2.31**) as our model substrate. The outcome of an initial catalyst screening is presented in Table 5.[30] Interestingly, the β-(*Z*) isomer was never observed under these conditions. In addition, the *N*-aryl substituted NHCs (entries 6–9) afford better selectivities and are more active than their *N*-alkyl counterparts (entries 2–5). One notable exception is the I*p*Tol derivative **2.15m**, which is one of the worst catalysts tested in this reaction (entry 1). It appears therefore, that the difference in reactivity between aryl- and alky-substituted (NHC)Pt(dvtms) complexes cannot be attributed to an electronic effect of the aromatic substituent. Unfortunately, the influence of a steric effect is also not clear at this point. Indeed, there is no correlation between the results obtained with methyl (entry 2), adamantyl (entry 3), cyclohexyl (entry 5) and mesityl (entry 6) substituents on nitrogen. However, it transpires clearly that an *ortho*, *ortho'* substitution pattern in complexes **2.15e-h** is essential to achieve high regiocontrol and activity (compare entry 1 with entries 6–9).

[30] G. De Bo, G. Berthon-Gelloz, B. Tinant, I. E. Markó, *Organometallics* **2006**, *25*, 1881.

Table 5. Catalyst screening for the hydrosilylation of 1-octyne.

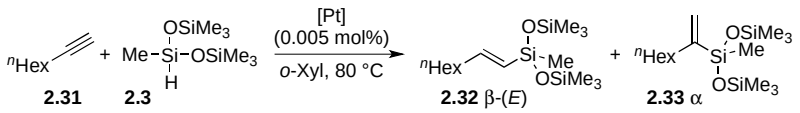

2.31 **2.3** **2.32** β-(*E*) **2.33** α

entry	catalyst	β-(*E*)/α[a]	time (h)[b]
1	(I*p*Tol)Pt(dvtms) **2.15m**	1.5	77
2	(IMe)Pt(dvtms) **2.15a**	1.6	44
3	(IAd)Pt(dvtms) **2.15d**	2.3	55
4	(I*t*Bu)Pt(dvtms) **2.15b**	2.5	55
5	(ICy)Pt(dvtms) **2.15c**	2.8	150
6	(IMes)Pt(dvtms) **2.15e**	5.8	49
7	(SIMes)Pt(dvtms) **2.15f**	6.4	6
8	(SIPr)Pt(dvtms) **2.15h**	10.1	3
9	(IPr)Pt(dvtms) **2.15g**	10.6	6

a Ratio determined by CG analysis of the crude reaction mixture. *b* Time to completion of reaction (>95% conversion).

As emphasized in Section 4.1, the X-ray crystal structures of the (NHC)Pt(dvtms) derivatives **2.15a-l** revealed that their carbene ring system is nearly orthogonal to the plane involving the Pt and its dvtms ligand, when *N*-alkyl substituted NHCs are present on the metal. However, it is tilted away in the *N*-aryl substituted analogs. Therefore, though the crystal structure of (I*p*Tol)Pt(dvtms) **2.15m** was unavailable, we decided to examine the relationship between this tilt angle θ and the regioselectivity observed in the hydrosilylation of alkynes. Interestingly, an excellent linear correlation was obtained (Figure 24).[30] This suggests that, while releasing their steric strain by tilting away from orthogonality, the *N*-aryl substituted NHCs bring their substituents in close proximity to the adjacent coordination sites and thus can influence the regioselectivity more effectively than their *N*-alkyl counterparts.

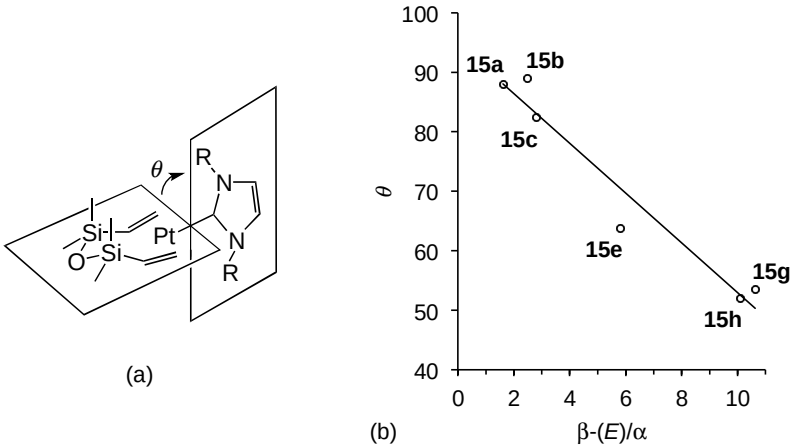

Figure 24. (a) Representation of the tilt θ angle. (b) Correlation between the tilt θ angle and the β-(*E*)/α ratio obtained using these catalysts. R^2 = 0.948.

Whilst the Tolman cone angle is a broadly used structural parameter for phosphines,[31] that depicts efficiently the volume occupied by these ligands in a metal complex, the *N*-heterocyclic carbenes do not possess such a valuable steric hindrance measure. In an effort to develop more predictive tools associating the nature of the carbene to the regioselectivity of the hydrosilylation reaction, we became interested in the A_H and A_L angles and the percent buried volume introduced by Nolan and co-workers.[32] Notably, the A_H angle was thought to reflect the size of the NHC in the direction that incorporates the crucial *ortho*, *ortho'* substitution pattern (Figure 25).

[31] Tolman, C. A. (1977) *Chem. Rev.*, **77** (3), 313–348.

[32] a) J. Huang, H.-J. Schanz, E. D. Stevens, S. P. Nolan, *Organometallics* **1999**, *18*, 2370. b) A. C. Hillier, W. J. Sommer, B. S. Yong, J. L. Petersen, L. Cavallo, S. P. Nolan, *Organometallics* **2003**, *22*, 4322. c) H. Clavier, S. P. Nolan, *Chem. Commun.* **2010**, *46*, 841.

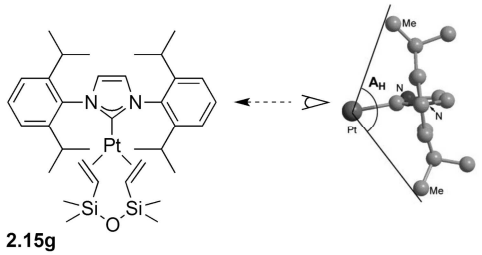

Figure 25. Depiction of Nolan's A_H angle. One of the aryl group and the diene ligand are omitted for clarity.

While the A_L angle and the percent buried volume do not correlate with the β-(*E*)/α ratio, the A_H angle proves to be nicely related to the regioselectivity of the process (Figure 26).[30] To the best of our knowledge, it is the first time that this structural descriptor is correlated successfully to an observed reactivity and/or selectivity. This relationship indicates that the higher the steric hindrance of the NHC in the direction orthogonal to the carbene plane, the greater the regioselectivity. It is interesting to point out that the distinctive behavior of (I*p*Tol)Pt(dvtms) **2.15m** (vide supra), as compared to the other *N*-aryl substituted NHCs, is perfectly represented.

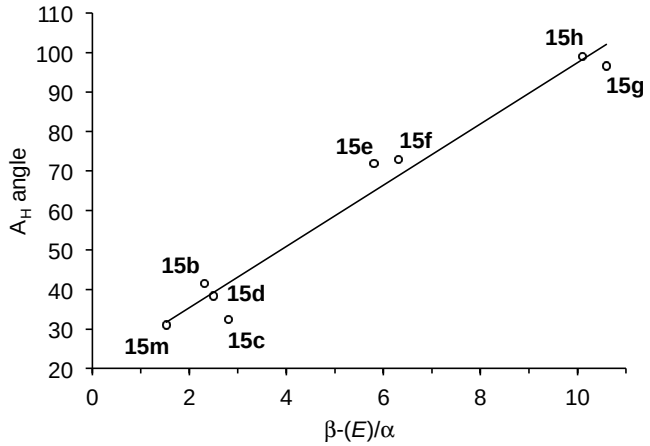

Figure 26. Correlation between the A_H angle and the β-(*E*)/α ratio obtained using these catalysts. R^2 = 0.965.

To further substantiate the validity of this correlation, we decided to probe the influence of the σ-donating ability of the NHC on the regioselectivity. For this purpose, the hydrosilylation of phenylacetylene by triethylsilane, under the standard conditions, was performed with three catalysts possessing the same limited steric hindrance but completely different electronic properties (Figure 27).[30] As can be seen, identical selectivities were obtained, despite the fundamental differences between the catalysts, thereby reinforcing our proposal that the regioselectivity of the hydrosilylation of alkynes is controlled essentially by steric parameters. It is noteworthy that the major isomer obtained in this case is the α adduct. This is not surprising since arylacetylenes are known to lead preferentially to regio-isomers opposite to those obtained during the reaction of alkylacetylenes.

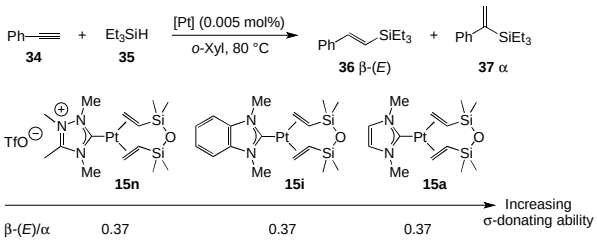

Figure 27. Influence of the σ-donating ability of the NHC on the regioselectivity.

5.2 Influence of the Silane on the Regioselectivity

The electronic and steric nature of the silane is usually decisive for the control of the selectivity of catalytic hydrosilylations. Therefore, the hydrosilylation of 1-octyne (**2.31**), in the presence of various silanes and under the usual conditions was studied (Table 6).[30] Due to his previous success, (IPr)Pt(dvtms) **2.15g** was selected to catalyze this reaction. However, since the effect of the silane should be assessed without interference of the NHC sterics, we performed the reactions with $PtCl_2$(cod), a source of platinum(0) species devoid of a bulky ligand, as control experiments. Whereas the influence of the electronic properties

of the silane is difficult to rationalize,[33] its steric hindrance proved again to be important. Indeed, the bulkier the silane, the higher the β-(*E*)/α ratio.

Table 6. Influence of the silane on the regioselectivity in the hydrosilylation of 1-octyne.

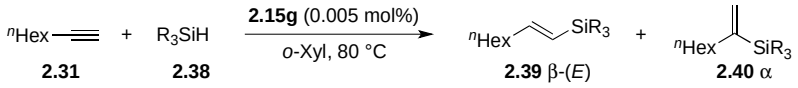

2.31 **2.38** **2.39** β-(*E*) **2.40** α

entry	silane	β-(*E*)/α[(a)]	time (h)	conversion (%)[(b)]
1	*t*-BuMe$_2$SiH	1 (1)	92	85
2	(EtO)$_3$SiH	2	150	>99
3	(Me$_3$SiO)Me$_2$SiH	4.3 (3.2)	3	54
4	Et$_3$SiH	6.3 (2.8)	42	87
5	(Me$_3$SiO)$_2$MeSiH	10.6 (2.9)	6	>99
6	Me$_2$PhSiH	11.5 (5.3)	22	>99
7	Ph$_3$SiH	15.7 (20)	22	88

[a] Ratio determined by GC analysis (gas chromatography) of the crude reaction mixture. Results obtained with PtCl$_2$(cod) are reported in brackets. [b] Conversion determined by GC analysis.

5.3 A Second Generation Catalyst for the Hydrosilylation of Alkynes

Despite the encouraging results obtained in the hydrosilylation of 1-octyne (**2.31**) with the (IPr)Pt(dvtms) catalyst **2.15g**, the *N*-heterocyclic carbene platinum complexes did not perform better than the catalysts employing bulky phosphines.[34] Specifically, the high

[33] The electronic effect of alkoxy groups on silicon does not correlate in a simple way with their electronegativity and their influence is difficult to rationalize.

[34] For selected examples, see: reference 24b, a) P. J. Murphy, J. L. Spencer, G. Procter, *Tetrahedron Lett.* **1990**, *31*, 1051. b) K. Takahashi, T. Minami, Y.

temperatures required to achieve completion and the initiation period, significantly longer than for 1-octene (**2.2**), have to be improved. Building upon our knowledge about the mechanism of the initiation step and since isomerization of the substrate is no longer an issue (see Section 4.3.1), we synthesized complex (IPr)Pt(AE) **2.45** (Figure 28).[21b] This platinum derivative is an analog of (IPr)Pt(dvtms) **2.15g**, in which the strongly binding dvtms ligand is replaced by the more labile diallyl ether (**2.43**), as in **2.24** (see Figure 13).

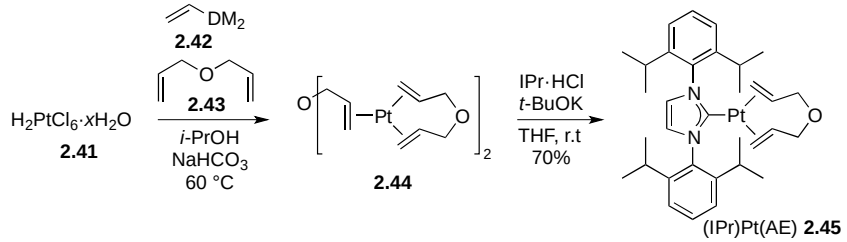

Figure 28. Synthesis of (IPr)Pt(AE) complex 2.45 starting from chloroplatinic acid.

This second generation catalyst rapidly showed its value and, after a small optimization of the reaction conditions, outstanding results were obtained in the hydrosilylation of 1-octyne (**2.31**) with bis(trimethylsilyloxy)methylsilane (**2.3**) (Figure 29).[35] The outcome of the reaction revealed it to be rather sensitive to catalyst loading and a significant decrease in selectivity was observed when less than 0.05 mol% of **2.45** was used. This observation will prove to be important for the complete elucidation of the mechanism (see Section 5.5).

Ohara, T. Hiyama, *Tetrahedron Lett.* **1993**, *34*, 8263. c) S. E. Denmark, Z. Wang, *Org. Lett.* **2001**, *3*, 1073. d) K. Itami, K. Mitsudo, A. Nishino, J.-I. Yoshida, *J. Org. Chem.* **2002**, *67*, 2645. e) W. Wu, C.-J. Li, *Chem. Commun. 2003*, 1668. f) H. Aneetha, W. Wu, J. G. Verkade, *Organometallics* **2005**, *24*, 2590. g) A. Hamze, O. Provot, J. D. Brion, M. Alami, M. *Synthesis* 2007, 2025. h) A. Hamze, O. Provot, J.-D. Brion, M. Alami, *Tetrahedron Lett.* **2008**, *49*, 2429. i) J. Montenegro, J. Bergueiro, C. Saá, S. López, *Org. Lett.* **2009**, *11*, 141.

[35] G. Berthon-Gelloz, J.-M. Schumers, G. De Bo, I. E. Markó, *J. Org. Chem.* **2008**, *73*, 4190.

Furthermore, dramatic rate acceleration was achieved using solventless conditions, without affecting the reaction yield and selectivity.[36]

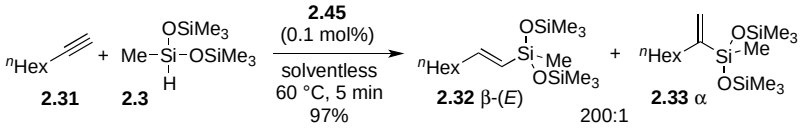

Figure 29. Optimized conditions for the hydrosilylation of 1-octyne (2.31) by MD'M (2.3) using second generation catalyst 2.45.

5.4 Functional Group Tolerance and Substrate Scope

Having optimized the conditions, the scope and limitations of this second generation catalyst **2.45** was investigated (Table 7).[35] The hydrosilylation of 1-octyne with dimethylphenylsilane proceeded with a rate and a selectivity similar to those observed using MD'M (**2.3**) (entry 1). However, the ratio of regioisomers was significantly improved in the case of phenylacetylene (entry 2 vs 3). It is worth noting that the β-(*E*) adduct is the major product under these conditions, in stark contrast to what was observed in Figure 27. This result is important for a good understanding of the reaction mechanism (see Section 5.5). Gratifyingly, free alcohols and amines, as well as ester functions, are tolerated by the catalytic system and no silylated alcohols or amines could be detected in the reaction mixture (entries 4–7). Benzylpropargyl ether proved to be a particularly challenging substrate, requiring long reaction times and leading to low selectivities if less than 1 mol% of **2.45** is used (entry 8). Finally, trimethylsilylacetylene is easily hydrosilylated to afford a *trans* bis-silyl ethylene species, an interesting building block for subsequent synthetic applications (entry 9).

[36] Similar observations were made by Stone, see: reference 24b.

Table 7. Hydrosilylation of terminal alkynes catalyzed by complex 2.45.

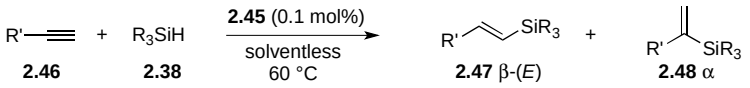

entry	major product	time (h)[a]	ratio[b] β-(*E*)/α	yield (%)[c]
1	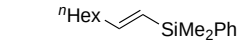	0.1	50:1	93
2		4	16:1	95
3	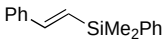	2	100:1	94
4		0.1	32:1	94
5	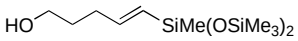	0.2	100:1	97
6	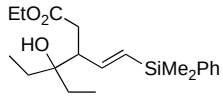	0.25	>20:1[d]	94
7[e]	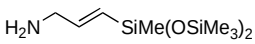	6	>20:1[d]	90
8[f]	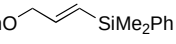	0.1	16:1	94
9	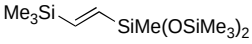	0.1	25:1	96

[a] Time for complete conversion determined by GC analysis. [b] Ratio of regioisomers determined by GC analysis of the crude reaction mixture. [c] Isolated yield of the mixture of regioisomers. [d] Ratio of regioisomers determined by ^{1}H NMR analysis of the crude reaction mixture. [e] 0.5 mol% of catalyst was used. [f] 1 mol% of catalyst was used, THF (1 mol L^{-1}), 20 °C.

The excellent regioselectivities obtained for terminal alkynes prompted us to investigate the much more challenging, and rather under developed, hydrosilylation of internal alkynes (Table 8).[35] While the hydrosilylation of 2-nonyne with bis(trimethylsilyloxy)methylsilane (**2.3**) affords modest discrimination between the methyl group and the *n*-hexyl chain (entry 1), the use of more sterically demanding silanes improves this selectivity issue (entries 2–4). Diphenylchlorosilane proved to be the best choice, affording a 6:1 ratio of the position isomers **2.50**/**2.51** (entry 5). Increasing the steric bias between the two substituents of the triple bond increases the regioselectivity to useful levels, even with MD'M (**2.3**). The newly incorporated silyl moiety being positioned further away from the bulkiest group (entries 1 vs 6–10). At this stage, minor electronic effects, that could influence this selectivity, have not been identified with certainty. It is worth noting that the presence of a quaternary carbon center adjacent to the alkyne does not preclude coordination of the triple bond to the catalyst (entry 6). Interestingly, a diethyl acetal protecting group is tolerated, in contrast to what is observed with the Karstedt's catalyst (**2.1**) (entry 9).

Table 8. Hydrosilylation of internal alkynes catalyzed by complex 2.45.

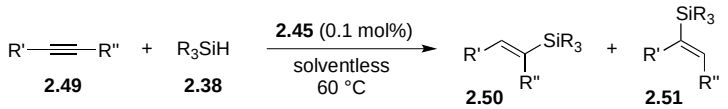

entry	major product	time (h)[a]	ratio[b] β-(*E*)/α	yield (%)[c]
1	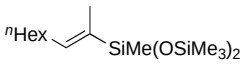	1	2:1	84
2	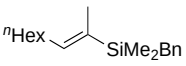	0.5	3.3:1	75
3	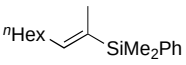	0.5	3.6:1	80
4	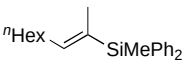	0.5	4.4:1	85
5	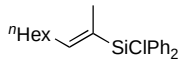	2	6.0:1	80
6	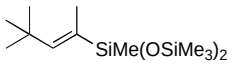	0.25	9:1	87
7	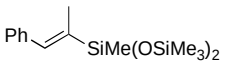	5	24:1	90
8	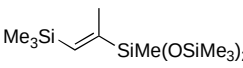	0.75	16:1	92
9[d]	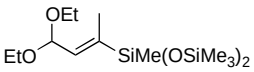	4	5:1[e]	75
10	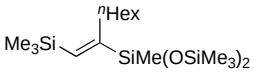	6	23:1	87

[a] Time for complete conversion determined by GC analysis. [b] Ratio of regioisomers determined by GC analysis of the crude reaction mixture. [c] Isolated yield of the mixture of regioisomers. [d] 0.5 mol% of catalyst was used, THF (1 mol L^{-1}). [e] Ratio determined by ^1H NMR analysis of the crude reaction mixture. [f] 1 mol% of catalyst was used.

Gratifyingly, (IPr)Pt(AE) **2.45** has also been used to catalyze the hydrosilylation of an elaborate 1,3-enyne **2.52** during the total synthesis of lactimidomycin by Fürstner (Figure 30).[37] The high selectivity observed for the addition of the silane onto the internal alkyne, instead of the terminal olefin, likely originates from the preferential coordination of the platinum(0) complex to alkynes. It is interesting to point out that the vinylsilanes obtained through hydrosilylation of alkynes with MD'M (**2.3**) are competent partners in the Hiyama–Denmark cross-coupling reaction.[35,38]

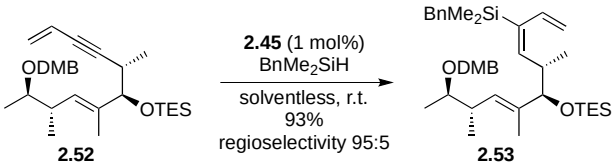

Figure 30. Hydrosilylation of a 1,3-enyne during the total synthesis of lactimidomycin.

5.5 Mechanistic Studies

5.5.1 Qualitative Kinetic Studies

The kinetic profile observed for the hydrosilylation of 1-octyne (**2.31**) catalyzed by (IPr)Pt(AE) **2.45** is presented in Figure 31.[35] The monitoring of the reaction was conducted at room temperature in order to obtain a more accurate definition of the curve. The sigmoidal shape

[37] D. Gallenkamp, A. Fürstner, *J. Am. Chem. Soc.* **2011**, *133*, 9232.

[38] a) Denmark have demonstrated that related disiloxanes give high yields in cross-coupling reactions under both fluoride-promoted and fluoride-free conditions: S. E. Denmark, C. S. Regens, *Acc. Chem. Res.* **2008**, *41*, 1486. b) For the seminal publication by Hiyama, see: Y. Hatanaka, T. Hiyama, *J. Org. Chem.* **1988**, *53*, 918. c) For a review about the Hiyama coupling, see: S. E. Denmark, R. F. Sweis, in *Metal-Catalyzed Cross-Coupling Reactions 2nd edition*; A. de Meijere, F. Diederich, ed.; Wiley-VCH, Weinheim, 2004, vol. 1, p 163.

strongly suggests that the mechanism of alkynes hydrosilylation proceeds *via* an activation process similar to the one observed in the case of the alkenes (see Figure 12). This activation period is greatly reduced when the labile diallyl ether ligand is employed. During the study of alkynes hydrosilylation, a decline of the activity and of the selectivity *during the course of the reaction* has been regularly observed,[22] indicating that a background hydrosilylation pathway is probably operating at a slower rate and with a lower selectivity. Moreover the extent of this competitive mechanism increases with time, at the expense of the principal catalytic cycle. Further support for this side reaction can be gathered in the fact that increasing the catalyst loading significantly improves the β-(*E*)/α ratio whilst decreasing the time necessary to reach completion.

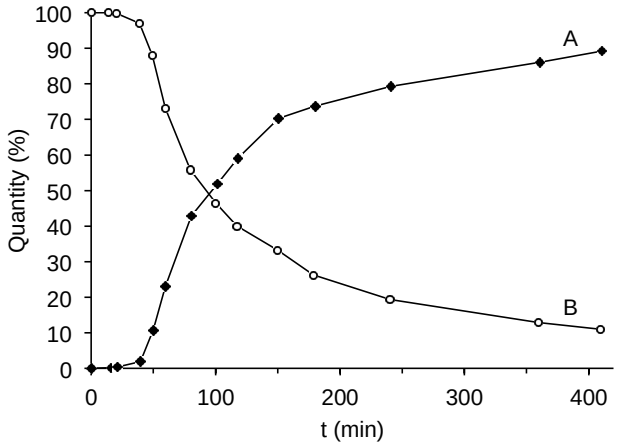

Figure 31. Kinetic profile for the hydrosilylation of 1-octyne (**2.31**) by MD'M (**2.3**) catalyzed by (IPr)Pt(AE) **2.45**. Curve (A): yield of the β-(*E*) isomer **2.32**. Curve (B): 1-octyne conversion. Reaction conditions: MD'M (1 mol L^{-1}), 1-octyne (1 mol L^{-1}), (IPr)Pt(AE) **2.45** (0.1 mol %), THF, 20 °C.

In order to collect more information about the mechanism of the reaction, we devised three independent experiments in which the three reactants (the alkyne, the silane and the catalyst) where incubated two by two at 60 °C for 3 h, before addition of the third component at 20 °C.[35] The results of these experiments are presented in Figure 32. As

can be seen, the addition of complex **2.45** to a mixture of alkyne and silane displays a kinetic profile identical to what was observed previously (curve A). However, when the silane was added to the alkyne, previously incubated with the precatalyst, a considerable reduction of the catalytic activity occurred (curve B). It thus transpires that the alkyne triggers somehow the deactivation of the catalyst. In stark contrast, a dramatic acceleration of the reaction rate, concomitant with the disappearance of the induction period, was observed when the catalyst was heated with the silane *prior to addition of the alkyne* (curve C). This last effect is reminiscent of what was observed upon repeated addition of fresh reactants during the hydrosilylation of alkenes (see Figure 11). Therefore, treating the precatalyst with a silane *before* adding the alkyne leads to a particularly active and selective catalyst.

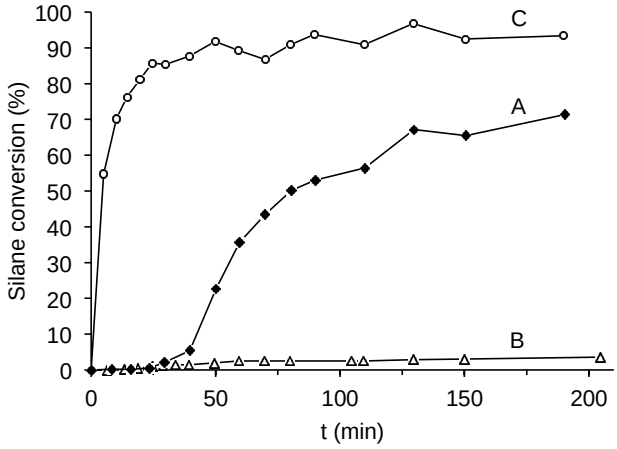

Figure 32. Effect of the different reaction components on the catalyst activation period. Curve (A): MD'M (**2.3**) and 1-octyne (**2.31**) for 3 h at 60 °C, followed by addition of (IPr)Pt(AE) **2.45** at 20 °C. Curve (B): (IPr)Pt(AE) **2.45** and 1-octyne (**2.31**) for 3 h at 60 °C, followed by addition of MD'M (**2.3**) at 20 °C. Curve (C): Reaction of (IPr)Pt(AE) **2.45** and MD'M (**2.3**) for 3 h at 60 °C, followed by addition of 1-octyne (**2.31**) at 20 °C. Reaction conditions: MD'M (1 mol L^{-1}), 1-octyne (1 mol L^{-1}), (IPr)Pt(AE) **2.45** (0.1 mol%), THF.

5.5.2 Catalyst Activation and Deactivation Pathways

Interested by the results of these qualitative kinetic studies, we undertook the isolation of the compounds produced under these conditions. To study the deactivation pathway, benzylpropargyl ether, a strongly binding alkyne we encountered during the study of the scope of this reaction, was selected (see Table 7). Unfortunately, the reaction between this alkyne and compound **2.45** leads to complex mixtures from which no single component could be isolated. Following this process by ^{1}H NMR, indicates that after several hours at 40 °C, the signals corresponding to the chelated diallyl ether have completely disappeared (Figure 33).[35] The region of the spectrum where the signals of the IPr methyl groups are located displays a multitude of peaks, characteristic of a complex mixture. More significantly, the signals corresponding to the imidazolium cation **2.54** appear, suggesting that the NHC is displaced from the coordination sphere of the metal and is protonated, probably by residual water.[39] The loss of the NHC from the Pt-complex generates probably alkyne-coordinated platinum species that can still promote hydrosilylation, albeit with reduced activity and regioselectivity. This deactivation pathway can be almost completely suppressed by adding slowly the alkyne to a mixture of the silane and the precatalyst.[12d]

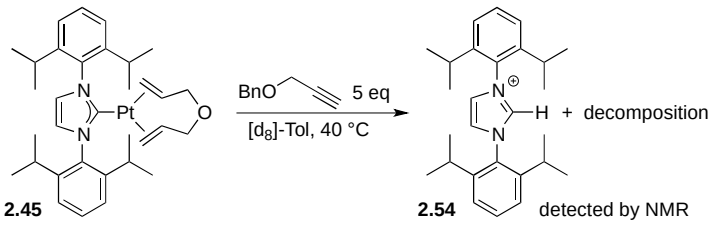

Figure 33. Deactivation of (IPr)Pt(AE) 2.45 by benzylpropargyl ether.

[39] The loss of NHC type ligands has been observed before, see: C. M. Crudden, D. P. Allen, *Coord. Chem. Rev.* **2004**, *248*, 2247.

Next, the activation pathway promoted by the silane was investigated. Whilst the reaction between (ICy)Pt(dvtms) **2.15c** and bis(trimethylsilyloxy)methylsilane (**2.3**) produced smoothly the dimer **2.25** (see Figure 15), treating the second generation derivative **2.45** with MD'M (**2.3**) generated a complex mixture upon attempted purification. Replacing MD'M by phenyldimethylsilane led to the bis-silyl complex **2.55** (Figure 34).[40] This compound is the first purely tricoordinated platinum(II) complex ever isolated. The full scope and application of this intermediate in hydrosilylation is explored in Chapter 3.

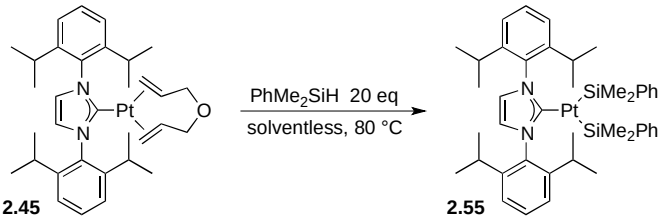

Figure 34. Synthesis of bis-silyl platinum carbene species 2.55.

5.5.3 Proposed Mechanism

Based upon the information gathered throughout these studies, a reasonable mechanism for the hydrosilylation of alkynes promoted by (IPr)Pt(AE) **2.45** can be proposed (Figure 35). Whilst reminiscent of the Chalk and Harrod mechanism (see Figure 3), it differs in several aspects.[10] During the activation period, the diallyl ether ligand of the precatalyst **2.45** is hydrosilylated to afford the active species **H**. Afterwards, the silane coordinates to the platinum(0) catalyst and undergoes an oxidative addition yielding the platinum(II) complex **J**. A 1,2-migratory insertion follows, leading to the alkenyl platinum compound **K**. Subsequently, a reductive elimination of the vinylsilane **2.47** completes the primary catalytic cycle and regenerates the catalyst

[40] G. Berthon-Gelloz, B. de Bruin, B. Tinant, I. E. Markó, *Angew. Chem. Int. Ed. 2009*, *48*, 3161.

H. The origin of the selectivity in favor of the β-(*E*) regioisomers remains unclear. We assume that upon coordination of the alkyne, two isomers **J** and **J'** can be formed and are most probably in equilibrium. In complex **2.57**, the larger substituent of the triple bond is facing the bulky carbene, generating repulsive steric interactions and shifting the equilibrium towards its isomer **J**. Accordingly, the subsequent hydride insertion produces almost exclusively intermediate **K**. Moreover, this adduct is thermodynamically favored over its regioisomers **K'** because of the reduced steric repulsion between IPr and the alkenyl substituent. Unfortunately, the alkyne can trigger several deactivation pathways by bonding strongly to the platinum(0) metal. Both precatalyst **2.45** and catalyst **H** can be transformed into the complex **2.57**. While being inactive, this intermediate can lose its NHC ligand yielding unidentified platinum species **L**. These catalysts enter a secondary catalytic cycle that displays lower activity and selectivity, presumably due to the lack of a bulky controlling ligand.

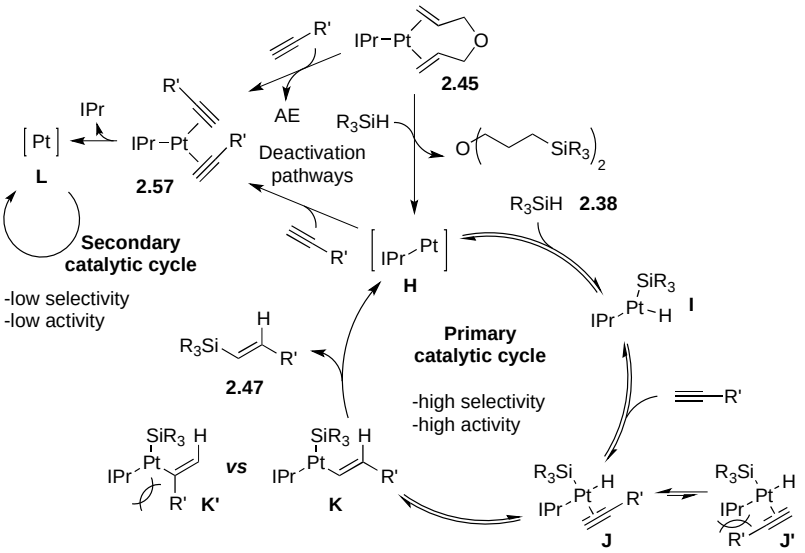

Figure 35. Proposed mechanism for the hydrosilylation of alkynes catalyzed by (IPr)Pt(AE) 2.45.

6. Conclusions

With the desire to address the shortcomings pertaining to the use of the Karstedt catalyst and its derivatives, our laboratory has developed since 1998 a whole family of *N*-heterocyclic carbene platinum(0) catalysts. These complexes are able to catalyze the hydrosilylation of alkenes and alkynes with high activities, exquisite stereoselectivities (up to above 100:1) and low catalyst loading (down to 0.005 mol%). They tolerate a wide range of functionalities and protecting groups that are rapidly decomposed by other catalysts. Moreover, they are readily available, insensitive towards air and moisture, bench-stable for extended periods of time and easy to handle. These qualities make them the ideal user-friendly catalysts for hydrosilylation. Indeed, all the reagents are mixed directly from their bottles and stirred in air without any special precaution. Since 2012, some of these catalysts are commercially available from Umicore AG (visit chemistry.umicore.com).

Chapter 3

New Platinum *N*-Heterocyclic Carbene Complexes for Catalytic Hydrosilylation

This Chapter will present some of our results on the hydrosilylation of carbon–carbon unsaturations catalyzed by *N*-heterocyclic carbene platinum(0) complexes. Furthermore, we will disclose how – on our journey to our objectives – intuitions, detailed mechanistic studies and serendipity proved to be key elements in the discovery of a new generation of precatalysts. Our progress toward the application of our silyl adducts in the synthesis of allenylsilanes, β-aminosilanes, and cyclopropane derivatives will also be discussed.

1. Origin and Objectives of this Research Project

During his master thesis, Dr. Jean-Marc Schumers achieved the synthesis of (*E*) 1,2-bis(silyl)vinyl species **3.3** through the hydrosilylation of silylated alkynes **3.1** with MD'M (**3.2**) catalyzed by (IPr)Pt(AE) (Figure 1, see also Chapter 2).[1,2] At the onset of this Ph.D. thesis, we recognized the efficiency of this reaction as well as the synthetic potential of these

[1] a) J.-M. Schumers, *Master thesis*, Université catholique de Louvain, 2006. b) G. Berthon-Gelloz, J.-M. Schumers, G. De Bo, I. E. Markó, *J. Org. Chem.* **2008**, *73*, 4190.

[2] For the preparation of such compounds without hydrosilylation, see: a) H. Ohmiya, H. Yorimitsu, K. Oshima, *Angew. Chem. Int. Ed.* **2005**, *44*, 3488. b) G. Auer, M. Oestreich, *Chem. Commun.* **2006**, 311.

products.[3] Therefore, we decided to further explore further this research topic and set out to (i) establish the substrate scope of the reaction, (ii) extend the methodology to the addition of other silanes, (iii) confirm that steric effects are controlling the stereoselectivity of the process and (iv) study the synthetic potential of building blocks **3.3** for the preparation of allenylsilanes.

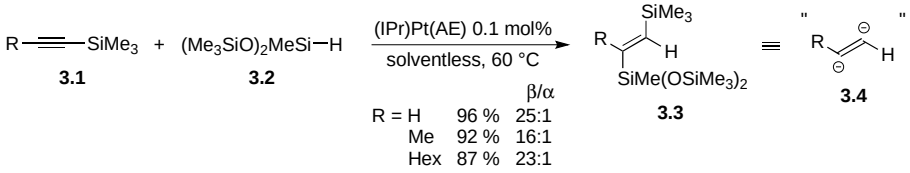

Figure 1. Hydrosilylation of silylated alkynes with MD'M.

2. Preparation of the Starting Materials

2.1 Synthesis of (IPr)Pt(dvtms) and (IPr)Pt(AE)

Obviously, to start this research project, we had to prepare the 2nd generation NHC platinum(0) complex (IPr)Pt(AE), required to catalyze the hydrosilylation of silylated alkynes. Additionally, we undertook the synthesis of the 1st generation precatalyst (IPr)Pt(dvtms) to enable comparison experiments. These two compounds were made in two steps starting from hexachloroplatinic acid and the corresponding carbene IPr.[4]

[3] For the synthetic utility of these species beyond Hiyama cross-coupling, see: a) I. Fleming, T. W. Newton, V. Sabin, F. Zammattio, *Tetrahedron* **1992**, *48*, 7775. b) M. Murakami, H. Oike, M. Sugawara, M. Suginome, Y. Ito, *Tetrahedron* **1993**, *49*, 3933. c) C. Thiot, C. Mioskowski, A. Wagner, *Eur. J. Org. Chem.* **2009**, 3219. d) D. Lee, S. J. Danishefsky, *J. Am. Chem. Soc.* **2010**, *132*, 4427. e) P. Pawluc, *Catal. Commun.* **2012**, *23*, 10.

[4] a) G. Berthon-Gelloz, O. Buisine, J.-F. Brière, G. Michaud, S. Stérin, G. Mignani, B. Tinant, J.-P. Declercq, D. Chapon, I. E. Markó, *J. Organomet. Chem.* **2005**, *690*, 6156. b) G. Berthon-Gelloz, J.-M. Schumers, F. Lucaccioni, B. Tinant, J. Wouters, I. E. Markó, *Organometallics* **2007**, *26*, 5731.

For the preparation of IPr•HCl (**3.7**), the imidazolium salt of IPr, the condensation of 2,6-diisopropylaniline (**3.5**) with aqueous glyoxal was carried out in methanol with excellent yields (Figure 2). During previous work in our lab, the resulting diazadiene **3.6** was transformed into the imidazolium salt **3.7**, in low yields, using a combination of paraformaldehyde and either (i) a dry solution of anhydrous hydrogen chloride in ethyl acetate[5] or (ii) aqueous tetrafluoroboric acid in toluene.[1a] This transformation could be dramatically improved with the use of trimethylsilyl chloride in ethyl acetate, according to a protocol disclosed by Hintermann.[6]

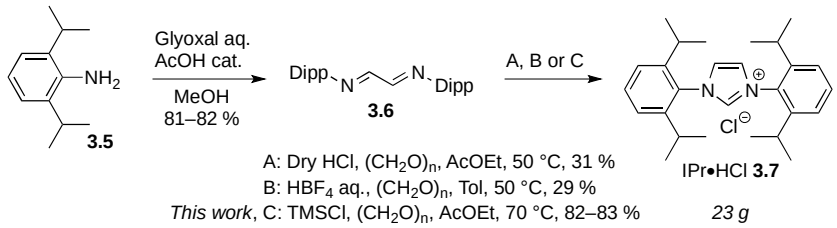

Figure 2. Synthesis of the imidazolium salt IPr•HCl.

Having secured a large scale and high yielding access to carbene precursor **3.7**, we turned our attention to the synthesis of NHC platinum(0) complexes. Initially, using a standard protocol,[1a] we easily prepared (IPr)Pt(dvtms) (**3.10**) through a ligand exchange on the Karstedt's catalyst (**3.9**),[7] itself obtained from hexachloroplatinic acid (**3.8**) (Figure 3).[8]

5 G. De Bo, *Master thesis*, Université catholique de Louvain, 2004.
6 L. Hintermann, *Beilstein J. Org. Chem.* **2007**, 3:22.
7 B. D. Karstedt, US Patent 3,775,452 (1973).
8 S. Dierick, G. Bastug, I. E. Markó, *Org. Synth.*, Accepted for checking.

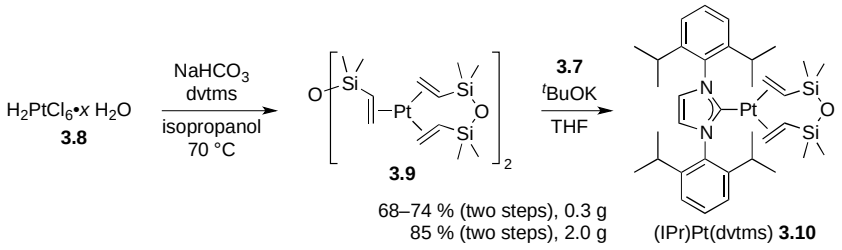

Figure 3. Synthesis of (IPr)Pt(dvtms).

Next, accessing (IPr)Pt(AE) (**3.12**) proved to be particularly troublesome though the synthetic sequence depicted in Figure 4 previously afforded the desired complex in 70 % yield.[4b] As we attempted to reproduce these experiments, we were initially restrained to 9–16 % yield. In order to improve these disappointing results, we examined the influence of the following reaction parameters: $Pt^{(IV)}$ source, water quantity, addition time, degassed isopropanol and inert atmosphere, concentration of the reagents and reaction time.[9] Finally, simply adding all the reagents at room temperature *before* heating the reaction mixture increased the yield to 42 %. Unfortunately, we were not able to improve further this procedure.

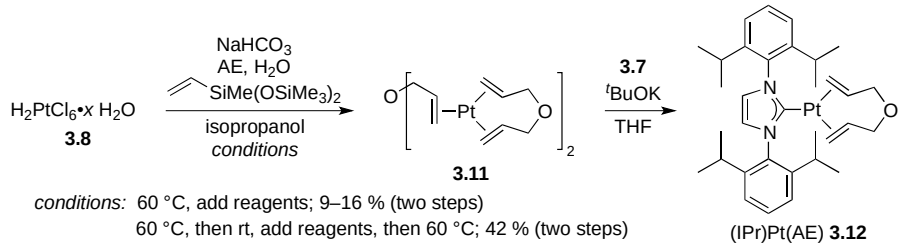

Figure 4. Synthesis of (IPr)Pt(AE).

Assuming that the problem encountered in the preparation of (IPr)Pt(AE) (**3.12**) was caused by the instability of intermediate **3.11**, we envisioned a different approach based upon the replacement of the divinyltetramethyldisiloxane ligand of **3.10** by diallyl ether (Table 1).

[9] The Author warmly thanks Mr. Fabio Lucaccioni for helpful discussions about the preparation of complexes **3.10** and **3.12**.

Merely stirring complex **3.10** with several equivalents of diallyl ether in absence of solvent did not displace the dvtms ligand, even under heating (entry 1). This confirmed that vinylsilanes bind more strongly to electron-rich transition metals than simple alkenes (see Chapter 2). As an alternative to the direct substitution, we tried to selectively destabilize and/or destroy dvtms through the introduction of some additives in the reaction mixture (entries 2–5). Unfortunately, we never observed any conversion. Nonetheless, a positive information could be extracted from these negative results, that is the stability of (IPr)Pt(dvtms) (**3.10**) under highly acidic or basic conditions.

Table 1. Attempts to convert (IPr)Pt(dvtms) into (IPr)Pt(AE).

(IPr)Pt(dvtms) **3.10** $\xrightarrow[conditions]{AE}$ (IPr)Pt(AE) **3.12**

entry	conditions	AE (equiv)	conversion
1	Solventless, 1 d, 60 °C	50	0 %
2	TBAF (3 equiv), THF, 2 d	5	0 %
3	TBAF (3 equiv), AcOH (2 equiv), THF, 2 d	5	0 %
4	NaOH (12 equiv), MeOH/THF 2:1, 5 d	5	0 %
5	AcOH/THF/H_2O 4:3:1, 3 d	5	0 %

2.2 Synthesis of Silylated Alkynes

At the time this project begun, the functional group tolerance of (IPr)Pt(dvtms) and (IPr)Pt(AE) under the hydrosilylation conditions was already well-established (see Chapter 2).[1b] Consequently, we undertook the synthesis of three families of silylated alkynes, devoided of functional group (Figure 5). With derivatives **3.13a–e** and **3.14a–e**, we planned to study the influence of the silyl group versus an *n*-hexyl chain or a phenyl ring, respectively. In contrast, compounds **3.15a–d** and **3.13a**, having a trimethylsilyl portion, should enable us to determine the steric impact of the carbon substituent. In the end, the review of their hydrosilylation outcome with various silanes would help

us to (i) establish the substrate scope of the reaction, (ii) extend the methodology to other silanes and (iii) confirm that steric hindrance controls stereoselectivity.

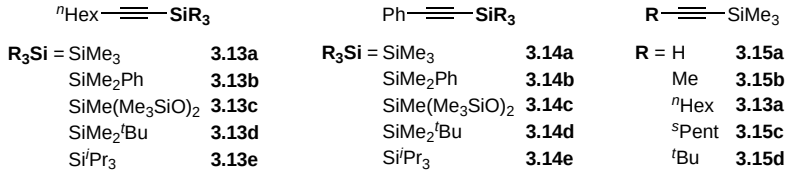

Figure 5. Three families of silylated alkynes with various steric hindrance.

All these substrates were prepared according to a standard protocol (Table 2). Thus, deprotonation of the corresponding alkynes **3.16** with *n*-butyllithium in cold tetrahydrofuran was followed by the capture of the resulting lithium acetylides **3.17** with the appropriate silyl chloride. Compounds **3.15a,b** being commercially available, they did not have to be synthesized.

All the alkynes **3.16** and the silyl chlorides that were needed were commercially available, except for bis(trimethylsilyloxy)methylsilyl chloride (**3.19**). However, this electrophile is readily accessible from the corresponding silane, MD'M (**3.2**), by a palladium(0) mediated exchange reaction with allyl chloride **3.18** (Figure 6).[10]

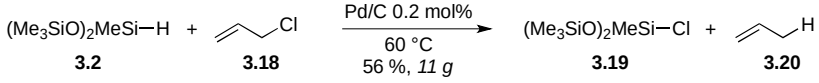

Figure 6. Synthesis of bis(trimethylsilyloxy)methylsilyl chloride.

[10] Y. M. Pai, K. L. Servis, W. L. Weber, *Organometallics* **1986**, *5*, 683.

Table 2. Synthesis of silylated alkynes.

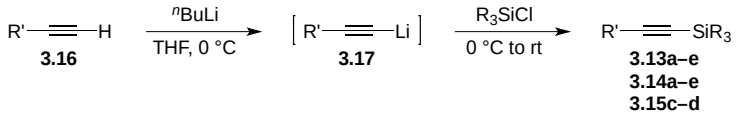

entry	R'	R_3Si	product	yield[(a)]
1	^{n}Hex	Me_3Si	**3.13a**	97 %
2	^{n}Hex	$PhMe_2Si$	**3.13b**	95 %
3	^{n}Hex	$(Me_3SiO)_2MeSi$	**3.13c**	98 %
4	^{n}Hex	$^{t}BuMe_2Si$	**3.13d**	98 %
5	^{n}Hex	$^{i}Pr_3Si$	**3.13e**	93 %
6	Ph	Me_3Si	**3.14a**	90 %
7	Ph	$PhMe_2Si$	**3.14b**	92 %
8	Ph	$(Me_3SiO)_2MeSi$	**3.14c**	51 %
9	Ph	$^{t}BuMe_2Si$	**3.14d**	43 %
10	Ph	$^{i}Pr_3Si$	**3.14e**	21 %
11	^{s}Pent	Me_3Si	**3.15c**	95 %
12	^{t}Bu	Me_3Si	**3.15d**	70 %[(b)]

[a] Isolated yield after aqueous work-up and removing of the volatiles, GC purity > 95 %. [b] Isolated yield after distillation, GC purity > 99 %.

3. An Unexpectedly Challenging Class of Substrates

3.1 Unpromising first results

At the very beginning of this work, the established protocol for the hydrosilylation of alkynes catalyzed by NHC platinum(0) complexes was the following:[1b]

> *"A mixture of silane (1.1 equiv) and alkyne (1 equiv) was dissolved in the appropriate solvent (1.0 mol L^{-1}, solvent can be omitted) and brought to 60 °C. To this mixture was added (IPr)Pt(AE) (THF solution, 10 mg mL^{-1}, 0.1 mol%). The reaction was heated until judged complete by GC analysis."*

Likewise, we applied these experimental conditions (without solvent) for the hydrosilylation of our three families of silylated alkynes. The results are collected in Table 3.[11] When R_3Si is a trimethylsilyl group, increasing the steric hindrance of the carbon on the other side of the triple bond decreases the selectivity (entries 1,8,9), excepted for R' = Ph, which gives poorer selectivity (entry 5). In the *n*-hexyl series, whilst replacing the TMS substituent by a *tert*-butyldimethylsilyl moiety is beneficial (entries 1 vs 4), the use of electron-withdrawing groups on silicon is detrimental (entries 1,4 vs 2,3). Finally, for the phenylacetylenes, an electron-withdrawing silyl group decreases the selectivity as well as, unexpectedly, a triisopropylsilyl substituent. Overall, the reactions are sluggish and afford disappointing levels of selectivity. Furthermore, we always observed an erosion of selectivity

[11] We determined which regioisomer is formed by comparing the chemical shift of the vinylic proton to known compounds. We then confirmed by a rigorous analysis of the coupling constants.

during the course of the reaction, particularly in the phenyl series or for electron-withdrawing silyl groups.

Table 3. Hydrosilylation of silylated alkynes.

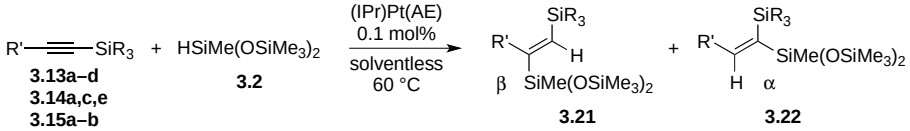

3.13a–d
3.14a,c,e
3.15a–b

3.2

3.21

3.22

entry	R'	R_3Si	reaction time	β/α[(a)]	conversion[(b)]
1	^{n}Hex	Me_3Si	18 h	11:1	100 %
2	^{n}Hex	$PhMe_2Si$	3 d	4:1	100 %
3	^{n}Hex	$(Me_3SiO)_2MeSi$	4 d	3:1	100 %
4	^{n}Hex	$^{t}BuMe_2Si$	2 d	12:1	96 %
5	Ph	Me_3Si	1.5 d	8:1	100 %
6	Ph	$(Me_3SiO)_2MeSi$	2 d	4:1	61 %
7	Ph	$^{i}Pr_3Si$	14 d	3:1	60 %
8	H	Me_3Si	3 h	21:1	100 %
9	Me	Me_3Si	7 h	14:1	100 %

[a] Determined by ^{1}H NMR of the crude reaction mixture. [b] Calculated by GC.

Assuming that the mechanism described for the hydrosilylation of terminal alkynes is still operating with silylated alkynes (see Chapter 2 and Figure 7), the following conclusions can be drawn:

- Silylated alkynes appear to bind more tightly to platinum(0) than simple alkynes and hence promote the corresponding deactivation pathways. This effect can certainly be linked to the lower energy of their LUMO.[12] Consequently, the secondary catalytic cycle is more important, resulting in slower and less selective hydrosilylations. This observation is in good agreement with the erosion of selectivity noticed during these reactions.

[12] The same effect is observed between olefins and vinylsilanes, see Chapter 2.

Furthermore, this phenomenon is reinforced in the phenyl series or for silyl groups bearing electron-withdrawing substituents.

- Increasing the steric bulk of the alkynes dramatically extends the reaction time. This could be attributed to increased steric interactions in intermediates **3.27** and **3.29**, which probably disfavor the coordination of the triple bond and slow the 1,2-migratory insertion step.
- The regioselectivity is apparently governed by a steric differentiation between the R' and R_3Si substituents in intermediates **3.27** and **3.29** (see Chapter 2). However, when the silicon atom is substituted by electron-withdrawing groups, the LUMO is further lowered and the deactivation pathways become more competitive. This leads to lower selectivities, despite the increased steric hindrance of the silyl group. The same trend is observed when comparing *n*-hexyl- and phenylacetylenes.
- Finally, the bulky triisopropylsilyl group afforded very low selectivity, for unknown reason.

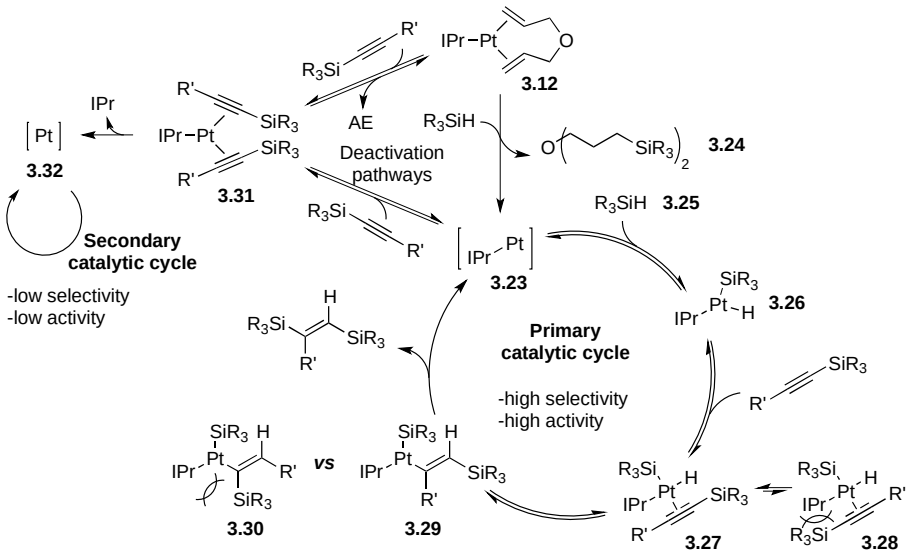

Figure 7. Proposed mechanism for the hydrosilylation of silylated alkynes catalyzed by (IPr)Pt(AE).

At this stage, it is also important to wonder if the regioselectivity might also be governed by an electronic effect of the silyl substituent rather than by a simple steric bias. Indeed, the silyl group induces a polarization of the triple bond as depicted in Figure 8. However, recent work of Ferreira,[13] Sumida and Hosoya[14] in the hydrosilylation of internal alkynes catalyzed by platinum(0) and palladium(0) complexes (Chalk–Harrod mechanism, see Chapter 1), supports the insertion of the hydride onto the more electron-poor position of the unsaturation. Hence, the silyl substituent electronically favors the opposite regioisomer. Nonetheless, both steric and electronic factors could be reconciled if an alternative catalytic cycle, based upon a silylmetallation step from intermediate **3.34**, reminiscent of an Ojima–Crabtree mechanism, is operational. Unfortunately, such a proposal appears unlikely since a silylmetallation has never been observed, or even postulated, for platinum(0) catalyzed hydrosilylation.[15] Furthermore, insertion reactions involving a hydrogen atom are usually much faster than those involving any other elements.[16]

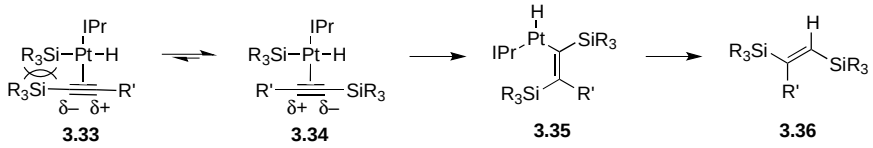

Figure 8. Unlikely mechanistic alternative for silylated alkynes hydrosilylation.

3.2 Optimization of the Reaction Conditions

Frustrated by our results obtained when hydrosilylating silylated alkynes, we considered the reagents purity, the glassware cleanliness, and we performed the reaction under an inert atmosphere using

[13] a) D. A. Rooke, E. M. Ferreira, *J. Am. Chem. Soc.* **2010**, *132*, 11926. b) D. A. Rooke, E. M. Ferreira, *Angew. Chem. Int. Ed.* **2012**, *51*, 3225.
[14] Y. Sumida, T. Kato, S. Yoshida, T. Hosoya, *Org. Lett.* **2012**, *14*, 1552.
[15] J. Y. Corey, *Chem. Rev.* **2011**, *111*, 863.
[16] R. H. Crabtree, *The Organometallic Chemistry of the Transition Metals*; Wiley: Hoboken, 2005, p 60.

degased reagents. No improvements were noticed. Therefore, we focused our efforts on the optimization of the reaction parameters, selecting trimethylsilyl phenylacetylene (**3.14a**) as our standard substrate. Our major findings are collected in Table 4. At the onset, it was found that performing the reaction in tetrahydrofuran had a deleterious effect on the selectivity and the time of reaction (entry 2 vs 1). Concerning the reagents addition order, as silylated alkynes are poisoning the precatalyst, we stirred the silane with (IPr)Pt(AE) (**3.12**) before the addition of the substrate (entry 3 vs 1). This led to an improvement in both the reaction rate and selectivity. Focusing on this interesting activation effect, we increased the temperature further (entry 4 vs 3). Albeit this was beneficial for the reaction time, the amount of unidentified side products unfortunately increased as well. The use of phenyldimethylsilane, a bulkier silane, decreased the reaction time and slightly improved the regioselectivity (entry 5 vs 3). However, diphenylmethylsilane, although more selective, was less active and produced more side products (entry 6 vs 3). Our last improvement consisted in raising the catalyst loading from 0.1 to 1 mol% (entry 7 vs 3). The reaction time was dramatically reduced while a good regioselectivity was retained. The purity of the crude product was also slightly improved. Interestingly, lowering the temperature decreased the rate of the reaction but the selectivity levels were maintained (entry 8 vs 7). At that moment, we ran out of precatalyst (IPr)Pt(AE) (**3.12**). Therefore, it was decided to test the 1st generation (IPr)Pt(dvtms) catalyst (**3.10**) in our optimized conditions (entry 9 vs 7). **Surprisingly, both complexes afforded similar results.** The activation time of the precatalyst was then varied and two hours appeared to be the optimum (entries 10 and 11 vs 9).

In summary, we improved the hydrosilylation of silylated alkynes by (i) stirring the silane and precatalyst together during 2 h before adding the substrate, (ii) increasing the loading of precatalyst from 0.1 to 1 mol% and (iii) replacing bis(trimethylsilyloxy)methyl silane by phenyldimethylsilane.

Table 4. Optimization of the hydrosilylation of trimethylsilyl phenylacetylene.

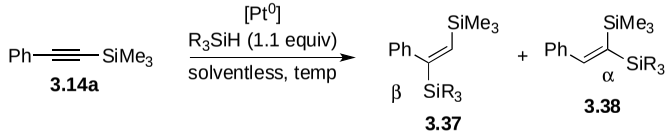

entry	[Pt^0] (mol%)	silane	activation time[a] (h)	temp (°C)	reaction time (h)	β/α[b]	crude purity[c] (%)	yield[d] (%)
1	(IPr)Pt(AE) 0.1	MD'M	0	60	36	8:1	n.d.	(100)
2[e]	(IPr)Pt(AE) 0.1	MD'M	0	60	>48	2.5:1	n.d.	(82)
3	(IPr)Pt(AE) 0.1	MD'M	2	60	18	10:1	91	87
4	(IPr)Pt(AE) 0.1	MD'M	2	80	4	10:1	78	69[f]
5	(IPr)Pt(AE) 0.1	$PhMe_2SiH$	2	60	3	12:1	96	60[g]
6	(IPr)Pt(AE) 0.1	Ph_2MeSiH	2	60	16	17:1	61	13[h]
7	(IPr)Pt(AE) 1	MD'M	2	60	3	10:1	95	84
8	(IPr)Pt(AE) 1	MD'M	2	40	12	10:1	96	88
9	(IPr)Pt(dvtms) 1	MD'M	2	60	3	10:1	94	88
10	(IPr)Pt(dvtms) 1	MD'M	4	60	5	10:1	94	83
11	(IPr)Pt(dvtms) 1	MD'M	1	60	4	10:1	95	86

[a] Time of activation of the precatalyst by the silane, before addition of the substrate. [b] Determined by ^{1}H NMR of the crude mixture. [c] Determined by GC. [d] Isolated yield after filtration over a plug of silica gel/celite/$MgSO_4$, GC purity > 95 %, (conversion calculated by GC). [e] Reaction performed in THF (1 mol L^{-1}). [f] GC purity = 84 %. [g] Due to a mistake upon purification. [h] Product degraded upon distillation.

3.3 A 3rd Generation of Precatalysts

While the accelerating effect of the increased catalytic loading is easily understandable, we were not able to explain the reason why better results are obtained when phenyldimethylsilane is employed instead of bis(trimethylsilyloxy)methylsilane. Furthermore, the activation effect of the silane on the precatalyst would have been challenging to rationalize if the two different precatalysts would not have performed similarly.[17] Indeed, this information suggests that, upon activation, both (IPr)Pt(dvtms) (**3.10**) and (IPr)Pt(AE) (**3.12**) lead to a common intermediate which is the real catalyst (or precatalyst) of the reaction.

In order to confirm our hypothesis, we undertook the isolation of this putative common intermediate. For that purpose, (IPr)Pt(dvtms) was reacted with MD'M during 2 h at 60 °C and the excess of silane was removed under reduced pressure (Figure 9). Unfortunately, the resulting yellow solid, washed with the silane, was very sensitive to air. Nevertheless, a ^{1}H NMR spectrum could be obtained. Though it was not very clean, it suggested that the carbene IPr was still coordinated to the platinum. Furthermore, there were siloxane proton signals but no trace of double bond.

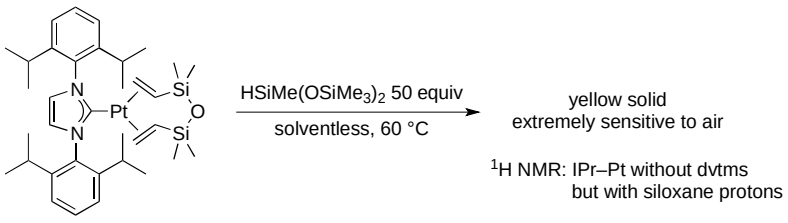

(IPr)Pt(dvtms) **3.10**

Figure 9. Reaction between (IPr)Pt(dvtms) and MD'M.

[17] At the time these experiments were conducted, the Author was not aware of the similar activation effect reported in Chapter 2.

Accordingly to these findings, it was postulated that the new compound was a (IPr)Pt complex bearing several silyl ligands. These observations indicated that the yellow solid might be an analog of the bis-silyl platinum complex **3.39**, previously isolated in our group (Figure 10).[18] It is worth noting that both generations of platinum precatalysts, under similar conditions, afford the same bis-silyl complex as previously postulated.

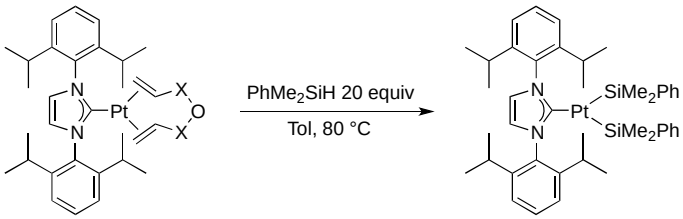

Figure 10. Isolation of a bis-silyl platinum complex.

Consequently, we synthesized (IPr)Pt($SiMe_2Ph$)$_2$ (**3.39**) and submitted this complex to the hydrosilylation of trimethylsilyl phenylacetylene (**3.14a**), stirring **3.39** with MD'M during 1 min before the addition of the substrate (Figure 11). Rewardingly, we observed the same outcome as when (IPr)Pt(AE) and (IPr)Pt(dvtms) were used in our optimized conditions (2 h activation). This result confirms that a bis-silyl platinum complex is indeed the common intermediate that we previously proposed.

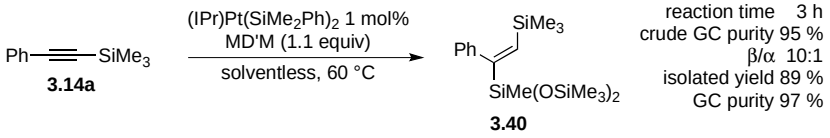

Figure 11. A bis-silyl platinum complex as hydrosilylation precatalyst.

[18] G. Berthon-Gelloz, B. de Bruin, B. Tinant, I. E. Markó, *Angew. Chem. Int. Ed.* **2009**, *48*, 3161.

According to these experimental results, we are now able to propose a mechanism for the hydrosilylation of alkynes when an activation effect is operating. Concerning this activation phase, Dr. Guillaume Berthon-Gelloz has demonstrated that the bis-silyl complex **3.39** requires an olefin or an alkyne in order to release its silyl ligands (vide infra).[19] Therefore, if we assume the same requirement, notwithstanding the nature of these ligands, the activation consists in the complete conversion of the precatalysts **3.10** or **3.12** into the new precatalyst **3.42** (Figure 12).

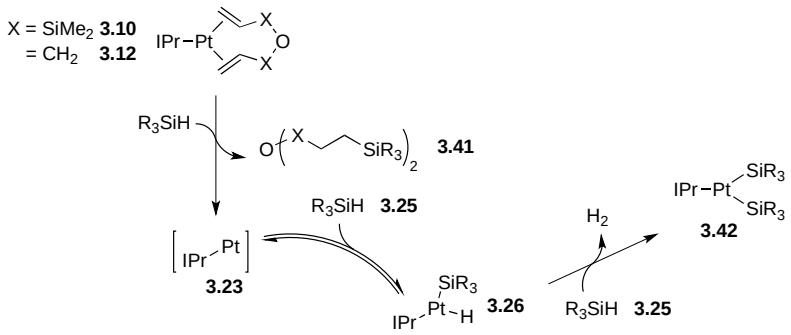

Figure 12. Activation phase.

Regarding the hydrosilylation phase – i.e. after adding the alkyne – the bis-silyl platinum complex **3.42** is able to enter the same classical catalytic cycle already described in Section 3.1 (Figure 13). However, two major differences appear here: (i) the precatalyst **3.42** is converted into **3.26** much more rapidly than the classical 1st and 2nd generation precatalysts **3.10** and **3.12** (vide infra) and (ii) there is one less deactivation pathway, since the precatalyst **3.42** is activated upon coordination of an alkyne and not deactivated as for **3.10** and **3.12** (Figure 7).

[19] G. Berthon-Gelloz, *Ph.D. thesis*, Université catholique de Louvain, 2007.

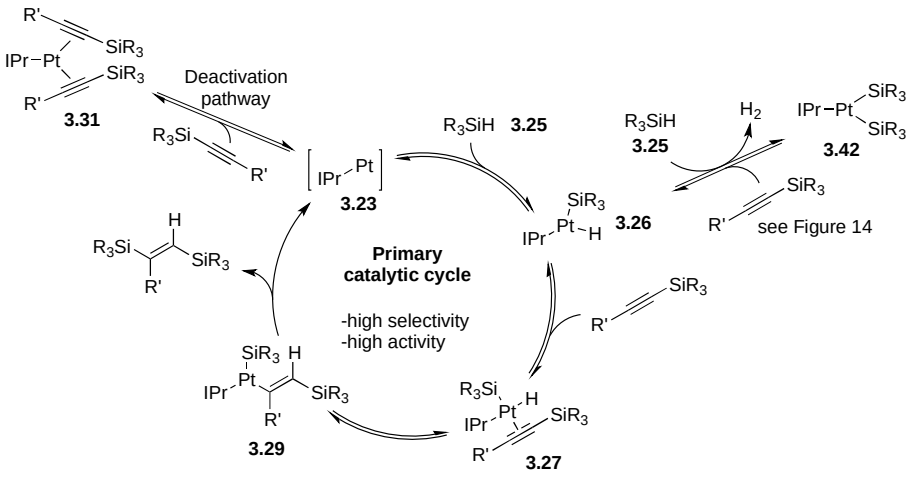

Figure 13. Hydrosilylation phase.

The two last points deserve some explanations. During his studies, Dr. Guillaume Berthon-Gelloz noticed that the addition of diallyl ether to complex **3.39** produced the parent complex **3.12**, bis-silylated diallyl ether **3.44** and the bis-silane **3.45** (Figure 14).[19] This observation suggests that two pathways are available for the precatalyst **3.39** to enter into the hydrosilylation catalytic cycle through the complex **3.43**: (i) a direct reductive elimination of bis-silane **3.45** or (ii) a bis-silylation of the incoming π-ligand. Moreover, kinetic studies have established that bis-silyl platinum complex **3.39** displays a much shorter induction period than diallyl ether complexes **3.12**.

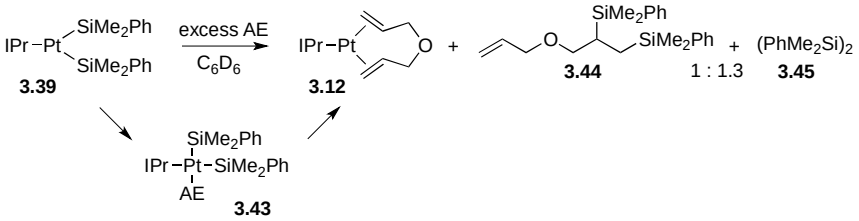

Figure 14. Reaction between bis-silyl complex 3.39 and diallyl ether.

This working mechanism has helped us to improve further our hydrosilylation protocol. Indeed, it is obvious that maintaining the

alkyne concentration as low as possible should limit the access to the deactivation pathway and hence the secondary catalytic cycle. Therefore, we added the substrate slowly using a syringe pump and observed a noticeable increase in regioselectivity (Figure 15).[20] The reaction was complete in less than 15 min after the end of the addition.

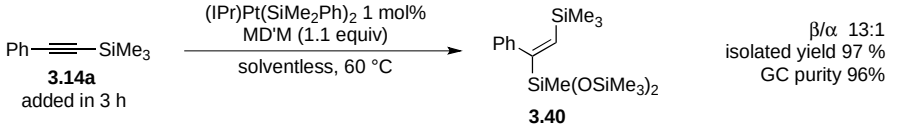

Figure 15. Slow-addition of trimethylsilyl phenylacetylene.

Finally, realizing that we had potentially in hand a 3rd generation of hydrosilylation platinum precatalysts, we decided to compare the three generations under the same conditions – i.e. by adding all the reagents at the same time – and using a fairly simple substrate: phenylacetylene (**3.14a**) (Table 5).[11] It rapidly transpired from these experiments that bis-silyl platinum complex **3.39** is indeed a potent hydrosilylation precatalyst, not only more efficient than the older precatalysts **3.10** and **3.12** in the difficult hydrosilylation of silylated alkynes, but also for the easier to hydrosilylate terminal alkynes.

Table 5. Comparison of the three generations of platinum precatalysts.

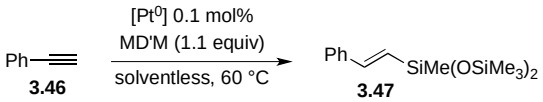

entry	precatalyst	reaction time (min)	β/α[a]	yield[b]
1	(IPr)Pt(dvtms)	420	12:1	95 %
2	(IPr)Pt(AE)	240	16:1	95 %
3	(IPr)Pt($SiMe_2Ph$)$_2$	60	>20:1	96 %

[a] Determined by ^{1}H NMR. [b] Isolated yield after filtration through a plug of silica gel/celite/$MgSO_4$, GC purity > 95 %.

[20] The increased yield is attributed to a better purification protocol.

3.4 Exploring the Potential of the 3rd Generation of Precatalysts

Recognizing that the complexes (IPr)Pt(SiR_3)$_2$ (**3.42**) are exceptional hydrosilylation precatalysts, we set out to explore their potential. However, the single isolated member of this family, (IPr)Pt($SiMe_2Ph$)$_2$ (**3.39**), could not be stored for more than one or two days. The only possibility is to keep it away from light and under high vacuum in a sealed ampoule. Therefore, we resolved to use the more convenient activation pathway of the (IPr)Pt(dvtms) **3.10** by the silane, hence generating the 3rd generation of precatalysts in situ for all our future hydrosilylations.

3.4.1 Silylated Alkynes

The outcome of the hydrosilylation of silylated alkynes by our methodology is presented in Table 6. For every substrate the selectivities and yields were excellent. Interestingly, whereas an *n*-hexyl or a phenyl substituent directed the incoming silyl group at the β position and afforded the expected (*E*) bis-silylvinyl products (entries 1 and 3),[8] a bulky *tert*-butyl group led to the opposite regioisomer (entry 2). This is in line with our selectivity model in which the more sterically demanding side of the unsaturation is placed in front of the hydride ligand in intermediate **3.27** (see Figure 7). We were also pleased to notice that arylsilanes were perfectly tolerated and led to a further increase in regioselectivity (entries 4,5). Finally, during the course of our studies toward the synthesis of allenylsilanes, we performed the hydrosilylation of propargylic alcohols (see Section 3.5). Though excellent regioselectivity was obtained for the primary alcohol (entry 6), the resulting vinylsilane proved to be particularly unstable, either thermally or on silica gel. The introduction of a cinnamyl side-chain stabilized the final product (entry 7), but resulted in a severe erosion of the regioselectivity due to the increased steric hindrance.

Table 6. Hydrosilylation of silylated alkynes.

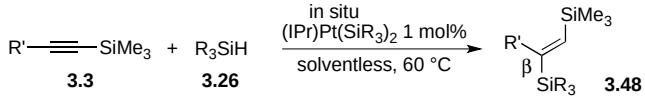

entry	R'	R_3SiH	β/α[a]	yield[b]
1[c]	^{n}Hex	$(Me_3SiO)_2MeSiH$	13:1	97 %
2	^{t}Bu	$(Me_3SiO)_2MeSiH$	1:14	82 %
3	Ph	$(Me_3SiO)_2MeSiH$	13:1	97 %
4	Ph	$PhMe_2SiH$	19:1	88 %
5	Ph	Ph_2MeSiH	>20:1	90 %
6	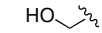	$(Me_3SiO)_2MeSiH$	>20:1	43 %[d]
7	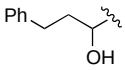	Ph_2MeSiH	4:1	61 %[e]

[a] Determined by ^{1}H NMR of the crude reaction mixture. [b] Isolated yield after filtration through a plug of silica gel/celite/$MgSO_4$, GC purity > 95 %. [c] 0.1 mol% catalyst was used. [d] Purification by column chromatography on silica gel. [e] Isolated yield of the pure β isomer after purification by column chromatography on silica gel.

3.4.2 Terminal Alkynes

The 3rd generation platinum precatalysts proved to be excellent reagents for the hydrosilylation of terminal alkynes, leading to exquisite selectivities for almost every substrate examined (Table 7, p 124). We first looked at the tolerance of the catalytic system toward various silanes. Surprisingly, triethylsilane afforded a relatively low regioselectivity level, though the yield was excellent (entry 1). We sought to improve this ratio by using the bulkier triisopropylsilane. Unfortunately, this resulted in the complete degradation of the reaction mixture (entry 2). However, we were pleased to discover that every other silane tested, including silyloxy-, aryl-, chloro- and alkoxysilanes, achieved outstanding yields and excellent selectivities (entries 3–11). It is noteworthy that the catalytic loading could be reduced to 0.01 mol% while still maintaining excellent selectivities (entries 5,6).[8] Moreover,

even phenylacetylene was successfully hydrosilylated (entry 12). Concerning functional group compatibility, alcohols, tertiary tosylamines and phtalimides were perfectly tolerated (entries 13–18). Finally, we were interested in the hydrosilylation of heteroatom substituted alkynes. Unfortunately, (phenylseleno)acetylene proved to be inert under our conditions (entry 19).

It is important to point out that the reaction of tosylamine derivative **3.51** (entry 16) represents three challenges: (i) both unsaturations can be hydrosilylated, (ii) the 1,6-enyne system might poison the catalyst by chelation and (iii) the double bond could direct the reversible 1,2-migratory insertion toward the α isomer (see Chapter 1). Accordingly, we introduced this substrate in one portion and increased the catalytic loading to 1 mol%. We were pleased to notice that there was no trace of hydrosilylation of the double bond and that the vinylsilane could be obtained with excellent regioselectivity. The perfect discrimination between the alkene and the alkyne is putatively attributed to the higher coordinating ability of the latter (alkynes are stronger π-acids).[21]

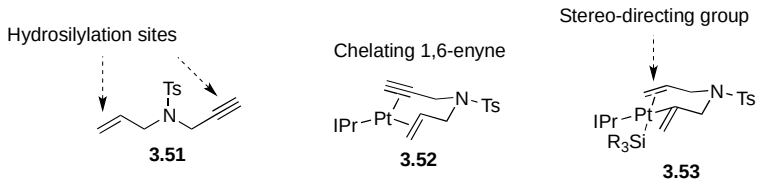

Figure 16. Challenges residing in the tosylamine 3.51.

[21] For similar selectivities in intermolecular version, see: C. A. Tsipis, *J. Organomet. Chem.* **1980**, *188*, 53.

Table 7. Hydrosilylation of terminal alkynes.

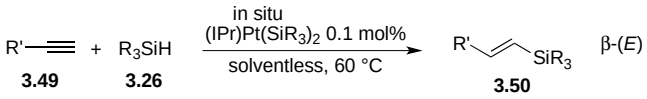

3.49 **3.26** **3.50**

entry	R'	R_3SiH	β(*E*)/α[a]	yield[b]
1	^{n}Hex	Et_3SiH	7:1	93 %
2[c]	^{n}Hex	$^i Pr_3SiH$	—	dec
3	^{n}Hex	$(Me_3SiO)Me_2SiH$	>20:1	94 %
4	^{n}Hex	$(Me_3SiO)_2MeSiH$	96:1[d]	98 %
5[e]	^{n}Hex	$(Me_3SiO)_2MeSiH$	41:1[d]	98 %
6[f]	^{n}Hex	$(Me_3SiO)_2MeSiH$	13.4:1[d]	92 %
7	^{n}Hex	$(Me_3SiO)_3SiH$	>20:1	96 %
8[g]	^{n}Hex	$PhMe_2SiH$	>20:1	86 %
9	^{n}Hex	Ph_2MeSiH	>20:1	96 %
10[h]	^{n}Hex	Ph_2ClSiH	>20:1	87 %
11[e,i]	^{n}Hex	$(EtO)_2MeSiH$	>20:1	98 %
12[c]	Ph	$(Me_3SiO)_2MeSiH$	>20:1	91 %
13		$(Me_3SiO)_2MeSiH$	>20:1	95 %
14		$(Me_3SiO)_2MeSiH$	>20:1	98 %
15	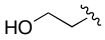	$PhMe_2SiH$	>20:1	97 %
16[c,j]	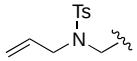	$PhMe_2SiH$	14:1	82 %[k]
17[g]	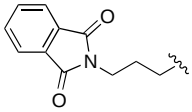	$PhMe_2SiH$	>20:1	86 %[k]
18[g]		Ph_2MeSiH	>20:1	76 %[k]
19[c]	PhSe	$(Me_3SiO)Me_2SiH$	—	n.c.

[a] Determined by ^{1}H NMR of the crude reaction mixture. [b] Isolated yield after filtration through a plug of silica gel/celite/$MgSO_4$, GC purity > 95 %. [c] 1 mol% catalyst. [d] Determined by GC of the crude reaction mixture. [e] 0.03 mol% catalyst. [f] 0.01 mol% catalyst. [g] 0.05 mol% catalyst. [h] Quenched with ethanol/triethylamine and isolated as diphenylhexylethoxysilane. [i] Performed by Mr. Thibaut Debande during his Master thesis. [j] The alkyne was dissolved in THF (1 mol L^{-1}) and added in one portion. [k] Isolated yield after column chromatography on silica gel, GC purity > 95 %.

3.4.3 Alkenes

Naturally, we became interested in evaluating our 3rd generation of precatalysts in the hydrosilylation of alkenes (Table 8). This work has been done in collaboration with Ms. Emilie Vercruysse.[22] 1-Octene and (+)-β-citronellene were straightforwardly hydrosilylated by MD'M with complete regiocontrol (entries 1,2). Epoxides (readily open by classical catalysts) and alcohols were tolerated, as well as allyl ethers (entries 3,4). Since Dow Corning showed some interest in the hydrosilylation of allyl esters and acrylates,[23] we assessed these substrates (entries 5–7). Allyl hexanoate led to excellent results. On the other hand, allyl methacrylate easily polymerized and we had to introduced BHT as a radical inhibitor to achieve a good yield. We observed that vinyl ethers and esters were unreactive under our reaction conditions (entries 8,9). Surprisingly, an olefin bearing a nitrile group could not be hydrosilylated (entry 10), but we were able to achieve the hydrosilylation of a 1,1-disubstitued alkene (entry 11). Cyclohexene did not react, even if we increased considerably the catalyst loading and the temperature (entry 12).

[22] E. Vercruysse, *Master thesis*, Université catholique de Louvain, 2012.
[23] Dow Corning, personal communication 2010.

Table 8. Hydrosilylation of alkenes

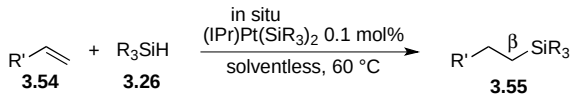

entry	alkene	R_3SiH	β/α[a]	yield[b]
1	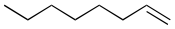	$(Me_3SiO)_2MeSiH$	>20:1	91 %
2	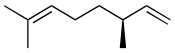	$(Me_3SiO)_2MeSiH$	>20:1	99 %
3	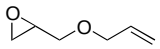	$(Me_3SiO)_2MeSiH$	>20:1	78 %[c]
4	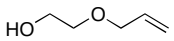	$(Me_3SiO)_2MeSiH$	>20:1	95 %[d]
5[e]	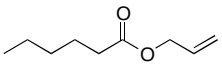	$(EtO)_3SiH$	>20:1	96 %
6[f]		$(EtO)_2MeSiH$	>20:1	86 %
7[g]	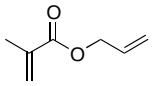	$(Me_3SiO)_2MeSiH$	>20:1	54 %[d]
8[h]	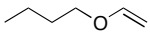	$PhMe_2SiH$	—	n.c.
9[h]	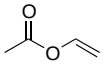	$PhMe_2SiH$	—	n.c.
10	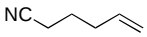	$(Me_3SiO)_2MeSiH$	—	n.c.
11[h]	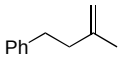	$(Me_3SiO)_2MeSiH$	>20:1	86 %
12[i]		$PhMe_2SiH$	—	n.c.

[a] Determined by ^1H NMR of the crude reaction mixture. [b] Isolated yield after filtration through a plug of silica gel/celite/$MgSO_4$, GC purity > 95 %. [c] Isolated yield after distillation, GC purity > 95 %. [d] Isolated yield after column chromatography on silica gel, GC purity > 95 %. [e] 0.05 mol% catalyst. [f] 0.025 mol% catalyst. [g] 1 mol% BHT introduced as radical inhibitor. [h] 1 mol% catalyst. [I] 5 mol% catalyst, 85 °C.

It is worthy of note that γ-functionalized propylsilanes, highly desired by the industry (see Chapter 1), could be accessed through our methodology. Indeed, as seen in Table 8, the hydrosilylation of allyl ethers and esters could be carried out in good yields and without degradation through π-allyl platinum intermediates. Therefore, Ms. Emilie Vercruysse studied the transformation of other allylic systems containing leaving groups of variable nucleofugacity.[22] Unfortunately, allyl chloride (**3.56**), allyl acetoacetate (**3.57**) and diethyl allyl phosphate (**3.58**) were completely unstable and led to the complete degradation of the reaction mixtures under our conditions (Figure 17).

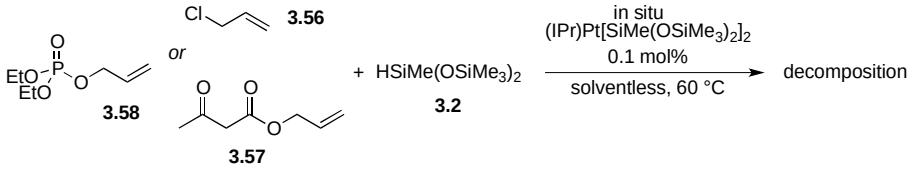

Figure 17. Attempts to hydrosilylate allylic system containing a leaving group.

We were intrigued by the reluctance of 5-hexenenitrile to undergo hydrosilylation (Table 8, entry 10). This phenomenon was attributed to a strong and non-productive coordination of the catalyst by the substrate. Indeed, there is a possibility for the nitrile function to bind to platinum through its nitrogen lone pair (**3.59**) or its π-system (**3.60**) (Figure 18). The second possibility is more likely since it would allow chelation using the carbon–carbon double bond.

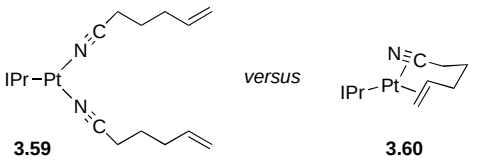

Figure 18. Proposed coordination mode of 5-hexenenitrile.

Thus, we sought to isolate a complex derived from the (IPr)Pt fragment and a nitrile ligand: 5-hexenenitrile, acetonitrile or adiponitrile. Unfortunately, a ligand exchange strategy starting from either (IPr)Pt(dvtms) (**3.10**) or (IPr)Pt($SiMe_2Ph$)$_2$ (**3.39**) proved to be unsuccessful (Figure 19).

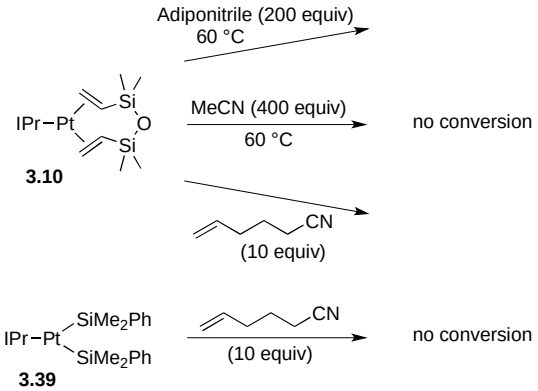

Figure 19. Attempts to isolate a platinum–nitrile complex.

3.4.4 Allenes

In the course of our efforts dedicated to the association of hydrosilylation and hydroamination reactions (see Section 3.6), we discovered an unexpected isomerization process. Interestingly, the hydrosilylation of a mixture of homopropargylic alcohol (**3.61**) and 2,3-butadiene-1-ol (**3.62**) afforded the β-(*E*) vinylsilane **3.63** without any trace of other stereoisomers or allylsilanes (Figure 20). The nearly quantitative yield of **3.63** led us to postulate that isomerization of the internal double bond of the allene should have taken place.

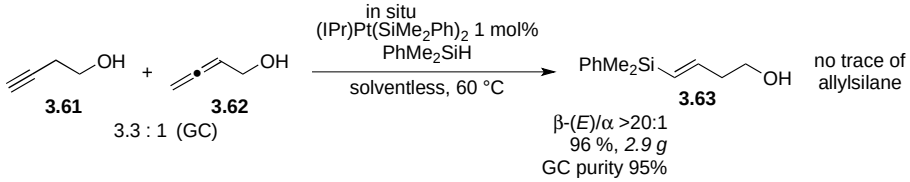

Figure 20. Concomitant isomerization–hydrosilylation processes.

The same reaction was repeated on 1,2-nonadiene (**3.64**). Surprisingly, we obtained a mixture of (*E*) allylsilane **3.65**, (*Z*) allylsilane **3.66** and α vinylsilane **3.67**. As there is no trace of β-(*E*) vinylsilane in the reaction mixture, isomerization should not have taken place in this specific case. This experiment suggests that, in the previous transformation, the isomerization of allene **3.62** occurs prior to the hydrosilylation step. Indeed, if it happened otherwise, we should have detected the regioisomer opposite to **3.63**, i.e. the α vinylsilane**.**

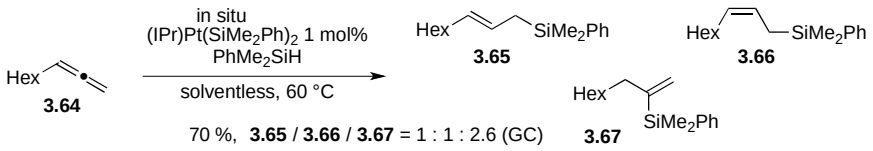

Figure 21. Hydrosilylation of 1,2-nonadiene.

As for the formation of the three isomers **3.65**–**3.67**, and assuming the mechanism described in Figure 13, all the potential complexes preceding the 1,2-migratory insertion step, which determines the regio- and stereoselectivity, are represented in Figure 22. After careful examination, it rapidly transpires that intermediates **3.68**, **3.70** and **3.73** are disfavored. Indeed, they all suffer from severe steric repulsions between the IPr carbene and the *n*-hexyl substituent of the allene. In contrast, species **3.71**, **3.72**, **3.77** and **3.78** are free of destabilizing steric interactions. Intriguingly, complex **3.75**, which apparently does not undergo steric congestion, as it is similar to **3.71** and **3.72**, is probably not formed during the reaction. Otherwise, the resulting vinylsilane **3.76** would have been observed. It is interesting to note that the preferred intermediates **3.71**, **3.72**, **3.77** and **3.78** are formed on an essentially statistical distribution basis, though the two formers complexes are slightly favored.

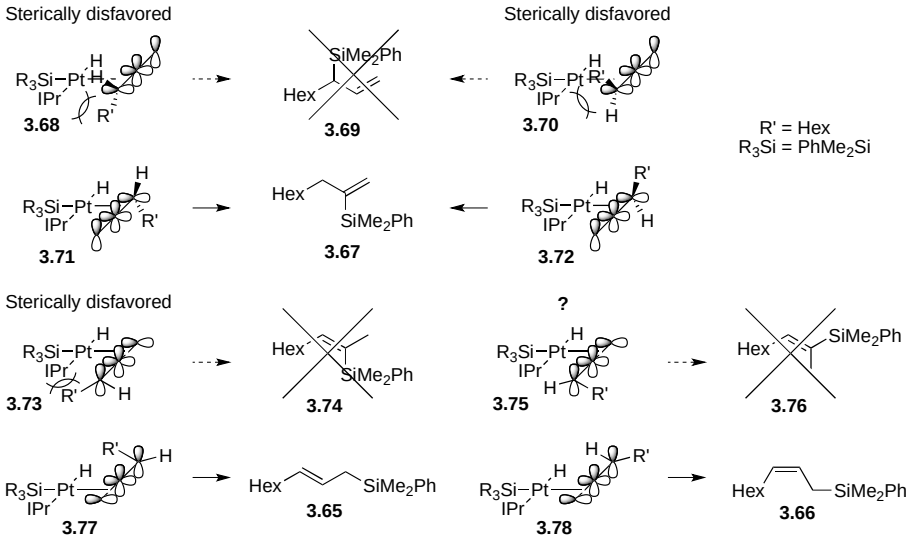

Figure 22. Potential complexes preceding the pivotal 1,2-migratory insertion step.

These results suggest that the free alcohol function of **3.62** is probably responsible for the isomerization process. Therefore, in an attempt to underpin the role played by the hydroxyl substituent, we protected the mixture of **3.61** and **3.62** as their silyl ethers **3.79** and **3.80**. A subsequent hydrosilylation afforded four compounds (Figure 23). Whilst the β-(*E*) vinylsilane **3.81** arises from the stereoselective hydrosilylation of the homopropargylic silyl ether **3.79**, products **3.82**–**3.84** originate from the allene **3.80**.[24] Based upon the hydrosilylation of 1,2-nonadiene (**3.64**), the theoretical ratio of products should be as follow: **3.81** / **3.82** / **3.83** / **3.84** = 18 : 2.6 : 1 : 1. The observed selectivity ratio being rather close to these values, it appears that protecting the alcohol function suppresses the isomerization pathway.[25] Therefore, a free hydroxyl substituent is required to drive this transformation.

[24] The α vinylsilane **3.82** is certainly not resulting from the hydrosilylation of **3.79** in reason of the outstanding regioselectivity usually obtained for such substrates (see Table 7 and Figure 20).

[25] The difference between the theoretical and the measured ratios are attributed to the lack of accuracy of the ^{1}H NMR integrations.

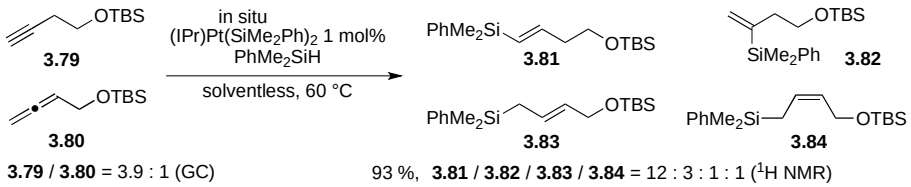

Figure 23. Hydrosilylation of silyl ethers 3.79 and 3.80.

Since our reaction conditions are definitely not basic or acidic enough to trigger the isomerization of the allene into the propargylic system, we propose the occurrence of a classical 1,2-migratory insertion–β-hydride elimination mechanism involving the vinyl-platinum intermediate **3.86** (Figure 24). Accordingly, our experiments imply that the β-hydride elimination toward derivatives **3.89** must occur faster than the competitive reductive eliminations leading to the allyl- and vinylsilanes when R' = OH ($k_{iso} > k_{\alpha}$). Furthermore, we know that the hydrosilylation of terminal alkyne largely favors the β-(*E*) vinylsilanes **3.91** (see Section 3.4.2). Conversely, when R' = OTBS or *n*-Pent, the β-hydride elimination is slower than the reductive eliminations ($k_{iso} < k_{\alpha}$).

In order to explain these kinetic differences, we can speculate on the inductive effects of the substituents. In stark contrast to what we have observed, it has been reported that electron-withdrawing groups slow down the β-hydride elimination from platinum(II) complexes.[26] Given the lack of the isomerization when the silyl ether **3.80** is employed, it is tempting to attribute the isomerization proficiency of **3.62** to the coordinating ability of its alcohol function. Unfortunately, β-hydride elimination from complex **3.87** should be disfavored. Indeed, square planar 16-electron complexes of platinum(II) are particularly reluctant to form 18-electron complexes and, without a prior ligand dissociation, no elimination would occur.[26,27]

[26] E. J. Alexanian, J. F. Hartwig, *J. Am. Chem. Soc.* **2008**, *130*, 15627.
[27] G. M. Whitesides, J. F. Gaasch, E. R. Stedronsky, *J. Am. Chem. Soc.* **1972**, *94*, 5258.

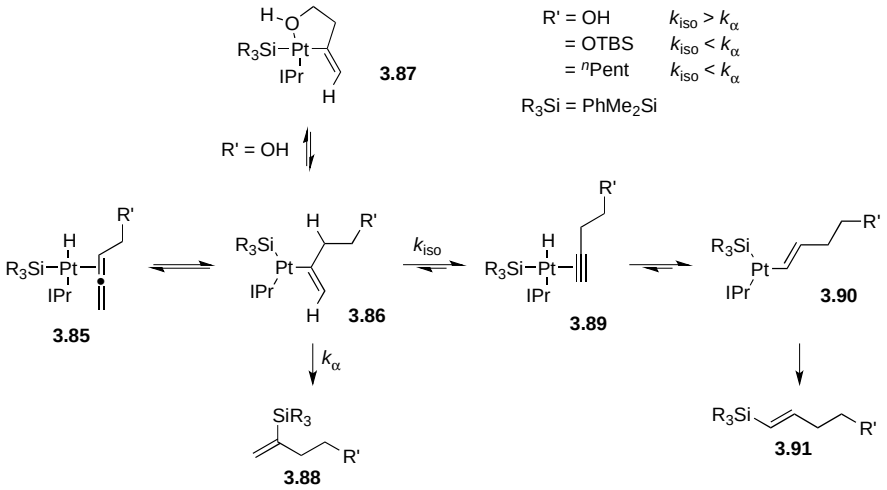

Figure 24. Proposed mechanism for the isomerization of allene derivatives.

3.5 Combining Hydrosilylation and Peterson Elimination

Allenylsilanes are promising building blocks for organic synthesis.[28] However, the lack of a general, flexible, enantioselective and mild access to these reagents has partially hampered their development.[28b,29] At the onset of this thesis, we envisioned to study and demonstrate the synthetic potential of building blocks **3.3** by their transformation into allenylsilanes (**3.94**). Indeed, the hydrosilylation of the propargylic alcohol **3.92** should afford the (*E*) 2,3-bis(silyl)allyl alcohol species **3.93**, which through a subsequent Peterson elimination would deliver the expected allenylsilanes **3.94**.[30,31] It is noteworthy that, if the starting alcohol **3.92** is optically enriched, then the chiral information will be transferred to the final product, affording optically active allene **3.94**.[32] Furthermore, by selecting the conditions of the elimination step – acidic

[28] For selected reviews about allenylsilanes, see: a) J. S. Panek, C. E. Masse, *Chem. Rev.* **1995**, *95*, 1293. b) J. A. Marshall, B. W. Gung, M. L. Grachan, in *Modern Allene Chemistry*; N. Krause, A. S. K. Hashmi, eds; Wiley-VCH: Weinheim, 2004, p 527.

[29] For selected recent methodologies, see reference 3d and: a) S. P. Marsden, P. C. Ducept, *Beilstein J. Org. Chem.* **2005**, 1:5. b) R. A. Brawn, J. S. Panek, *Org. Lett.* **2007**, *9*, 2689. c) H. Ohmiya, H. Ito, M. Sawamura, *Org. Lett.* **2009**, *11*, 5618. d) M. Ogasawara, A. Okada, V. Subbarayan, S. Sörgel, T. Takahashi, *Org. Lett.* **2010**, *12*, 5736.

[30] For a review about the Peterson olefination, see: N. Kano, T. Kawashima, in *Modern Carbonyl Olefination*; T. Takeda, ed; Wiley-VCH: Weinheim, 2004, p 18.

[31] For Peterson elimination in the preparation of allenes, see reference 29d and: a) M. Suginome, A. Matsumoto, Y. Ito, *J. Org. Chem.* **1996**, *61*, 4884. b) M. A. Tius, S. K. Pal, *Tetrahedron Lett.* **2001**, *42*, 2605. c) A. Tsubouchi, T. Kira, T. Takeda, *Synlett* **2006**, 2577.

[32] For reviews about the asymmetric synthesis of propargylic alcohols, see: a) B. M. Trost, A. H. Weiss, *Adv. Synth. Catal.* **2009**, *351*, 963. (b) K. Ishihara, M. Hatano, *Synthesis* **2008**, 1647. (c) M. Shibasaki, M. Kanai, *Chem. Rev.* **2008**, *108*, 2853. (d) J. S. Yadav, S. Chandrasekhar, in *Drug Discovery and Development*; M. S. Chorghade, ed; Wiley: Hoboken, 2007, vol. 2, p 141. (e) A. S. C. Chan, G. Lu, X. Li, in *Methodologies in Asymmetric Catalysis*; S. V. Malhotra, ed; American Chemical Society: Washington, 2004, p 103. (f) L. Pu, *Tetrahedron* **2003**, *59*, 9873.

or basic – one can produce both enantiomers of allene **3.94** starting from any enantiomer of alcohol **3.92**.

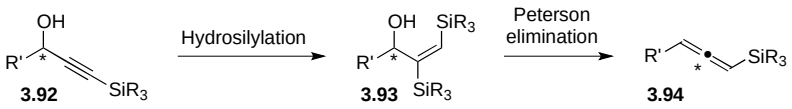

Figure 25. Proposed synthetic pathway toward allenylsilanes.

We began our study with the preparation of two bis(silyl)allyl alcohols **3.95** and **3.97** by hydrosilylation of the corresponding alkynes (see Section 3.4.1). Slow addition of **3.95** to a suspension of potassium hydride led to complete conversion of the starting material. Alas, the desired trimethylallenylsilane (**3.96**) was not detected (Figure 26). We suspected that this highly volatile allene was lost upon evaporation of the solvent.

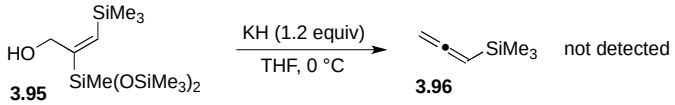

Figure 26. Peterson elimination on allyl alcohol 3.95.

Therefore, we focused our attention on the less volatile cinnamyl alcohol **3.97** (Table 9). Unfortunately, under our previous conditions, the use of potassium hydride or KHMDS resulted in the complete decomposition of the reaction mixture (entries 1,2). A careful examination of the literature revealed that α-silyl allylic alcohols are particularly prone to protodesilylation via a 1,3-Brook rearrangement in the presence of remaining hydroxyl protons.[3d,31b,c] In order to overcome this phenomenon, it is recommended to (i) produce a lithium alkoxide, which does not undergo 1,3-Brook rearrangement or Peterson elimination, and (ii) activate this tight ion pair by adding a polar solvent or initiating a transmetallation to potassium. Even if this literature precedent does not provide us with an explanation for the degradation of our starting material, it suggests standard conditions for the

transformation of this class of substrates.[3d,31c] Sadly, submitting our substrate to these protocols did not provide us with the desired allene (entries 3,4). Unexpectedly, when we replaced DMF by TMEDA at a lower temperature, we were able to isolate the oxasilacycle **3.99** (entry 5). Finally, employing boron trifluoride etherate also failed to initiate the desired Peterson elimination (entry 6).

Table 9. Peterson elimination conditions tested on cinnamyl alcohol 3.97.

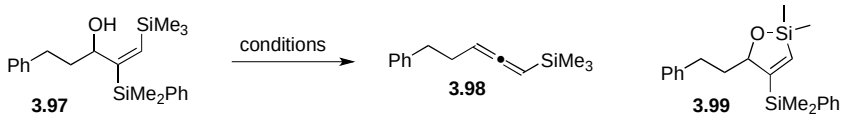

entry	conditions	result
1	**3.97** added onto KH (1.2 equiv), THF, 0 °C	dec
2	**3.97** added onto KHMDS (1.2 equiv), THF, 0 °C	dec
3	*i*. ^{n}BuLi (1.2 equiv), Et_2O, 0 °C *ii*. DMF, 50 °C	dec
4	*i*. ^{n}BuLi (1.2 equiv), Et_2O, –78 °C *ii*. ^{t}BuOK (1 equiv), –78 °C to rt	dec
5	*i*. ^{n}BuLi (1.1 equiv), Et_2O, –78 °C *ii*. TMEDA (20 equiv), –78 °C to 0 °C	**3.99** 77 %
6	BF_3•OEt_2 (0.2 equiv), CH_2Cl_2, –78 °C to 0 °C	dec

The isolation of side product **3.99** suggests that, upon formation of a reactive alkoxide **3.100**, the 5-membered cyclic species **3.101** is formed preferentially over the desired but more strained oxasilacyclobutane **3.102** (Figure 27). Subsequent degradation pathways are then operative, except when TMEDA is present in the reaction medium. The exact role of TMEDA is unknown for the moment.

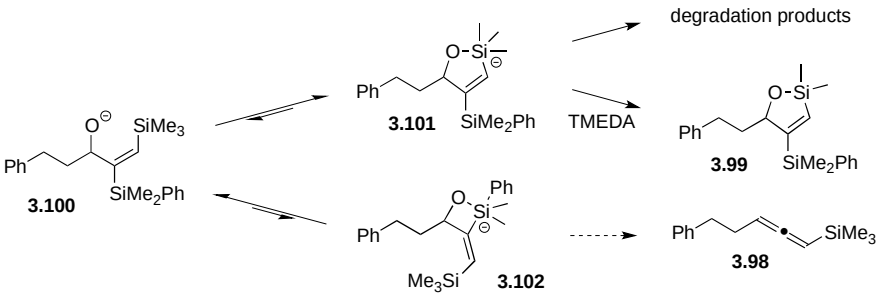

Figure 27. Rationalization for the failed Peterson elimination of 3.100.

A plausible solution to avoid the formation of the oxasilacycle **3.101**, would be to replace the terminal trimethylsilyl substituent by a more sterically demanding group. However, we know that the hydrosilylation of the corresponding silylated alkynes could be problematic (see Table 3). Another possibility to circumvent this difficulty would involve a variant of the Peterson reaction based upon an *anti* elimination of the corresponding esters or trimethylsilyl ether (Figure 28).[30,33]

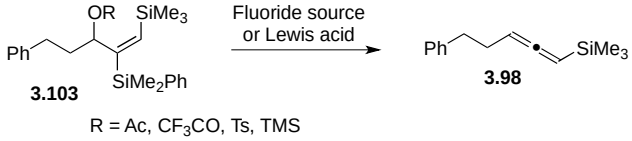

Figure 28. Perspectives for the Peterson elimination.

3.6 Combining Hydrosilylation and Hydroamination

During his post-doctoral stay, Dr. Alexandre Drouin demonstrated that a small amount of *n*-butyllithium catalyzed the addition of secondary amines **3.104** to vinyldimethylphenylsilane (**3.105**) (Figure 29).[34,35] He

[33] For a review, see: T.-H. Chan, *Acc. Chem. Res.* **1977**, *10*, 442.

[34] A. Drouin, M.-C. Tremblay, F. Lucaccioni, S. Dierick, I. E. Markó, *manuscript in preparation*.

[35] For publications from our team about hydroamination of olefins, see: a) C. Quinet, A. Ates, I. E. Markó, *Tetrahedron Lett.* **2008**, *49*, 5032. b) C. Quinet, P. Jourdain, C. Hermans, A. Ates, I. Lucas, I. E. Markó, *Tetrahedron* **2008**, *64*,

also reported that this reaction could be performed intramolecularly to prepare substituted pyrrolidine derivatives. Advantageously, this hydroamination approach for the formation of C–N bonds is atom-economic, cheap and employs readily available starting material.[36]

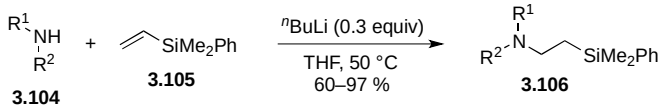

Figure 29. Hydroamination of vinyldimethylphenylsilane.

Interested by this innovative assembly of β-aminosilanes, we devised a synthesis of compound **3.108**, a model of the natural product (±)-xenovenine (**3.107**), a recurrent target in our laboratory (Figure 30).[37] According to our synthetic plans, pyrrolizidine **3.108** would be produced by a double intramolecular hydroamination of secondary amine **3.109**. This amine might be obtained from the bromide **3.110**, through a Grignard addition onto ethyl formate followed by a Mitsunobu reaction. Finally, the vinylsilane **3.110** would be prepared via the hydrosilylation of homopropargylic alcohol **3.61** followed by a subsequent bromination.

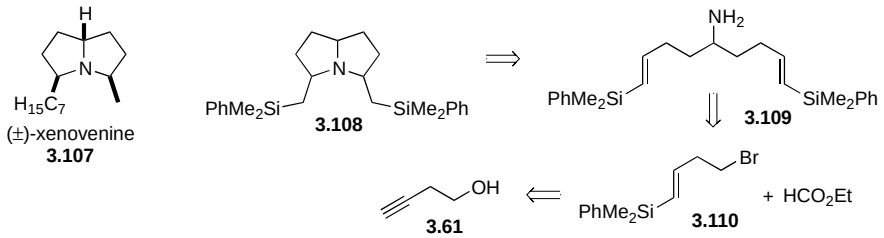

Figure 30. Retrosynthetic analysis of a (±)-xenovenine model.

1077. c) C. Quinet, L. Sampoux, I. E. Markó, *Eur. J. Org. Chem.* **2009**, 1806. d) H. Lee, S. Dochain, C. Eviolitte, I. E. Markó, *manuscript in preparation*.

36 For a review, see: T. E. Müller, M. Beller, *Chem. Rev.* **1998**, *98*, 675.

37 This retrosynthetic analysis is largely inspired by precedent studies realized in our group, see references 35b,c.

The facile preparation of the vinylsilane **3.63** has already been presented in Section 3.4.2 and 3.4.4 (Figure 31). We repeated this reaction on a large-scale without any loss in regioselectivity. The bromination step was first carried out with phosphorus tribromide buffered by triethylamine but resulted in the decomposition of the vinylsilane moiety. Therefore, we successfully used the Appel reaction, again on a large-scale.

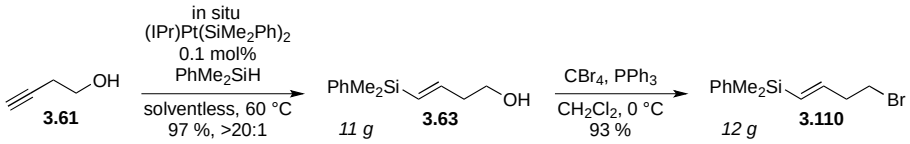

Figure 31. Large-scale preparation of bromide 3.110.

The preparation of the Grignard reagent derived from **3.110** and its subsequent addition onto ethyl formate proved more difficult than anticipated and remains unresolved to date (Table 10). The classical Grignard reaction in tetrahydrofuran afforded a complicated mixture, whereas in diethyl ether it resulted in no conversion (entries 1,2). Hence, we turned our attention to the conditions developed by Knochel using lithium chloride (entry 3).[38] We observed the reduction of the C–Br bond concomitant with the formation of diene **3.113**. Thus, the allylic protons of the starting material **3.110** are too acidic and reduce the organometallic species as soon as it is produced. To avoid this unwanted reaction, we decided to employ Barbier's method. However, we never could prepare the Grignard reagent in the presence of ethyl formate (entry 4). For our last attempt, we decided to use samarium(II) iodide, well-known for successfully performing Barbier type reactions.[39] Alas, the expected alcohol **3.111** was again absent in the reaction mixture (entry 5). Intriguingly, although the samarium reagent was completely

[38] a) F. M. Piller, P. Appukkuttan, A. Gavryushin, M. Helm, P. Knochel, *Angew. Chem. Int. Ed.* **2008**, *47*, 6802. b) T. D. Bluemke, F. M. Piller, P. Knochel, *Chem. Comm.* **2010**, *46*, 4082.

[39] For a review, see: A. Krief, A.-M. Laval, *Chem. Rev.* **1999**, *99*, 745.

consumed, the starting material was entirely recovered (entries 5,6). Furthermore, increasing the reduction potential of SmI_2 by the addition of hexamethylphosphoramide resulted in the complete degradation of the reaction mixture (entry 7).

Table 10. Grignard addition to ethyl formate.

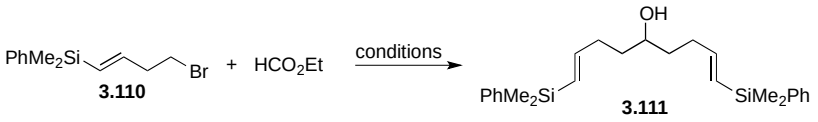

3.110 **3.111**

entry	conditions	result
1	*i*. Mg, THF, reflux *ii*. HCO_2Et, rt	dec
2	*i*. Mg, Et_2O, reflux *ii*. HCO_2Et	n.c.
3	*i*. Mg, LiCl, THF, 10 °C *ii*. HCO_2Et, 10 °C to rt	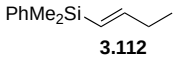 **3.112** 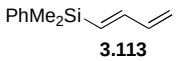 **3.113**
4	Mg, LiCl, HCO_2Et, THF, 10 °C to reflux	n.c.
5	SmI_2, HCO_2Et, THF, rt	n.c.[a]
6	SmI_2, THF, rt	n.c.[a]
7	SmI_2, HMPA, THF, rt	dec[a]

[a] Samarium(II) iodide was completely consumed.

The lack of success of a Grignard-based approach to **3.109** led us to propose an alternative route using the natural polarity of the carbon–bromine bond. In addition, we would like to avoid the Mitsunobu step. To fulfill both criteria, we need a synthetic equivalent to the synthon **3.114** (Figure 32). The obvious reagent would be nitromethane (**3.115**). Unfortunately, its anion is known to be a particularly poor partner for

alkylation of halogenoalkanes.[40] Therefore, this approach would probably require the condensation of the nitro ester anion **3.116**. The deprotonated imine **3.117** would also be a plausible alternative.[41,42]

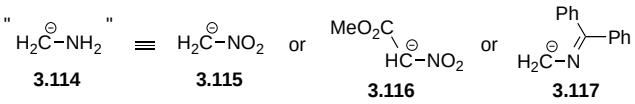

3.114 **3.115** **3.116** **3.117**

Figure 32. Synthetic equivalents to the methylamine anion.

3.7 Combining Hydrosilylation, Cyclopropanation and Hiyama Cross-Coupling

The addition of carbenoid reagents to carbon–carbon double bonds is probably the most practical route toward cyclopropanes.[43] Unfortunately, the application of this strategy to polyene substrates is particularly troublesome, due to obvious chemoselectivity issues. A solution to this synthetic problem is to introduce the cyclopropane unit via the cross-coupling reaction of a cyclopropylmetal derivative. Our research group has been studying this approach for a long time and applied it recently to the total syntheses of dictyopterene A (**3.118**) and B (**3.119**),[44] (+)-ambruticin S (**3.120**),[45] as well as the retinoid X receptor activator (RXR activator) (Figure 33).[46]

[40] Our research team has regularly been confronted to this limitation in the field of hydroamination. Accordingly, the literature is particularly scarce on this topic. Nonetheless, nitroethane and higher nitroalkyls are valuable alkylating agents. See: N. Ono, *The Nitro Group in Organic Synthesis*; Wiley-VCH: New York, 2001, p 126.

[41] a) V. N. Gogte, A. A. Natu, V. S. Pore, *Synth. Commun.* **1987**, *17*, 1421. b) B. Snider, Q. Che, *Tetrahedron* **2002**, *58*, 7821.

[42] a) P. Hullot, T. Cuvigny, *Bull. Soc. Chim. Fr.* **1973**, 2989. b) T. Kauffmann, H. Berg, E. Kiippelmann, D. Kuhlmann, *Chem. Ber.* **1977**, *110*, 2659.

[43] For selected reviews, see: a) D. Y.-K. Chen, R. H. Pouwer, J.-A. Richard, *Chem. Soc. Rev.* **2012**, *41*, 4631. b) H. Lebel, J.-F. Marcoux, C. Molinaro, A. B. Charette, *Chem. Rev.* **2003**, *103*, 977.

[44] T. Pospisil, *Ph.D. thesis*, Université catholique de Louvain, 2011.

[45] Y. Chen, *Post-doctoral report*, Université catholique de Louvain, 2010.

[46] F. Schevenels, *Ph.D. thesis*, Université catholique de Louvain, 2013.

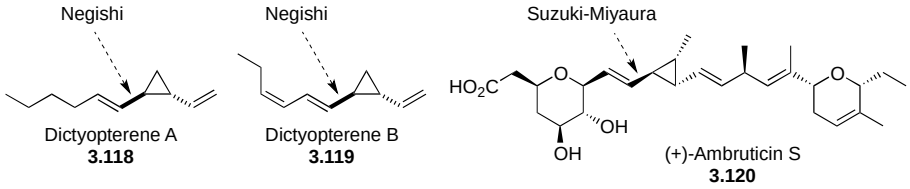

Figure 33. Dictyopterene A and B, and (+)-ambruticin S.

During their Ph.D. studies, Dr. Mélanie Marchant and Dr. Guillaume Berthon-Gelloz have observed that a palladium(0) analog **3.122** of the Karstedt complex was an outstanding catalyst for the cyclopropanation of vinylsilanes (Figure 34).[47]

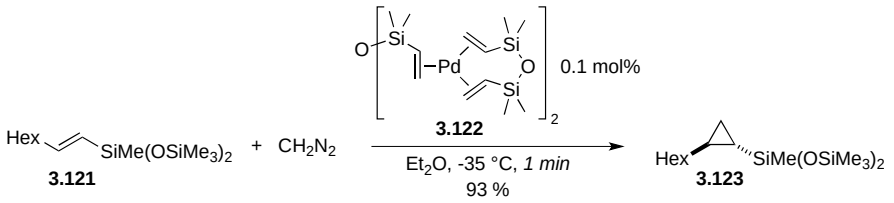

Figure 34. Cyclopropanation of vinylsilane using a palladium(0) catalyst.

Inspired by these brilliant reports, we recognized that cyclopropylsilanes **3.124** could be potential partners for Hiyama cross-coupling reactions (Figure 35).[48] Interestingly, all the vinylsilane stereoisomers are accessible through the hydrosilylation of alkynes (see Chapter 1, 2 and 3). Their cyclopropanation by alkyldiazo compounds is usually highly diastereoselective,[47] and this approach benefits from all the advantages inherent to silicon derivatives over their tin and boron equivalents (see Chapter 1).

[47] G. Berthon-Gelloz, M. Marchant, B. F. Straub, I. E. Markó, *Chem. Eur. J.* **2009**, *15*, 2923.

[48] To the best of our knowledge, there is only one publication on this subject, see: L.-P. Beaulieu, L. B. Delvos, A. B. Charette, *Org. Lett.* **2010**, *12*, 1348.

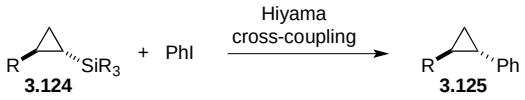

Figure 35. Hiyama cross-coupling of cyclopropylsilanes.

This topic constitutes the research project of the master thesis of Mr. Thibaut Debande.[49] Unfortunately, and despite numerous attempts, the cross-coupling of the cyclopropane **3.123** with phenyliodide under palladium catalysis has not yet been successfully accomplished.

4. Conclusions and Perspectives

4.1 Conclusions

At the onset of this Ph.D. thesis, we assigned ourselves four objectives dedicated to the hydrosilylation of silylated alkynes **3.1**: (i) establish the substrate scope of the reaction, (ii) extend the methodology to the addition of various silanes, (iii) confirm that steric hindrance controls the stereoselectivity and (iv) study the synthetic potential of the resulting (*E*) 1,2-bis(silyl)vinyl species **3.3**.

We began our work using the 2nd generation of platinum precatalyst, (IPr)Pt(AE) (**3.12**). Initially, we confirmed that the regioselectivity of the hydrosilylation is indeed dictated by a steric bias between each side of the unsaturation. Simultaneously, we established that silylated alkynes **3.1** are poisons for platinum(0) compounds. Therefore, we optimized the reaction conditions and independently discovered a 3rd generation of platinum precatalysts: (IPr)Pt(SiR_3)$_2$ (**3.42**). Thrilled by this unexpected development, we established the scope and limitation of the hydrosilylation of silylated alkynes by these new precatalysts. Furthermore, we also explored the hydrosilylation of terminal alkynes and alkenes, using numerous silanes. Outstanding yields and

[49] T. Debande, *Master thesis*, Université catholique de Louvain, 2013.

stereoselectivities, high functional group compatibilities and very low catalyst loadings are the hallmark of this new hydrosilylation protocol. Additionally, we studied the hydrosilylation of allenes and discovered an unexpected isomerization process triggered by a free alcohol group.

Having accomplish our first goals, we set out to develop a novel access to the allenylsilanes starting from (*E*) 2,3-bis(silyl)allyl alcohol species **3.93**. However, the Peterson elimination of these compounds proved to be particularly difficult and has not been accomplished so far. In addition, we began the synthesis of a model of the natural product (±)-xenovenine (**3.107**) employing a combination of hydrosilylation and hydroamination reactions. Finally, we initiated a research program on the Hiyama cross-coupling of cyclopropylsilanes.

4.2 Perspectives

Besides pursuing our efforts toward the synthesis of allenylsilanes and of a model of (±)-xenovenine, there is another important ambition that should be satisfied. The only isolated member of our 3rd generation of platinum precatalysts, (IPr)Pt($SiMe_2Ph$)$_2$ (**3.39**), could not be stored for more than one or two days. To date, the only possibility is to keep it away from light and under high vacuum in a sealed ampoule. Despite our convenient in situ preparation protocol from the bench-stable and user-friendly 1st generation complex (IPr)Pt(dvtms) (**3.10**), this limitation severely hampers the industrial development of these brilliant precatalysts.[50]

We reason that the stabilization of these complexes might be achieved by increasing the π-backbonding from the metal to the silyl ligands. Indeed, it is the reduction of this crucial electronic effect which is responsible for the relative instability of the 2nd generation precatalysts, as compared to the 1st generation (see Chapter 2). Silyl ligands are

[50] R. Karch, V. Raab, A. Rivas Nass, Umicore AG, personal communication 2013.

π-acceptors via their $\sigma^*_{(Si-R)}$ orbitals.[15,51] Therefore, introducing more electron-withdrawing groups (alkoxy-, chloro-, aryl-) on the silicon atom should lower the energy level of these orbitals and increase the π-backbonding.[15] Furthermore, replacing the IPr carbene by a more σ-donating ligand, like **3.126** or the mesoionic carbene **3.127**, should also increase the π-backbonding (Figure 36).[52] This synthetic endeavor is currently pursued by Dr. François Chellé.

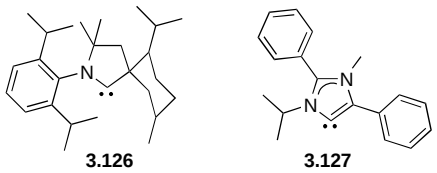

3.126 **3.127**

Figure 36. Highly σ-donating carbene ligands.

Finally, the presence of two silyl ligands onto platinum immediately suggests the possibility to catalyze the bis-silylation of multiple C–C bonds (Figure 37). To the best of our knowledge, only catalytic systems based upon palladium enable this reaction.[53] However, the oxidative insertion of platinum(0) into Si–Si bonds has also been reported.[54] Moreover, the addition of an alkene to complex **3.39** produces both the bis-silylated adduct and the bis-silane (see Figure 14), supporting the viability of our proposition.

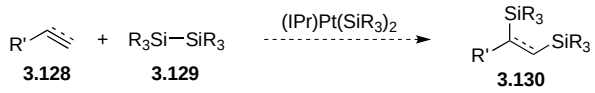

3.128 **3.129** **3.130**

Figure 37. Proposed bis-silylation reaction.

51 R. H. Crabtree, *The Organometallic Chemistry of the Transition Metals*; Wiley: Hoboken, 2005, p 68.

52 a) A. R. Chianese, A. Kovacevic, B. M. Zeglis, J. W. Faller, R. H. Crabtree, *Organometallics* **2004**, *23*, 2461. b) V. Lavallo, Y. Canac, C. Präsang, B. Donnadieu, G. Bertrand, *Angew. Chem. Int. Ed.* **2005**, *44*, 5705.

53 For a review, see: H. K. Sharma, K. H. Pannell, *Chem. Rev.* **1995**, *95*, 1351.

54 H. Arii, M. Takahashi, M. Nanjo, K. Mochida, *Dalton Trans.* **2010**, *39*, 6434.

Chapter 4

IPr*$^{(2\text{-Np})}$ — An Exceedingly Bulky *N*-Heterocyclic Carbene

This Chapter is dedicated to a new *N*-heterocyclic carbene designed during the course of this Ph.D. thesis.[1] After a brief overview of the research context, we will present some of our efforts devoted to the synthesis and coordination properties of this NHC. This work has been done in collaboration with Mr. Damien Dewez.[2]

1. Introduction

Since Bertrand's pioneering discovery and Arduengo's tour de force,[3] *N*-heterocyclic carbenes (NHCs) have developed into ubiquitous ligands, finding widespread applications in coordination chemistry, [4]

[1] Part of this chapter has been submitted for publication: S. Dierick, D. F. Dewez, I. E. Markó, 2013.

[2] D. Dewez, *Bachelor thesis*, Institut Paul Lambin, 2012.

[3] a) A. Igau, H. Grutzmacher, A. Baceiredo, G. Bertrand, *J. Am. Chem. Soc.* **1988**, *110*, 6463. b) A. J. Arduengo III, R. L. Harlow, M. Kline, *J. Am. Chem. Soc.* **1991**, *113*, 361.

[4] a) F. E. Hahn, M. C. Jahnke, *Angew. Chem. Int. Ed.* **2008**, *47*, 3122. b) D. Martin, M. Soleilhavoup, G. Bertrand, *Chem. Sci.* **2011**, *2*, 389. c) J. C. Y. Lin, R. T. W. Huang, C. S. Lee, A. Bhattacharyya, W. S. Hwang, I. J. B. Lin, *Chem. Rev.* **2009**, *109*, 3561. d) P. L. Arnold, I. J. Casely, *Chem. Rev.* **2009**, *109*, 3599.

metal-based catalysis,[5] organocatalysis,[6] material science,[7] and even in medicine.[7,8] Playing the role of ancillary ligands or organocatalysts, the NHCs are becoming increasingly popular as their talent to accommodate an ever larger repertoire of electronic and structural properties intensifies over time.[9] Notably, bulky and flexible carbenes possessing strong σ-donating abilities represent the state of the art on the catalysis forefront, particularly for palladium-catalyzed cross-coupling processes.[5b-d] Indeed, they enable the kinetic stabilization of low-coordinated catalytic intermediates whilst adjusting themselves to the incoming substrates. Henceforth, the rates of discrete catalytic steps are enhanced, selectivities are improved and deactivation pathways are delayed.[10] It is therefore no wonder that the development of such

[5] a) S. Díez-González, N. Marion, S. P. Nolan, *Chem. Rev.* **2009**, *109*, 3612. b) E. A. B. Kantchev, C. J. O'Brien, M. G. Organ, *Angew. Chem. Int. Ed.* **2007**, *46*, 2768. c) G. C. Fortman, S. P. Nolan, *Chem. Soc. Rev.* **2011**, *40*, 5151. d) N. Marion, S. P. Nolan, *Acc. Chem. Res.* **2008**, *41*, 1440. e) S. Würtz, F. Glorius, *Acc. Chem. Res.* **2008**, *41*, 1523. f) F. Wang, L.-j. Liu, W. Wang, S. Li, M. Shi, *Coord. Chem. Rev.* **2012**, *256*, 804. g) S. P. Nolan (Ed.), *N-Heterocyclic carbenes in synthesis*, Wiley-VCH, Weinheim, **2006**. h) F. Glorius (Ed.), *Top. Organomet. Chem.* **2007**, *21*, 1.

[6] a) V. Nair, S. Vellalath, B. P. Babu, *Chem. Soc. Rev.* **2008**, *37*, 2691. b) D. Enders, O. Niemeier, A. Henseler, *Chem. Rev.* **2007**, *107*, 5606. c) N. Marion, S. Díez-González, S. P. Nolan, *Angew. Chem. Int. Ed.* **2007**, *46*, 2988. d) D. Enders, T. Balensiefer, *Acc. Chem. Res.* **2004**, *37*, 534.

[7] L. Mercs, M. Albrecht, *Chem. Soc. Rev.* **2010**, *39*, 1903.

[8] a) K. M. Hindi, M. J. Panzner, C. A. Tessier, C. L. Cannon, W. J. Youngs, *Chem. Rev.* **2009**, *109*, 3859. b) M.-L. Teyssot, A.-S. Jarrousse, M. Manin, A. Chevry, S. Roche, F. Norre, C. Beaudoin, L. Morel, D. Boyer, R. Mahiou and A. Gautier, *Dalton Trans.* **2009**, 6894.

[9] a) T. Dröge, F. Glorius, *Angew. Chem. Int. Ed.* **2010**, *49*, 6940. b) S. Díez-González, S. P. Nolan, *Coord. Chem. Rev.* **2007**, *251*, 874. c) H. Clavier, S. P. Nolan, *Chem. Commun.* **2010**, *46*, 841. d) D. J. Nelson, S. P. Nolan, *Chem. Soc. Rev.* **2013**, *42*, 6723.

[10] a) F. Glorius, G. Altenhoff, R. Goddard, C. Lehmann, *Chem. Commun.* **2002**, 2704. b) G. Altenhoff, R. Goddard, C. W. Lehmann, F. Glorius, *Angew. Chem. Int. Ed.* **2003**, *42*, 3690. c) G. Altenhoff, R. Goddard, C. W. Lehmann, F. Glorius, *J. Am. Chem. Soc.* **2004**, *126*, 15195. d) V. Lavallo, Y. Canac, C. Präsang, B. Donnadieu, G. Bertrand, *Angew. Chem. Int. Ed.* **2005**, *44*, 5705. e) V. Lavallo, Y. Canac, A. DeHope, B. Donnadieu, G. Bertrand, *Angew. Chem. Int. Ed.* **2005**, *44*, 7236. f) Lavallo, G. D. Frey, S. Kousar, B. Donnadieu, G.

appreciated performers has captured the interest of many research groups (Figure 1).[11]

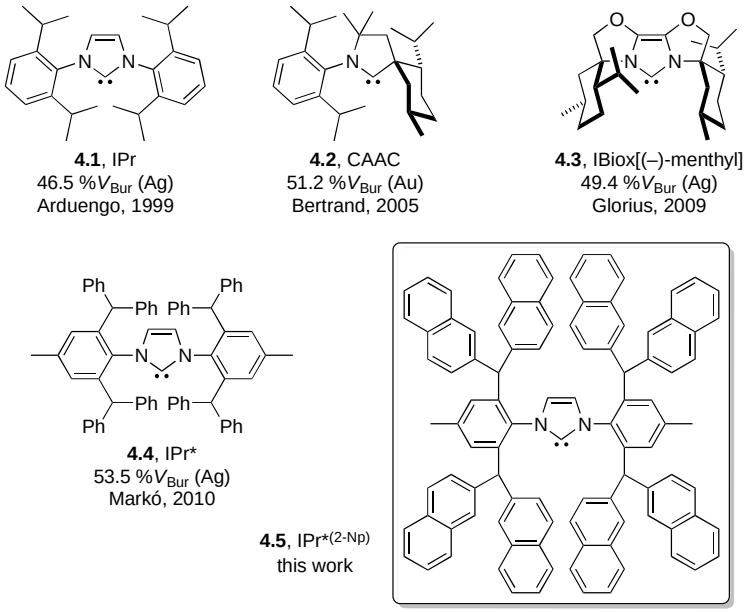

Figure 1. State-of-the-art bulky *N*-heterocyclic carbenes.

Our first contribution to this field involved the preparation and complete characterization of IPr* (**4.4**).[12] This massive *N*-heterocyclic carbene is one of the biggest NHC described to date and it rapidly

Bertrand, *Proc. Natl. Acad. Sci. USA* **2007**, *104*, 13569. g) S. Würtz, F. Glorius, *Acc. Chem. Res.* **2008**, *41*, 1523. h) V. Lavallo, G. D. Frey, B. Donnadieu, M. Soleilhavoup, G. Bertrand, *Angew. Chem. Int. Ed.* **2008**, *47*, 5224. i) S. Würtz, C. Lohre, R. Fröhlich, K. Bergander, F. Glorius, *J. Am. Chem. Soc.* **2009**, *131*, 8344. j) M. G. Organ, S. Çalimsiz, M. Sayah, K. H. Hoi, A. J. Lough, *Angew. Chem. Int. Ed.* **2009**, *48*, 2383.

11 For leading examples, see: reference 10 and a) A. J. Arduengo III, R. Krafczyk, R. Schmutzler, H. A. Craig, J. R. Goerlich, W. J. Marshall, M. Unverzagt, *Tetrahedron* **1999**, *55*, 14523. b) L. Jafarpour, E. D. Stevens, S. P. Nolan, *J. Organomet. Chem.* **2000**, *606*, 49. (c) L. Hintermann, *Beilstein J. Org. Chem.* **2007**, 3:22.

12 G. Berthon-Gelloz, M. A. Siegler, A. L. Spek, B. Tinant, J. N. H. Reek, I. E. Markó, *Dalton Trans.* **2010**, *39*, 1444.

attracted the attention of the scientific community.[13] Interestingly, it proved to be a particularly efficient ligand for the Buchwald–Hartwig amination of arylchlorides[13h–k] and for the Suzuki–Miyaura cross-coupling of hindered substrates.[13g] Several analogues of IPr* have since been prepared and their use in important catalytic transformations reported.[14]

2. A New Generation of Sterically Demanding NHC

2.1 Synthesis of the Imidazolium Salt IPr*$^{(2\text{-Np})}$•HCl

In echo to the success encountered by IPr* (**4.4**), we set out to elaborate a new generation of even more sterically hindered carbenes. It was recognized at the onset of this work that, for a ligand to be attractive among numerous others, its synthesis must be short, practical and

[13] a) C. A. Laskowski, A. J. M. Miller, G. L. Hillhouse, T. R. Cundari, *J. Am. Chem. Soc.* **2011**, *133*, 771. b) A. Gómez-Suárez, R. S. Ramón, O. Songis, A. M. Z. Slawin, C. S. J. Cazin, S. P. Nolan, *Organometallics* **2011**, *30*, 5463. c) B. M. Prince, T. R. Cundari, *Organometallics* **2012**, *31*, 1042. d) L. Candish, D. W. Lupton, *Chem. Sci.* **2012**, *3*, 380. e) J. Balogh, A. M. Z. Slawin, S. P. Nolan, *Organometallics* **2012**, *31*, 3259. f) S. Manzini, C. A. Urbina Blanco, A. M. Z. Slawin, S. P. Nolan, *Organometallics* **2012**, *31*, 6514. g) A. Chartoire, M. Lesieur, L. Falivene, A. M. Z. Slawin, L. Cavallo, C. S. J. Cazin, S. P. Nolan, *Chem. Eur. J.* **2012**, *18*, 4517. h) A. Chartoire, X. Frogneux, S. P. Nolan, *Adv. Synth. Catal.* **2012**, *354*, 1897. i) S. Meiries, A. Chartoire, A. M. Z. Slawin, S. P. Nolan, *Organometallics* **2012**, *31*, 3402. j) A. Chartoire, X. Frogneux, A. Boreux, A. M. Z. Slawin, S. P. Nolan, *Organometallics* **2012**, *31*, 6947. k) A. Chartoire, A. Boreux, A. R. Martin, S. P. Nolan, *RSC Adv.* **2013**, *3*, 3840. l) C. Dash, A. Das, M. Yousufuddin, H. V. R. Dias, *Inorg. Chem.* **2013**, *52*, 1584. m) A. Gómez-Suárez, Y. Oonishi, S. Meiries, S. P. Nolan, *Organometallics* **2013**, *32*, 1106. n) A. Poater, L. Falivene, C. A. Urbina-Blanco, S. Manzini, S. P. Nolan, L. Cavallo, *Dalton Trans.* **2013**, *42*, 7433.

[14] a) S. G. Weber, C. Loos, F. Rominger, B. F. Straub, *ARKIVOC* **2012**, *3*, 226. b) S. G. Weber, F. Rominger, B. F. Straub, *Eur. J. Inorg. Chem.* **2012**, 2863. c) A. R. Martin, A. Chartoire, A. M. Z. Slawin, S. P. Nolan, *Beilstein J. Org. Chem.* **2012**, *8*, 1637. d) S. Meiries, K. Speck, D. B. Cordes, A. M. Z. Slawin, S. P. Nolan, *Organometallics* **2013**, *32*, 330.

cheap. Thus, we planned to use the same design as for IPr*. Careful examination of the X-ray structure of IPr*AgCl (Figure 2),[12] suggested that replacing the eight phenyl rings by 2-naphthyl (2-Np) surrogates might increase the steric demand of the carbene in the first coordination sphere.[15] Indeed, assuming that the ligand will retain the same conformation as depicted in Figure 2, extending the aromatic planes wrapped around the metal center should bury it even more deeply within the cavity created by the longer walls of the ligands.

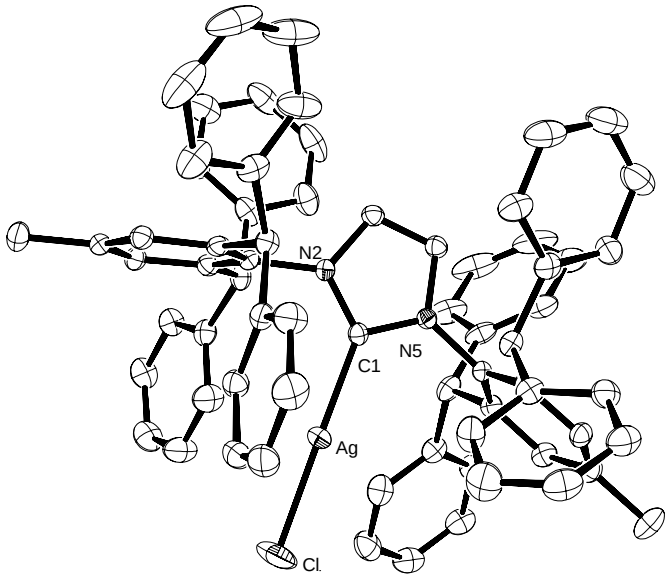

Figure 2. Displacement ellipsoid plot (50% probability level) of IPr*AgCl. Hydrogen atoms and lattice molecules are omitted for clarity. Selected bond lengths [Å] and angle [°]: Ag–C1 2.081(2), Ag–Cl 2.3189(9), C1–Ag–Cl 174.29(7).

Conveniently, the preparation of the targeted imidazolium salt IPr*(2-Np)•HCl (**4.10**) requires only four steps and is easy to scale up (Figure 3). Hence, the addition of the Grignard reagent derived from inexpensive 2-bromonaphthalene (**4.6**) to ethyl formate affords alcohol

[15] For other approach which proved unsuccessful, see reference 2.

7 in excellent yields. A Friedel–Crafts alkylation of *p*-toluidine, followed by the condensation of the resulting aniline **4.8** with aqueous glyoxal, delivers the desired diazadiene **4.9** in good yields. As feared, the final cyclization step using paraformaldehyde proved to be particularly difficult, most probably due to the increased steric hindrance around the two nitrogen atoms of **4.9**. Nonetheless, after careful optimization of the reaction conditions and the purification procedure, which confirmed the crucial role played by zinc chloride,[16] the sought-after imidazolium salt **4.10** was obtained on a 3.6-gram scale!

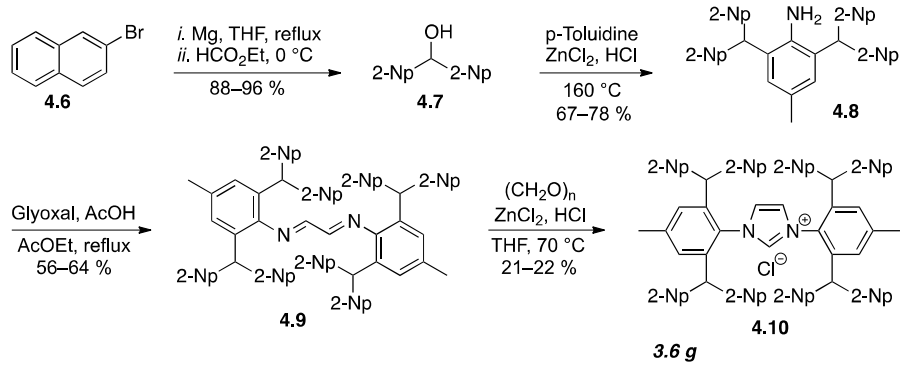

Figure 3. Synthesis of IPr*$^{(2\text{-Np})}$•HCl (10).

The structure of IPr*$^{(2\text{-Np})}$•HCl (**4.10**) has been unambiguously established by single-crystal X-ray diffraction analysis (Figure 4). As in the case of its parent, the imidazolium salt precursor of IPr* (**4.4**), the symmetric architecture of **4.10** results in simplified NMR spectra, apart for their aromatic regions. Interestingly, the signal of the iminium hydrogen is found at 13.8 ppm in the ^{1}H NMR spectrum ($CDCl_3$). To the best of our knowledge, it is the most downfield chemical shift reported to date for any imidazolium compound, nearly 1 and 4 ppm downfield from the same hydrogen present in IPr*•HCl and IPr•HCl, respectively. Such a shift is presumably due to a strengthening of the hydrogen bond

[16] Zinc chloride is thought to reorganize the intermediate prior to cyclization from the favored s-*trans* to the required s-*cis* conformation. For more information, see reference 12.

between this acidic hydrogen and the chloride ion. This interaction is enhanced by the hydrophobic pocket built around the anion by the phenyl and naphthyl framework. On the other hand, the two remaining protons of the imidazolium core are shifted to 5.4 ppm, some 0.1 and 2.4 ppm upfield from the corresponding protons of IPr*•HCl and IPr•HCl, respectively. This shielding is probably caused by the ring currents produced by the naphthyl groups in close proximity to these hydrogens.

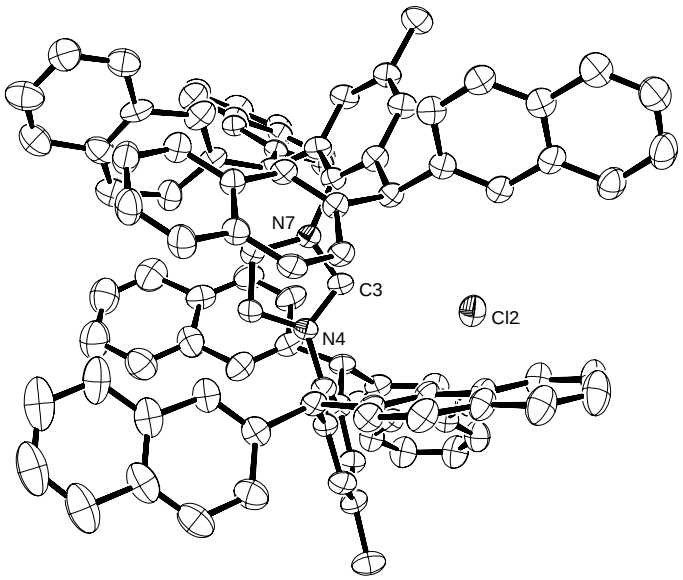

Figure 4. Displacement ellipsoid plot (30% probability level) of IPr*(2-Np)•HCl (**4.10**). Hydrogen atoms and lattice molecules are omitted for clarity.

2.2 Coordination Chemistry of IPr*(2-Np)

Having successfully prepared the desired imidazolium salt, the coordination chemistry of IPr*(2-Np) **4.5** was investigated (Figure 5). Surprisingly, and despite its rather enormous size, carbene **4.5** reacted smoothly, affording compounds **4.11**–**4.15** in a straightforward manner. As expected, the linear structures of silver(I) **4.11** and copper(I) **4.12** complexes, both bearing a chloride atom *trans* to the bulky carbene

substituent, are easily contained within the cavity defined by the NHC ligand. It is noteworthy that IPr*(2-Np) was also able to accommodate standard ligands such as a η^3-cinnamyl moiety and a η^4-1,5-cyclooctadiene, as in complexes **4.13** and **4.14**, respectively. The σ-donating effect of this massive *N*-heterocyclic carbene was measured by infrared spectroscopy of the corresponding rhodium carbonyl complex **4.15**.[9] Pleasingly, IPr*(2-Np) appeared to be among the highest donating NHCs reported, with CO stretching frequencies of 2075 cm^{-1} (ν_{sym}) and 1994 cm^{-1} (ν_{asym}). These values are identical to those of IPr* (**4.4**)[12] and comparable to the ones of the Bertrand CAAC ligand **4.2** (ν_{sym} = 2077 cm^{-1}, ν_{asym} = 1994 cm^{-1}).[10d]

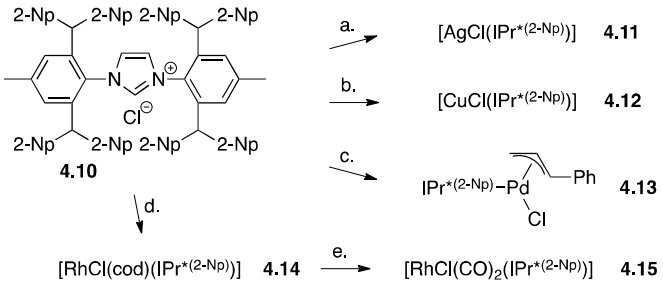

Figure 5. Synthesis of IPr*(2-Np) complexes. (a) Ag_2O, CH_2Cl_2, 91 %. (b) *t*BuOK, CuCl, CH_2Cl_2, 59 %. (c) *t*BuOK, $[PdCl(\pi\text{-cinnamyl})]_2$, THF, 72 %. (d) $[RhCl(cod)]_2$, *t*BuOK, THF, 0 °C, then rt, 97%. (e) CO, CH_2Cl_2, 100 %.

Single-crystal X-ray diffraction analysis revealed the intimate structures of compounds **4.11** and **4.12** (Figure 6 and Figure 7). The silver(I) complex **4.11** deviates only slightly from linearity (C3–Ag1–Cl2 178.30°) and the NHC–metal distance (2.068 Å) is in the range of similar molecules.[12,17] As anticipated (vide supra), out of the eight naphthyl moieties, four are directed toward the backside of the complex (i.e. opposite to the metal), whilst the four remaining aryl groups are located around the metal center and the chlorine atom. As far as we know, this is the first example of a monodentate ligand able to extend *beyond* the substituent positioned at the *trans* coordination site, additionally

[17] J. C. Garrison, W. J. Youngs, *Chem. Rev.* **2005**, *105*, 3978.

building a hydrophobic cavity around it. The copper(I) complex **4.12** displays the same features, while being less linear (C3–Cu1–Cl2 175.11°) and having a shorter NHC–metal bond (1.882 Å), as in other (NHC)CuCl complexes.[18]

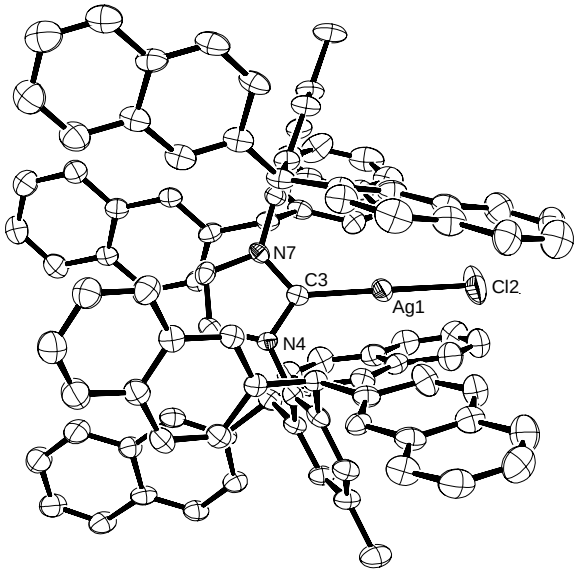

Figure 6. Displacement ellipsoid plot (30% probability level) of IPr*(2-Np)AgCl (**4.11**). Hydrogen atoms, lattice molecules and disorder are omitted for clarity.

[18] a) H. Kaur, F. K. Zinn, E. D. Stevens, S. P. Nolan, *Organometallics* **2004**, *23*, 1157. b) S. Díez-González, E. C. Escudero-Adán, J. Benet-Buchholz, E. D. Stevens, A. M. Z. Slawin, S. P. Nolan, *Dalton Trans.* **2010**, *39*, 7595.

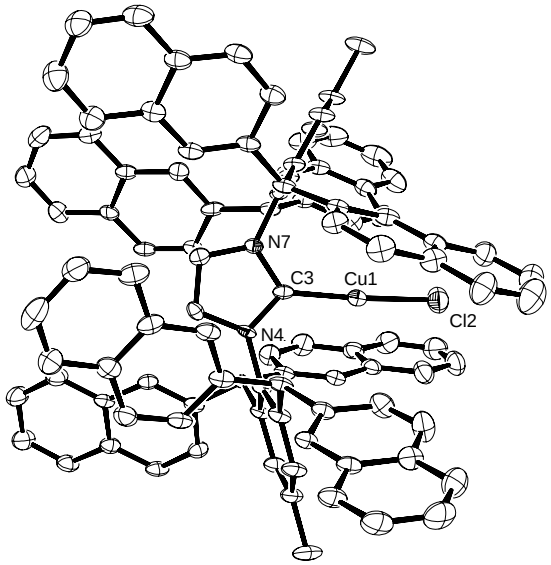

Figure 7. Displacement ellipsoid plot (30% probability level) of IPr*$^{(2\text{-Np})}$CuCl (**4.12**). Hydrogen atoms, lattice molecules and disorder are omitted for clarity.

Based upon the crystal structures of **4.10**–**4.12**, the bulkiness and flexibility of IPr*$^{(2\text{-Np})}$ (**4.5**) could be estimated. The percent buried volumes (%V_{Bur}), a descriptor of the steric demand of a ligand, were calculated via the application Samb*V*ca.[19] These data represent the fraction of volume occupied by a ligand in a sphere centered on an imaginary metal center (Figure 8).

[19] For a description of %V_{bur} and the web-based Sam*V*ca applet, see: a) A. Poater, B. Cosenza, A. Correa, S. Giudice, F. Ragone, V. Scarano, L. Cavallo, *Eur. J. Inorg. Chem.* **2009**, 1759. b) The calculations used the following parameters: radius of sphere, 3.5 Å; distance from sphere, 2.0 Å; mesh step, 0.05 Å; H atoms omitted; bondi radii scaled by 1.17 Å.

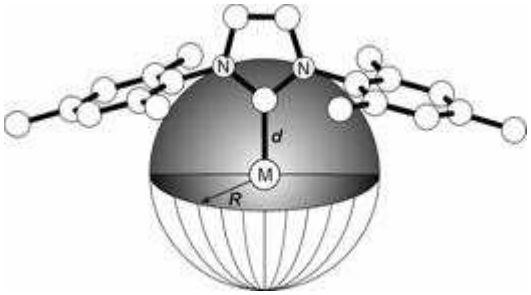

Figure 8. Graphical representation of the sphere used to calculate the %V_{Bur}. Courtesy of Prof. Luigi Cavallo.

The values obtained for **4.10**, **4.11** and **4.12** are 49.7 %V_{Bur}, 57.4 %V_{Bur} and 57.1 %V_{Bur}, respectively. To the best of our knowledge, IPr*(2-Np) appears to be the most sterically demanding, yet flexible, NHC known, in terms of percent buried volume (see Figure 1).[20] Regarding its flexibility, the torsion angles defined by the imidazolyl moiety and the phenyl rings can vary significantly, ranging from 69.80° for complex **4.10**, to 85.7° for **4.11** and 86.0° for **4.12**, respectively. It thus transpires that this carbene occupies a much smaller volume when a small hydrogen atom is present inside the cavity created by the aromatic rings (structure **4.10**). To enable the insertion of a metal, the NHC has to reorganize its structure. For that purpose, it can open its cavity by modifying the orientations of the naphthyl groups. The overall volume of the complexes is thus increased, as in **4.11** and **4.12**. This key structural information therefore suggests that IPr*(2-Np) is able to reshuffle its entire conformation to adjust it to various environments.

[20] A percent buried volume of 80.5 % for an imidazolium salt, which requires 13 synthetic steps, was recently reported. However, this NHC precursor is conformationally rigid and its coordination chemistry has not been described yet. See: J.-N. Levy, C. M. Latham, L. Roisin, N. Kandziora, P. Di Fruscia, A. J. P. White, S. Woodward, M. J. Fuchter, *Org. Biomol. Chem.* **2012**, *10*, 512.

3. Conclusions and perspectives

To summarize, using a rational approach based upon crystal structures of **4.4**, we have designed an exceptionally bulky *N*-heterocyclic carbene. IPr*$^{(2\text{-Np})}$ (**4.5**) is readily available in useful quantities through a cheap, expedient and convenient synthetic sequence devoided of tedious purification steps. This new ligand was fully characterized and was engaged in the formation of several organometallic complexes. Its electron releasing effect, flexibility and steric demand have been evaluated and IPr*$^{(2\text{-Np})}$ appears to be the most sterically demanding *N*-heterocyclic carbene reported to date. Its ability to modify its overall shape enables IPr*$^{(2\text{-Np})}$ to accommodate various metals inside the cavity created by the aromatic rings whilst still remaining one of the most σ-donating NHCs.

In view of these rather exceptional properties, we believe that IPr*$^{(2\text{-Np})}$ might rapidly become a unique ligand among all the NHCs. Naturally, the next step in its development would be to evaluate its catalytic properties. In this regard, the palladium complex **4.13** can be directly used in the Suzuki–Miyaura cross-coupling of hindered substrates and in the Buchwald–Hartwig amination of arylchlorides, two applications in which IPr* has already been successful (vide supra). The extreme bulkiness of this new NHC might also enable us to isolate sensitive complexes or reactive intermediates. Indeed, the flexible hydrophobic pocket IPr*$^{(2\text{-Np})}$ is rather reminiscent of the active pocket of some enzymes or supramolecular assemblies. It might therefore protect the reactive center of the sensitive complexes by forbidding other reagents to come to its close proximity. Based upon this structural feature, one can imagine generating artificial metallo-enzymes, tailored with specific binding and reacting residues.

The structures of both IPr* and IPr*$^{(2\text{-Np})}$ complexes are characterized by the aromatic rings surrounding the metal centers. We propose to leave

the two-dimensional world of these ligands to reach the third dimension afforded by sp^3-hybridized substituents. Figure 9 depicts our proposal toward a new *N*-heterocyclic carbene: IPr*(1-Ad). Replacing the phenyl or 2-naphthyl groups by 1-adamantyl moieties should increase the space occupied by the NHC in the coordination sphere of the metal. Furthermore, it will suppress the aromatic ring current effects present in the former complexes, as well as simplify the NMR spectra due to the highly symmetric nature of the adamantane unit.

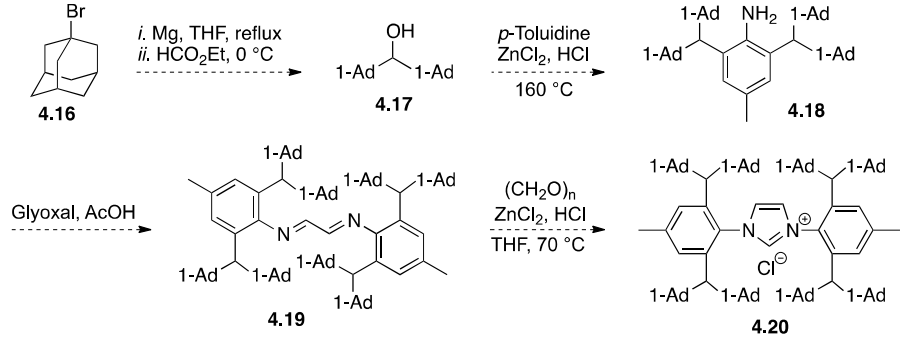

Figure 9. Synthetic plan toward an expectedly bulkier NHC: IPr*(1-Ad).

Chapter 5

Conclusions

At the beginning of this work, we were interested in the hydrosilylation of silylated alkynes **5.1** which affords stereoselectively 1,2-bis(silyl)vinyl species **5.4** (Figure 1). Our objectives were to (i) establish the substrate scope of the reaction, (ii) extend this transformation to various silanes, (iii) study the origin of the stereoselectivity and (iv) explore the synthetic potential of the adducts **5.4**.

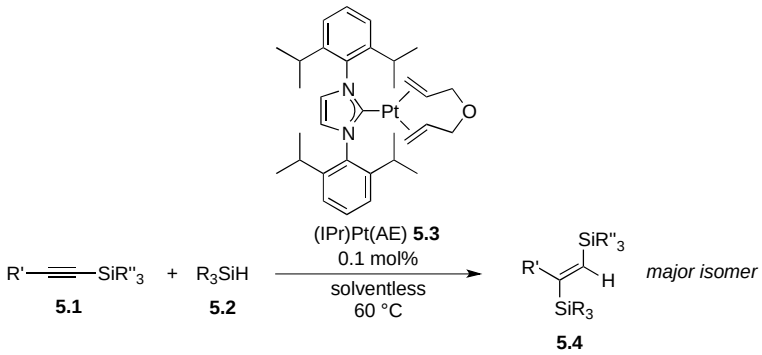

Figure 1. Hydrosilylation of silylated alkynes.

By the careful examination of the hydrosilylation of various silylated alkynes, we confirmed that the regioselectivity of the process originates from a steric differentiation between the two substituents of the triple bond in the key intermediates **5.5** and **5.6** (Figure 2).

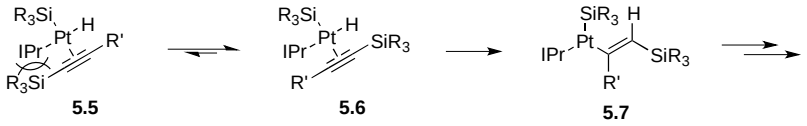

Figure 2. Origin of the regioselectivity in silylated alkynes hydrosilylation.

Furthermore, disappointed by the low rates, yields and selectivities afforded by this transformation, we undertook a careful optimization of the reaction conditions. This study led to the discovery of a 3rd generation of NHC platinum(0) precatalysts **5.8** (Figure 3).

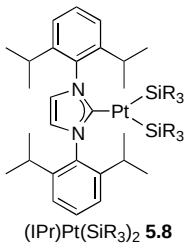

Figure 3. Third generation hydrosilylation precatalysts.

Thrilled by the efficiency of these complexes as compared to that of the previous generations, we set out to establish the substrate scope and the chemocompatibility of these reagents in the hydrosilylation of silylated alkynes, terminal alkynes and olefins (Figure 4). Various silanes we also employed. We were pleased to confirm that these bis-silyl platinum complexes are the best hydrosilylation precatalysts developed to date in our laboratory, with regard to their levels of selectivity and to their rate of the reaction. This increased efficiency has been attributed to a faster initiation process and the suppression of one of the possible deactivation pathways.

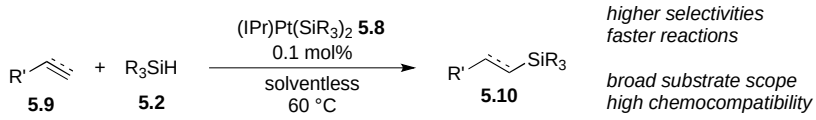

Figure 4. Hydrosilylation catalyzed by (IPr)Pt(SiR3)2 complexes.

In order to extend further the synthetic potential of the resulting hydrosilylation products, we envisioned a novel access to the underdeveloped family of allenylsilanes **5.13** (Figure 5). However, the Peterson elimination of the β-silyl alcohol intermediates **5.12** proved to be particularly difficult and has not yet been accomplished successfully.

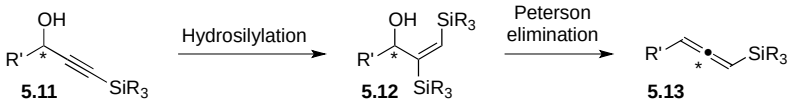

Figure 5. Synthetic pathway toward allenyl silanes.

In addition, we began the synthesis of a model of the natural product (±)-xenovenine (**5.14**) through a combination of the hydrosilylation and hydroamination reactions (Figure 6). Up to now, we have been unable to mediate the addition of intermediate **5.17** onto ethyl formate via the formation of a derived organometallic reagent.

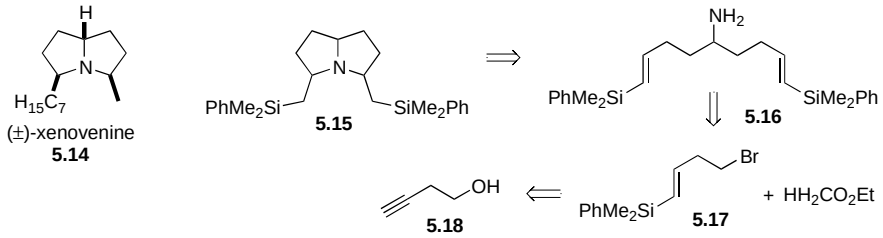

Figure 6. Retrosynthetic analysis of a model of (±)-xenovenine.

On the other hand, we have also been interested in the study of sterically demanding *N*-heterocyclic carbenes. Therefore, we imagined and synthesized, IPr*$^{(2\text{-Np})}$ (**5.19**), the bulkiest NHC reported to date, building upon the structural information gathered from the X-ray structures of IPr* (Figure 7).

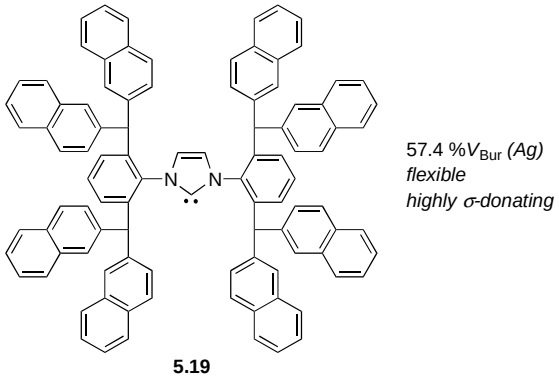

5.19

Figure 7. An exceedingly bulky *N*-heterocyclic carbene.

Gratifyingly, this new ligand is readily available, in useful quantities and in only four steps, from 2-bromonaphthalene. Its massive size does not preclude its coordination to various metals and it was engaged in the formation of complexes with silver(I), copper(I), rhodium(I) and palladium(II) (Figure 8).

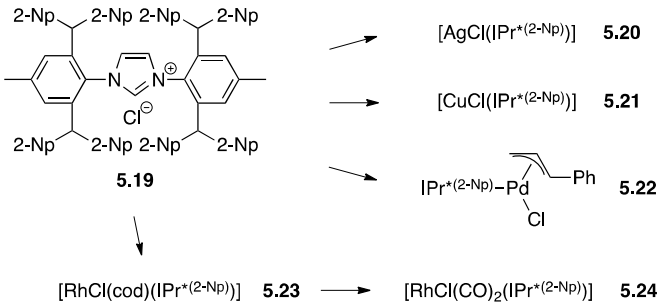

Figure 8. Complexes based upon IPr*(2-Np).

Chapter 6

Experimental Section

1. Instrumentation

^{1}H and ^{13}C nuclear magnetic resonance spectra were recorded on Brucker Avance II-300 spectrometers (^{1}H 300 MHz and ^{13}C 75 MHz). ^{1}H chemical shifts are reported in ppm downfield from internal tetramethylsilane (δ = 0 ppm) or $CHCl_3$ (δ = 7.261 ppm) in the case of silicon containing compounds. ^{13}C NMR spectra are reported using $CDCl_3$ as the internal standard (δ = 77.16 ppm). Splitting patterns are designed as: s = singlet; d = doublet; t = triplet; q = quartet; qui = quintet; sex = sextet; sep = septet; b = broad; and m = multiplet. ^{195}Pt NMR spectra were recorded on a Brucker Avance 500 spectrometer (107 MHz) and externally referenced to H_2PtCl_6 in H_2O (δ = 0 ppm).

In stark contrast to usual olefins, 1,2-disubstitued vinylsilanes usually display ^{3}J coupling constants between their vinylic protons of 18–20 Hz and 14–16 Hz for (*E*) and (*Z*) double bonds, respectively.[1] On the other hand, 1,1-disubstituted vinylsilanes present ^{2}J coupling constants, where measurable, of 2–3 Hz.

[1] C. S. Aricó, L. R. Cox, *Org. Biomol. Chem.* **2004**, *2*, 2558.

Nuclear Overhauser effect difference spectroscopy experiments were performed by Dr. Cécile Le Duff from the Nuclear Magnetic Spectroscopy Service, Université catholique de Louvain.

Infrared spectra were recorded by transmittance on a Shimadzu FTIR-8400S spectrometer and reported in wavenumber (cm^{-1}). The samples were analyzed as thin films deposited on a ZnSe ATR crystal by solvent evaporation. Signal intensities are denoted as: s = strong; m = medium; w = weak and b = broad.

Elemental analyses were carried out by Dr. J. Opitz from the Institut für Organische Chemie, Universität Stuttgart (Germany), for liquids; and by Prof. György Hajós and Dr. Zsuzsanna Riedl from the Chemical Research Center, Hungarian Academy of Sciences (Hungary), for solids.

Low- and high-resolution mass spectra were recorded by Mr. Alexandre Spote or Mr. Raoul Rozenberg from the Mass Spectrometry Service, Université catholique de Louvain. Several high-resolution mass spectra were recorded by Dr. Lisa D. Harris from the Mass Spectrometry Facility, University College London (United Kingdom).

Melting points were measured on a Buchï B-545 melting point apparatus and are uncorrected.

Single-crystal X-ray diffractions were measured and the crystal structures determined by Dr. Koen Robeyns from the Crystallography Service, Université catholique de Louvain.

Gas–liquid chromatographies were performed on a Thermo-Finnigan Trace GC chromatograph equipped with an FID detector and a fused silica capillary column (Alltech EC-5, 30 m × 0.25 mm, DF = 0.25 μm) using helium as the carrier gas. Injector temperature: 300 °C. FID detector temperature: 250 °C. Pressure at the head of the column:

13 psi. Split injection ratio: 1/40. A standard temperature program was used for most of the GC analyses: 60 °C (1 min), 20 °C/min, 280°C (3 min).

2. Procedures

All the experiments were performed in air with magnetic stirring unless otherwise stated. When inert atmosphere was required, the glassware was assembled, purged with argon and flame dried under a stream of argon until the glass emitted an orange light. Argon was previously dried by passing it through a bed of silica gel doped with cobalt(II) chloride.

All the reagents were used as received apart from the followings. Magnesium turnings were cleaned by washing them successively with HCl_{aq} 1 M and acetone, and dried overnight in an oven (110 °C). Ethyl formate was distilled from phosphorus pentoxide. *p*-Toluidine was dried in a desiccator under high vacuum over phosphorus pentoxide. Zinc chloride was dried in a Kugelrohr apparatus (100 °C) under high vacuum. Copper(I) chloride was dissolved in concentrated HCl_{aq} (36 %), precipitated by dilution with water, filtered, washed with ethanol and diethyl ether, and dried in a desiccator under high vacuum over phosphorus pentoxide. Trimethysilyl chloride and triethylamine were distilled from calcium hydride. TMEDA was distilled under vacuum from sodium.

All the solvents were analytical grade and used as received unless otherwise stated. Dry tetrahydrofuran, diethyl ether and 1,4-dioxane were distilled from sodium benzophenone ketyl. Dry dichloromethane and toluene were distilled from calcium hydride. Technical grade ethyl acetate and petroleum ether (40 to 65 °C fraction) were evaporated under reduced pressure.

Degassed solvents were prepared on a small scale (< 15 mL) by five freeze–pump–thaw cycles in Schlenk tube. On a larger scale, argon was bubbled through the solvent for at least 30 minutes using a fritted gas dispersion tube and under sonication.

Thin layer chromatographies were performed on Merck Millipore F_{254} silica gel 60 plates (200 µm thickness, aluminum supported). The plates were visualized using ultra-violet light (254 nm) and stained using an alkaline $KMnO_4$ solution. Conveniently, simple heating of the plates revealed platinum containing compounds as black dots. Column chromatographies were performed under pressure with the stated solvents using Sigma-Aldrich silica gel 60 (70–230 mesh).

3. Compounds Synthesized in Chapter 3

3.1 Preparation of the Precatalysts

The imidazolium salt IPr•HCl (**3.7**) was prepared according to Hintermann from 2,6-diisopropylaniline and dried in a desiccator under high vacuum over phosphorus pentoxide.[2]

Karstedt's catalyst (3.9)[3] CAS: 68478-92-2

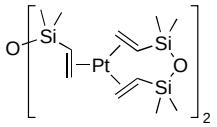

A two-necked round-bottomed flask, equipped with a thermometer and a septum, was charged with hexachloroplatinic acid hydrate (300 mg, 0.615 mmol, 1 equiv) and 4.4 mL of isopropanol (*caution: H_2PtCl_6 is toxic, corrosive and very hygroscopic*). The orange mixture was stirred at 70 °C for 30 min and then cooled to 25 °C. Solid sodium hydrogen carbonate (413 mg, 4.92 mmol, 8 equiv) was added

[2] L. Hintermann, *Beilstein J. Org. Chem.* **2007**, 3 :22.
[3] For more details, see: S. Dierick, G. Bastug, I. E. Markó, *Org. Synth.*, Accepted for checking.

portionwise over 5 min and the flask was left open (*caution: vigorous CO_2 gas evolution!*). After 10 min, 1,3-divinyltetramethyldisiloxane (1.1 mL, 4.9 mmol, 8 equiv) was added, the reaction vessel was capped with a rubber septum and heated to 70 °C for 60 min. After confirming the completion of the reaction by TLC, the final off white suspension was cooled to room temperature. The reaction mixture was filtered through a plug of silica gel/Celite/$MgSO_4$ (v/v/v 1:1:1), eluting with diethyl ether. The filtrate was concentrated by rotary evaporation (200 mmHg, 25 °C), to ca. 4–5 mL, affording a yellow solution of Karstedt's catalyst, stabilized by excess 1,3-divinyltetramethyldisiloxane in isopropanol, used without further purification.

This solution must not be further concentrated otherwise its platinum(0) content will be degraded resulting in significantly lower yields. Storage at –20 °C under an argon atmosphere for several days showed no degradation.

(IPr)Pt(dvtms) (3.10)[3] CAS: 849830-54-2

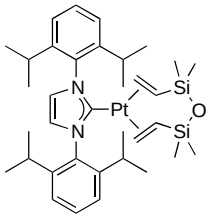

To the flask containing the solution of Karstedt's catalyst (**3.9**) prepared previously was added 6.2 mL of dry tetrahydrofuran. Then, IPr•HCl (**3.7**) (314 mg, 0.738 mmol, 1.2 equiv) was introduced, followed immediately by potassium *tert*-butoxide (75 mg, 0.74 mmol, 1.2 equiv). The resulting solution was then stirred at room temperature for 60 min. After confirming the completion of the reaction by TLC, the mixture was diluted with 10 mL of water. The aqueous layer was separated and extracted with dichloromethane (3 × 10 mL). The combined organic layers were dried over magnesium sulfate, filtered and evaporated to dryness yielding a yellow solid (349–406 mg). The crude product was crystallized with a minimal amount of isopropanol (ca. 4.2–4.8 mL) at 100 °C. The crystals were rinsed with cold isopropanol (3 × 1 mL) and dried under high vacuum to give (IPr)Pt(dvtms) (322–351 mg, 68–74% yield for 2 steps) as off white needles.

^{1}H NMR (300 MHz, $CDCl_3$) δ: 7.36 (t, 2 H, *J* = 7.8 Hz, H_{Ar}), 7.21–7.16 (m, 6 H, H_{Ar}), 2.97 (sep, 4 H, *J* = 6.7 Hz, $CHMe_2$), 1.79–1.19 (m, 6 H, H_{Vi}), 1.24 (d, 12 H, *J* = 6.9 Hz, $C(CH_3)_2$), 1.13 (d, 12 H, *J* = 6.9 Hz, $C(CH_3)_2$), 0.13 (s, 6 H, $SiCH_{3\ eq}$), –0.76 (s, 6 H, $SiCH_{3\ ax}$) ppm. **^{13}C NMR** (75 MHz, $CDCl_3$) δ: 186.1 (t, $^{1}J_{Pt-C}$ = 1412.3 Hz, $C_{carbene}$), 145.9 (C_{Ar}), 136.8 (t, $^{4}J_{Pt-C}$ = 9.8 Hz, C_{Ar}), 129.5 (C_{Ar}), 124.0 (t, $^{3}J_{Pt-C}$ = 42.0 Hz, C_{Im}), 123.7 (C_{Ar}), 41.9 (t, $^{1}J_{Pt-C}$ = 165.0 Hz, =CHSi), 35.6 (t, $^{1}J_{Pt-C}$ = 119.3 Hz, $=CH_2$), 28.5 ($CHMe_2$), 26.0 ($CHCH_3$), 22.6 ($CHCH_3$), 1.7 ($SiCH_{3\ eq}$), –2.2 ($SiCH_{3\ ax}$) ppm. **^{195}Pt NMR** (107 MHz, $CDCl_3$) δ: –5340 ppm. **IR** (thin film): 3135 (m), 2962 (s), 1463 (s), 1401 (s), 1385 (s), 1322 (s), 1246 (s), 1179 (s), 1059 (s), 977 (s), 781 (s) cm^{-1}. **MS** (ESI) m/z: 793-792-791 (97-100-70 %, $[M+Na]^+$), 743-742-741 (89-99-66 %, $[M-C_2H_3]^+$), 390-389 (4-16 %, $[IPr+H]^+$), 385 (6 %, $[IPr+H-2H_2]^+$). **Anal. calcd** for $C_{35}H_{54}N_2OPtSi_2$: C, 54.59; H, 7.07; N, 3.64; found: C, 54.44; H, 7.10; N, 3.50. **mp**: 158–159 °C (dec).

Platinum(0) diallyl ether complex (3.11) CAS: 441018-57-1

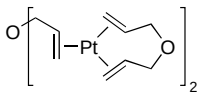

A two-necked round-bottomed flask, equipped with a thermometer and a septum, was charged with hexachloroplatinic acid hydrate (150 mg, 0.307 mmol, 1 equiv) and 2.3 mL of isopropanol (*caution: H_2PtCl_6 is toxic, corrosive and very hygroscopic*). The orange mixture was stirred at 60 °C for 30 min and then cooled to 25 °C. Solid sodium hydrogen carbonate (200 mg, 2.40 mmol, 8 equiv) was added portionwise over 5 min and the flask was left open (*caution: vigorous CO_2 gas evolution!*). After 10 min, methylbis(trimethylsilyloxy)vinylsilane (0.45 mL, 1.5 mmol, 5 equiv), one drop of water and diallyl ether (0.37 mL, 3.0 mmol, 10 equiv) were added, the reaction vessel was capped with a rubber septum and heated to 60 °C for 8 h. After confirming the completion of the reaction by TLC, the final off white suspension was cooled to room temperature. The reaction mixture was filtered through a plug of silica gel/Celite (v/v 1:1), eluting with diethyl ether. The filtrate was concentrated by rotary evaporation (200 mmHg, 25 °C), to ca. 3 mL, affording a yellow solution

of the complex, stabilized by excess diallyl ether in isopropanol, used without further purification.

This solution must not be further concentrated otherwise its platinum(0) content will be degraded resulting in significantly lower yields. Storage at –20 °C under an argon atmosphere for several days showed no degradation.

(IPr)Pt(AE) (3.12)

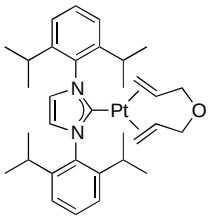

To the flask containing the solution of complex **3.11** prepared previously was added 3 mL of dry tetrahydrofuran. Then, IPr•HCl (**3.7**) (205 mg, 0.480 mmol, 1.6 equiv) was introduced, followed immediately by potassium *tert*-butoxide (54 mg, 0.48 mmol, 1.6 equiv). The resulting solution was then stirred at room temperature for 6 h. After confirming the completion of the reaction by TLC, the black mixture was filtered through a plug of silica gel/Celite (v/v 1:1), eluting with diethyl ether. After evaporation of the solvent under reduced pressure, the crude product was purified by column chromatography on silica gel (Et_2O/PE 1:9) to afford (IPr)Pt(AE) (85 mg, 41% yield for 2 steps) as a white solid.

^{1}H NMR (500 MHz, $CDCl_3$) δ: 7.35 (t, 2 H, *J* = 7.7 Hz, H_{Ph}), 7.20 (s, 2 H, $^4J_{Pt–H}$ = 9.0 Hz, H_{Im}), 7.17 (d, 4 H, *J* = 7.7 Hz, H_{Ph}), 3.95 (dd, 2 H, *J* = 12.0, 3.5 Hz, $^3J_{Pt–H}$ = 34.4 Hz, $H_{allyl\ eq}$), 2.97 (sep, 4 H, *J* = 6.7 Hz, $CHMe_2$), 2.44 (dt, 2 H, *J* = 10.9, 2.8 Hz, $^3J_{Pt–H}$ = 30.0 Hz, $H_{allyl\ ax}$), 1.62 (tt, 2 H, *J* = 11.6, 5.6 Hz, CH=), 1.32 (dd, 2 H, *J* = 8.3, 1.0 Hz, $^3J_{Pt–H}$ = 61.6 Hz, $=CH_2$), 1.18 (d, 12 H, *J* = 6.9 Hz, $C(CH_3)_2$), 1.15 (d, 12 H, *J* = 6.9 Hz, $C(CH_3)_2$), 0.85 (dd, 2 H, *J* = 10.7, 1.0 Hz, $^3J_{Pt–H}$ = 60.0 Hz, $=CH_2$) ppm. **^{13}C NMR** (75 MHz, $CDCl_3$) δ: 187.5 ($C_{carbene}$), 146.0 (C_{Ph}), 136.9 (C_{Ph}), 129.5 (C_{Ph}), 123.3 (C_{Ph}), 123.1 (t, $^3J_{Pt–C}$ = 40.6 Hz, C_{Im}), 69.2 (t, $^2J_{Pt–C}$ = 30.4 Hz, CH_2O), 47.8 (t, $^1J_{Pt–C}$ = 143.2 Hz, =CH), 32.1 (t, $^1J_{Pt–C}$ = 196.0 Hz, $=CH_2$), 28.4 ($CHMe_2$), 25.7 (CH_3), 22.6 (CH_3) ppm. **^{195}Pt NMR** (107 MHz, $CDCl_3$): –5574 ppm. **IR** (thin film): 3165 (w), 3124 (m), 3090 (w), 3037 (w), 2962 (s), 2869 (s), 2839 (m), 1560 (m), 1467 (s), 1446 (s), 1395 (s), 1385 (m), 1362 (m),

1330 (s), 1260 (s), 1178 (s), 1059 (s), 929 (s), 858 (m), 801 (s), 757 (s), 697 (m), 609 (m) cm^{-1}. **MS** (ESI) m/z: 681-680-599 $[M+H]^+$, 625-624-623 $[(IPr)Pt(CH_2{=}CH{-}CH_2)]^+$, 599-598-597 $[(IPr)Pt(CH_3)]^+$. **Anal. calcd** for $C_{33}H_{46}N_2OPt$: C, 58.13; H, 6.80; N, 4.11; found: C, 58.19; H, 6.82; N 4.04. **mp**: 158–161 °C (dec).

(IPr)Pt(SiMe$_2$Ph)$_2$ (3.39)

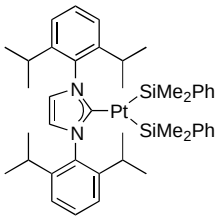

A Schlenk tube, flame-dried under a stream of argon, was charged with (IPr)Pt(dvtms) (**3.10**) (500 mg, 0.650 mmol, 1 equiv) and phenyldimethylsilane (5.0 mL, 25 mmol, 38 equiv). The white suspension was degased and then heated to 110 °C for 14 h under argon. The resulting homogeneous orange solution was evaporated to dryness under high vacuum. The orange-brown solid residue was washed with pentane (3 × 0.5–1 mL) and then dried under high vacuum to afford (IPr)Pt(SiMe$_2$Ph)$_2$ (368 mg, 431 mmol, 66 %) as a light-yellow solid.

^{1}H NMR (500 MHz, C_6D_6) δ: 7.61 (bs, 4 H, SiPh), 7.37 (t, 2 H, *J* = 7.7 Hz, NPh), 7.27 (bs, 6 H, SiPh), 7.22 (d, 4 H, *J* = 7.8 Hz, NPh), 6.53 (s, 2 H, H_{Im}), 3.08 (sep, 4 H, *J* = 6.7 Hz, $CHMe_2$), 1.46 (d, 12 H, *J* = 6.8 Hz, $C(CH_3)_2$), 1.09 (d, 12 H, *J* = 6.8 Hz, $C(CH_3)_2$), 0.41 (s, 12 H, $SiCH_3$) ppm. **^{13}C NMR** (75 MHz, $CDCl_3$) δ: 219.7 ($C_{carbene}$), 147.7 (C_{Ar}), 145.6 (C_{Ar}), 134.7 (CH_{Ar}), 130.0 (CH_{Ar}), 126.5 (CH_{Ar}), 126.3 (CH_{Ar}), 124.3 (CH_{Ar}), 123.5 (C_{Im}), 28.7 $CHMe_2$), 25.2 ($CHCH_3$), 23.7 ($CHCH_3$), 5.0 ($SiCH_3$) ppm. **^{29}Si NMR** (99 MHz, $CDCl_3$) δ: 8.4 (s) ppm. **^{195}Pt NMR** (107 MHz, $CDCl_3$) δ: –5493 ppm. **Anal. calcd** for $C_{43}H_{59}N_2PtSi_2{\bullet}CH_2Cl_2$: C, 56.27; H, 6.44; N, 2.98; found: C, 56.58; H, 6.52; N 3.17. **mp**: 168–170 °C (dec).

3.2 Preparation of the Substrates.

Dr. Alexandre Drouin and Mr. Fabio Lucaccioni synthesized and hydrosilylated *N*-(pent-4-ynyl)phthalimide.[4] Dr. Florian Schevenels provided (phenylseleno)acetylene.[5] Ms. Emilie Vercruysse carried out the preparation of allyl methacrylate and 2-methyl-4-phenyl-1-butene.[6]

Silylated alkynes **3.15d**,[7] silyl chloride **3.19**,[8] 3-trimethylsilylpropargyl alcohol,[9] 5-phenyl-1-trimethylsilyl-pentyn-3-ol,[10] *N*-allyl-*N*-propargyltosylamine,[11] 1,2-nonadiene (**1.64**),[12] and the mixture of silyl ethers **1.79** and **1.80**[13] were obtained according to literature protocols. The mixture of homopropargyl alcohol (**1.61**) and 2,3-butadiene-1-ol (**1.62**) resulted from the distillation of the former from potassium carbonate.

The silylated alkynes **3.13a–e**, **3.14a–e** and **3.15a–c** were synthesized according to the following procedure:

A round-bottomed flask, flame-dried under a stream of argon, was charged with a terminal alkyne (1 equiv) and dry tetrahydrofuran (0.5 mol L^{-1}). The solution was cooled to 0 °C and *n*-butyllithium (2.5 mol L^{-1} in hexanes, 1.1 equiv) was added dropwise. After 30 min,

4 A. Drouin, *Post-doctoral report*, Université catholique de Louvain, 2012.
5 F. Schevenels, *Ph.D. thesis*, Université catholique de Louvain, 2013
6 E. Vercruysse, *Master thesis*, Université catholique de Louvain, 2012.
7 R. B. Miller, G. McGarvey G. *J. Org. Chem.* **1978**, *43*, 4424.
8 Y. M. Pai, K. L. Servis, W. L. Weber, *Organometallics* **1986**, *5*, 683.
9 E. J. Corey, G. W. J. Fleet, M. Kato, *Tetrahedron Lett.* **1973**, *14*, 3963.
10 Y. Kiyotsuka, Y. Kobayashi, *J. Org. Chem.* **2009**, *74*, 7489.
11 a) O. Miyata, Y. Ozawa, I. Ninomiya, T. Naito, *Tetrahedron* **2000**, *56*, 6199. b) S. E. Gibson, D. J. Hardick, P. R. Haycock, K. A. C. Kaufmann, A. Miyazaki, M. J. Tozer, A. J. P. White, *Chem. Eur. J.* **2007**, *13*, 7099.
12 a) M. Makisza, M. Wawrzyniewicz, *Tetrahedron Lett.* **1969**, *10*, 4659. b) L. Brandsma, H. D. Verkruijsse, *Synthesis of Acetylenes, Allenes and Cumulenes*; Elsevier: Amsterdam, 1981, p 139.
13 H. Clavier, K. Le Jeune, I. de Riggi, A. Tenaglia, G. Buono, *Org. Lett.* **2011**, *13*, 308. 1 equiv of alcohols and 1.1 equiv of silylating agent were used.

the silyl chloride (1.1 equiv) was introduced dropwise. The reaction mixture was warmed to room temperature and stirred for 1–16 h. A saturated aqueous solution of ammonium chloride was added and the aqueous layer was extracted three times with ethyl acetate. The combined organic layers were washed with water, dried over magnesium sulfate and concentrated under reduced pressure. The last traces of volatiles were removed under high vacuum to afford the pure product as a colorless or light-yellow liquid. The analytical data were in good agreement with those reported in the literature.

3.3 Hydrosilylation

The substrates were hydrosilylated according to the following procedure, unless otherwise stated:

(IPr)Pt(dvtms) (**3**) (0.1 mol%) and the silane (1.1 equiv) were stirred in a round-bottomed flask at 60 °C for 1 h. To the resulting yellow solution, the substrate (1 equiv) was introduced slowly with a syringe pump (0.5–3 mmol h^{-1}). After confirming the completion of the reaction by GC, the reaction mixture was cooled to room temperature and filtered through a pad of silica gel/Celite/$MgSO_4$ (v/v/v 1:1:1), eluting with petroleum ether or diethyl ether (depending on product polarity). The filtrate was concentrated under reduced pressure and the last traces of volatiles were removed under high vacuum to afford the product as a colorless or light-yellow liquid. If necessary, analytically pure sample can usually be obtained by Kugelrhor distillation.

3.3.1 Hydrosilylation of Silylated Alkynes

(*E*)-2-bis(trimethylsilyloxy)methylsilyl-1-trimethylsilyl-1-octene
CAS: 1032732-57-2

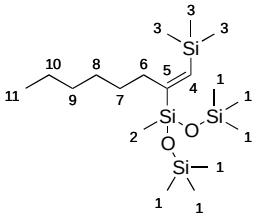

^{1}H NMR (300 MHz, $CDCl_3$) δ: 6.06 (s, 1 H, H-4), 2.22 (t, *J* = 7.8 Hz, 2 H, H-6), 1.41–1.26 (m, 8 H, H-7-8-9-10), 0.89 (t, *J* = 6.8 Hz, 3 H, H-11), 0.15 (s, 3 H, H-2), 0.11 (s, 9 H, H-3), 0.09 (s, 18 H, H-1) ppm. **^{13}C NMR** (75 MHz, $CDCl_3$) δ: 163.8 (C-5), 142.2 (C-4), 36.3 (C-6), 32.1-31.0-30.2 (C-7-8-9), 22.9 (C-10), 14.2 (C-11), 2.0 (C-1), 0.5 (C-3), 0.1 (C-2) ppm. **IR** (thin film): 2957 (m), 2929 (m), 2856 (m), 1250 (s), 1045 (s), 868 (s) cm^{-1}. **MS** (CI) m/z: 405 (10 %, $[M+H]^+$), 390 (100 %, $[M–CH_3]^+$), 221 (80 %, $[(Me_3OSi)_2MeSi]^+$). **Anal. calcd** for $C_{18}H_{44}O_2Si_4$: C, 53.40; H, 10.95; found: C, 53.32; H, 10.82.

(*E*)-2-bis(trimethylsilyloxy)methylsilyl-1-trimethylsilyl-1-propene
CAS: 1032732-50-5

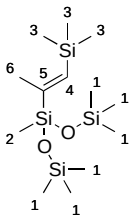

^{1}H NMR (300 MHz, $CDCl_3$) δ: 6.13 (q, ^{4}J = 1.4 Hz, 1 H, H-4), 1.87 (d, ^{4}J = 1.4 Hz, 3 H, H-6), 0.14 (s, 9 H, H-3), 0.10 (s, 21 H, H-1-2) ppm. **^{13}C NMR** (75 MHz, $CDCl_3$) δ: 158.0 (C-4), 142.0 (C-5), 20.0 (C-6), 1.9 (C-1), 0.0 (C-3), –1.4 (C-2) ppm. **IR** (thin film): 2957 (m), 1250 (s), 1045 (s) cm^{-1}. **MS** (CI) m/z: 336 (15 %, $[M+H]^+$), 319 (100 %, $[M–CH_3]^+$), 221 (42 %, $[(Me_3OSi)_2MeSi]^+$). **Anal. calcd** for $C_{13}H_{34}O_2Si_4$: C, 46.65; H, 10.24; found: C, 45.61; H, 10.16.

(*E*)-1-bis(trimethylsilyloxy)methylsilyl-2-trimethylsilylethene
CAS: 1032732-32-3

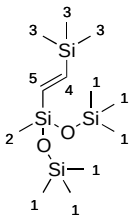

^{1}H NMR (300 MHz, $CDCl_3$) δ: 6.67 (d, *J* = 22.7 Hz, 1 H, H-4 or H-5), 6.38 (d, *J* = 22.7 Hz, 1 H, H-5 or H-4), 0.08 (s, 18 H, H-1), 0.05 (s, 12 H, H-2-3) ppm. **^{13}C NMR** (75 MHz, $CDCl_3$) δ:

152.2 (C-4 or C-5), 147.8 (C-5 or C-4), 1.8 (C-1), 1.5 (C-3), 0.5 (C-2) ppm. **IR** (thin film): 2958 (s), 2900 (m), 1258 (s), 1172 (m), 1050 (s), 840 (s), 789 (m), 755 (m) cm^{-1}. **MS** (CI) m/z: 321 (15 %, $[M+H]^+$), 306 (100 %, $[M-CH_3]^+$), 221 (15 %, $[(Me_3OSi)_2MeSi]^+$), 73 (17 %, $[Me_3Si]^+$). **Anal. calcd** for $C_{12}H_{32}O_2Si_4$: C, 44.94; H, 10.06; found: C, 44.66; H, 10.03.

(*E*)-2-bis(trimethylsilyloxy)methylsilyl-1-trimethylsilyl-3,3-dimethyl-1-butene

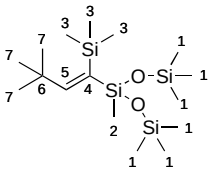

^{1}H NMR (300 MHz, $CDCl_3$) δ: 6.88 (s, 1 H, H-4), 6.20 (s, 0.07 H, $H_{\beta\text{-}(E)}$), 1.11 (s, 9 H, H-7), 0.23 (s, 9 H, H-3), 0.13 (s, 3 H, H-2), 0.10 (s, 18 H, H-1) ppm. **^{13}C NMR** (75 MHz, $CDCl_3$) δ: 169.4 (C-5), 135.9 (C-4), 36.4 (C-6), 30.7 (C-7), 3.5 (C-3), 2.0 (C-1), 1.4 (C2) ppm. **IR** (thin film): 2955 (m), 2901 (w) 2361 (m), 2341 (m), 1556 (m), 1250 (s), 1034 (s), 837 (s), 783 (s) cm^{-1}. **MS** (ESI) m/z: 399 (21 %, $[M+Na]^+$), 355 (60 %), 239 (55 %, $[(Me_3SiO)_2MeSiOH_2]^+$), 167 (60 %, $[(Me_3SiO)MeSi(OH)_2+H]^+$), 91 (100 %, $[Me_3SiOH_2]^+$). **HRMS** (ESI) m/z calcd for $[C_{16}H_{40}O_2NaSi_4]^+$: 399.1998, found: 399.1999. The regio- and stereochemistry were determined by comparison of the chemical shifts of the vinylic protons with know compounds for all possible isomers. Furthermore, nuclear Overhauser effect difference spectroscopy substantiated the stereochemistry of the major isomer:

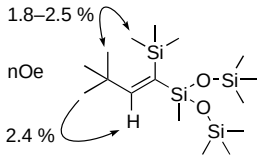

(*E*)-1-bis(trimethylsilyloxy)methylsilyl-1-phenyl-2-trimethylsilylethene

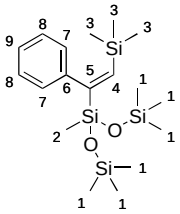

^{1}H NMR (300 MHz, $CDCl_3$) δ: 7.24–7.14 (m, 3 H, H-8-9), 7.03–6.99 (m, 2 H, H-7), 6.43 (s, 1 H, H-4), 0.09 (s, 3 H, H-2), 0.03 (s, 18 H, H-1), –0.17 (s, 9 H, H-3) ppm. **^{13}C NMR** (75 MHz, $CDCl_3$) δ: 164.0 (C-5), 145.4 (C-4), 144.5 (C-6), 127.9 (C-7 or C-8), 127.6 (C-8 or C-7), 126.0 (C-9), 1.9 (C-1), 0.1 (C-3), –0.6 (C-2) ppm. **IR** (thin film): 2957 (m), 2899 (w), 1487 (w), 1441 (w), 1410 (w), 1250 (s), 1047 (s), 835 (s), 785 (s), 700 (s) cm^{-1}. **MS** (ESI) m/z: 397 (2 %, $[M+H]^+$), 311 (8 %), 239 (100 %, $[(Me_3SiO)_2MeSiOH_2]^+$), 221 (14 %, $[(Me_3SiO)_2MeSi]^+$), 91 (26 %, $[Me_3SiOH_2]^+$). **HRMS** (ESI) m/z calcd for $[C_{18}H_{37}O_2Si_4]^+$: 397.1865, found: 397.1865.

(*E*)-1-dimethylphenylsilyl-1-phenyl-2-trimethylsilylethene

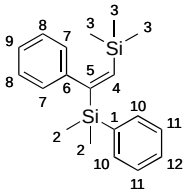

^{1}H NMR (300 MHz, $CDCl_3$) δ: 7.48–7.45 (m, 2 H, H-10 or H-11), 7.36–7.32 (m, 3 H, H-12, H-11 or H-10), 7.20–7.13 (m, 3 H, H-9, H-7 or H-8), 6.84–6.81 (m, 2 H, H-8 or H-7), 6.39 (s, 1 H, H-4), 0.32 (s, 6 H, H-2), -0.21 (s, 9 H, H-3) ppm. **^{13}C NMR** (75 MHz, $CDCl_3$) δ: 164.3 (C-5), 146.3 (C-4), 145.1 (C-6), 138.0 (C-1), 134.3 (C-10), 129.1 (C-12), 127.8-127.6 (C-7-8-11), 125.8 (C-9), 0.2 (C-3), –2.9 (C-2) ppm. The analytical data were in good agreement with those reported in the literature.[14]

(*E*)-1-methyldiphenylsilyl-1-phenyl-2-trimethylsilylethene

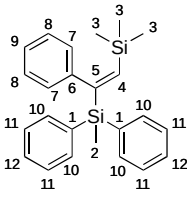

^{1}H NMR (300 MHz, $CDCl_3$) δ: 7.51–7.48 (m, 4 H, H-10 or H-11), 7.39–7.31 (m, 6 H, H-12, H-11 or H-10), 7.15–7.11 (m, 3 H, H-9, H-7 or H-8), 6.88–6.84 (m, 2 H, H-8 or H-7), 6.45 (s, 1 H, H-4), 0.53 (s, 3 H, H-2), -0.19 (s,

[14] A. Naka, S. Okazaki, M. Hayashi, M. Ishikawa, *J. Organomet. Chem.* **1995**, *499*, 35.

9 H, H-3) ppm. **^{13}C NMR** (75 MHz, $CDCl_3$) δ: 161.7 (C-5), 149.6 (C-4), 145.0 (C-6), 136.0 (C-1), 135.4 (C-10), 129.4 (C-12), 127.87-127.85 (C-8-11), 127.7 (C-7), 126.0 (C-9), 0.2 (C-3), –3.6 (C-2) ppm. **IR** (thin film): 3069 (m), 3049 (m), 2953 (m), 2895 (w), 1589 (w), 1549 (w), 1487 (s), 1427 (s), 1111 (s), 932 (s), 852 (s), 779 (s), 688 (s) cm^{-1}. **MS** (ESI) m/z: 373 (17 %, $[M+H]^+$), 215 (100 %), 197 (8 %, $[Ph_2MeSi]^+$) 181 (24 %), 95 (38 %, $[MeSi(OH)_3+H]^+$), 77 (29 %, $[Ph]^+$). **HRMS** (ESI) m/z calcd for $[C_{24}H_{28}NaSi_2]^+$: 395.1622, found: 395.1618.

(*E*)-2-bis(trimethylsilyloxy)methylsilyl-3-trimethylsilyl-2-propen-1-ol (3.95)

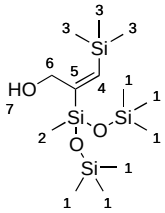

^{1}H NMR (300 MHz, $CDCl_3$) δ: 6.26 (s, 1 H, H-4), 4.32 (d, *J* = 4.8 Hz, 2 H, H-6), 1.84 (t, *J* = 5.6 Hz, 1 H, H-7), 0.17 (s, 3 H, H-2), 0.14 (s, 9 H, H-3), 0.11 (s, 18 H, H-1) ppm. **^{13}C NMR** (75 MHz, $CDCl_3$) δ: 161.2 (C-5), 145.1 (C-4), 65.6 (C-6), 2.0 (C-1), 0.3 (C-3), 0.1 (C-2) ppm. **IR** (thin film): 2954 (w), 1250 (m), 1041 (s), 839 (s), 785 (m), 754 (w) cm^{-1}. **MS** (ESI) m/z: 373 (100 %, $[M+Na]^+$), 239 (6 %, $[(Me_3SiO)_2MeSiOH_2]^+$), 91 (13 %, $[Me_3SiOH_2]^+$), 73 (18 %, $[Me_3Si]^+$). **HRMS** (ESI) m/z calcd for $[C_{13}H_{34}O_3NaSi_4]^+$: 373.1477, found: 373.1479.

3.3.2 Hydrosilylation of Terminal Alkynes

(*E*)-1-triethylsilyl-1-octene CAS: 31930-43-5

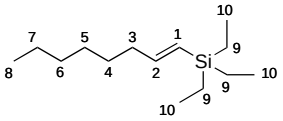

^{1}H NMR (300 MHz, $CDCl_3$) δ: 6.03 (dt, *J* = 18.7, 6.3 Hz, 1 H, H-2), 5.53 (dt, *J* = 18.7, 1.5 Hz, 1 H, H-1), 2.15–1.99 (m, 2 H, H-3), 1.41–1.26 (m, 8 H, H-4-5-6-7), 0.96–0.86 (m, 12 H, H-8-10), 0.54 (q, *J* = 7.7 Hz, 6 H, H-9) ppm. **^{13}C NMR** (75 MHz, $CDCl_3$) δ: 149.0 (C-2), 125.6 (C-1), 37.3 (C-3), 31.9 (C-6), 29.0 (C-4-5), 22.8 (C-7), 14.2 (C-8), 7.5 (C-10), 3.7 (C-9) ppm. **IR** (thin film): 2953 (s), 2926 (s), 2874 (s), 1616 (m), 1458 (m), 1462 (m), 1236 (m), 1014 (s), 989 (s) cm^{-1}. **MS** (CI) m/z: 197 (100 %, [M–

$C_2H_5]^+$), 115 (35 %, $[Et_3Si]^+$). The analytical data were in good agreement with those reported in the literature.[15]

(*E*)-1-(trimethylsilyloxy)dimethylsilyl-1-octene

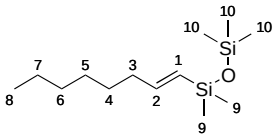

^{1}H NMR (300 MHz, $CDCl_3$) δ: 6.09 (dt, *J* = 18.6, 6.2 Hz, 1 H, H-2), 5.59 (dt, *J* = 18.6, 1.4 Hz, 1 H, H-1), 2.13–2.06 (m, *J* = 13.7, 7.1 Hz, 2 H, H-3), 1.39–1.27 (m, 8 H, H-4-5-6-7), 0.88 (t, *J* = 6.7 Hz, 3 H, H-8), 0.09 (d, *J* = 11.3 Hz, 12 H, H-9-10) ppm. **^{13}C NMR** (75 MHz, $CDCl_3$) δ: 148.3 (C-2), 129.5 (C-1), 36.7 (C-3), 31.9 (C-6), 29.1 (C-4 or C-5), 28.7 (C-5 or C-4), 22.8 (C-7), 14.3 (C-8), 2.2 (C-10), 0.9 (C-9) ppm. The analytical data were in good agreement with those reported in the literature.[16]

(*E*)-1-bis(trimethylsilyloxy)methylsilyl-1-octene (3.121)

CAS: 885456-00-8

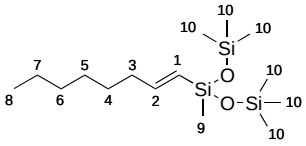

^{1}H NMR (300 MHz, $CDCl_3$) δ: 6.13 (dt, *J* = 18.6, 6.4 Hz, 1 H, H-2), 5.47 (dt, *J* = 18.6, 1.4 Hz, 1 H, H-1), 2.13–2.06 (m, 2 H, H-3), 1.41–1.28 (m, 8 H, H-4-5-6-7), 0.88 (t, *J* = 6.8 Hz, 3 H, H-8), 0.10–0.07 (m, 21 H, H-9-10) ppm. **^{13}C NMR** (75 MHz, $CDCl_3$) δ: 149.3 (C-2), 127.8 (C-1), 36.6 (C-3), 31.9 (C-6), 29.0 (C-4 or C-5), 28.6 (C-5 or C-8), 22.8 (C-7), 14.3 (C-8), 2.0 (C-10), 0.1 (C-9) ppm. **IR** (thin film): 2958 (s), 2927 (s), 2856 (m), 1620 (m), 1258 (s), 1048 (s) cm^{-1}. **MS** (ESI) m/z: 355 (100 %, $[M+Na]^+$), 314 (28 %), 208 (24 %, $[(Me_3SiO)SiOH(Me_2SiO)]^+$), 167 (10 %, $[(Me_3SiO)MeSi(OH)_2+H]^+$), 91 (2%, $[Me_3SiOH_2]^+$). **HRMS** (ESI) m/z calcd for $[C_{15}H_{36}O_2NaSi_3]^+$: 355.1915, found: 355.1916. **Anal. calcd** for $C_{15}H_{36}O_2Si_3$: C, 54.15; H, 10.91; found: C, 53.90; H, 10.82. **bp**: 86–89 °C. For more information, see reference 3.

---

15 R. Takeuchi, S. Nitta, D. Watanabe, *J. Org. Chem.* **1995**, *60*, 3045.

16 K. Hirabayashi, E. Takahisa, Y. Nishihara, A. Mori, T. Hiyama, *Bull. Chem. Soc. Jpn.* **1998**, *71*, 2409.

(*E*)-1-tris(trimethylsilyloxy)silyl-1-octene

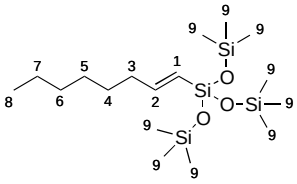

^{1}H NMR (300 MHz, $CDCl_3$) δ: 6.19 (dt, *J* = 18.6, 6.3 Hz, 1 H, H-2), 5.35 (dt, *J* = 18.5, 1.5 Hz, 1 H, H-1), 2.10 (td, *J* = 7.7, 1.4 Hz, 2 H, H-3), 1.42–1.28 (m, 8 H, H-4-5-6-7), 0.88 (t, *J* = 6.7 Hz, 3 H, H-8), 0.10 (s, 27 H, H-9) ppm. **^{13}C NMR** (75 MHz, $CDCl_3$) δ: 150.3 (C-2), 123.8 (C-1), 36.4 (C-3), 31.7 (C-6), 28.8 (C-4 or C-5), 28.4 (C-5 or C-4), 22.6 (C-7), 14.1 (C-8), 1.8 (C-9) ppm. **IR** (thin film): 2957 (m), 2927 (m), 2856 (w), 1624 (w), 1456 (w), 1250 (s), 1047 (s), 862 (s), 839 (s), 794 (m), 754 (m), 685 (m) cm^{-1}. **MS** (ESI) m/z: 407 (10 %, $[M+H]^+$), 299 (13 %), 225 (100 %), 109 (10 %, $[C_8H_{13}]^+$), 93 (52 %). **HRMS** (ESI) m/z calcd for $[C_{17}H_{43}O_3Si_4]^+$: 407.2284, found: 407.2274.

(*E*)-1-dimethylphenylsilyl-1-octene CAS: 116488-00-7

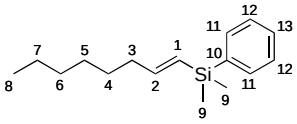

^{1}H NMR (300 MHz, $CDCl_3$) δ: 7.54–7.51 (m, 2 H, H-11 or H-12), 7.36–7.33 (m, 3 H, H-13, H-12 or H-11), 6.12 (dt, *J* = 18.5, 6.2 Hz, 1 H, H-2), 5.75 (dt, *J* = 18.6, 1.3 Hz, 1 H, H-1), 2.17–2.11 (m, 2 H, H-3), 1.40–1.27 (m, 8 H, H-4-5-6-7), 0.88 (t, *J* = 6.6 Hz, 3 H, H-8), 0.32 (s, 6 H, H-9) ppm. **^{13}C NMR** (75 MHz, $CDCl_3$) δ: 149.6 (C-2), 139.5 (C-10), 134.0 (C-11), 128.9 (C-13), 127.8 (C-12), 127.3 (C-1), 37.0 (C-3), 31.9 (C-6), 29.1 (C-4 or C-5), 28.8 (C-5 or C-4), 22.8 (C-7), 14.3 (C-8), –2.3 (C-9) ppm. **IR** (thin film): 2956 (s), 2926 (s), 2855 (m), 1616 (m), 1427 (m), 1247 (s), 1113 (s), 840 (s), 821 (s) cm^{-1}. **MS** (APCI) m/z: 247 (21 %, $[M+H]^+$), 232 (15 %, $[M+H-CH_3]^+$), 169 (42 %, $[M-Ph]^+$), 135 (54 %, $[PhMe_2Si]^+$), 84 (100 %, $[Me_2Si-CH=CH]^+$). The analytical data were in good agreement with those reported in the literature.[17]

[17] K. Itami, K. Mitsudo, A. Nishino, J.-i. Yoshida, *J. Org. Chem.* **2002**, *67*, 2645.

(*E*)-1-methyldiphenylsilyl-1-octene

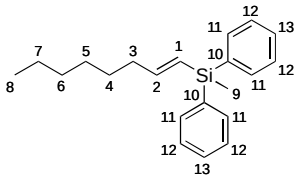

^{1}H NMR (300 MHz, $CDCl_3$) δ: 7.54–7.51 (m, 4 H, H-11 or H-12), 7.38–7.33 (m, 6 H, H-13, H-12 or H-11), 6.16 (dt, *J* = 18.5, 6.1 Hz, 1 H, H-2), 5.93 (dt, *J* = 18.5, 1.2 Hz, 1 H, H-1), 2.22–2.15 (m, 2 H, H-3), 1.44–1.29 (m, 8 H, H-4-5-6-7), 0.89 (t, *J* = 6.7 Hz, 3 H, H-8), 0.60 (s, 3 H, H-9) ppm. **^{13}C NMR** (75 MHz, $CDCl_3$) δ: 151.8 (C-2), 137.3 (C-10), 135.0 (C-11), 129.3 (C-13), 127.9 (C-12), 125.2 (C-1), 37.1 (C-3), 31.9 (C-6), 29.0 (C-4 or C-5), 28.7 (C-5 or C-4), 22.8 (C-7), 14.3 (C-8), –3.5 (C-9) ppm. The analytical data were in good agreement with those reported in the literature.[18]

(*E*)-1-ethoxydiphenylsilyl-1-octene

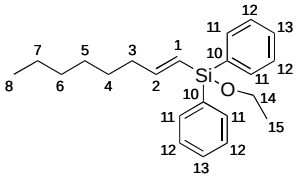

The reaction was performed under an inert atmosphere on 3 mmol of 1-octyne. Hydrosilylation was carried out using the standard procedure. After confirming the completion of the reaction by GC, the reaction vessel was cooled to 0 °C and 3 mL of tetrahydrofuran were added. Triethylamine (2 equiv) and ethanol (2 equiv) were successively introduced dropwise. The reaction mixture was slowly warmed to room temperature and stirred overnight. A saturated aqueous solution of ammonium chloride was added and the aqueous layer was extracted three times with ethyl acetate. The combined organic layers were washed with water, dried over magnesium sulfate and concentrated under reduced pressure. The last traces of volatiles were removed under high vacuum to afford the pure product as a light-yellow liquid.

^{1}H NMR (300 MHz, $CDCl_3$) δ: 7.62–7.59 (m, 4 H, H-11 or H-12), 7.42–7.35 (m, 6 H, H-13, H-12 or H-11), 6.28 (dt, *J* = 18.7, 6.2 Hz, 1 H, H-2), 5.97 (dt, *J* = 18.6, 1.3 Hz, 1 H, H-1), 3.82 (q, *J* = 7.0 Hz, 2 H, H-14), 2.24–2.18 (m, 2 H, H-3), 1.43–1.31 (m, 2 H, H-7), 1.28–1.22 (m, 6 H, H-4-5-6),

[18] B. J. Truscott, A. M. Z. Slawin, S. P. Nolan, *Dalton Trans.* **2013**, *42*, 270.

1.23 (t, *J* = 7 Hz, 3 H, H-15), 0.88 (t, *J* = 6.7 Hz, 3 H, H-8) ppm. **^{13}C NMR** (75 MHz, $CDCl_3$) δ: 154.1 (C-2), 135.4 (C-10), 135.1 (C-11), 129.9 (C-13), 127.9 (C-12), 123.4 (C-1), 59.6 (C-14), 37.0 (C-3), 31.8 (C-6), 29.0 (C-4 or C-5), 28.5 (C-5 or C-4), 22.8 (C-7), 18.6 (C-15), 14.2 (C-8) ppm. **IR** (thin film): 3069 (w), 3049 (w), 2957 (m), 2924 (s), 2871 (m), 2854 (m), 1958 (w), 1886 (w), 1823 (w), 1774 (w), 1616 (m), 1589 (w), 1427 (s), 1109 (s), 1076 (s), 948 (s), 791 (s), 735 (s), 698 (s) cm^{-1}. **MS** (ESI) m/z: 329 (2 %, $[M+H]^+$), 311 (100 %, $[M–Et+H_2]^+$), 293 (8 %, $[M–EtO]^+$), 279 (28 %, $[M–Ph+H_2O]^+$), 251 (5 %, $[M–Et–Ph+H_2O]^+$) 245 (59 %), 217 (43 %, $[Ph_2Si(OH)_2+H]^+$), 157 (22 %, $[PhSi(OH)_3+H]^+$), 97 (30 %, $[Si(OH)_4+H]^+$). **HRMS** (ESI) m/z calcd for $[C_{22}H_{31}OSi]^+$: 339.2139, found: 339.2138.

(*E*)-1-diethoxymethylsilyl-1-octene CAS: 89984-52-1

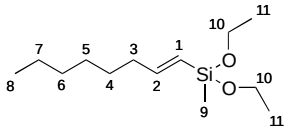

^{1}H NMR (300 MHz, $CDCl_3$) δ: 6.30 (dt, *J* = 18.8, 6.2 Hz, 1 H, H-2), 5.53 (dt, *J* = 18.8, 1.5 Hz, 1 H, H-1), 3.77 (q, *J* = 7.0 Hz, 4 H, H-10), 2.17–2.10 (m, 2 H, H-3), 1.45–1.35 (m, 2 H, H-7), 1.33–1.25 (m, 6 H, H-4-5-6), 1.22 (t, *J* = 7.0 Hz), 0.88 (t, *J* = 6.7 Hz, 3 H, H-8), 0.18 (s, 3 H, H-9) ppm. **^{13}C NMR** (75 MHz, $CDCl_3$) δ: 152.3 (C-2), 123.5 (C-1), 58.3 (C-10), 36.8 (C-3), 31.8 (C-6), 29.0 (C-4 or C-5), 28.5 (C-5 or C-4), 22.7 (C-7), 18.5 (C-11), 14.2 (C-8), 4.2 (C-9) ppm. The analytical data were in good agreement with those reported in the literature.[19] Synthesized by Mr. Thibaut Debande.

(*E*)-1-bis(trimethylsilyloxy)methylsilyl-2-phenylethene
CAS: 198623-99-3

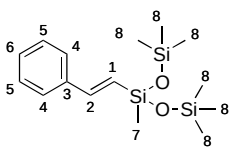

^{1}H NMR (300 MHz, $CDCl_3$) δ: 7.46–7.43 (m, 2 H, H-4 or H-5), 7.37–7.28 (m, 3 H, H-6, H-5 or H-4), 6.96 (d, *J* = 19.2 Hz, 1 H, H-2), 6.26 (d, 1 H, H-1), 0.18 (s, 3 H, H-7), 0.13 (s, 18 H, H-8) ppm. **^{13}C NMR** (75 MHz,

[19] K. Tamao, M. Kumada, K. Maeda, *Tetrahedron Lett.* **1984**, *25*, 321.

$CDCl_3$) δ: 145.2 (C-2), 138.3 (C-3), 128.7 (C-4 or C-5), 128.4 (C-6), 126.7 (C-1, C-4 or C-5), 2.1 (C-8), 0.2 (C-7) ppm. **IR** (thin film): 2957 (m), 1607 (w), 1575 (w), 1495 (w), 1447 (w), 1250 (s), 1041 (s), 837 (s), 812 (s) cm^{-1}. **MS** (EI) m/z: 324 (21 %, $[M]^+$), 309 (100 %, $[M–CH_3]^+$), 221 (84 %, $[(Me_3SiO)_2MeSi]+$). **HRMS** (ESI) m/z calcd for $[C_{15}H_{28}O_2NaSi_3]^+$: 347.1289, found: 347.1290. **Anal. calcd** for $C_{15}H_{28}O_2Si_3$: C, 55.50; H, 8.61; found: C, 55.54; H, 8.61.

(*E*)-3-bis(trimethylsilyloxy)methylsilyl-2-propen-1-ol
CAS: 1032732-22-1

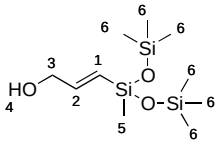

^{1}H NMR (300 MHz, $CDCl_3$) δ: 6.29 (dt, *J* = 18.9, 4.2 Hz, 1 H, H-2), 5.76 (dt, *J* = 18.9, 1.8 Hz, 1 H, H-1), 4.20 (dd, *J* = 4.2, 1.9 Hz, 2 H, H-3), 1.73 (bs, 1 H, H-4), 0.10 (s, 21 H, H-5-6) ppm. **^{13}C NMR** (75 MHz, $CDCl_3$) δ: 146.7 (C-2), 126.8 (C-1), 65.2 (C-3), 2.0 (C-6), 0.1 (C-5) ppm. **IR** (thin film): 3307 (bs), 2958 (m), 2900 (m), 2866 (m), 1624 (w), 1252 (s), 1045 (s), 896 (s), 754 (s) cm^{-1}. **MS** (CI) m/z: 279 (25 %, $[M+H]^+$), 261 (100 %, $[M–CH_3–H_2]^+$), 221 (40 %, $[(Me_3SiO)_2MeSi]^+$). **Anal. calcd** for $C_{10}H_{26}O_3Si_3$: C, 43.12; H, 9.41; found: C, 42.88; H, 9.38.

(*E*)-4-bis(trimethylsilyloxy)methylsilyl-2-methyl-3-buten-2-ol

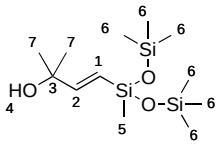

^{1}H NMR (300 MHz, $CDCl_3$) δ: 6.25 (d, *J* = 19.0 Hz, 1 H, H-2), 5.65 (d, *J* = 19.0 Hz, 1 H, H-1), 2.01 (bs, 1 H, H-4), 1.30 (s, 6 H, H-7), 0.10 (s, 21 H, H-5-6) ppm. **^{13}C NMR** (75 MHz, $CDCl_3$) δ: 155.0 (C-2), 122.7 (C-1), 71.9 (C-3), 29.3 (C-7), 2.0 (C-6), 0.0 (C-5) ppm. **IR** (thin film): 3371 (bs), 2959 (m), 2901 (w), 1618 (w), 1456 (w), 1404 (w), 1361 (w), 1252 (s), 1218 (w), 1041 (s), 837 (s), 786 (s) cm^{-1}. **MS** (ESI) m/z: 329 (14 %, $[M+Na]^+$), 297 (51 %), 283 (75 %), 225 (100 %), 91 (65 %, $[Me_3SiOH_2]^+$), 73 (37 %, $[C_4H_9O]^+$). **HRMS** (ESI) m/z calcd for $[C_{12}H_{30}O_3NaSi_3]^+$: 329.1395, found: 329.1394.

(*E*)-4-dimethylphenylsilyl-3-buten-1-ol (3.63) CAS: 104080-51-5

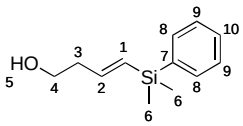

^{1}H NMR (300 MHz, $CDCl_3$) δ: 7.53–7.50 (m, 2 H, C-8 or C-9), 7.38–7.33 (m, 3 H, H-10, C-9 or C-8), 6.10 (dt, *J* = 18.6, 6.2 Hz, 1 H, H-2), 5.92 (dt, *J* = 18.6, 1.2 Hz, 1 H, H-1), 3.71 (dd, *J* = 12.2, 6.2 Hz, 2 H, H-4), 2.44 (qd, *J* = 6.3, 1.2 Hz, 2 H, H-3), 1.33 (t, *J* = 5.8, 1 H, H-5), 0.34 (s, 6 H, H-6) ppm. **^{13}C NMR** (75 MHz, $CDCl_3$) δ: 144.8 (C-2), 138.8 (C-7), 133.8 (C-8), 131.3 (C-10), 129.0 (C-1), 127.8 (C-9), 61.5 (C-4), 40.1 (C-3), –2.5 (C-6) ppm. The analytical data were in good agreement with those reported in the literature.[20]

(*E*)-*N*-allyl-*N*-(3-(dimethylphenylsilyl)allyl)-tosylamine

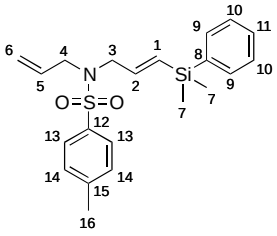

The reaction was performed according to the standard procedure, excepted that (i) 1 mol% of catalyst was used, (ii) 1.05 equiv of silane was used and (iii) the substrate was dissolved in tetrahydrofuran (1 mol L^{-1}) and added in one portion.

^{1}H NMR (300 MHz, $CDCl_3$) δ for major isomer: 7.69 (d, *J* = 8.3 Hz, 1.84 H, H-13), 7.45–7.42 (m, 2 H, H-9 or H-10), 7.37–7.33 (m, 3 H, H-11, H-10 or H-9), 7.26 (d, *J* = 8.3 Hz, 2 H, H-14), 5.88 (d, *J* = 18.6 Hz, H-1), 5.79 (dd, *J* = 18.6, 4.8 Hz, 1 H, H-2), 5.61 (ddt, *J* = 16.7, 10.3, 6.3 Hz, 1 H, H-5), 5.14–5.06 (m, 2 H, H-6), 3.87 (d, *J* = 4.5 Hz, 2 H, H-3), 3.79 (d, *J* = 6.3 Hz, 2 H, H-4), 2.42 (s, 3 H, H-16), 0.27 (s, 5.28 H, H-7) ppm. δ for minor isomer: 7.62 (d, *J* = 8.5 Hz, 0.11 H, H-13), 7.56–7.53 (m, 0.26 H, H_{Ar}), 5.36–5.31 (m, 0.07 H, H_{Vi}), 4.97–4.90 (m, 0.13 H, H_{Vi}), 3.66 (d, *J* = 6.9 Hz, 0.11 H, H-4), 0.33 (s, 0.74 H, H-7) **^{13}C NMR** (75 MHz, $CDCl_3$) δ for major isomer: 143.3 (C-15), 141.7 (C-1), 138.1 (C-8), 137.5 (C-12), 133.7 (C-9 or C-10), 132.8 (C-2 or C-5), 132.6 (C-5 or C-2), 129.7 (C-14), 129.1 (C-11), 127.9 (C-10 or C-9), 127.2 (C-13), 119.0 (C-6), 51.7, (C-3), 49.8 (C-4), 21.6 (C-16), 2.7 (C-7) ppm. **IR** (thin film): 3069 (w), 2955 (w),

[20] S. Couty, C. Meyer, J. Cossy, *Tetrahedron* **2009**, *65*, 1809.

1618 (w), 1597 (w), 1495 (w), 1427 (m), 1346 (s), 1248 (s), 1155 (s), 1113 (s), 1092 (s), 991 (m), 927 (m), 814 (s) cm^{-1}. **MS** (ESI) m/z: 386 (10 %, $[M+H]^+$), 209 (6 %, $[M–Ph_2MeSiC_3H_4–H]^+$), 195 (47 %, $[M–Ph_2MeSiC_3H_4–H–CH_3]^+$), 175 (57 %, $[M–C_3H_5NTs]^+$), 119 (100 %, $[C_3H_5NSO_2]^+$) 93 (90 %, $[Tol+H]^+$). **HRMS** (ESI) m/z calcd for $[C_{21}H_{28}O_2N_1S_1Si_1]^+$: 386.1605, found: 386.1606.

3.3.3 Hydrosilylation of Alkenes

bis(trimethylsilyloxy)methyloctylsilane CAS: 17955-88-3

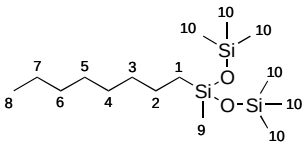

^{1}H NMR (300 MHz, $CDCl_3$) δ: 140–1.21 (m, 12 H, H-2-3-4-5-6-7), 0.88 (t, *J* = 6.6 Hz, 3 H, H-8), 0.45 (t, *J* = 7.6 Hz, 2 H, H-1), 0.12 (s, 18 H, H-10, 0.10 (s, 3 H, H-9) ppm. **^{13}C NMR** (75 MHz, $CDCl_3$) δ: 33.3 (C-3 or C-6), 31.9 (C-6 or C-3), 29.7 (C-4 or C-5), 29.4 (C-5 or C-4), 23.1 (C-2 or C-7), 22.7 (C-7 or C-2), 17.6 (C-1), 14.1 (C-8), 1.9 (C-10), –0.3 (C-9) ppm. **MS** (APCI) m/z: 334 (100 %, $[M]^+$), 319 (18%, $[M–CH_3]^+$), 221 (6 %, $[(Me_3SiO)_2MeSi]^+$). The analytical data were in good agreement with those reported in the literature.[21] Synthesized by Ms. Emilie Vercruysse.

(*S*)-1-bis(trimethylsilyloxy)methylsilyl-3,7-dimethyl-6-octene

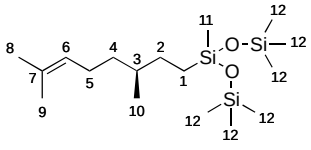

^{1}H NMR (300 MHz, $CDCl_3$) δ: 5.14–5.09 (m, 1 H, H-6), 1.97 (sep, *J* = 7.5 Hz, 2 H, H-5), 1.69 (s, 3 H, H-8), 1.61 (s, 3 H, H-9), 1.36–1.29 (m, 3 H, H-2-3-4), 1.15–1.10 (m, 2 H, H-2'-4'), 0.86 (d, *J* = 6.2 Hz, 3 H, H-10), 0.48–0.38 (m, 2 H, H-1), 0.10 (s, 18 H, H-12), 0.01 (s, 3 H, H-11) ppm. **^{13}C NMR** (75 MHz, $CDCl_3$) δ: 130.9 (C-7), 125.1 (C-6), 36.6 (C-4), 34.9 (C-3), 29.9 (C-2), 25.7 (C-8), 25.6 (C-5), 19.1

[21] J. Pernak, A. Swierczynska, M. Kot, F. Walkiewicz, H. MacIejewski, *Tetrahedron Lett.* **2011**, *52*, 4342.

(C-10), 17.6 (C-9), 14.5 (C-1), 1.9 (C-12), –0.4 (C-11) ppm. **IR** (thin film): 2959 (m), 2914 (m), 2866 (m), 1257 (s), 1043 (s) 839 (s) cm^{-1}. Synthesized by Ms. Emilie Vercruysse.

1-bis(trimethylsilyloxy)methylsilyl-3-(oxiran-2-ylmethoxy)-1-propanol

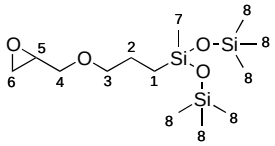

^{1}H NMR (300 MHz, $CDCl_3$) δ: 3.70 (dd, *J* = 11.5, 3.1 Hz, 1 H, H-4), 3.50–3.36 (m, 3 H, H-3-4'), 3.18–3.12 (m, 1 H, H-5), 2.81–2.78 (m, 1 H, H-6), 2.61 (dd, *J* = 5.0, 2.7 Hz, H-6'), 1.66–1.58 (m, 2 H, H-2), 0.48–0.42 (m, 2 H, H-1), 0.08 (s, 18 H, H-8), 0.01 (s, 3 H, H-7) ppm. **^{13}C NMR** (75 MHz, $CDCl_3$) δ: 74.3 (C-3), 71.4 (C-4), 50.9 (C-5), 44.4 (C-6), 23.3 (C-2), 13.5 (C-1), 1.9 (C-8), –0.4 (C-7) ppm. **IR** (thin film): 2961 (m), 2918 (m), 2860 (m), 1254 (s), 1039 (s), 839 (s) cm^{-1}. **MS** (ESI) m/z: 359 (100 %, $[M+Na]^+$), 342 (13 %), 247 ($[M–Me_3SiO]^+$), 195 (12 %). **HRMS** (ESI) m/z calcd for $[C_{13}H_{32}O_4NaSi_3]^+$: 359.1501, found: 359.1502. Synthesized by Ms. Emilie Vercruysse.

1-bis(trimethylsilyloxy)methylsilyl-3-(2-hydroxyethoxy)-1-propanol

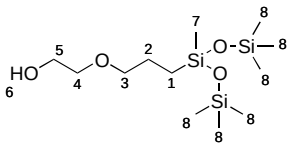

^{1}H NMR (300 MHz, $CDCl_3$) δ: 3.76–3.71 (m, 2 H, H-5), 3.54 (t, *J* = 4.9 Hz, 2 H, H-4), 3.43 (t, *J* = 6.9 Hz, 2 H, H-3), 1.99 (t, *J* = 6.1 Hz, 1 H, H-6), 1.66–1.58 (m, 2 H, H-2), 0.48–0.43 (m, 2 H, H-1), 0.09 (s, 18 H, H-8), 0.02 (s, 3 H, H-7) ppm. **^{13}C NMR** (75 MHz, $CDCl_3$) δ: 73.9 (C-3), 71.6 (C-4), 61.9 (C-5), 23.3 (C-2), 13.5 (C-1), 1.9 (C-8), –0.3 (C-7) ppm. **IR** (thin film): 3300 (bm), 1257 (s), 1045 (s), 840 (s) cm^{-1}. **MS** (ESI) m/z: 347 (100 %, $[M+Na]^+$), 248 (9 %, $[M–H–C_3H_7O_2]^+$), 145 (9 %), 105 (12 %). **HRMS** (ESI) m/z calcd for $[C_{12}H_{32}O_4NaSi_3]^+$: 347.1501, found: 347.1502. Synthesized by Ms. Emilie Vercruysse.

3-triethoxysilyl-propyl hexanoate

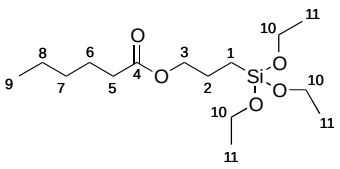

^{1}H NMR (300 MHz, $CDCl_3$) δ: 4.04 (t, *J* = 6.8 Hz, 2 H, H-3), 3.82 (q, *J* = 7.0 Hz, 6 H, H-10), 2.29 (t, *J* = 7.5 Hz, 2 H, H-5), 1.79–1.69 (m, 2 H, H-2), 1.67–1.57 (m, 2 H, H-6), 1.35–1.20 (m, 4 H, H-7-8), 1.23 (t, *J* = 7.0 Hz, 12 H, H-11), 0.89 (t, *J* = 6.9 Hz, 3 H, H-9), 0.68–0.62 (m, 2 H, H-1) ppm. **^{13}C NMR** (75 MHz, $CDCl_3$) δ: 174.0 (C-4), 66.4 (C-3), 58.5 (C-10), 34.4 (C-5), 31.4 (C-7), 24.8 (C-6), 22.4 (C-2 or C-8), 22.3 (C-8 or C-2), 18.3 (C-11), 14.0 (C-9), 6.6 (C-1) ppm. **IR** (thin film): 2972 (m), 2928 (m), 2885 (m), 1736 (s), 1442 (w), 1389 (m), 1244 (m), 1167 (s), 1101 (s), 1076 (s), 957 (s), 775 (s) cm^{-1}. **MS** (ESI) m/z: 321 (5 %, $[M+H]^+$), 293 (10 %, $[M-C_2H_5+2\ H]^+$), 251 (100 %), 177 (31 %), 125 (80 %), 99 (76 %, $[C_5H_{11}CO]^+$) 71 (70 %, $[C_5H_{11}]^+$). **HRMS** (ESI) m/z calcd for $[C_{15}H_{32}O_5NaSi]^+$: 343.1911, found: 343.1911.

3-diethoxymethylsilyl-propyl hexanoate

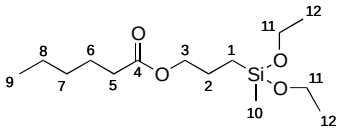

^{1}H NMR (300 MHz, $CDCl_3$) δ: 4.03 (t, *J* = 6.9 Hz, 2 H, H-3), 3.82–3.69 (m, 4 H, H-11), 2.29 (t, *J* = 7.5 Hz, 2 H, H-5), 1.74–1.58 (m, 4 H, H-2-6), 1.36–1.19 (m, 4 H, H-7-8-12), 0.89 (t, *J* = 6.9 Hz, 3 H, H-9), 0.65–0.60 (m, 2 H, H-1), 0.13 (s, 3 H, H-10) ppm. **^{13}C NMR** (75 MHz, $CDCl_3$) δ: 173.9 (C-4), 66.5 (C-3), 58.2 (C-11), 34.4 (C-5), 31.4 (C-7), 24.8 (C-6), 22.4 (C-2 or C-8), 22.3 (C-8 or C-2), 18.4 (C-11), 13.94 (C-9), 10.0 (C-1), –4.9 (C-10) ppm. **IR** (thin film): 2957 (m), 2928 (m), 2874 (m), 1736 (s), 1460 (w), 1389 (m), 1258 (m), 1257 (m), 1167 (s), 1101 (s), 1076 (s), 950 (s), 794 (s) cm^{-1}. **MS** (ESI) m/z: 313 (100 %, $[M+Na]^+$), 270 (15 %), 229 (16 %), 175 (4 %, $[M-C_5H_{11}CO_2]^+$). **HRMS** (ESI) m/z calcd for $[C_{14}H_{30}O_4NaSi]^+$: 313.1806, found: 313.1804.

3-bis(trimethylsilyloxy)methylsilyl-propyl methacrylate

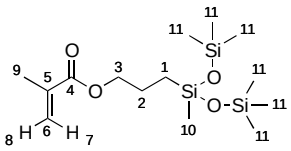

^{1}H NMR (300 MHz, $CDCl_3$) δ: 6.11 (s, 1 H, H-7), 5.55 (s, 1 H, H-8), 4.09 (t, *J* = 6.8 Hz, 2 H, H-3), 1.95 (s, 3 H, H-9), 1.73–1.63 (m, 2 H, H-2), 0.53–0.47 (m, 2 H, 1), 0.10 (s, 18 H, H-11), 0.09 (s, 2 H, H-9) ppm. **^{13}C NMR** (75 MHz, $CDCl_3$) δ: 167.5 (C-4), 136.6 (C-5), 125.1 (C-6), 67.0 (C-3), 22.5 (C-2), 18.4 (C-9), 13.6 (C-1), 1.8 (C-11), –0.9 (C-10) ppm. **IR** (thin film): 1722 (s), 1454 (w), 1257 (s), 1163 (m), 1049 (s) cm^{-1}. **MS** (ESI) m/z: 349 (100 %, $[M+H]^+$), 168 (21 %), 124 (5 %). **HRMS** (ESI) m/z calcd for $[C_{14}H_{32}O_4NaSi_3]^+$: 371.1501, found: 371.1503. Synthesized by Ms. Emilie Vercruysse.

1-bis(trimethylsilyloxy)methylsilyl-2-methyl-4phenylbutane

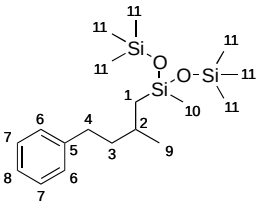

^{1}H NMR (300 MHz, $CDCl_3$) δ: 7.25–7.24 (m, 2 H, H-7), 7.19–7.16 (m, 3 H, H-6-8), 2.66–2.53 (m, 2 H, H-4), 1.72–1.53 (m, 2 H, H-3), 1.51–1.44 (m, 1 H, H-2), 0.98 (d, *J* = 6.4 Hz, 3 H, H-9), 063 (dd, *J* = 14.7, 4.6 Hz, 1 H, H-1), 0.41 (dd, *J* = 14.7, 8.4 Hz, H-1', 0.08 (s, 18 H, H-11), 0.01 (s, 3 H, H-10) ppm. **^{13}C NMR** (75 MHz, $CDCl_3$) δ: 143.1 (C-5), 128.4 (C-6 or C-7), 128.2 (C-7 or C-6), 125.5 (C-8), 42.3 (C-4), 33.7 (C-3), 28.5 (C-2), 26.1 (C-1), 22.5 (C-9), 1.9 (C-11), 0.9 (C-10) ppm. **IR** (thin film): 2956 (m), 2916 (m), 2869 (m), 1496 (m), 1251 (s), 1029 (bs), 754 (s), 696 (s) cm^{-1}. **MS** (ESI) m/z: 391 (100 %, $[M+Na]^+$), 369 (38 %, $[M+H]^+$), 304 (65 %), 282 (70 %), 102 (93 %). **HRMS** (ESI) m/z calcd for $[C_{18}H_{36}O_2NaSi_3]^+$: 391.1915, found: 391.1915. Synthesized by Ms. Emilie Vercruysse.

3.4 Transformations of the Vinylsilanes

5-cinnamyl-2,2-dimethyl-4-dimethylphenylsilyl-2,5-dihydro-[1,2]oxasilole

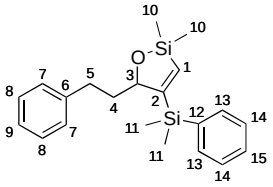

A round-bottomed flask, flame-dried under a stream of argon, was charged with the corresponding alcohol (369 mg, 1.00 mmol, 1 equiv), and dry diethylether (10 mL). The solution was cooled to −78 °C and *n*-butyllithium (freshly titrated, 2.33 mol L^{-1} in hexanes, 0.47 mL, 1.10 mmol, 1.1 equiv) was added dropwise over 5 min. After 15 min, dry TMEDA (3.0 mL, 20 mmol, 20 equiv) was introduced in one portion. The mixture was warmed to 0 °C, stirred for 6 h. Water was added (10 mL) and the aqueous layer was extracted with diethyl ether (2 × 5 mL). The combined organic layers were washed with a saturated solution of ammonium chloride (3 × 10 mL) and brine (1 × 5 mL), dried over magnesium sulfate and concentrated under reduced pressure. The last traces of volatiles were removed under high vacuum to afford the product (270 mg, 0.767 mmol, 77 %) as a light-yellow liquid.

^{1}H NMR (300 MHz, $CDCl_3$) δ: 7.52–7.49 (m, 2 H, H-13 or H-14), 7.38–7.32 (m, 3 H, H-15, H-14 or H-13), 7.22–7.09 (m, 3 H, H-9, H-7 or H-8), 6.95–6.93 (m, 2 H, H-8 or H-7), 6.59 (d, *J* = 2 Hz, 1 H, H-1), 4.92–4.88 (m, 1 H, H-3), 2.64–2.45 (m, 2 H, H-5), 2.03–1.92 (m, 1 H, H-4), 1.59–1.47 (m, 1 H, H-4'), 0.42 (s, 6 H, H-11), 0.29 (s, 3 H, H-10), 0.26 (s, 3 H, H-10') ppm. **^{13}C NMR** (75 MHz, $CDCl_3$) δ: 169.9 (C-2), 142.4 (C-6), 141.8 (C-1), 137.5 (C-12), 134.0 (C-13), 129.3 (C-15), 128.5-128.3-128.1 (C-7-8-14), 126.6 (C-9), 86.2 (C-3), 38.9 (C-4), 31.1 (C-5), 1.4 (C-10), 0.7 (C-10'), -1.8 (C-11), −2.6 (C-11') ppm. **IR** (thin film): 3067 (w), 3026 (w), 2955 (w), 2928 (w), 1858 (w), 1603 (w), 1497 (m), 1454 (m), 1427 (m), 1248 (s), 1112 (m), 1041 (s), 970 (s), 864 (s), 829 (s), 775 (s) cm^{-1}. **MS** (ESI) m/z: 353 (6 %, $[M+H]^+$), 217 (30 %, $[M-PhMe_2Si]^+$), 167 (100 %), 149 (19 %), 93 (24%, $[Tol+H]^+$). **HRMS** (ESI) m/z calcd for $[C_{21}H_{29}OSi_2]^+$: 353.1752, found: 353.1751.

(*E*)-4-bromo-1-dimethylphenylsilyl-1-butene CAS: 1194063-80-3

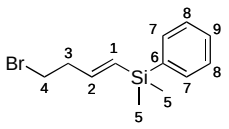

A 500-mL round-bottomed flask, was charged with the corresponding alcohol (10.82 g, 52.43 mmol, 1.08 equiv), carbon tetrabromide (15.98 g, 48.18 mmol, 1 equiv) and dry dichloromethane (100 mL). The solution was cooled to 0 °C and a solution of triphenylphosphine (13.16 g, 50.18 mmol, 1.05 equiv) in dry dichloromethane (40 mL) was added dropwise over 1 h. After 1 h, the completion of the reaction was checked by TLC and the reaction mixture was concentrated under reduced pressure. The resulting dark yellowish-green solid was triturated overnight in petroleum ether (300 mL), filtered and washed with petroleum ether (3 × 50 mL). The filtrate was concentrated under reduced pressure to afford the crude product contaminated with bromoform and traces of triphenylphosphine oxide. Purification by column chromatography on silica gel (PE to AcOEt/PE 3:97) yielded the pure product (12.06 g, 44.78 mmol, 93 %) as a light-yellow liquid.

^{1}H NMR (300 MHz, $CDCl_3$) δ: 7.54–7.50 (m, 2 H, H-7 or H-8), 7.37–7.34 (m, 3 H, H-9, H-8 or H-7), 6.06 (dt, *J* = 18.6, 5.9 Hz, 1 H, H-2), 5.90 (dt, *J* = 18.5, 1.1 Hz, 1 H, H-1), 3.43 (t, *J* = 7.1 Hz, 2 H, H-4), 2.71 (qd, *J* = 7.1, 1.1 Hz, 2 H, H-3), 0.34 (s, 6 H, H-5) ppm. **^{13}C NMR** (75 MHz, $CDCl_3$) δ: 144.7 (C-2), 138.6 (C-6), 133.9 (C-7), 131.5 (C-1), 129.1 (C-9), 127.9 (C-8), 39.8 (C-3), 31.6 (C-4), –2.5 (C-5) ppm. The analytical data were in good agreement with those reported in the literature.[22]

[22] J. Lange, E. Schaumann, *Eur. J. Org. Chem.* **2009**, *27*, 4674.

4. Compounds Synthesized in Chapter 4

4.1 Synthesis of the Imidazolium Salt IPr*$^{(2\text{-Np})}$•HCl

Alcohol 4.7 CAS: 4809-95-4

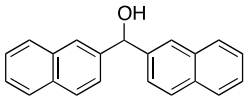

A 500-mL, three-necked, round-bottomed flask was equipped with a 20-cm condenser, a 250-mL dropping funnel and a septum. The flask was charged with a 2.5-cm oval stir bar and magnesium turnings (4.38 g, 180 mmol, 2.1 equiv) before it was flame-dried under a stream of argon. One crystal of iodine and 60 mL of dry tetrahydrofuran were introduced and heated to reflux. After 10 min, a few mL of 2-bromonaphthalene (37.31 g, 180.2 mmol, 2.1 equiv), dissolved in 90 mL of dry tetrahydrofuran, were added in one portion. After decolorization (10–15 min), the remaining 2-bromonaphthalene was added dropwise over 3 h. The resulting black mixture was stirred for 90 min under reflux and then cooled with an ice bath. Ethyl formate (6.90 mL, 85.8 mmol, 1 equiv) was added over 1 h using a syringe pump. The resulting suspension was warmed slowly to room temperature overnight and then cooled with an ice bath before carefully adding 150 mL of HCl_{aq} 1M. The aqueous layer was acidified to pH ~ 2 with concentrated HCl_{aq} (36%). The organic phase was diluted with ethyl acetate until both layers had the same volume. The aqueous phase was extracted with ethyl acetate (3 × 50 mL). The combined organic layers were washed with brine (100 mL), dried over magnesium sulfate, filtered and concentrated under reduced pressure to yield a beige solid. The crude product was triturated with a minimum amount of petroleum ether overnight, filtered, washed with petroleum ether and dried under high vacuum to afford the alcohol **4.7** (23.37 g, 96 %) as a white solid.

^{1}H NMR ($CDCl_3$, 300 MHz) δ: 7.92 (s, 2 H), 7.84–7.76 (m, 6 H), 7.50–7.43 (m, 6 H), 6.13 (d, *J* = 3.1 Hz, 1 H), 2.45 (d, *J* = 3.5 Hz, 1 H) ppm. **^{13}C NMR**

($CDCl_3$, 75 MHz) δ: 141.1, 133.4, 133.0, 128.5, 128.2, 127.8, 126.4, 126.2, 125.4, 125.0, 76.6 ppm. **IR** (thin film): 2947 (m), 2920 (m), 2906 (m), 2854 (m), 1599 (m), 1506 (m), 1362 (m), 1261 (m), 1161 (m), 1118 (m), 1024 (s), 822 (s), 785 (s), 756 (s) cm^{-1}. **MS** (APCI) m/z: 283 (12 %, $[M–H]^+$), 267 (100 %). **mp**: 112 °C. The analytical data were in good agreement with those reported in the literature.[23]

Aniline 4.8

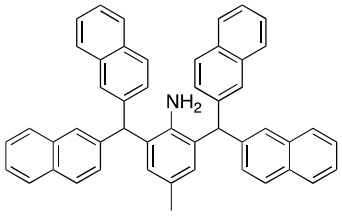

Alcohol **4.7** (23.37 g, 82.17 mmol, 2 equiv) and *p*-toluidine (4.40 g, 41.1 mmol, 1 equiv) were mixed and finely powdered together in a mortar. This solid blend was introduced in a 250-mL Schlenk round-bottomed flask equipped with a 2.5-cm dumbbell-shaped stir bar and heated in an oil bath (110 °C, external temperature) until liquefaction. Separately, zinc chloride (2.80 g, 20.6 mmol, 0.5 equiv) was dissolved in concentrated HCl (36 % in water, 3.60 mL, 41.1 mmol, 1 equiv) and then added over 1 min under vigorous stirring (*caution: this addition is accompanied by vigorous gas evolution!*). The Schlenk flask was sealed with a screw cap immediately after the end of the addition. The reaction mixture solidified rapidly and was heated to 160 °C (external temperature). After 2 h, the solid was cooled slowly to room temperature and then dissolved in 120 mL of dichloromethane. The organic layer was washed with saturated ammonium chloride (100 mL) and brine (100 mL) and dried over potassium carbonate. Silica gel was added (10 g) and the suspension was stirred and filtered after 10 min. Evaporation of the solvent under reduced pressure afforded the crude product as a brown solid, which was purified by trituration with 1-butanol (350 mL) under reflux for 4 hours. The suspension was cooled with an ice bath, filtered and washed with cold 1-butanol (3 × 20 mL). The resulting beige solid was dried

[23] B. S. Park, S. W. Lee, I. T. Kim, J. S. Tae, S. H. Lee, *Heteroatom Chem.* **2012**, *23*, 66–73.

under high vacuum at 50 °C, yielding the pure aniline **4.8** (20.48 g, 78 %).

^{1}H NMR ($CDCl_3$, 300 MHz) δ: 7.82–7.76 (m, 8 H), 7.71–7.68 (m, 4 H), 7.51 (s, 4 H), 7.45–7.42 (m, 8 H), 7.35 (d, *J* = 8.4 Hz, 4 H), 6.52 (s, 2 H), 5.78 (s, 2 H), 3.40 (s, 2 H), 1.99 (s, 3 H) ppm. **^{13}C NMR** ($CDCl_3$, 75 MHz) δ: 140.3, 140.1, 133.6, 132.5, 129.7, 129.1, 128.5, 128.3, 128.1, 127.7, 126.2, 125.9, 52.8, 21.1 ppm. **IR** (thin film): 3043 (s), 1630 (s), 1601 (s), 1506 (s), 1464 (s), 1265 (m), 858 (m), 820 (m), 748 (s) cm^{-1}. **MS** (ESI) m/z: 640 (44 %, $[M+H]^+$), 374 (100 %), 267 (25 %), 246 (10 %). **HRMS** (ESI) m/z calcd for $[C_{49}H_{38}N_1]^+$: 640.2999, found: 640.2993. **Anal. calcd** for $C_{49}H_{37}N_1$: C, 91.98; H, 5.83; N, 2.19; found: C, 92.02; H, 5.86; N, 1.89. **mp**: 150 °C.

Diazadiene 4.9

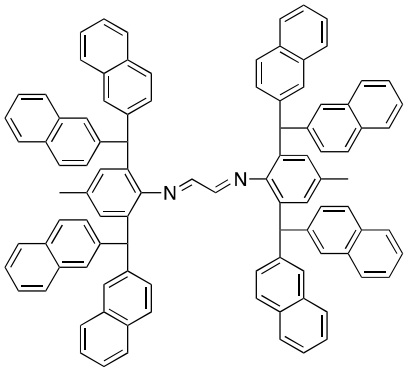

A 50-mL, two-necked, round-bottomed flask was equipped with a 10-cm condenser and a septum. The flask was charged with a 1-cm oval stir bar, aniline **4.8** (10.00 g, 15.63 mmol, 2 equiv), 20 mL of ethyl acetate and 5 drops of acetic acid. The white suspension was stirred vigorously under reflux and glyoxal (40 % in water, 0.89 mL, 7.8 mmol, 1 equiv) was added in one portion. A yellow precipitate appeared rapidly and the reaction mixture was stirred overnight under reflux. The suspension was cooled with an ice bath, filtered and washed with cold ethyl acetate (3 × 15 mL). The resulting yellow solid was dried under high vacuum, yielding the diazadiene **4.9** (6.51 g, 64 %).

^{1}H NMR ($CDCl_3$, 300 MHz) δ: 7.69 (d, *J* = 7.5 Hz, 8 H), 7.61–7.57 (m, 16 H), 7.42–7.34 (m, 18 H), 7.29 (s, 8 H), 7.10 (d, *J* = 8.4 Hz, 8 H), 6.73 (s, 4 H), 5.45 (s, 4 H), 2.08 (s, 6 H) ppm. **^{13}C NMR** ($CDCl_3$, 75 MHz) δ: 163.6, 146.8, 141.2, 134.0, 133.4, 132.3, 131.9, 129.6, 128.5, 128.2 (2 C), 128.1,

127.7, 126.1, 125.8, 51.5, 21.5 ppm. **IR** (thin film): 2921 (s), 1630 (s), 1601 (s), 1506 (s), 1452 (m), 1360 (w), 1271 (m), 1200 (m), 1124 (m), 906 (s), 858 (s), 820 (s), 733 (s) cm^{-1}. **MS** (ESI) m/z: 1302 (7 %, $[M+H]^+$), 1272 (100%), 1218 (41 %), 1024 (65 %), 887 (26 %). **HRMS** (ESI) m/z calcd for $[C_{100}H_{73}N_2]^+$: 1301.5768, found: 1301.5785. **Anal. calcd** for $C_{100}H_{72}N_2$: C, 92.27; H, 5.58; N, 2.15; found: C, 90.96; H, 5.54; N, 1.78. **mp**: 247 °C (dec).

Imidazolium salt IPr*$^{(2\text{-Np})}$•HCl (4.10)

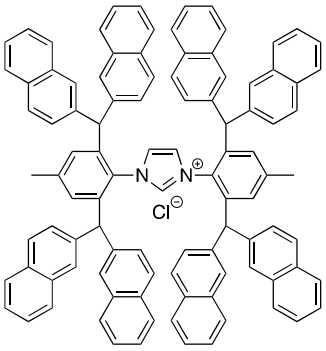

A 1-L, two-necked, round-bottomed flask was equipped with a 20-cm condenser, a septum and a 2.5-cm oval stir bar and flame-dried under a stream of argon. The flask was charged with diazadiene **4.9** (16.77 g, 12.88 mmol, 1 equiv) and 400 mL of dry tetrahydrofuran and heated with an oil bath (70 °C, external temperature). Zinc chloride (1.76 g, 12.9 mmol, 1 equiv), HCl 4M in 1,4-dioxane (4.0 mL, 16 mmol, 1.25 equiv) and paraformaldehyde (423 mg, 14.1 mmol, 1.1 equiv) were added successively and rapidly. The color of the homogeneous solution evolved from yellow to deep red immediately. The progress of the reaction was followed by TLC (toluene, imidazolium salt **4.10** R_f = 0; aniline **4.8** R_f = 0.40; diazadiene **4.9** R_f = 0.84). After 12 h, the black homogeneous mixture was cooled to room temperature and concentrated to dryness under reduced pressure. The solid residue was dissolved in ethyl acetate (100 mL) and water (50-mL). The organic layer was washed with water (2 × 50 mL) and brine (50 mL), dried over magnesium sulfate, filtered and evaporated under reduced pressure to afford a brown solid. The crude product was purified by trituration with dichloromethane/hexane (1:2, 100 mL) under reflux overnight. The suspension was cooled with an ice bath, filtered and washed with a *minimum amount* of cold dichloromethane until the filtrate was colorless. (*Notice: the product is soluble in dichloromethane*). The resulting off-white solid was dried

under high vacuum, yielding the imidazolium salt IPr*$^{(2\text{-Np})}$•HCl (**4.10**) (3.60 g, 21 %).

^{1}H NMR ($CDCl_3$, 300 MHz) δ: 13.82 (s, 1H), 7.80–7.75 (m, 8 H), 7.71–7.66 (m, 12 H), 7.51 (s, 4 H), 7.43–7.30 (m, 20 H), 7.27–7.20 (m, 4 H), 7.05 (s, 4 H), 6.88 (s, 4 H), 6.74 (dd, *J* = 8.4, 1.5 Hz, 4 H), 5.73 (s, 4 H), 5.41 (d, *J* = 0.9 Hz, 2 H), 2.16 (s, 6 H) ppm. **^{13}C NMR** ($CDCl_3$, 75 MHz) δ: 141.8, 140.1, 140.0, 139.8, 133.4, 133.1, 132.6, 132.3, 131.7, 130.6, 129.2, 128.9, 128.8, 128.6, 128.4, 127.9, 127.72, 127.68, 127.6, 126.4, 126.3, 126.00, 125.95, 123.4, 51.8, 22.1 ppm. **IR** (thin film): 3053 (w), 1630 (w), 1599 (m), 1529 (w), 1506 (m), 1458 (w), 1361 (w), 1271 (m), 860 (s), 822 (s), 748 (s) cm^{-1}. **MS** (APCI) m/z: 1314 (69 %, $[M\text{-}Cl]^+$), 663 (100 %), 650 (47 %), 551 (55 %), 338 (65 %), 215 (54 %). **HRMS** (ESI) m/z calcd for $[C_{101}H_{73}N_2]^+$: 1314.5852, found: 1314.5815. **Anal. calcd** for $C_{101}H_{73}ClN_2$: C, 89.85; H, 5.45; N, 2.07; found: C, 88.80; H, 5.56; N, 1.70. **mp**: 220–221 °C (dec). Single-crystals suitable for X-ray diffraction analysis were obtained by slow diffusion of hexane into a benzene solution.

4.2 Synthesis of the organometallic complexes

Silver(I) complex 4.11

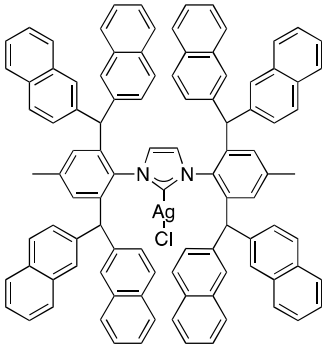

A 10-mL round-bottomed flask was equipped with a septum and a 1-cm oval stir bar, and flame-dried under a stream of argon. The flask was charged with the imidazolium salt **4.10** (145 mg, 0.107 mmol, 1.9 equiv) and 5 mL of dry dichloromethane. Silver(I) oxide (13 mg, 0.056 mmol, 1 equiv) was introduced and the resulting suspension was stirred away from light overnight. The reaction mixture was filtered through celite, eluting with

dichloromethane, concentrated under reduced pressure and dried under high vacuum to afford the silver(I) complex **4.11** (142 mg, 91 %) as a white solid.

^{1}H NMR ($CDCl_3$, 300 MHz) δ: 7.74 (d, *J* = 7.8 Hz, 4 H), 7.68–7.64 (m, 8 H), 7.54 (dd, *J* = 14.0, 8.5 Hz, 4 H), 7.47–7.31 (m, 26 H), 7.26–7.24 (m, 4 H), 7.19 (dd, *J* = 8.4, 1.8 Hz, 4 H), 7.04 (dd, *J* = 8.5, 1.7 Hz, 4 H), 6.96 (s, 4 H), 5.84 (d, *J* = 1.8 Hz, 2 H), 5.59 (s, 4 H), 2.20 (s, 6 H) ppm. **^{13}C NMR** ($CDCl_3$, 75 MHz) δ: 140.8, 140.5, 139.8, 134.7, 133.4, 133.3, 132.4, 130.9, 128.8, 128.5, 128.2, 128.0, 127.9, 127.7, 127.6, 126.4, 126.2, 126.1, 125.9, 124.2, 124.1, 51.8, 22.0 ppm. No signal detected for the carbon coordinated to silver. **IR** (thin film): 3053 (w), 1630 (w), 1601 (m), 1506 (s), 1472 (m), 1408 (w), 1364 (w), 1263 (m), 858 (s), 820 (s), 777 (m), 748 (s) cm^{-1}. **MS** (ESI) m/z: 1420 (6 %, $[M–Cl]^+$), 1313 (22 %), 797 (8 %), 662 (10 %), 522 (21 %), 267 (100 %). **HRMS** (ESI) m/z calcd for $[C_{101}H_{72}AgN_2]^+$: 1419.4741, found: 1419.4738. A satisfactory elemental analysis could not be obtained despite several attempts; **Anal. calcd** for $C_{101}H_{72}AgClN_2$: C, 83.36; H, 4.98; N, 1.92; found: C, 81.31; H, 4.91; N, 1.59. **mp**: 212–213 °C (dec). Single-crystals suitable for X-ray diffraction analysis were obtained by slow diffusion of hexane into a chloroform solution.

Copper(I) complex 4.12

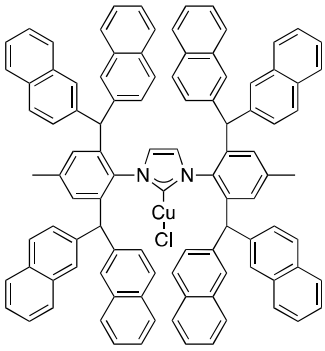

A 10-mL round-bottomed flask was equipped with a septum and a 1-cm oval stir bar, and flame-dried under a stream of argon. The flask was charged with the imidazolium salt **4.10** (170 mg, 0.125 mmol, 1 equiv), copper(I) chloride (12 mg, 0.13 mmol, 1 equiv) and 4.2 mL of dry dichloromethane. Potassium *tert*-butoxide (21 mg, 0.19 mmol, 1.5 equiv) was introduced and the resulting homogeneous brown solution was stirred overnight. The reaction mixture was filtered through celite, eluting with

dichloromethane, and concentrated under reduced pressure to afford a brown solid. The crude product was triturated for 1 h in 2.5 mL of dichloromethane and then 2.5 mL of pentane were added. The supernatant was removed and the resulting white solid was triturated with pentane (3 × 2 mL) and dried under high vacuum to yield of copper(I) complex **4.12** (104 mg, 59 %).

^{1}H NMR ($CDCl_3$, 300 MHz) δ: 7.73 (d, *J* = 8.3 Hz, 4 H), 7.66 (d, *J* = 7.7 Hz, 8 H), 7.53 (dd, *J* = 8.5 Hz, 3.3 Hz, 8 H), 7.48 (s, 4 H), 7.44–7.30 (m, 24 H), 7.22 (s, 4 H), 7.02 (d, *J* = 8.7 Hz, 4 H), 6.95 (s, 4 H), 5.74 (s, 2 H), 5.66 (s, 4 H), 2.20 (s, 6 H) ppm. **^{13}C NMR** ($CDCl_3$, 75 MHz) δ: 140.8, 140.5, 140.4, 140.1, 134.5, 133.3, 133.2, 132.39, 132.36, 130.8, 128.6, 128.4, 128.3, 128.1, 127.9, 127.7, 127.6, 126.3, 126.1, 126.0, 125.8, 123.6, 51.8, 22.0 ppm. No signal detected for the carbon coordinated to copper. **IR** (thin film): 3053 (w), 1632 (w), 1601 (m), 1506 (s), 1470 (m), 1406 (w), 1364 (w), 1263 (m), 858 (s), 820 (s), 777 (m), 748 (s) cm^{-1}. **MS** (ESI) m/z: 1314 (100 %, $[M–CuCl]^+$), 1045 (13 %), 520 (8 %), 267 (30 %). **HRMS** (ESI) m/z calcd for $[C_{101}H_{72}CuN_2]^+$: 1375.4986, found: 1375.4968. **Anal. calcd** for $C_{101}H_{72}CuClN_2$: C, 85.87; H, 5.14; N,1.98; found: C, 85.25; H, 5.37; N, 1.60. **mp**: >250 °C. Single-crystals suitable for X-ray diffraction analysis were obtained by slow evaporation of a chloroform solution.

Palladium(II) complex 4.13

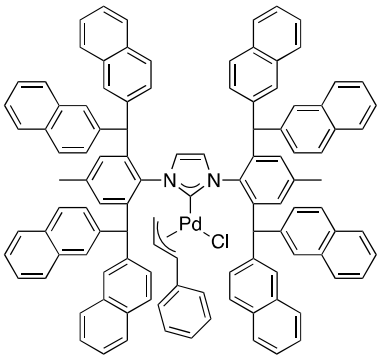

A 10-mL round-bottomed flask was equipped with a septum and a 1-cm oval stir bar, and flame-dried under a stream of argon. The flask was charged with the imidazolium salt **4.10** (191 mg, 0.141 mmol, 2.4 equiv) and 5 mL of dry tetrahydrofuran. Potassium *tert*-butoxide (16 mg, 0.14 mmol, 2.4 equiv) was introduced, followed after 15 min by palladium(π-cinnamyl) chloride dimer (30 mg,

0.059 mmol, 1 equiv). The reaction mixture was stirred overnight and then concentrated under reduced pressure. The solid residue was dissolved in dichloromethane, filtered through silica gel/celite (1:1 v/v), eluting with dichloromethane, and concentrated under reduced pressure to afford a yellow solid. The crude product was triturated with pentane (3 × 1 mL) and dried under high vacuum to yield the palladium(II) complex **4.13** (160 mg, 72 %) as a yellow solid.

^{1}H NMR ($CDCl_3$, 300 MHz) δ: 7.88–7.73 (m, 12 H), 7.69–7.50 (m, 13 H), 7.49–7.31 (m, 20 H), 7.28–7.15 (m, 10 H), 7.08 (d, *J* = 11.3 Hz, 4 H), 6.89 (s, 4 H), 6.79 (d, *J* = 8.4 Hz, 2 H), 6.66 (d, *J* = 8.0 Hz, 2 H), 6.44 (s, 2 H), 6.14 (s, 2 H), 5.37–5.25 (m, 1 H), 5.14 (s, 2 H), 4.98 (d, *J* = 13.2 Hz, 1 H), 3.09 (d, *J* = 6.3 Hz, 1 H), 2.19 (s, 6 H), 1.87 (d, *J* = 11.1 Hz, 1 H) ppm. **^{13}C NMR** ($CDCl_3$, 75 MHz) δ: 182.3, 141.7, 141.5, 141.4, 141.0, 140.5, 138.8, 137.8, 136.3, 133.4, 133.2, 132.4, 132.1, 131.0, 129.5, 129.2, 129.0, 128.8, 128.2, 128.1, 128.0, 127.7, 127.6, 127.3, 126.02, 125.95, 125.8, 123.4, 109.3, 92.4, 51.8, 47.4, 22.0 ppm. **IR** (thin film): 3051 (m), 3020 (w), 2955 (w), 2922 (w), 2853 (w), 1630 (w), 1599 (m), 1506 (s), 1460 (m), 1400 (w), 1265 (m), 858 (s), 820 (s), 777 (m), 746 (s), 692 (s) cm^{-1}. **MS** (ESI) m/z: 1536 (2 %, $[M–Cl]^+$), 1431 (12 %), 1314 (30 %), 621 (37 %), 596 (28 %), 493 (100 %), 355 (28 %), 265 (82 %). **HRMS** (ESI) m/z calcd for $[C_{110}H_{81}N_2Pd]^+$: 1535.5429, found: 1535.5453. **Anal. calcd** for $C_{110}H_{81}ClN_2Pd$: C, 84.01; H, 5.19; N, 1.78; found: C, 83.85; H, 5.30; N, 1.36. **mp**: 206–207 °C (dec).

Rhodium(I) (cod) complex 4.14

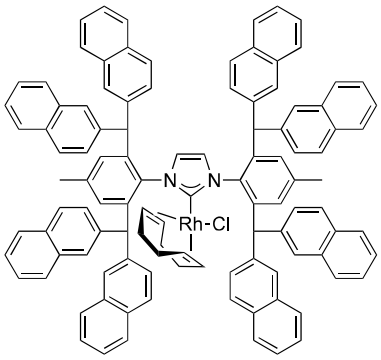

A 25-mL round-bottomed flask was equipped with a septum and a 1-cm oval stir bar, and flame-dried under a stream of argon. The flask was charged with potassium *tert*-butoxide (13 mg, 0.11 mmol, 2.2 equiv) and 8 mL of dry tetrahydrofuran, and cooled with an ice bath. 1,5-Cyclooctadienerhodium(I)

chloride dimer (25 mg, 0.051 mmol, 1 equiv) was introduced and the resulting orange solution was stirred 15 min in the ice bath, and then 45 min at room temperature. The imidazolium salt **4.10** (152 mg, 0.112 mmol, 2.2 equiv) was added and the reaction mixture evolved progressively from orange to yellow. After 7 h, the homogeneous solution was filtered through celite, eluting with dichloromethane, and concentrated under reduced pressure to afford a yellow solid. The crude product was dissolved in a minimum amount of chloroform and precipitated with pentane. The supernatant was removed and the resulting yellow solid was triturated with pentane (3×2 mL) and dried under high vacuum to yield the rhodium(I) (cod) complex **4.14** (154 mg, 97 %) as a yellow solid. This complex appeared to be relatively unstable and was used in the next step without delay.

^{1}H NMR ($CDCl_3$, 300 MHz) δ: 8.20 (d, *J* = 8.4 Hz, 2 H), 7.83–7.17 (m, 44 H), 7.14–7.02 (m, 7 H), 6.94–6.85 (m, 9 H), 6.61–6.48 (m, 6 H), 6.24 (s, 2 H), 5.42 (s, 2 H), 4.88 (s, 2 H), 3.75 (s, 2 H), 2.53–2.38 (m, 2 H), 2.20 (s, 6 H), 2.08–1.81 (m, 4 H), 1.68–1.54 (m, 2 H) ppm. **^{13}C NMR** ($CDCl_3$, 75 MHz) δ: 181.2 (d, $^1J_{C–Rh}$ = 52 Hz), 142.3, 142.2, 141.6, 140.8, 140.4, 138.4, 137.0, 133.4, 133.2, 133.0, 132.3, 132.2, 132.0, 131.5, 130.6, 130.3, 129.7, 129.1, 128.8, 128.3, 128.1, 127.9, 127.6, 127.5, 127.1, 126.1, 126.0, 125.6, 125.5, 123.8, 97.3 (d, $^1J_{C–Rh}$ = 7.3 Hz), 71.0 (d, $^1J_{C–Rh}$ = 13.8 Hz), 51.8, 51.5, 32.9, 28.8, 21.9 ppm. **IR** (thin film): 3053 (m), 3018 (w), 2918 (w), 2878 (w), 2829 (w), 1630 (w), 1599 (m), 1506 (m), 1458 (m), 1391 (w), 1271 (w), 906 (s), 858 (s), 820 (s), 779 (m), 730 (s) cm^{-1}. **MS** (ESI) m/z: 1525 (100 %, $[M–Cl]^+$), 1315 (24 %), 625 (25 %). **HRMS** (ESI) m/z calcd for $[C_{109}H_{85}N_2Rh]^+$: 1524.5762, found: 1524.5691. **mp**: 87–88 °C (dec). Due to the lack of stability of this complex, an elemental analysis was not carried out.

Rhodium(I) $(CO)_2$ complex 4.15

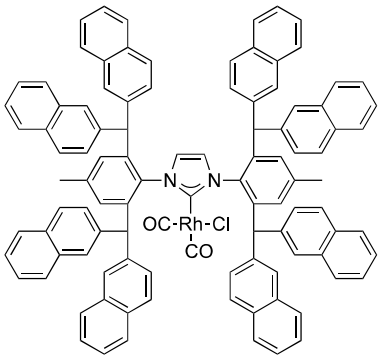

A 10-mL round-bottomed flask was equipped with a septum and a 1-cm oval stir bar. The flask was charged with rhodium (cod) complex **4.14** (154 mg, 0.0987 mmol) and 4 mL of dry dichloromethane. Carbon monoxide was bubbled through the solution for 30 min. The reaction mixture was then concentrated under reduced pressure to dryness. The resulting yellow solid was triturated with pentane (5×5 mL) and dried under high vacuum to yield of rhodium(I) $(CO)_2$ complex **4.15** (148 mg, 100 %) as a yellow solid.

^{1}H NMR ($CDCl_3$, 300 MHz) δ: 7.84–7.78 (m, 12 H), 7.62–7.59 (m, 8 H), 7.52 (s, 4 H), 7.46–7.33 (m, 14 H), 7.23–7.20 (m, 11 H), 7.03 (s, 4 H), 6.87 (s, 4 H), 6.70 (dd, J = 8.4, 1.2 Hz, 4 H), 6.27 (s, 4 H), 4.96 (s, 2 H), 2.19 (s, 6 H) ppm. **^{13}C NMR** ($CDCl_3$, 75 MHz) δ: 185.3 (d, $^1J_{C–Rh}$ = 54 Hz), 182.6 (d, $^1J_{C–Rh}$ = 74 Hz), 178.0 (d, $^1J_{C–Rh}$ = 46 Hz), 141.5, 141.0, 139.3, 135.2, 133.4, 133.1, 132.4, 132.1, 131.1, 129.6, 129.3, 128.2, 128.1, 127.94, 127.89, 127.7, 127.6, 127.3, 126.1, 126.0, 125.9, 123.5, 52.0, 22.0 ppm. **IR** (thin film): 3053 (m), 3018 (w), 2075 (s), 1994 (s), 1956 (w), 1923 (w), 1630 (w), 1599 (m), 1506 (m), 1458 (m), 1402 (m), 1273 (m), 906 (s), 858 (s), 820 (s), 777 (s), 758 (s), 731 (s), 704 (s) cm^{-1}. **MS** (ESI) m/z: 1445 (3 %, $[M–CO–Cl]^+$), 1345 (3 %), 1315 (100 %). **HRMS** (ESI) m/z calcd for $[C_{102}H_{73}ONRh]^+$: 1444.4773, found: 1444.4727.

4.3 X-Ray Structures Determination

CCDC 946320 (**4.10**), CCDC 946317 (**4.11**) and CCDC 946318 (**4.12**) contain the supplementary crystallographic data for this thesis. These data can be obtained free of charge from the Cambridge Crystallographic Data Center via www.ccdc.cam.ac.uk/data_request/cif.

Table 1. Crystal data and refinement parameters.

	IPr*$^{(2\text{-Np})}$•HCl (**4.10**)	IPr*$^{(2\text{-Np})}$AgCl (**4.11**)	IPr*$^{(2\text{-Np})}$CuCl (**4.12**)
Refined formula	$C_{101}H_{73}ClN_2$•C_6H_6	$C_{101}H_{72}AgClN_2$•2 $CHCl_3$	$C_{101}H_{72}ClCuN_2$•3 $CHCl_3$
M_r (g mol^{-1})	1428.17	1695.66	1770.70
Crystal dimensions (mm)	$0.3 \times 0.3 \times 0.23$	$0.35 \times 0.22 \times 0.17$	$0.12 \times 0.12 \times 0.10$
Crystal system	monoclinic	triclinic	triclinic
Space group	C 2/c	P–1	P–1
a (Å)	39.809(2)	14.0393(11)	14.1747(4)
b (Å)	14.0313(7)	14.4179(10)	14.3542(2)
c (Å)	37.0198(16)	24.8519(17)	25.0078(8)
α (°)		73.245(5)	73.281(2)
β (°)	105.718(5)	82.809(6)	82.616(3)
γ (°)		77.903(6)	78.712(2)
V (Å^3)	19904.7(18)	4698.6(6)	4764.7(2)
Z	8	2	2
ρ_{calc} (g cm^{-3})	0.953	1.199	1.234
$2\theta_{max}$ (°)	40.388	42.98	46.52
Radiation	MoKα	MoKα	MoKα

	IPr*$^{(2\text{-Np})}$•HCl (**4.10**)	IPr*$^{(2\text{-Np})}$AgCl (**4.11**)	IPr*$^{(2\text{-Np})}$CuCl (**4.12**)
λ (Å)	0.71073	0.71073	0.71073
F(000)			
T (K)	150(2)	150(2)	150(2)
Measured reflections	28445	21145	25766
Unique reflections	9469	10243	12881
Observed reflections ($I_o > 2\sigma(I_o)$)	6647	6944	9681
Parameters refined	993	1239	1275
Restraints	291	1075	935
R_1	0.0908	0.0784	0.0896
ωR_2[a]	0.2217	0.2142	0.2542
R_1 (all data)	0.1220	0.1080	0.1093
ωR_2 (all data)	0.2427	0.2356	0.2701
GOOF			
R_{int}	0.0573	0.0608	0.0363
μ (mm^{-1})	0.080	0.459	0.556
Squeeze details nr of sites (P1 cell)	4	3	6
Total e⁻ count	586	163	137
Total void volume	5916	733	500

5. Compounds Synthesized in the Annex Chapter

The starting materials were commercially available or prepared according to standard literature protocols.

General procedure for the reduction of ketones: In a flame-dried round-bottomed flask, thiophenol (4.12 mmol, 1.1 equiv) was added dropwise at 0 °C to triethylaluminum (1 mol L^{-1} in hexane, 4.20 mmol, 1.12 equiv). After stirring 20 min at room temperature, dry toluene (7 mL) was added and the reaction mixture was cooled to −78 °C. This solution was cannulated slowly (over 45 min) into a Schlenk flask (along the glass), previously cooled at −78 °C, containing the aldehyde (3.73 mmol, 1 equiv) and the ketone (3.73 mmol, 1 equiv) in dry toluene (5 mL). The round-bottomed flask was rinsed with cold and dry toluene (1 mL) and the resulting mixture was stirred 20 min at −78 °C. Diisobutylaluminum hydride (1 mol L^{-1} in toluene, 4.48 mmol, 1.2 equiv) was added dropwise to this solution (over 15 min) at −78 °C. Completion of the reaction was checked by TLC or GC. The mixture was then carefully poured into a stirred 1 mol L^{-1} aqueous solution of HCl (150 mL) at 0 °C. The aqueous layer was extracted with dichloromethane (3 × 50 mL) at room temperature. The organic layer was washed with brine, dried over magnesium sulfate, filtered and concentrated under reduced pressure. The crude product was purified by column chromatography on silica gel.

General procedure for the reduction of methyl esters: In a flame-dried round-bottomed flask, thiophenol (4.12 mmol, 1.1 equiv) was added dropwise at 0 °C to triethylaluminum (1 mol L^{-1} in hexane, 4.20 mmol, 1.12 equiv). After stirring 20 min at room temperature, dry toluene (7 mL) was added and the reaction mixture was cooled to -78 °C. This solution was cannulated slowly over (45 min) into a Schlenk flask (along the glass), previously cooled at −78 °C, containing the aldehyde (3.73 mmol, 1 equiv) and the methyl ester (3.73 mmol,

1 equiv) in dry toluene (5 mL). The round-bottomed flask was rinsed with cold and dry toluene (1 mL) and the resulting mixture was stirred 20 min at –78 °C. Diisobutylaluminum (1 mol L^{-1} in toluene, 8.21 mmol, 2.2 equiv) was added dropwise to this solution (over 15 min) at –78 °C and the reaction mixture was stirred at 0 °C. Completion of the reaction was checked by TLC or GC. The mixture was then carefully poured into a stirred 1 mol L^{-1} aqueous solution of HCl (150 mL) at 0 °C. The aqueous layer was extracted with dichloromethane (3×50 mL) at room temperature. The organic layer was washed with brine, dried over magnesium sulfate, filtered and concentrated under reduced pressure. The crude product was purified by column chromatography on silica gel.

General procedure for the preparation of acetate derivatives: In a flame-dried round-bottomed flask, triethylamine (5.60 mmol, 1.5 equiv) and 4-dimethylaminopyridine (0.19 mmol, 0.05 equiv) were added to the alcohol (3.73 mmol, 1 equiv) in dry dichloromethane (7.5 mL) at 0 °C, then acetic anhydride (7.46 mmol, 2 equiv) was added dropwise. The resulting solution was stirred at room temperature and completion of the reaction was checked by TLC. The reaction mixture was then quenched with water (10 mL) and the aqueous layer was extracted with dichloromethane (3 × 10 mL). The organic layer was dried over magnesium sulfate, filtered and concentrated under reduced pressure. The crude product was purified by column chromatography on silica gel.

4-Phenyl-2-butanol (A.18) CAS: 2344-70-9

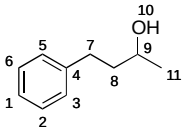

Eluent: AcOEt 2/ PE 8. **^{1}H NMR** (300 MHz, $CDCl_3$) δ: 7.31–7.16 (m, 5 H, H_{Ar}), 3.82 (sex, *J* = 6.2 Hz, 1 H, H-9), 2.81–2.62 (m, 2 H, H-7), 1.81–1.73 (m, 2 H, H-8), 1.47 (br s, 1 H, H-10), 1.23 (d, *J* = 6.2 Hz, 3 H, H-11) ppm. **^{13}C NMR** (75 MHz, $CDCl_3$) δ: 142.2 (C-4), 128.5 (C-2-3-5-6), 125.9 (C-1), 67.6 (C-9), 41.0 (C-8), 32.3 (C-7), 23.8 (C-11) ppm. **HRMS** (EI) m/z calcd for $[C_{10}H_{14}O]^+$: 150.1039, found: 150.1037.

1-Phenyl-3-pentanol (A.20) CAS: 71747-37-0

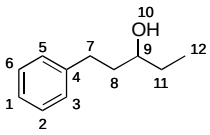

Eluent: AcOEt 1/ PE 9. **^{1}H NMR** (300 MHz, $CDCl_3$) δ: 7.30–7.15 (m, 5 H, H_{Ar}), 3.59–3.51 (m, 1 H, H-9), 2.84–2.61 (m, 2 H, H-7), 1.84–1.67 (m, 2 H, H-8), 1.57–1.42 (m, 3 H, H-10-11), 0.94 (t, *J* = 7.5 Hz, 3 H, H-12) ppm. **^{13}C NMR** (75 MHz, $CDCl_3$) δ: 142.3 (C-4), 128.5 (C-2-3-5-6), 125.9 (C-1), 72.8 (C-9), 38.7 (C-8), 32.2 (C-7), 30.4 (C-11), 10.0 (C-12) ppm. **IR** (thin film): 3335, 3085, 3062, 3026, 2964, 2934, 2877, 1120 cm^{-1}. **HRMS** (CI) m/z calcd for $[C_{11}H_{15}]^+$: 147.1174, found: 147.1175.

4,4-Dimethyl-1-phenyl-3-pentanol (A.22) CAS: 18335-33-6

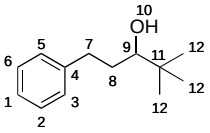

Eluent: dichloromethane. **^{1}H NMR** (300 MHz, $CDCl_3$) δ: 7.32–7.12 (m, 5 H, H_{Ar}), 3.20 (dd, *J* = 10.6, 1.8 Hz, 1 H, H-9), 2.97–2.88 (m, 1 H, H-7), 2.67–2.57 (m, 1 H, H-7'), 1.90–1.79 (m, 1 H, H-8), 1.65–1.52 (m, 1 H, H-8'), 1.45 (br s, 1 H, H-10), 0.89 (s, 9 H, H-12) ppm. **^{13}C NMR** (75 MHz, $CDCl_3$) δ: 142.4 (C-4), 128.4 (C-2-6 or C-3-5), 128.3 (C-3-5 or C-2-6), 125.7 (C-1), 79.3 (C-9), 34.9 (C-11), 33.4 (C-7 or C-8), 33.3 (C-8 or C-7), 25.6 (C-12) ppm. **IR** (thin film): 3500, 3026, 2955, 2866, 1605, 1497, 1479, 1392, 1364, 1074, 1047, 1010 cm^{-1}. **HRMS** (CI) m/z calcd for $[C_{13}H_{19}]^+$: 175.1486, found: 175.1482.

1-Phenyl-1-ethanol (A.25) CAS: 98-85-1

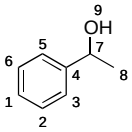

Eluent: AcOEt 2/ PE 8. **^{1}H NMR** (300 MHz, $CDCl_3$) δ: 7.37–7.25 (m, 5 H, H_{Ar}), 4.90 (q, *J* = 6.4 Hz, 1 H, H-7), 1.84 (br s, 1 H, H-9), 1.50 (d, *J* = 6.3 Hz, 3 H, H-8) ppm. **^{13}C NMR** (75 MHz, $CDCl_3$) δ: 145.9 (C-4), 128.5 (C-2-6 or C-3-5), 127.5 (C-1), 125.5 (C-3-5 or C-2-6), 70.4 (C-7), 25.2 (C-8) ppm.

1-Phenyl-1-propanol (A.27) CAS: 93-54-9

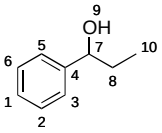

Eluent: AcOEt 2/ PE 8. **^{1}H NMR** (300 MHz, $CDCl_3$) δ: 7.38–7.24 (m, 5 H, H_{Ar}), 4.60 (t, *J* = 6.8 Hz, 1 H, H-7), 1.91–

1.68 (m, 3 H, H-8-9), 0.92 (t, *J* = 7.4 Hz, 3 H, H-10) ppm. **^{13}C NMR** (75 MHz, $CDCl_3$) δ: 144.7 (C-4), 128.5 (C-2-6 or C-3-5), 127.6 (C-1), 126.1 (C-3-5 or C-2-6), 76.1 (C-7), 32.0 (C-8), 10.2 (C-10) ppm.

2-Methyl-1-phenyl-1-propanol (A.29) CAS: 611-69-8

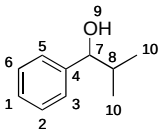

Eluent: AcOEt 2/ PE 8. **^{1}H NMR** (300 MHz, $CDCl_3$) δ: 7.36–7.25 (m, 5 H, H_{Ar}), 4.36 (d, *J* = 6.9 Hz, 1 H, H-7), 2.02–1.90 (m, 1 H, H-8), 1.87 (br s, 1 H, H-9), 1.00 (d, *J* = 6.6 Hz, 3 H, H-10), 0.80 (d, *J* = 6.6 Hz, 3 H, H-10') ppm. **^{13}C NMR** (75 MHz, $CDCl_3$) δ: 143.8 (C-4), 128.3 (C- C-2-6 or C-3-5), 127.6 (C-1), 126.7 (C-3-5 or C-2-6), 80.2 (C-7), 35.4 (C-8), 19.1 (C-10), 18.4 (C-10') ppm. **IR** (thin film): 3426, 3086, 3063, 3028, 2960, 2926, 2873 cm^{-1}. **MS** (CI) m/z: 149 (10 %, $[M–H]^+$), 134 (21 %), 133 (100 %, $[M–OH]^+$), 107 (51 %, $[M–C_3H_7]^+$), 93 (19 %), 73 (30 % $[M–Ph]^+$).

6-Acetoxyheptanal (from A.33) CAS: 113434-69-8

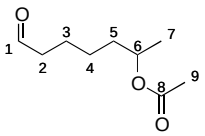

Eluent: AcOEt 15/ PE 85. **^{1}H NMR** (300 MHz, $CDCl_3$) δ: 9.77 (s, 1 H, H-1), 4.90 (sex, *J* = 6.2 Hz, 1 H, H-6), 2.45 (t, *J* = 7.2 Hz, 2 H, H-2), 2.03 (s, 3 H, H-9), 1.67–1.49 (m, 4 H, H-3-5), 1.41–1.31 (m, 2 H, H-4), 1.21 (d, *J* = 6.3 Hz, 3 H, H-7) ppm. **^{13}C NMR** (75 MHz, $CDCl_3$) δ: 202.4 (C-1), 170.8 (C-8), 70.6 (C-6), 43.8 (C-2), 35.7 (C-5), 25.0 (C-4), 21.9 (C-3), 21.4 (C-9 or C-7), 20.0 (C-7 or C-9) ppm.

6-Acetoxy-6-phenylhexanal (from A.35)

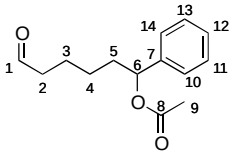

Eluent: AcOEt 1/ PE 9. **^{1}H NMR** (300 MHz, $CDCl_3$) δ: 9.72 (t, *J* = 1.5 Hz 1 H, H-1), 7.36–7.24 (m, 5 H, H_{Ar}), 5.72 (t, *J* = 6.9 Hz, 1 H, H-6), 2.40 (td, *J* = 7.3, 1.5 Hz, 2 H, H-2), 2.06 (s, 3 H, H-9), 1.99–1.87 (m, 1 H, H-5), 1.84–1.72 (m, 1 H, H-5'), 1.63 (quin, *J* = 7.3 Hz, 2 H, H-3), 1.44–1.18 (m, 2 H, H-4) ppm. **^{13}C NMR** (75 MHz, $CDCl_3$) δ: 202.0 (C-1), 170.0 (C-8), 140.2 (C-7), 128.2 (C-11-13 or C-10-14), 127.6 (C-12), 126.2 (C-10-14 or

C-11-13), 75.4 (C-6), 43.3 (C-2), 35.7 (C-5), 24.8 (C-4), 21.4 (C-3), 20.9 (C-9) ppm. **IR** (thin film): 2910, 2900, 1728, 1704, 1454, 1371, 1234, 1022 cm^{-1}. **HRMS** (CI) m/z calcd for $[C_{13}H_{17}O_2]^+$: 205.1229, found: 205.1225.

Benzylalcohol (A.37) CAS: 100-51-6

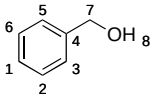

Eluent: AcOEt 2/ PE 8. **^{1}H NMR** (300 MHz, $CDCl_3$) δ: 7.39–7.32 (m, 5 H, H_{Ar}), 4.65 (s, 2 H, H-7), 2.53 (br s, 1 H, H-8) ppm. **^{13}C NMR** (75 MHz, $CDCl_3$) δ: 140.9 (C-4), 128.6 (C-2-6), 127.6 (C-1), 127.1 (C-3-5), 65.2 (C-7) ppm.

Cyclohexanemethanol (A.39) CAS: 100-49-2

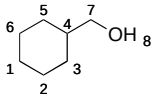

Eluent: AcOEt 2/ PE 8. **^{1}H NMR** (300 MHz, $CDCl_3$) δ: 3.44 (d, *J* = 6.6 Hz, 2 H, H-7), 1.77–1.66 (m, 5 H, H-1_{eq}-2_{eq}-3_{eq}-5_{eq}-6_{eq}), 1.55–1.41 (m, 2 H, H-4-8), 1.32–1.14 (m, 3 H, H-1_{ax}-2_{ax}-6_{ax}), 0.99–0.88 (m, 2 H, H-3_{ax}-5_{ax}) ppm. **^{13}C NMR** (75 MHz, $CDCl_3$) δ: 68.9 (C-7), 40.6 (C-4), 29.7 (C-3-5), 26.7 (C-1), 26.0 (C-2-6) ppm.

6-Acetoxyhexanal (from A.41) CAS: 68750-25-4

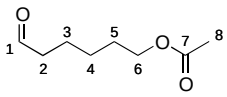

Eluent: AcOEt 5/ PE 95. **^{1}H NMR** (300 MHz, $CDCl_3$) δ: 9.78 (t, *J* = 1.6 Hz, 1 H, H-1), 4.06 (t, *J* = 6.6 Hz, 2 H, H-6), 2.46 (td, *J* = 7.3, 1.6 Hz, 2 H, H-2), 2.05 (s, 3 H, H-8), 1.72–1.61 (m, 4 H, H-3-5), 1.43–1.34 (m, 2 H, H-4) ppm. **^{13}C NMR** (75 MHz, $CDCl_3$) δ: 202.3 (C-1), 171.1 (C-7), 64.1 (C-6), 43.7 (C-2), 28.4 (C-5), 25.5 (C-4), 21.6 (C-3), 21.0 (C-8) ppm. **IR** (thin film): 2947, 2866, 1730, 1714, 1462, 1435, 1390, 1365, 1230, 1199, 1145, 1038 cm^{-1}. **HRMS** (EI) m/z calcd for $[C_8H_{13}O_3]^+$: 157.0859, found: 157.0859.

Annex Chapter

Chemoselective Reduction of Carbonyl Groups in the Presence of Aldehydes

This chapter describes the chemoselective reduction of ketones and methyl esters, in the presence of aldehydes, using a combination of diethylaluminum benzenethiolate and diisobutylaluminum hydride.[1] After a brief survey of the literature, we will detail our efforts dedicated to the elaboration of this new methodology and finally present some opportunities for its development. This work has been done in collaboration with Dr. Gulluzar Bastug and Dr. Frédéric Lebreux.[1,2]

1. State of the Art

Functional Group Interconversions (FGIs) form a central theme in organic chemistry.[3] Among them, modifying the oxidation state of carbonyl groups is of crucial importance.[3, 4] The chemoselective

[1] Part of this chapter has already been published in: G. Bastug, S. Dierick, F. Lebreux, I. E. Markó, *Org. Lett.* **2012**, *14*, 1306; which was written by the Author of this manuscript.

[2] F. Lebreux, *Master thesis*, Université catholique de Louvain, 2004.

[3] E. J. Corey, X.-M. Cheng, *The Logic of Chemical Synthesis*; Wiley: New-York, 1995.

[4] a) K. C. Nicolaou, E. J. Sorensen, *Classics in Total Synthesis*; VCH: Weinheim, 1996. b) T. Hudlicky, J. W. Reed, *The Way of Synthesis*; Wiley-VCH: Weinheim, 2007.

reduction of aldehydes in the presence of less reactive carbonyl functions can be easily achieved using specially designed reagents.[5] However, the opposite transformation – i.e. the reduction of a carbonyl group, such as a ketone or an ester, in the presence of an aldehyde – remains elusive.

Although specific protecting groups for aldehydes have been introduced,[6] several drawbacks still persist. In particular, their use in polyfunctional molecules is sometimes challenging and unselective. Moreover, this protecting group methodology requires a three-step process: protection, reaction, and deprotection. Accordingly, it is hardly surprising that modern synthetic endeavors, aimed at efficiency and convergency, will try to avoid such practice by attempting to minimize the number of steps, decreasing the amount of byproduct and saving time.[7]

A more elegant strategy can solve most of these shortcomings. Indeed, the aldehyde can be reversibly transformed in situ in an unreactive derivative, leaving other untouched carbonyl groups to react. This principle has been successfully applied by Reetz and Yamamoto for the chemoselective alkylation of ketones in the presence of aldehydes.[8] In his pioneering work, Luche used lanthanoids for the hydration of aldehydes, enabling the selective reduction of ketones by sodium

5 S. D. Burke, R. L. Danheiser, *Handbook of Reagents for Organic Synthesis. Oxidizing and Reducing Agents*; Wiley: Chichester, 1999.

6 a) P. J. Kocienski, *Protecting Groups*, 3th ed.; Thieme: Stuttgart, 2004. b) P. G. M. Wuts, T. W. Greene, *Greene's Protective Groups in Organic Synthesis*, 4th ed.; Wiley: Hoboken, 2007.

7 a) J. B. Hendrickson, *J. Am. Chem. Soc.* **1975**, *97*, 5784. b) P. S. Baran, T. J. Maimone, J. M. Richter, *Nature* **2007**, *446*, 404. c) T. Newhouse, P. S. Baran, R. W. Hoffmann, *Chem. Soc. Rev.* **2009**, *38*, 3010. d) I. S. Young, P. S. Baran, *Nat. Chem.* **2009**, *1*, 193.

8 a) M. T. Reetz, B. Wenderoth, R. J. Peter, *Chem. Soc., Chem. Commun.* **1983**, 406. b) K. Maruoka, Y. Araki, H. Yamamoto, *Tetrahedron Lett.* **1988**, *29*, 3101.

borohydride (Figure 1).[9] Unfortunately, this aqueous system displays only good to moderate selectivities and is limited to aliphatic substrates. In a one-pot procedure, Paradisi preferentially converted aldehydes into *tert*-butyl imines before reducing ketones with an aluminohydride reagent, eventually releasing the unreacted aldehyde.[10] However, the intermediate imine is too reactive to extend this methodology to other transformations. During our own study, Colby described the use of dialkylaluminum *N*,*O*-dimethylhydroxylamine complexes as reagents to mask carbonyl groups in situ.[11] Although interesting, the selectivities have not been measured and this system requires excess of the nucleophile.

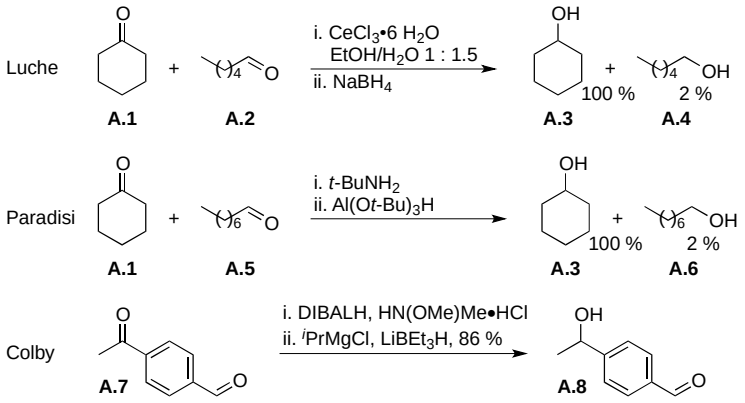

Figure 1. Chemoselective reduction of ketones in the presence of aldehydes.

[9] a) A. L. Gemal, J.-L. Luche, *J. Org. Chem.* **1979**, *44*, 4187. b) J.-L. Luche, A. L. Gemal, *J. Am. Chem. Soc.* **1979**, *101*, 5848.

[10] M. P. Paradisi, G. P. Zecchini, G. Ortar, *Tetrahedron Lett.* **1980**, *21*, 5085.

[11] a) F. J. Barrios, X. Zhang, D. A. Colby, *Org. Lett.* **2010**, *12*, 5588. b) F. J. Barrios, B. C. Springer, D. A. Colby, *Org. Lett.* **2013**, *15*, 3082.

2. When Serendipity Comes into Play

As part of an ongoing research program, aimed at the efficient assembly of α-methylene-γ-butyrolactones, our research team has reported recently a novel tandem Claisen–ene rearrangement (Figure 2).[12] In the course of this process, diethylaluminum benzenethiolate,[13] which was used as a mild Lewis acid to catalyze the initial Claisen rearrangement, added to the in situ generated aldehyde as soon as it was formed. The resulting *O*,*S*-aluminum acetal **A.10** proved to be surprisingly robust, and the aldehyde **A.11**, needed for the subsequent ene reaction, had to be unmasked by the addition of phenylsulfenyl chloride. It is noteworthy that, introducing this last reagent, afforded not only inert diphenyl disulfide, but also diethylaluminum chloride, the Lewis acid required for the ene reaction, thereby increasing further the efficiency of the overall process.

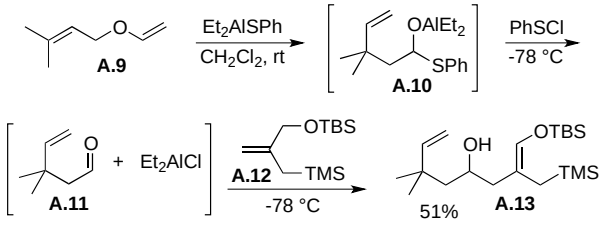

Figure 2. Tandem Claisen–ene rearrangement.

Attracted by this unexpected reactivity, we investigated the behavior of this particular Lewis acid toward various aldehydes and ketones. In the event, hydrocinnamaldehyde (**A.14**) and benzylacetone (**A.16**) were reacted individually, at –78 °C, with diethylaluminum benzenethiolate in

[12] C. Leclercq, I. E. Markó, *Tetrahedron Lett.* **2005**, *46*, 7229.

[13] a) K. Takai, I. Mori, K. Oshima, H. Nozaki, *Bull. Chem. Soc. Jpn.* **1984**, *57*, 446. b) I. Mori, K. Takai, K. Oshima, H. Nozaki, *Tetrahedron* **1984**, *40*, 4013. c) K. Takai, I. Mori, K. Oshima, H. Nozaki, H. *Tetrahedron Lett.* **1981**, *22*, 3985.

hexane giving the corresponding *O*,*S*-aluminum acetals **A.15** and **A.17**, respectively (Figure 3).

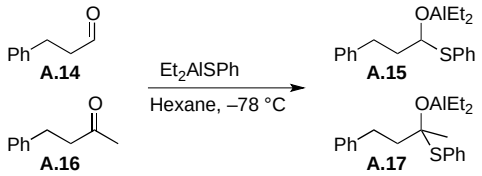

Figure 3. Addition of Et_2AlSPh to hydrocinnamaldehyde and benzylacetone.

According to the ^{13}C NMR analyses of the crude reaction mixtures measured at 25 °C (Figure 4), we were pleased to notice that (i) aldehyde **A.14** was completely transformed into the acetal **A.15** and did not undergo a Tishchenko reaction (spectrum A)[14] and (ii) ketone **A.16** reacted partially to give ketal **A.17** (spectrum B). The presence of several signals around 83 ppm in the ^{13}C NMR spectrum of **A.15** suggests that this species might exist in a dimeric form or even as an oligomeric assembly. In a competitive experiment, hydrocinnamaldehyde (**A.14**) and benzylacetone (**A.16**) were treated with 1 equiv of Et_2AlSPh. Gratifyingly, aldehyde **A.14** was smoothly converted into the acetal **A.15** while the ketone **A.16** remained unaltered (spectrum C).

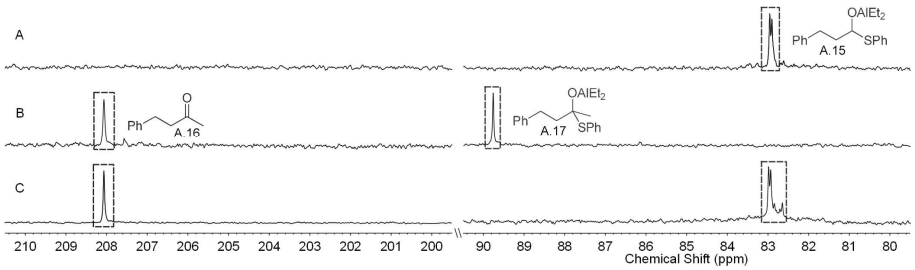

Figure 4. Partial ^{13}C NMR spectra of the aluminum adducts.

[14] L. Cronin, F. Manoni, C. J. O'Connor, S. J. Connon, *Angew. Chem. Int. Ed.* **2010**, *49*, 3045.

3. Chemoselective Reduction of Carbonyl Groups in the Presence of Aldehydes

3.1 Optimization Study

Encouraged by these preliminary observations, we designed a protocol for the selective reduction of benzylacetone (**A.16**) in the presence of an equimolar amount of hydrocinnamaldehyde (**A.14**). Some relevant results are presented in Table 1. It transpires, from this optimization study, that the temperature for the formation of the acetal is, as expected, crucial; the lower the temperature, the better the selectivity and the higher the yield (entries 2–5). Another important parameter to control proved to be the quantity of diethylaluminum benzenethiolate. Indeed, if a near-stoichiometric quantity of this reagent is employed, the selectivity drops to 78 % (entry 6). On the other hand, the use of 1.4 equiv of this Lewis acid provides the highest levels of chemoselectivity albeit at the expense of the conversion (entry 7). Clearly, using a large excess of Et_2AlSPh leads to the partial hemi-thioketalization of the ketone, which could not be reduced further. The best compromise between high selectivity and good yields involves the use of 1.1 equiv of diethylaluminum benzenethiolate. Furthermore, the temperature of reduction has also some influence on the selectivity and it should be performed at –78 °C or below. Finally, replacing toluene with dichloromethane or tetrahydrofuran does not improve the yield but decreases the selectivity (entries 8, 9).

Table 1. Optimization of the chemoselective reduction of hydrocinnamaldehyde in the presence of benzylacetone.

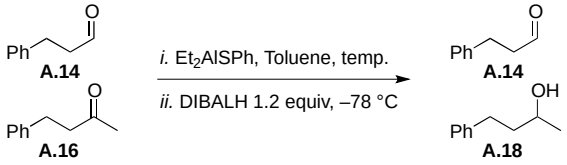

entry	temperature	Et_2AlSPh	selectivity[a]	yield[b]
1[c]	—	0 equiv	0 %	50 %
2	rt	1.1 equiv	42 %	65 %
3[d]	–15 °C	1.1 equiv	48 %	68 %
4	–15 °C	1.1 equiv	66 %	77 %
5	–78 °C	1.1 equiv	98 %	89 %
6	–78 °C	1.02 equiv	78 %	81 %
7	–78 °C	1.4 equiv	99 %	72 %
8[e]	–78 °C	1.1 equiv	88 %	86 %
9[f]	–78 °C	1.1 equiv	85 %	89 %

[a] Selectivity is defined as (secondary alcohol – primary alcohol) / (secondary alcohol + primary alcohol) and determined by GC. [b] GC yields measured with dodecane (1 equiv) as an internal standard. [c] 1.0 equiv of diisobutylaluminum hydride was used. [d] Reduction was performed at –15 °C. [e] Toluene was replaced by CH_2Cl_2. [f] Toluene was replaced by THF.

3.2 Chemoselective Reduction of Ketones

With the optimization study completed, the scope and limitations of this novel chemoselective reduction methodology were next investigated (Table 2). In the aliphatic series, increasing the steric hindrance around the ketone function has little effect on the selectivity and yield. Both remain excellent (entries 1–3). The aromatic substrates give slightly lower yields and selectivities (entries 4–6). It is worth noting that, in these cases, an important influence of steric hindrance is operating, with the isopropyl group significantly raising the selectivity. An impressive result arises from the reduction of benzylacetone in the presence of pivalaldehyde. In this case, no trace of neopentyl alcohol could be detected (entry 7). Thus, a quaternary center α to the aldehyde group does not prevent the formation of the corresponding *O*,*S*-acetal. Moreover, functionalities sensitive to diisobutylaluminum hydride, such as alkynes and nitriles, are well tolerated under these conditions (entries 8, 9). Finally, the synthetically useful intramolecular version of our protocol proceeds smoothly to give outstanding selectivities and good yields (entries 10, 11).[15]

[15] Since the resulting hydroxy aldehydes were in equilibrium with their hemiacetal forms, they were acetylated in order to obtain unambiguous characterization data.

Table 2. Chemoselective reduction of ketones.

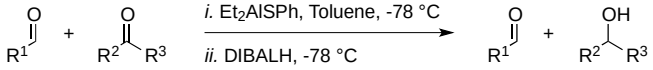

entry	aldehyde	ketone	product	selectivity[a]	yield[b]
1	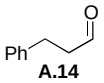 A.14	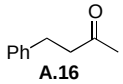 A.16	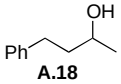 A.18	98 %	89 %
2	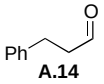 A.14	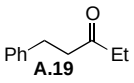 A.19	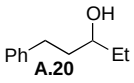 A.20	97 %	85 %
3	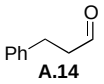 A.14	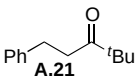 A.21	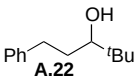 A.22	99 %	84 %
4	 A.23	 A.24	 A.25	91 %	85 %
5	 A.23	 A.26	 A.27	91 %	82 %
6	 A.23	 A.28	 A.29	97 %	82 %
7	 A.30	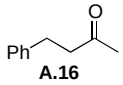 A.16	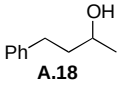 A.18	>99 %[c]	91 %[d]
8[e]	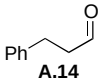 A.14	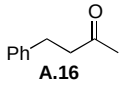 A.16	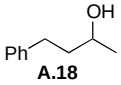 A.18	97 %	89 %
9	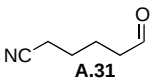 A.31	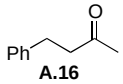 A.16	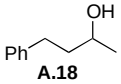 A.18	97 %	86 %
10	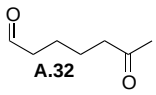 A.32		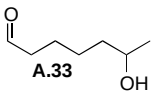 A.33	92 %	69 %[d,f]
11	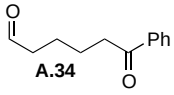 A.34		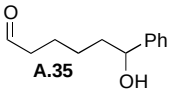 A.35	98 %	79 %[d,f]

[a] Selectivity is defined as (secondary alcohol – primary alcohol)/(secondary alcohol + primary alcohol) and determined by GC for intermolecular reaction and by ^{1}H NMR for intramolecular reaction. [b] GC yields measured with dodecane (1 equiv) as an internal standard. [c] No trace of neopentylalcohol was detected in the crude mixture by GC. [d] Isolated yields after column chromatography on silica gel. [e] Performed in the presence of 1-octyne (1 equiv). [f] Isolated as the acetate derivative.[15]

3.3 Chemoselective Reduction of Methyl Esters

Having successfully demonstrated the synthetic potential of our methodology, we next turned our attention to the more challenging reduction of methyl esters in the presence of aldehydes. Some of our results are collected in Table 3. In these cases, 2 equiv of diisobutylaluminum hydride have been used in the reduction step which was performed at 0 °C. Pleasingly, the reduction of both aromatic and aliphatic methyl esters could be accomplished in good yields and with excellent levels of chemoselectivity in the presence of an aliphatic aldehyde (entries 1, 2). An intramolecular version of this process gave remarkable selectivity, though the yield was slightly lower (entry 3).[15]

Table 3. Chemoselective reduction of methyl esters.

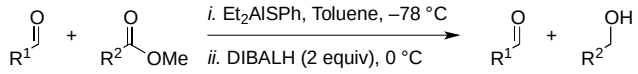

entry	aldehyde	ester	product	selectivity[a]	yield[b]
1	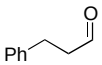 **A.14**	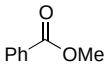 **A.36**	 **A.37**	>99 %[c]	97 %
2	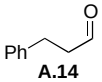 **A.14**	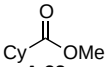 **A.38**	 **A.39**	>99 %[c]	93 %
3	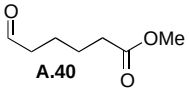 **A.40**	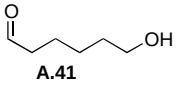 **A.41**		98 %	71 %[d]

[a] Selectivity is defined as (alcohol from ester – alcohol from aldehyde)/(alcohol from ester + alcohol from aldehyde) and determined by GC for intermolecular reaction and by ^{1}H NMR for intramolecular reaction. [b] Isolated yields after column chromatography on silica gel. [c] No trace of hydrocinnamic alcohol was detected in the crude mixture by GC. [d] Isolated as the acetate derivative.[15]

4. Conclusions and Perspectives

In summary, the reduction of ketones and methyl esters in the presence of aldehydes was achieved with high yields and excellent chemoselectivity. The method is efficient for both aliphatic and aromatic substrates and tolerates increasing steric hindrance around both carbonyl groups. Moreover, all the reagents employed in this reaction are commercially available and cheap.[16]

The in situ masking of aldehyde as *O*,*S*-aluminum acetals is certainly not limited to the chemoselective reduction of other carbonyl moiety. Obviously, this tactic could be use to protect aldehyde towards various transformations (olefination, hydroboration, aldol reaction…) in the presence of less reactive functions. Dr. Huoming Li has begun to study the alkylation of ketones with Grignard reagents in the presence of aldehydes (Figure 5).[17] Whilst encouraging, these preliminary results remain to be improved.

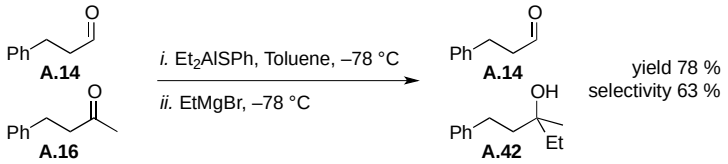

Figure 5. Chemoselective alkylation of benzylacetone.

Furthermore, building on our facile preparation of thioacetals, we propose to develop a one-pot synthesis of thioethers from aldehyde (Figure 6). Indeed, adding a hard Lewis acid to the *O*,*S*-acetal **A.44** should selectively trigger the formation of the thionium cation **A.46**.

[16] Diethylaluminum benzenethiolate is easily prepared in situ from triethylaluminum and thiophenol.

[17] H. Li, *Post-doctoral report*, Université catholique de Louvain, 2012.

Addition of a nucleophile, inter- or intramolecularly, would then afford the thioether **A.47**.[18]

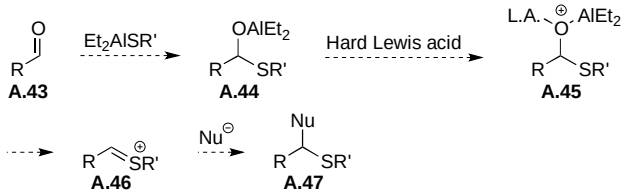

Figure 6. One-pot synthesis of thioesters from aldehydes.

Recently, Procter described a similar sequence, named connective Pummerer rearrangement (Figure 7).[19] While substantiating our proposal, this system is limited to the intramolecular Friedel–Crafts alkylation of thionium cation; generated by the addition of an excess of trifluoroacetic anhydride and boron trifluoride diethyl etherate to a mixture of thiol and glyoxamide. We could reasonably presume that our approach would benefit from (i) the possibility to form the thioacetals from various precursors and (ii) the departure of the oxygen moiety under milder conditions, due to the assistance of the aluminum Lewis acid.

[18] For selected examples of the addition of nucleophiles to thionium cation prepared from thioacetals, see: a) I. Mori, P. A. Bartlett, C. H. Heathcock, *J. Org. Chem.* **1990**, *55*, 5966. b) J.-i. Uenishi, A. Sohma, O. Yonemitsu, *Chem. Lett.* **1996**, 595. c) W. Priebe, A. Zamojski, *Tetrahedron* **1980**, *36*, 287. d) K. C. Nicolaou, J. Ladduwahetty, J. L. Randall, A. Chuchdowski, *J. Am. Chem. Soc.* **1986**, *108*, 2466.

[19] a) L. A. McAllister, R. A. McCormick, S. Brand, D. J. Procter, *Angew. Chem. Int. Ed.* **2005**, *44*, 452. b) L. A. McAllister, R. A. McCormick, K. M. James, S. Brand, N. Willetts, D. J. Procter, *Chem. Eur. J.* **2007**, *13*, 1032. c) M. Miller, W. Tsang, A. Merritt, D. J. Procter, *Chem. Commun.* **2007**, 498. d) C. Ovens, N. G. Martin, D. J. Procter, *Org. Lett.* **2008**, *10*, 1441. e) C. Ovens, J. C. Vogel, N. G. Martin, D. J. Procter, *Chem. Commun.* **2009**, 3101. f) M. Miller, J. C. Vogel, W. Tsang, A. Merrit, D. J. Procter, *Org. Biomol. Chem.* **2009**, *7*, 589. g) L. H. Smith, T. T. Nguyen, H. F. Sneddon, D. J. Procter, *Chem. Commun.* **2011**, *47*, 10821. h) M. T. Levick, S. C. Coote, I. Grace, C. Lambert, M. L. Turner, D. J. Procter, *Org. Lett.* **2012**, *14*, 5744.

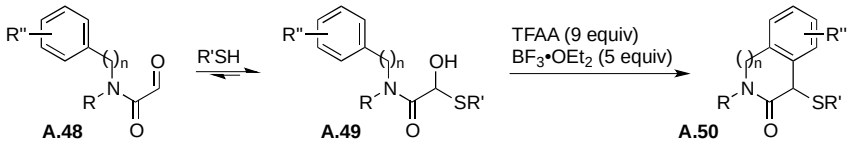

Figure 7. Connective Pummerer rearrangement as reported by Procter.